5th International Probabilistic Workshop

Luc Taerwe & Dirk Proske Editors

28-29 November 2007 Ghent, Belgium

acco

Proceedings
of the
5th International
Probabilistic Workshop

28-29 November 2007
Ghent, Belgium

Edited by
Luc Taerwe & Dirk Proske

Preface

These are the proceedings of the 5th International Probabilistic Workshop. Even though the 5th anniversary of a conference might not be of such importance, it is quite interesting to note the development of this probabilistic conference. Originally, the series started as the 1st and 2nd Dresdner Probabilistic Symposium, which were launched to present research and applications mainly dealt with at Dresden University of Technology. Since then, the conference has grown to an internationally recognised conference dealing with research on and applications of probabilistic techniques, mainly in the field of structural engineering. Other topics have also been dealt with such as ship safety and natural hazards. Whereas the first conferences in Dresden included about 12 presentations each, the conference in Ghent has attracted nearly 30 presentations. Moving from Dresden to Vienna (University of Natural Resources and Applied Life Sciences) to Berlin (Federal Institute for Material Research and Testing) and then finally to Ghent, the conference has constantly evolved towards a truly international level. This can be seen by the language used. The first two conferences were entirely in the German language. During the conference in Berlin however, the change from the German to English language was especially apparent as some presentations were conducted in German and others in English. Now in Ghent all papers will be presented in English. Participants now, not only come from Europe, but also from other continents.

Although the conference will move back to Germany again next year (2008) in Darmstadt, the international concept will remain, since so much work in the field of probabilistic safety evaluations is carried out internationally. In two years (2009) the conference will move to Delft, The Netherlands and probably in 2010 the conference will be held in Szczecin, Poland.

Coming back to the present: the editors wish all participants a successful conference in Ghent.

Conference Chairman

Prof. Dr. Ir. Luc Taerwe

Organizing Committee

Prof. Dr. Ir. Luc Taerwe
Department of Structural Engineering
Magnel Laboratory for Concrete Research
Technologiepark-Zwijnaarde 904
B-9052 Ghent, Belgium
Luc.Taerwe@UGent.be

ir. Robby Caspeele
Department of Structural Engineering
Magnel Laboratory for Concrete Research
Technologiepark-Zwijnaarde 904
B-9052 Ghent, Belgium
Robby.Caspeele@UGent.be

Marijke Reunes
Department of Structural Engineering
Magnel Laboratory for Concrete Research
Technologiepark-Zwijnaarde 904
B-9052 Ghent, Belgium
Marijke.Reunes@UGent.be

Dr.-Ing. D. Proske
University of Natural Resources and
Applied Life Sciences, Vienna
Institute of Mountain Risk Engineering
Peter Jordan-Strasse 82
1190 Wien, Austria
dirk.proske@boku.ac.at

Monika Stanzer
University of Natural Resources and
Applied Life Sciences, Vienna
Institute of Mountain Risk Engineering
Peter Jordan-Strasse 82
1190 Wien, Austria
monika.stanzer@boku.ac.at

Magnel Laboratory for Concrete Research
Ghent University, Ghent, Belgium

University of Natural Resources and Applied Life Sciences, Vienna
Department of Civil Engineering and Natural Hazards, Austria

Supported by the European Safety and Reliability Association

Scientific Committee

Content

Opening lecture: Innovative Technologies to Upgrade Fire Safety of Existing Tunnels

Konrad Bergmeister
Institute of Structural Engineering,
University of Natural Resources and Applied Life Sciences, Vienna

Abstract: A European research program called UPTUN, incorporating 41 partners, takes care on the fire protection of tunnels. The main objectives of this program are "Development of innovative technologies to upgrade fire safety of existing tunnels." Tunnel fires may release huge amount of energy. The recent fires in Europe have demonstrated that the energy generated by a fire can be as much as 30 - 150 Megawatts. In addition, there are requirements for protecting against such events. This paper shows developments within the project according to (a) fire and smoke as well as toxicity monitoring systems, and (b) efficient techniques increasing the fire protection. Associated investigations are performed in close collaboration with industrial partners and universities in laboratories and existing tunnels.

1   Introduction

There are rare real-scale fire tests for Tunnel Structures (Memorial Tunnel Fire Tests, Eureka Project, Safety Test, etc.) performed all over the world. The objectives of such tests are (a) the adaptation of Temperature versus Time curves, (b) the validation of the behavior of materials exposed to high temperatures, (c) corrosion tests of steel reinforcement, (d) the formulation of standards related to fire resistance of concrete structures. The European project UPTUN, which is the acronym for Cost-effective, Sustainable and Innovative Upgrading Methods for Fire Safety in Existing Tunnels; a European RTD-project funded by the European Commission in FP5, performed by industrial companies and universities (e.g. University of Natural Resources and Applied Sciences), comprises the mentioned objectives. Beyond these objectives a main interest are in the development of computation methods for the description of fire scenarios in tunnels. In addition to the computational methods, the targets of this paper are the presentation of safety elements developed during the project. The validation of safety features and monitoring devices allow to properly install systems, identified and studied to upgrade tunnels for the fire protection. Unfortu-

nately, simulation of realistic fire scenarios is necessary due to number and catastrophic real events. Full scale experiments and laboratory tests provide valuable knowledge for comprehensive and foresighted planning in many areas of tunnel safety.

2 Experiments reducing fire effects in existing Tunnels

2.1 General

The Virgolo tunnel in South Tyrol, Italy serves for four fire demonstrations, using diesel contained in stainless steel pools with a surface of 2 m^2 (Fig. 1) each (thermo energy E_{th} = 5 MW), to investigate the itemized objectives. A specially designed compartment (Mini-tunnel) was built, on whose walls and roof concretes, mortars and anchorages were applied and exposed to extremely high temperatures. The realization of real scale fire demonstration as performed in the Virgolo tunnel required the collaboration of local partners (high-way police, professional and voluntary fire brigades, emergency units, local agencies for ambient), Universities (10 institutes) and external partners.

Fig.1. Fire pools on rail tracks used for heating the concrete surface of the Minitunnel (right picture)

All of those mentioned institutions as well as designers and rescuers among others are predominant interested in the development of temperature fields in tunnels and the bearing elements of tunnels. In addition, they are interested in innovative tunnel facilities, which provide the possibility to control temperature fields and its effects on components. Following systems, elements and facilities have been installed and demonstrated in the Virgolo tunnel:

- 100 m of pipes of the water mist system for fire suppression,
- two Water shields for smoke containment,
- two Air-plugs for smoke containment,
- six optical signalling systems,
- several stationary and mobile samplers for air quality evaluation during fire,

- 80 m rail tracks,
- 18 m3 compartment (Minitunnel) for materials and anchorages tests,
- six innovative fire resistant concretes and mortars applied on the Virgolo tunnel walls,
- one fire resistant paint applied on the Virgolo tunnel walls,
- anchorage systems for illumination and ventilation systems.
- several fire detection and monitoring systems
- five video cameras, among which two stereoscopic and an infrared one
- Hundreds of sensors (air and concrete temperature, concrete resistance, wind (ventilation), opcacity/visibility, gas analysis, LVDT for anchor slip, etc.)

More than 300 temperature sensors distributed at different heights and depths in the tunnel walls provide data during four fire scenarios. The temperature measurements of these test-series build the basis for comparable numerical models and analyses. The measurements also served for the adaptation of fire fighting systems such as a fire section creator. For example, a fire fighting system and fire section creator, proved during the project, achieved some restriction of the convectional temperature be valuated as a valid measure to reduce smoke concentration in neighbouring sections. Another tested fire suppression technique is the water mist system. Figure 2 shows the effectiveness of this system. The second temperature increase after activation of the system is a result of the combined relationship through "burning oil and water". The clear increase in the CO concentration after activation can be explained by the lowered energy in the combustion process due to the water. The positive effect is that this system requires only about 10 % of the water required by conventional extinguisher systems. As a result, the energy adsorption of the fire from the water is lowered as is the CO concentration.
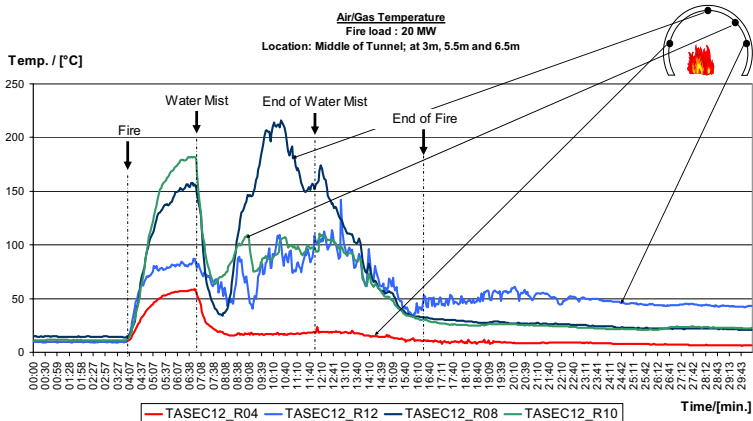
Fig.2. 20 MW test - Water Mist System

The research project also takes care on (a) risks caused by fastening elements under fire, (b) facilities increasing the probability of saving people involved in a tunnel fire scenario. In addition, a Traficon video based smoke detection system turns out as an effective tool to trigger an alarm and record video sequences. The tested video based fire detection system demonstrate a rapidly and reliably detection method despite unfavourable light and environmental conditions in the tunnel. Even if the very high smoke and temperature concentration caused the camera to fail after the first fire simulation, a fire event can be captured and signalled. Fibre optic cable indicators are alternative systems to detect fire very quickly and reliably after ignition. Because the system is able to locate the exact location of the fire, it is possible to conceive various emergency plans for one tunnel according to the detected fire location. Another advantage is the long life time of this system. The fibre optic sensor cable has an expected life expectancy of over 30 years as a passive measuring element. For example, the fibre optic cable within the Virgolo tunnel was still functional after all tests were carried out. Beyond these active protecting systems, there are also structural tunnel elements, such as shotcrete, that can be used to decrease risks caused by fire scenarios (e.g., partial collapse of a structural systems).

2.2   Shotcrete as fire protecting system

The first patent to spray concrete through a jet is known from the year 1898. At that time, a kind of the dry-shotcrete spraying machine has been used. 1908 CARL E. AKELY invented his "Cement Gun" [1]. Most ideas of using shotcrete where developed almost 100 years ago. However, commercial use of shotcrete started about 30 years ago. Today shotecrete is used in two fields of engineering applications. On the one hand shotcrete is used for maintenance and upgrading existing structures and on the other hand it is applied especially for tunnel linings. In February 2005 a real scale test was carried out in the previously mentioned tunnel at the Brenner Motorway/Virgolo tunnel in the context of the European research project UPTUN. Seven different fire resistant shotcrete mixtures from different manufactures, including the original concrete where applied on the tunnel wall (see Fig. 3). The fire load applied was between 10 MW and 30 MW.

Fig. 3. Areas of the shotcrete mixtures, [2]

Each area was instrumented with temperature sensors in different depths. The shotcrete mixtures essentially differ by:

- Various fire-resistant aggregates (e.g. magnesium iron hydro silicate minerals)
- Special fibres
- Special admixtures
- Various Filler
- Other additional additives

Cores where taken from seven areas, made of the previously mentioned mixtures, before and after the real scale test and analyzed with focus on chemical changes and changes of the pore size distribution. After the real scale fire test, laboratory fire test where carried out on special specimens which where instrumented as well with temperature - and electrical resistance sensors in several depths (see Fig. 4).
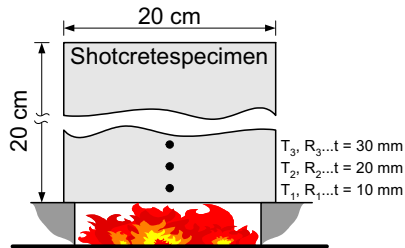
Fig. 4. Instrumented shotcrete specimen under fire load [3]

The temperature time distribution by using 92 thermocouples where investigated during the fire test in different depths. Figure 5 shows a temperature profile during a test by using water shields and a water mist system (with special nozzles). The temperature measured at the surface was about 340°C. The maximum temperature at the depth of 5 mm was about 175°C. A comprehensive documentation of all associated performed experiments is given in [2].
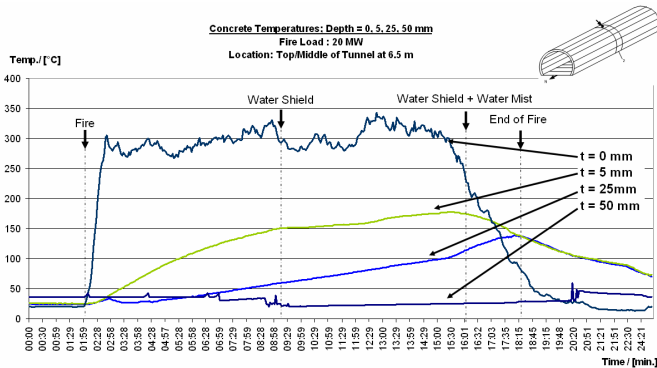
Fig. 5. Concrete temperature distribution in the depths of 0, 5, 25 and 50 mm, [2]

In addition, laboratory tests where carried out for detailed temperature analyses. Relations of the maximum temperatures in the different depths of 10 mm and 30 mm were calculated and are announced as a "Temperature Decreasing Index" (TDI). In Tab. 1 the TDI of concrete samples is presented, as well as the change of the electrical resistance in the depth of 30 mm.

Tab. 1. Temperature parameters of the various shotcrete mixtures

Product Number	TDI / [-]	ΔR / [Ω] t=30 mm	Short description
1	35 %	-1053	Constructive repair mortar – with thermal shield capabilities
2	29 %	-1243	Constructive, fire resistant shotcrete
3	49 %	-552	Thermal shield
4	34 %	-782	Constructive, fire resistant shotcrete
5	33 %	-1421	Constructive, fire resistant shotcrete
6	-	-	Thermal shield
*	72 %	-	Thermal shield

* An additional Thermal shield to product Nr. 1

TDI's between 29% and 72 % where measured. Changes in electrical resistance in a depth of 30 mm where between -552 Ω and -1421 Ω. The electrical resistance is influenced by the water saturation, which depends again form the porosity and the free ions movement. Therefore, the interpretation of the electrical resistance as a governing factor for the fire resistance is quite complicated. A big range of different parameters were carried out in real – and laboratory fire test. All shotcrete mixtures are actually on the market and offered as "fire resistant concrete". According to Tab. 1 it can be realized, that an effective fire resistant constructive shotcrete has a TDI of about 35 %. A comprehensive consideration of the concrete parameters show (a) a strong dependence of the mechanical from the physical parameters, and (b) the change of the electrical resistance is not only caused by change of water saturation. However, water can escape according to the pore size distribution. Changes in pore size causes changes in permeability, which is again dependent on the elasticity and therefore on the concrete tensile and compressive capacity. If the pore size increases, than micro cracks can be expected and therefore a loss of tensile and compressive strength. Therefore, the presence and the melting of PP-fibers helps to increase the permeability, but on the same time the strength and the structural stability of the concrete will be reduced. This means, it has to be defined an equilibrium between the permeability (elasticity) and the structural strength (high concrete tensile capacity and ductile after crack behavior) of the shotcrete mixtures. To avoid the appearance of to many micro cracks no silica aggregates (stones, sand) should be used in the shotcrete. One alternative is the use of "magnesium iron hydro silicate minerals" which has no modification jump and a higher (1700°C) melting point.

3 Integrated Structure Analyse Tool

A major innovation of the Uptun project was also the holistic approach for modelling and analyzing numerically the phenomenon of a fire in a tunnel and its effects on the structure, see Fig. 6. Thanks to the developed tools, the whole scenario of a tunnel fire can now be evaluated, considering thermodynamic modelling, determination of the material behavior and response of the whole structure, inverse analysis and a probabilistic based reliability analysis.
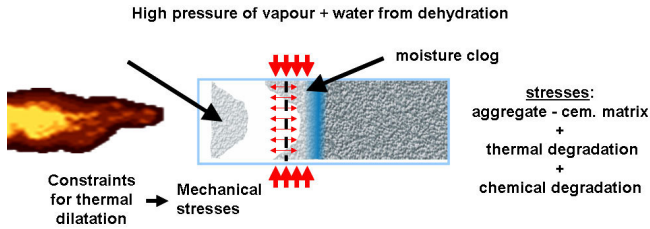
Fig. 6. Causes of thermal spalling phenomenon

In collaboration with the project partners Brennero, IKI, Cervenka Consulting, CISM, ENEA and the University of Padova considerable work on modelling and analyzing the Virgolo tunnel on a numerical basis has been done. Based on the acquired test data, different approaches of modelling have been developed and combined (Hitecosp, Faust, ATENA [3], etc.) on a micro-, meso- and macroscale level [4] [5] in order to optimize the validity of the numerical analysis. A series of numerical calculations and simulations have been performed for the experimentally investigated test specimens and materials. Finally also the verification of the numerical modelling and analyzing part with the collected data from both the real scale and the laboratory test has been a fundamental part for Analysis of Results and Validation of Theoretical Models. The combination of the micro- and mesoscale models/tools has been realised with a special coupling code (FaHiCoVMaC) developed within the Uptun project. The special feature of computing the safety level on a macroscale level is based on the probabilistic modelling and evaluation of materials properties and their influence on the structural response. The microscale analysis has been done in close collaboration with Prof. SCHREFLER [6] and the University of Padova. The mathematical model used for thermo-structural analysis (HITECOSP -HIgh TEmperature COncrete and SPalling,) considers concrete as multiphase porous material, where pores are partly filled with liquid water and partly with gas.

The model consists of four balance equations: mass conservation of dry air, mass conservation of the water species (both in liquid and gaseous state, taking phase changes, i.e. evaporation/condensation, adsorption/desorption and hydration/dehydration process, into account), enthalpy conservation of the whole medium (latent heat of phase changes and heat effects of hydration or dehydration processes are considered) and linear momentum of the multiphase system. They are completed by an appropriate set of constitutive and state equations, as well as some thermodynamic relationships. At the University of Barcelona

(UPC) a CfD Program called FAUST was developed by Prof. CODINA. Together with this group calculations related to the Virgolo tunnel fire experiment were done on a mesoscale level. The computational fluid dynamics formulation consists of a stabilized finite element approximation of the Low Mach number equations based on the subgrid scale concept.

On a macro scale level, a further class of numerical analysis and evaluation was done in collaboration with BRENNERO, IKI, and CERVENKA Consulting [7][8][9], who did a series of calculations based on a probabilistic FE concept (SARA/FREET/ATENA) with an integration of the developed thermal modules. First the real scale and laboratory experiments were simulated in order to precisely determine the thermal properties (i.e. temperature dependent capacitance and conductivity) of the materials. The thermal module of ATENA [7][8] was used in this study together with the probabilistic software package FREET. ATENA software was used for the thermal analysis of the laboratory specimens.

3.1 Thermal properties of shotcrete based on inverse analyses applied to small scale cubes

Heat transfer calculations require the knowledge about the relevant thermal properties of materials and heat transfer coefficients at the medium interfaces during the entire temperature interval. Essential parameters are the heat conductivity (K–value) and heat capacitivity (C–value) of the material. Both of them are varying with increasing temperature. These thermal properties are indicators of a material for the insulating performance against an increasing temperature (e.g., shotcrete). For the ATENA Temperature transfer computations these properties are extracted by stochastic inverse analyses from experimental laboratory and full scale tests provided by BOKU and ICASA. FREET, a statistical software, allowed the probabilistic (sensitivity factor based fitting) of the numerical results to the experimental outcomes and finally the determination of the thermal properties. Figure 7 shows temperature dependent PDF's used for generating a stochastic bundle of conductivity distributions, which are the basis for the fitting and sensitivity studies with respect to the experimental data.
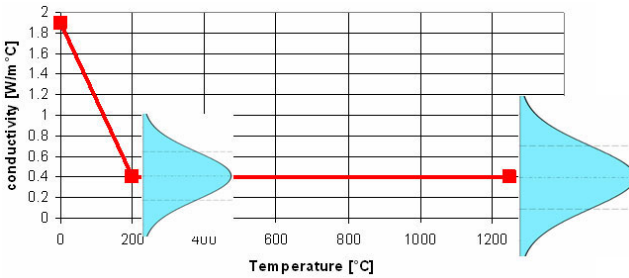
Fig. 7. Temperature dependent PDFs used for fitting the experimental obtained conductivity

Numerical parameter studies were based on laboratory test results obtained from cubes, which are made of shotcrete types, shown in Table 1, and a side length of 20 cm. The cubes were isolated on five sides and heated by gas burners with a fire load of 12 kW on the remaining free side. During the heating process the development of the temperature fields are measured by sensors positioned in different depths of the cube. In addition, the development of the temperature fields associated with the different shotcrete materials provide the basis for the stochastic parameter identification, thermal capacitivity and conductivity, by using the numerical ATENA thermal module. Figure 8 shows the mean distribution of the measured (exact), the inverse numerical obtained (matched), and the numerical approximated conductivity and capacity. The final deviation of the temperature gradients associated with the identified *C* and *K* functions (see Fig. 9) constitutes a maximum of 4.5%. These deviations occur mainly due to the inaccuracies of the temperature gradient at the beginning.
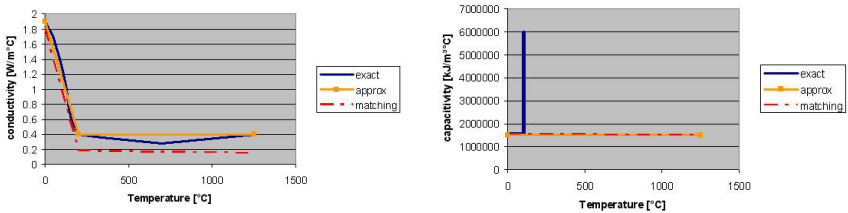
Fig. 8. The mean distribution of the measured (exact), the inverse numerical obtained (matched), and the numerical approximated temperature depended conductivity and capacity of shotcrete product N° 3
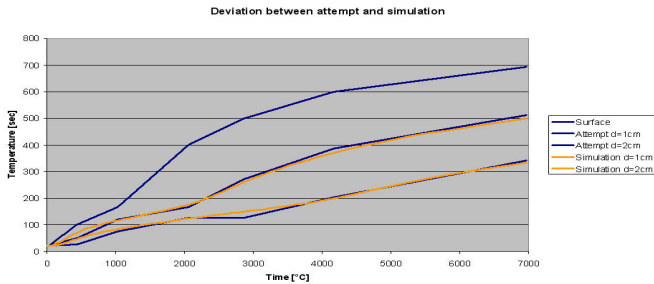
Fig. 9. (Probabilistic fitted – simulated and measured temperature gradients in different depths of the 20cm cubes of material N°3

3.2   Thermal Analysis

The thermal analysis algorithm included in ATENA is divided in two parts (a) thermal analysis, and (b) mechanical analysis. The temperature fields for the mechanical stress/ strain analysis are determined by a separate thermal analysis as follows.

$$C_T \cdot \frac{\partial T}{\partial t} = -div(J_T), \ where \ J_T = -K_T \cdot grad(T) \tag{1}$$

In the above standard diffusion formula, T denotes temperature and t represents time. C_T and K_T is thermal capacitity and conductivity respectively. Both capacitity and conductivity are, as previously mentioned, functions of the current temperature. Modified Crank-Nicholson integration scheme [8] is used to integrate the non-linear set of equations. The resulting iterative correction of unknown temperatures $\Delta\psi$ at time $t+\Delta t$ is calculated by the following formula:

$$\Delta\psi = (\widetilde{K})^{-1} \cdot \widetilde{J} \tag{2}$$

where

$$\widetilde{K} = \left(K \cdot \theta + \frac{1}{\Delta t} \cdot C \right) \tag{3}$$

and

$$\widetilde{J} = \bar{J} - K\left(\theta^{t+\Delta t} \cdot \psi + (1-\theta)^t \cdot \psi \right) - C \cdot \frac{1}{\Delta t} \cdot \left({}^{t-\Delta t}\psi - {}^t\psi \right) \tag{4}$$

C and **K** is the capacitity and conductivity matrix respectively after spatial discretization by finite element method. θ is the integration parameter. For $\theta = 0.5$ the Crank-Nicholson formulation is recovered. $\theta = 0$ corresponds to Euler explicit scheme, and the Euler implicit formulation is obtained when $\theta = 1$. The known oscillatory behaviour of the Crank-Nicholson formulation is addressed by introducing the following iterative damping [8].

$$^{t+\Delta t}\psi = {}^{t+\Delta t(i)}\psi = {}^{t+\Delta t(i-1)}\psi + {}^{t+\Delta t(i)}\eta \cdot \Delta\psi \tag{5}$$

The recommended value of the damping parameter η is in the interval of $\langle 0.3; 1 \rangle$.

3.3 Mechanical Analysis

The material models for concrete as well as reinforcement are formulated in a purely incremental manner, and the selected material parameters are temperature dependent. The temperature dependent evolution laws of these parameters are shown in subsequent figures. They have been derived based on Eurocode 2 and by matching experimental results of CASTILLO & DURANI. [5]. An analogical dependence is used also for the stress-strain law for reinforcement. The stress-strain diagram is scaled based on the maximally reached temperature at each reinforcement element based on the Eurocode 2 formulas.

Six fire resistance shotcrete mixes, mentioned previously, were tested in order to evaluate their effectiveness as fire protection barrier for reducing the damage to structural concrete. The large-scale test was supplemented by the previous presented laboratory experiments of the shotcrete specimens. The experimental program was supported by numerical simulation using the presented material models. The results from laboratory tests were used to calibrate the thermal properties of the shotcrete types. The obtained material laws were then used to simulate the behaviour of a tunnel wall protected by the tested materials. The main goal was to qualitatively evaluate the damage to tunnel lining and compare it to the damage of an unprotected wall.
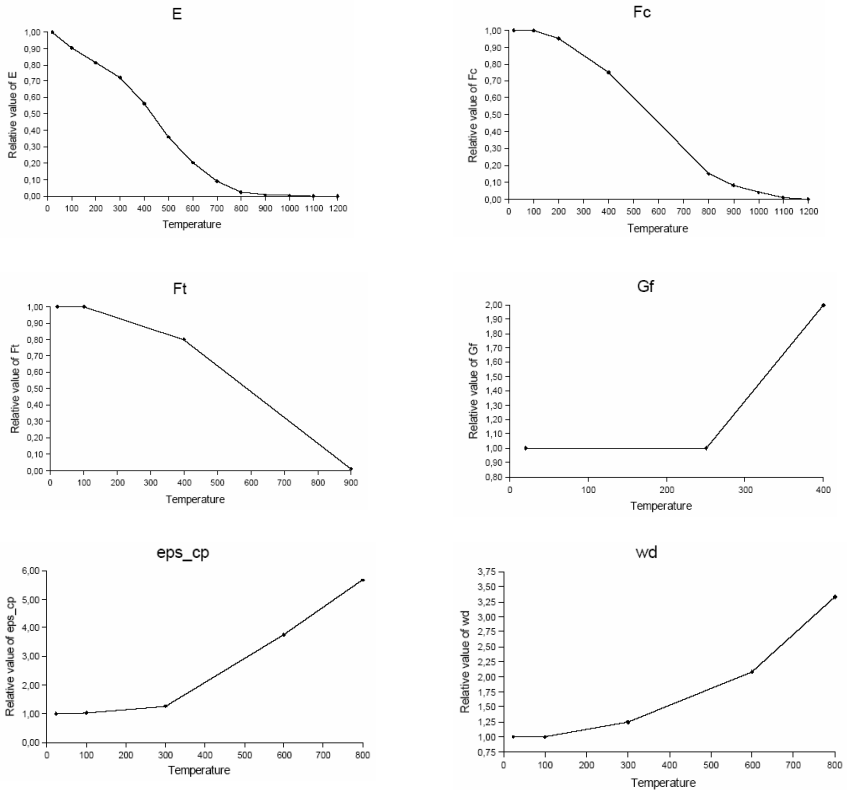
Fig. 10. The mean distribution of the measured (exact), the inverse numerical obtained (matched), and the numerical approximated temperature depended conductivity and capacity of shotcrete product N° 3

In addition, the model shown in Fig. 11 was subjected to modified hydrocarbon fire up to 1300°C. In the interior of the tunnel a 50 mm layer of shotcrete material was applied. The shotcrete layer was modeled by 4 finite elements while for the tunnel lining 7 elements were used through its thickness. The tunnel wall was made of concrete class C25/30 using Eurocode 2 classification.

The thermal analyses and the consecutive mechanical analyses performed on sections of the existing tunnel walls lead to thermal and mechanical property changes in the shotcrete. Figure 11 shows (a) the temperature distribution and (b) the evolution of concrete degradation at various depths for a typical wall section. The degradation is described as relative concrete strength. As it can be seen from this illustration, the tensile strength of the shotcrete N°3 decreased in 5 cm depth at first after 1000 seconds heating and decreases to 20% after 10000 seconds. This effect in 9 cm depth, which is the location of the reinforcement, is delayed of about 5000 seconds. Nevertheless, the temperature development in the region

of the reinforcement is of essential interest. Figure 12a shows the temperature development in different depths of the wall, which indicates the heating isolation effect of the investigated shotcrete with respect to e.g., the first layer of the reinforcement. The considered shotcrete N°3 demonstrated a high isolation effect and protection of the reinforcement. Table 1 presents recommended design criteria, such as (a) the temperature at the interface between the fire protection layer and original concrete wall (< 300°C), and (b) the temperature at the depth of reinforcement location (< 250°C), against the simulated temperature fields. Both of the mentioned criteria could be satisfied for a thickness of 50 mm of shotcrete N°3.
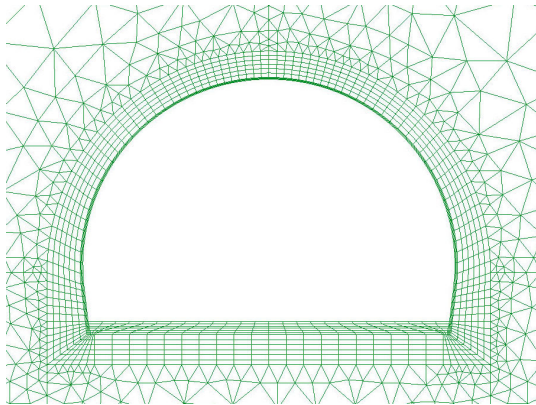
Fig. 11. The Numerical model for Virgolo tunnel analysis
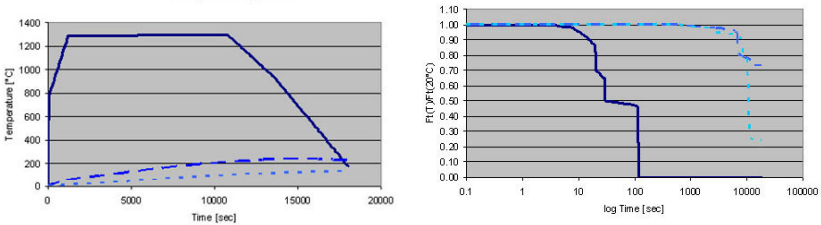
(a) Temperature distribution at different depth, 0cm, 5cm and 9 cm

(b) Relative tensile strength at different depth, 0cm, 5cm and 9 cm

Fig. 12. Temperature distribution and material degradation

Tab. 2. Temperature Limit State

Depth from the Wall Surface	Limit State	Simulated Temperature
50 mm	300°C	214°C
90 mm	250°C	141°C

In addition, a probabilistic optimization of the thickness of the protective layer with respect to the effectiveness in reducing the temperature on the concrete-shotcrete interface as well as on reducing the temperature at the depth of possible reinforcement location was performed by complying a $p_f = 10^{-3}$. These studies leads to a optimized thickness $d = 30$mm for shotcrete N° 3.

4   Conclusion

In conclusion, it is emphasized that fire protecting measures as well as systems, as proposed and tested within the UPTUN project, are powerful tools for increasing the safety of people and rescuers using tunnel systems and for diminishing effects of fire scenarios on tunnel structures. It could be demonstrated by testing and numerical methods that even the adjustment of materials such as shotcrete shells allows the increasing of safety in tunnels. Numerical methods are powerful tools for the optimization of structural elements against fire loading. For instance heating tests on small scale cubes provided the basis for the development of coupled algorithms (thermal and mechanical). In addition, these algorithms served for the improvement of shotcrete layers with respect to the protection of reinforcement against unaccepted heating in existing tunnel walls. The project UPTUN allows the verification of the developed numerical methods by a real fire test in the existing Virgolo tunnel and the development of novel shotcrete techniques. However, much future effort has to be devoted to integrate these tools in an overall life-cycle and safety management of tunnel infrastructure systems.

5   Acknowledgements

6   Literature

[1]   Ruffert, G., (1991): "Spritzbeton", Beton-Verlag GmbH, Düsseldorf

[2]   UPTUN – Report/WP6: Draft: "Test report Virgl/Virgolo Tunnel No. 875-05-2004; Real Scale Tunnel Fire Tests, Rev. 1.2", August 2005

[3]   ATENA 2005. Program Documentation, Cervenka Consulting, Prague, Czech Re-
       public, www.cervenka.cz

[4]   Bažant, Z.P. & Oh, B.H. 1983. Crack band theory for fracture of concrete, Materials
       and Structures, Vol. 16, pp. 155-177

[5]   Castillo, C. & Durani, A.J. 1990. Effect of transient high temperature on high-
       strength concrete, ACI Materials Journal, V. 87 n 1, pp. 47-53

[6]   Gawin, D., Pesavento, F., Schrefler, B.A. 2003. Modelling of hygro-thermal behav-
       iour of concrete at high temperature with thermo-mechanical and mechanical mate-
       rial degradation, CMAME, 192, pp. 1731-1771.

[7]   Cervenka, J., Surovec, J., Kabele, P., 2006, Modelling of reinforced concrete struc-
       tures subjected to fire, Proc. EuroC-2006, ISBN 0415397499, pp. 515-522

[8]   Jendele, L. 2001. Atena Pollutant Transport Module - Theory. Prague: Edited PIT,
       ISBN 80-902722-4-X

[9]   Jendele, L., Cervenka, V., 2006. A General Form of Dirichlet Boundary Conditions
       Used in Finite Element Analysis. Paper 165, Proc. Eighth International Conference
       on Computational Structures Technology, ed. B.H.V. Topping,

Keynote lecture: Optimization of road tunnel safety

Milan Holický & Dimitris Diamantidis
Klokner Institute, Czech Technical University in Prague and
University of Applied Sciences, Regensburg

Abstract: Probabilistic methods of risk optimization are applied to identify the most effective safety measures considered in design of road tunnels. The total consequences of alternative tunnel arrangements are assessed using Bayesian networks supplemented by decision and utility nodes. It is shown that the probabilistic optimization based on the comparison of societal and economic consequences may provide valuable information enabling a rational decision concerning effective safety measures. Thereby risk acceptability criteria are critically reviewed. A general procedure is illustrated by the optimization of a number of escape routes. It appears that the discount rate and specified life time of a tunnel affect the total consequences and the optimum arrangements of the tunnel more significantly than the number of escape routes. The optimum number of escape routes is also significantly dependent on the ratio of the cost of one escape route and acceptable expenses for averting a fatality based on the Life quality index. Further investigation of relevant input data including societal and economic consequences of various hazard scenarios as well as experience related to the effectiveness of safety systems are needed.

1 Introduction

Tunnel structures usually represent complex technical systems that may be exposed to hazard situations leading to unfavourable events with serious consequences. Moreover, the risk during a tunnel operation has increased in recent years. This has been manifested in significant accidents occurred in the last decade, such as the Kings Cross fire in London, the fire in the Mont-Blanc tunnel in France and the accident in the Tauern tunnel in Austria. The combination of mixed traffic and extreme length (5 to 20 kilometres in case of road tunnels) has a significant impact on the inherent safety of a tunnel system. Consequently, safety becomes an important criterion with respect to the selection of design parameters of a long tunnel such as tunnel configuration, tunnel cross section area, prevention measures and emergency systems.

Minimum safety requirements for tunnels in the trans-European road network are provided in the Directive of the European Parliament and of the Council 2004/54/ES [6]. The Directive also gives general recommendations concerning risk management, risk assessment and analysis.

Methods of risk assessment and analysis are more and more frequently applied in various technical systems (MELCHERS [17], STEWART & MELCHERS [23] including road tunnels (HOLICKÝ & ŠAJTAR [4]). This is a consequence of recent tragic events in various tunnels and of an increasing effort to take into account societal, economic and ecological consequences of unfavourable events. Available national and international documents (NS [18], CAN/CSA [3], ISO [8], ISO [9], ISO [10] and ISO [11] try to harmonize general methodical principles and terminology that can be also applied in the risk assessment of road tunnels.

The submitted contribution, based on previous studies (VROUWENVELDER et al. [24], WORM [26], BRUSSARD et al. [1], VROUWEVELDER & KROM [25], KRUISKAMP et al. [14], RUFFIN et al. [22] and KNOFLACHER & PFAFFENBICHLER [13]) and recent PIARC working documents, attempts to apply methods of probabilistic risk optimization using Bayesian networks supplemented by decision and utility nodes (JENSEN [12]). It appears that Bayesian networks provide an extremely effective tool for investigating the safety of road tunnels.

2 Risk analysis

Probabilistic methods of risk analysis are based on the concept of conditional probabilities $P_{fi} = P\{F|H_i\}$ of the event F providing a situation H_i occurs. In general this probability can be found using statistical data, experience or a theoretical analysis of the situation H_i.

If the situation H_i occurs with the probability $P(H_i)$ and the event F during the situation H_i occurs with the conditional probability $P(F|H_i)$, then the total probability P_F of the event F is given as

$$P_F = \sum_i P(F \mid H_i) P(H_i) \tag{1}$$

Equation (1) makes it possible to harmonize partial probabilities $P(F|H_i)$ $P(H_i)$ related to the situation H_i.

The main disadvantage of the purely probabilistic approach is the fact that possible consequences of the events F related to the situation H_i are not considered. Equation (1) can be, however, modified to take the consequences into account.

A given situation H_i may lead to a set of events E_{ij} (for example fully developed fire, explosion), which may have societal consequences R_{ij} or economic consequences C_{ij}. It is assumed that the consequences R_{ij} and C_{ij} are unambiguously assigned to events E_{ij}. If the consequences include only societal components R_{ij}, then the total expected risk R is

$$R = \sum_{ij} R_{ij} \mathrm{P}(E_{ij} \mid H_i) \mathrm{P}(H_i) \qquad (2)$$

If the consequences include only economic consequences C_{ij}, then the total expected consequences C are given as

$$C = \sum_{ij} C_{ij} \mathrm{P}(E_{ij} \mid H_i) \mathrm{P}(H_i) \qquad (3)$$

The computed risk is compared to the acceptable risk. When the acceptability criteria are not satisfied, then it may be possible to apply a procedure of risk treatment. Additional safety measures (prevention and mitigation measures), for example escape routes, technological equipments and traffic restrictions may be considered. Such measures might, however, require substantial costs that should be taken into account when deciding about the optimum tunnel arrangements.

3 Risk appraisal

In most practical studies the aforementioned societal risk of a project is given in the form of a numerical F-N-curve. An F-N-curve (N represents the number of fatalities, F the frequency of accidents with more than N fatalities) shows the relationship between the annual frequency F of accidents with N or more fatalities. It expresses both the probability and the consequence associated with given activities. Usually risk curves are shown in a log-log plot with the annual frequency on the vertical axis and the number of fatalities on the horizontal axis. Upper and lower bound curves are recommended based on gained experience with similar projects/activities and the ALARP (As Low As Reasonably Practical) acceptability criterion is obtained as the domain between the aforementioned limits [16, 5]. The upper limit represents the risk that can be tolerated in any circumstances while below the lower limit the risk is of no practical interest. Such acceptability curves have been developed by DIAMATIDIS et al. [5] for various industrial fields including the chemical and the transportation industry.

The ALARP recommendations can be represented in a so-called risk-matrix. For that purpose qualitative hazard probability levels have been defined together with hazard severity levels of accidental consequences. The hazard probability levels and the hazard severity levels can be combined to generate a risk classification matrix.

A number of areas of concern have been pointed out regarding the validity of the ALARP criteria including public participation, political reality, morality and economics [16]. The problem of identifying an acceptable level of risk is in most practical cases formulated as an economic decision problem. The optimal level of safety corresponds to the point of minimal cost. The optimisation problem can be solved using the Life Quality Index (LQI) approach. The strategy is based on a social indicator that describes the quality of life as a function of the gross domestic product, life expectation, and the life working time. The LQI [4, 20, 21] is a compound societal indicator, which is defined as a monotonously increasing function of two societal indicators: the gross domestic product per person per year, g, and the life expectancy at birth, e.

$$L = g^w \, e^{\,(1-w)} \tag{4a}$$

The exponent w is the proportion of life spent in economic activity. In developed countries it is assumed that $w \approx 1/8$. Using this Life Quality Index Criterion, the optimum acceptable Implied Cost of Averting a Fatality (ICAF) can then be deduced:

$$ICAF = \frac{ge}{4}\frac{1-w}{w} \tag{4b}$$

It is noted that the value expressed by equation (3) is not the value of one life since the human life is beyond price. ICAF is also not the amount of a possible monetary compensation for the relatives of the victims of the occurrence. ICAF is just the monetary value, which society should be willing to invest for saving one life according to its ethical principles. The ICAF value brings up also several new problems that should be considered. For example the gross domestic product per capita parameter implies that all kinds of production and domestic services are included. Also the exponent w, which represents the ratio of an average work to leisure time available to members of the society, has been discussed in the literature [19, 20, 21]. The ICAF values are of the order of 3 Million US$ for developed countries and below 500 000 US$ for underdeveloped countries. The values are not far away from the amount insurance companies' pay for human losses. The LQI principle offers a possible tool for justifying investments in major projects such as road tunnels. The values related to human lives may thereby tentatively be used in cost benefit analyses on behalf of the involuntary risk of the public. Further aspects and developments related to the LQI principle and to the evaluation of human life losses can be found in [21].

4 Principles of risk optimization

The total consequences $C_{tot}(k,p,n)$ relevant to the construction and performance of a tunnel are generally expressed as a function of the decisive parameter k (for example of the number k of escape routes), discount rate p (commonly about $p \approx 0.03$) and life time n (commonly $n = 100$ let). The decisive parameter k usually represents a one-dimensional or multidimensional quantity significantly affecting tunnel safety.

The fundamental model of the total consequences may be written as a sum of partial consequences as

$$C_{tot}(k,p,n) = R(k,p,n) + C_0 + \Delta C(k) \tag{5}$$

In equation (5) $R(k,p,n)$ denotes the expected societal risk that is dependent on the parameter k, discount rate p and life time n. C_0 denotes the basic of construction cost independent of k, and $\Delta C(k)$ additional expenses dependent on k. Equation (5) represents, however, only a simplified model that does not reflect all possible expenses including economic consequences of different unfavourable events and maintenance costs.

The societal risk $R(k,p,n)$ may be estimated using the following formulae

$$R(k,p,n) = N(k)\, R_1\, Q(p,n), \quad Q(p,n) = \frac{1 - 1/(1+p)^n}{1 - 1/(1+p)} \tag{6}$$

In equation (6) $N(k)$ denotes the number of expected fatalities per one year (dependent on k), R_1 denotes acceptable expenses for averting a fatality ICAF as explained above (or societal compensation cost (RACKWITZ [20, 21]), and p the discount rate (commonly within the interval from 0 to 5 %). The quotient q of the geometric row is given by the fraction $q = 1/(1+p)$. The discount coefficient $Q(p,n)$ makes it possible to express the actual expenses R_1 during a considered life time n in current cost considered in (5). In other words, expenses R_1 in a year i correspond to the current cost $R_1 q^i$. The sum of expenses during n years is given by the coefficient $Q(p,n)$.

A necessary condition for the minimum of the total consequences (5) is given by the vanishing of the first derivative with respect to k written as

$$\frac{\partial N(k)}{\partial k} R_1 Q(p,n) = -\frac{\partial \Delta C(k)}{\partial k} \tag{7}$$

In some cases this condition may not lead to a practical solution, in particular when the discount rate p is small (a corresponding discount coefficient $Q(p,n)$ is large) and when the number of escape routes k can not be arbitrarily increased.

5 Standardized consequences

The total consequences given by equation (5) may be in some cases simplified to a dimensionless standardized form and the whole procedure of optimization may be generalized. Consider as an example the optimization of the number k of escape routes. It is assumed that involved additional costs $\Delta C(k)$ due to the number of escape routes k may be expressed as the product $k C_1$, where C_1 denotes the cost of one escape route, then equation (5) becomes

$$C_{\text{tot}}(k,p,n) = N(k) R_1 Q(p,n) + C_0 + k C_1 \tag{8}$$

This function can be standardized as follows

$$\kappa(k,p,n) = \frac{C_{tot}(k,p,n) - C_0}{R_1} = N(k)Q(p,n) + k\frac{C_1}{R_1} \tag{9}$$

Here $\zeta = C_1/R_1$ denotes the cost ratio. An advantage of standardized consequences is the fact that they are independent of C_0 and the cost ratio $\zeta = C_1/R_1$.

Both variables $C_{\text{tot}}(k,p,n)$ and $\kappa(k,p,n)$ are mutually dependent and have the extremes (if exist) for the same number of escape routes k. A necessary condition for the extremes follows from equation (7) as

$$\frac{\partial N(k)}{\partial k} = -\frac{C_1}{Q(p,n)R_1} = -\frac{1 - 1/(1+p)}{1 - 1/(1+p)^n} \frac{C_1}{R_1} \tag{10}$$

A first approximation may be obtained assuming that C_1 is in the order of R_1 (assumed also in a recent study by VROUWENVELDER & KROM [25]), where $C_1 \approx R_1 \approx 3$ MEUR), and then the cost ratio $\zeta = C_1/R_1 \approx 1$.

6   Model of a tunnel

The main model of a road tunnel is indicated in Fig. 1. The tunnel considered here is partly adopted from a recent study by VROUWENVELDER & KROM [25]. It is assumed that the tunnel has a length of 4 000 m and two traffic lanes in one direction. The traffic consists of heavy goods vehicles HGV, dangerous goods vehicles DGV and Cars. The main model includes three sub-models for heavy goods vehicles HGV, dangerous goods vehicles DGV and Cars. Fig. 2 shows a sub-model for dangerous goods vehicles DGV.
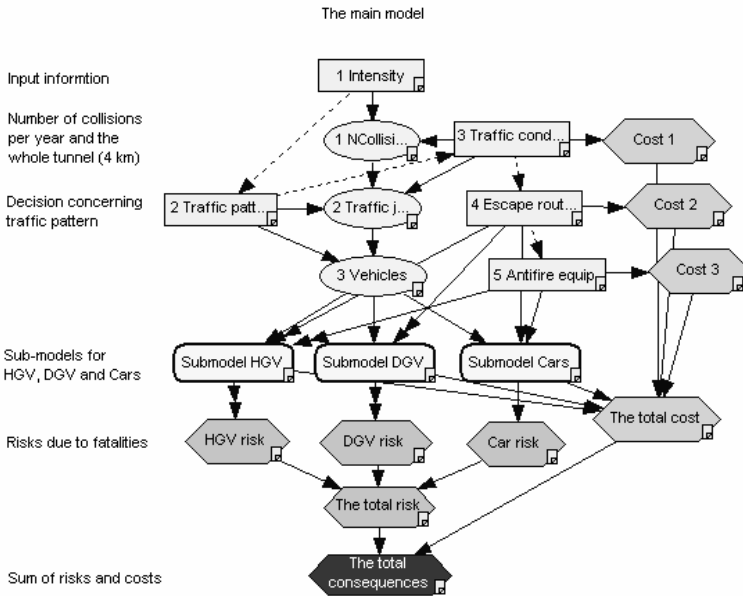
Fig. 1: Main model of a tunnel

The total traffic intensity in one direction is 20×10^6 vehicles per year (27 400 vehicles in one lane per day). The number of individual types of vehicles is assumed to be HGV:DGV:Cars = 0.15:0.01:0.84.

The frequency of serious accidents assuming basic traffic conditions (that might be modified) is considered as 1×10^{-7} per one vehicle and one km (VROUWENVELDER & KROM [25]), thus 8 accidents in the whole tunnel per year. The Bayesian networks used here need a number of other input data. Some of them are adopted from the study by VROUWENVELDER & KROM [25] (based on the event tree method), the other are estimated or specified using an expert judgment. Note that different types of hazard scenarios are distinguished as they may cause different consequences. Similar sub-models are used also for heavy goods vehicles HGV and Cars.
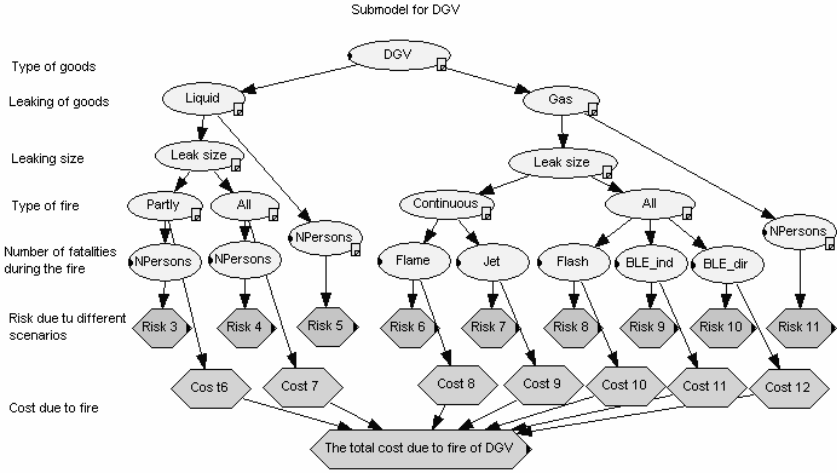
Fig. 2: Sub-model for dangerous goods vehicles DGV

7   Risk optimization

Risk optimization of the above described tunnel is indicated in Fig. 3, 4 and 5 showing the variation of standardized total consequences $\kappa(k,p,n)$, given by equation (9), with the number of escape routes k for selected discount rates p (up to 5 %) and a life time n (= 50 and 100 years) assuming the cost ratio $\zeta = C_1/R_1 \approx 1$.
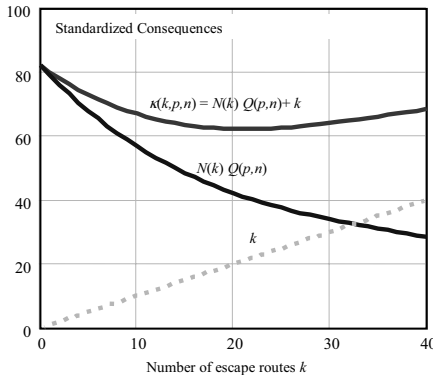
Fig. 3: Variation of the components of standardized total consequences $\kappa(k,p,n)$ with k for a discount rate $p = 0.03$, a cost ratio $\zeta = C_1/R_1 = 1$ and a life time $n = 100$ years

Standardized consequences
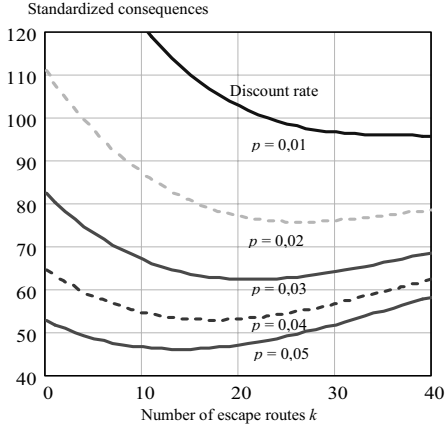
Fig. 4: Variation of standardized total consequences $\kappa(k,p,n)$ with k for the cost ratio $\zeta = C_1/R_1 = 1$, selected discount rates p and a life time $n = 50$ years.

Standardized consequences
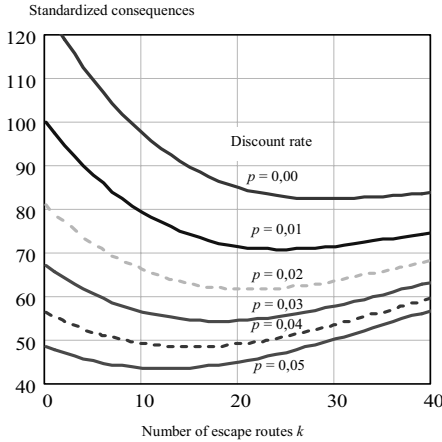
Fig. 5: Variation of standardized total consequences $\kappa(k,p,n)$ with k for selected discount rates p, the cost ratio $\zeta = C_1/R_1 = 1$ and a life time $n = 100$ years

Figure 3 shows the variation of the components of standardized total consequences $\kappa(k,p,n)$ with the number of escape routes k for a common value of the discount rate $p = 0.03$ and an assumed life time $n = 100$ years. Fig. 4 shows the variation of standardized total consequences $\kappa(k,p,n)$ with k for selected discount rates p and a life time $n = 50$ years only. Fig. 5 shows similar curves as Fig. 4, but for an expected life time $n = 100$ years (common value).

8 Effect of cost ratio

The cost ratio $\zeta = C_1/R_1$ may also affect the optimum number of escape routes. Note that the approximations $\zeta = C_1/R_1 \approx 1$ assumed above have recently been accepted in the study by VROUWENVELDER & KROM [25] (where the cost $C_1 \approx R_1 \approx 3$ MEUR is mentioned). Figures 6 and 7 show the variation of total standardized consequences with the number of escape routes k and cost ratios ζ (considered within the interval from 0.5 to 2), a discount rate $p = 0.03$ and a life time $n = 100$ years.

Standardized consequences
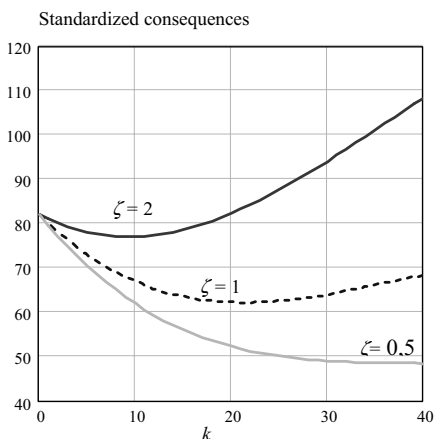
Fig. 6: Variation of standardized total consequences $\kappa(k,p,n)$ with the number of escape routes k for selected cost ratios ζ, a discount rate $p = 0.03$, a life time $n = 100$ years

Fig. 6 and 7 clearly indicate that the optimum number of escape routes k is significantly dependent on the cost ratio $\zeta = C_1/R_1$. In general the optimum number of escape routes k increases with decreasing cost ratio ζ, i.e. with increasing expenses R_1 (an expected result). An interactive effect of both quantities k and $\zeta = C_1/R_1$ on the total consequences is obvious from Fig. 7.

For example, for $\zeta = 2$ the optimum k is about 9, for $\zeta = 1$ the optimum k is about 20 and for $\zeta = 0.5$ the optimum k is more than 40. The last case seems to be an unrealistic solution as it would lead to a distance of escape routes less than 100 m. It is noted further here that the safety measures of a tunnel such as the discussed escape routes are also reviewed based on current design and safety provisions of road tunnels (such as [6], [20], or [2]), in order to come up with an overall safety package which fulfils the acceptability criteria ([4]).
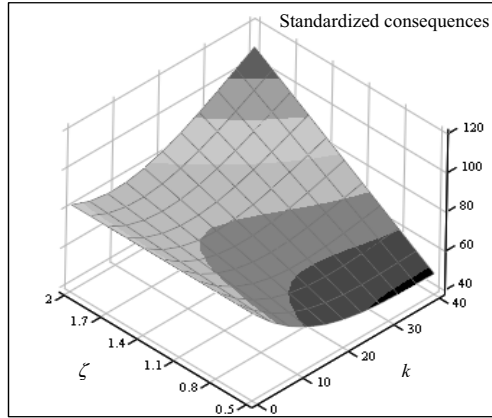
Fig. 7: Variation of total consequences $\kappa(k,p,n)$ with the number of escape routes k and cost ratios ζ, a discount rate $p = 0.03$, a life time $n = 100$ years

9 Conclusions

The following conclusions may be drawn from the submitted study of probabilistic risk optimization of road tunnels using Bayesian networks:

The risk of road tunnels must meet modern risk acceptability criteria and safety measures must be compatible to current provisions.

Probabilistic risk optimisation may provide background information valuable for a rational decision concerning effective safety measures applied to road tunnels.

It is shown that the optimum number of escape routes may be specified from the requirement for the minimum of total consequences covering the societal and economic aspects.

The optimum number of escape routes depends generally on the discount rate, required life time and the ratio between the cost for one escape route and acceptable expenses that a society is able to afford for averting one fatality (societal compensation cost).

It appears that the total consequences are primarily affected by the discount rate and less significantly by the assumed life time, cost ratio and the number of escape routes.

Bayesian networks supplemented by decision and utility nodes seem to provide an effective tool for risk analysis and optimization.

Further investigations of relevant input data concerning conditional probabilities describing individual hazard scenarios and models for their societal and economic consequences are needed.

There are three specific aspects that are of uttermost importance for an advanced risk assessment and optimization of road tunnels: the specification of discount rate and required design life time, and the costs of alternative safety measures foreseen in the design stage and the expenses for averting a fatality (called also societal compensation costs) that can be accepted by a society. Wrong or inadequate data may obviously lead to incorrect decisions. It should be mentioned that specification of the expenses for averting a fatality is a delicate philosophical and socio-economic task. It appears, however, that the concept of Life Quality Index (LQI) provides a tool for decision making.

10   References

[1]   Brussaard, L.A.; Kruiskamp, M.M.; Oude Essink, M.P.: The Dutch model for the quantitative risk analysis of road tunnels. In: *Proc. of the ESREL conference*, Berlin, 2004.

[2]   *Bundesamt für Strassen,* ASTRA Task Force, Schlussbericht, Bern, Switzerland, 2000.

[3]   CAN/CSA-Q634-91, Risk analysis requirements and guidelines, Ottawa, 1991.

[4]   Diamantidis, D.: Risk Analysis versus Risk Acceptability in Major European Tunnel Projects. In: *Proceedings* of *1st Asia Pacific Conference on Risk Management and Safety*, Hong Kong, 2005.

[5]   Diamantidis, D.; Zuccarelli, F.; Westhäuser, A.: Safety of long railway tunnels. In: *Reliability Engineering and System Safety 67*, 2000, pp. 135-145.

[6]   Directive 2004/54/EC of the European Parliament and of the Council of 29 April 2004 on minimum safety requirements for tunnels in the trans-European road network. Official Journal of the European Union L 201/56 of 7 June, 2004.

[7]   Holický, M.; Šajtar, L.: Risk Assessment of road tunnels based on Bayesian network. In: *Proc. of the Advances in Safety and Reliability, ESREL 2005*, London: Taylor & Francis Group, 2005, pp. 873-879.

[8]   ISO/IEC Guide 51, Safety aspects – Guidelines for their inclusion in standards, ISO/IEC, 1999.

[9]   ISO/IEC Guide 73, Risk management – Vocabulary - Guidelines for use in standards, 2002.

[10]   ISO 2394, General principles on reliability for structures, ISO, 1998.

[11]   ISO 9000, Quality management systems – Fundamentals and vocabulary, ISO, 2000.

[12] Jensen, F.V.: *Introduction to Bayesian networks*, Aalborg University, Denmark, 1996.

[13] Knoflacher H.; Pfaffenbichler, P.C.: A comparative risk analysis for selected Austrian tunnels. In: *Proc. of the 2nd International Conference Tunnel Safety and Ventilation*. Graz, 2004.

[14] Kruiskamp, M.M.; Weger D. de ; Hoeksma, J.: TUNprim - A Spreadsheet model for the calculating road tunnels risk. In: *Tunnels Management International*, Volume 5, Number 1, 2002, pp. 6 – 12.

[15] Martens, M.H.; Kaptein N.A. Guidelines and Standards for tunnels on Motorways, SAFESTAR deliverable 2.2, VTT, Finland, 2004.

[16] Melchers, R.E.: On the ALARP approach to risk management. In: *Reliability Engineering and System Safety*, n.71, 2000, pp. 201-208.

[17] Melchers, R.E.: *Structural reliability analysis and prediction*, Chichester: John Wiley&Sons, 1999.

[18] NS 5814, Requirements for risk analysis, 1991.

[19] Pandley, M.D.; Nathwani, J.S.: Life quality index for the estimation of societal willingness-to-pay for safety. In: *Structural Safety*, n. 26, 2004, pp. 181-199.

[20] Rackwitz, R.: Optimization and risk acceptability criteria based on the life quality index. In: *Structural Safety,* n. 24, 2002, pp. 297-331.

[21] Rackwitz, R.: The Philosophy behind the Life quality Index and Empirical Verification. Working material of JCSS, 2005.

[22] Ruffin, E.; Cassini, P.; Knoflacher, H.: Transport of hazardous goods. *The Handbook of Tunnel Fire Safety.* London: Thomas Telford Ltd, 2005, pp. 354-387.

[23] Stewart, M.S.; Melchers, R.E.: *Probabilistic risk assessment of engineering system.* London: Chapman & Hall, 1997.

[24] Vrouwenvelder, A.C.W.M.; Holický, M.; Tanner, C.P.; Lovegrove, D.R.; Canisius, E.G.: *Risk assessment and risk communication in civil engineering*, CIB Publication 259, 2001.

[25] Vrouwenvelder, A.C.W.M.; Krom, A.H.M.: Hazard and the Consequences for Tunnels Structures and Human Life. In: *Proc. of the 1st International Symposium Safe and Reliable Tunnels in Prague*. The Netherlands: CUR, Gouda, 2004, pp. 23-32.

[26] Worm, E.W.: Safety concept of Westershelde tunnel, manuscript provided by SATRA, Prague, 2002.

Analysis of Tunnel accidents by using Bayesian Networks

Jochen Köhler, Matthias Schubert & Michael Habro Faber
Institute of Structural Engineering IBK, ETH Zurich
ETH Hönggerberg, CH-8093 Zürich, Switzerland

Abstract: Accidents in tunnels and other underground structures often lead to serious consequences, more serious in general than would have been the case in open air. Tunnels often have to pass through mountainous regions with a lack of redundant detour routes. Additionally to the serious direct consequences in the tunnel, large societal consequences are associated with the closure of such life lines. For this reason careful consideration of risk and safety in tunnels is necessary.

Accidents are normally caused by a combination of several factors. In the case of accident in tunnels these factors could be related to characteristics of the, (e.g. the length of the tunnel, the illumination, the portal height, the curviness, the longitudinal gradient), they could be related to the characteristics of the traffic (e.g. the AADT, the HGV, the average speed) or these factors could be related to characteristics of the drivers and their vehicles involved.

In the presentation a Bayesian Network is developed based on a database containing accident rates, tunnel characteristics and traffic characteristics from 126 Swiss road tunnels is utilized in this study. The accident rates and the traffic characteristics are measured over 5 years. The causal relationships leading to accidents in tunnels are assessed directly based on this data by using the so called EM learning algorithm and the conditional probabilities of the network are calibrated. It is demonstrated how new information, in form of data or in form of expert opinion can be utilized to update the conditional probability tables in the network. The predictive ability of the network is compared with the predictions of a conventional regression model (with parameters fitted to the same database). The paper closed with some outlook to further application of this tool in tunnel risk assessment and management.

Probabilistic Safety Concept for Fire Safety Engineering based on Natural Fires

Astrid Weilert & Dietmar Hosser

Institute of Building Materials, Concrete Construction and Fire Protection,
Technical University of Braunschweig, Germany

Abstract: The existing German regulations for the design of fire protection measures for structures are based on the "prescriptive rules" of the State Building Codes. The safety requirements evolved on the basis of long-term experience. For this reason, no uniform safety level exists which would allow the comparison of protection measures prescribed for different types of buildings and occupancies with those derived from performance based fire safety engineering. Therefore it is necessary to establish uniform safety requirements based on definite objectives and to define the required system-reliability of fire protection measures for different types of buildings. Furthermore, statistical data describing the reliability of each fire protection measure and its effect on overall system reliability have to be collected. Using such kinds of probabilistic information, it is possible to analyse the existing fire protection concepts, to determine the resulting reliability and to compare it with the required system reliability as defined before. The probabilistic safety concept is planned to be included in the National Appendix for Eurocode 1 part 1-2 [1] as well as into the German „Guideline for Fire Safety Engineering Methods" [2].

1 Basic principles of the safety concept

Building design has to take into account not only permanent or variable loads, but also accidental events, such as fire. The most important factor for fire safety in the design of the construction is the time-dependent temperature-load on the structural members. „Prescriptive codes" have been predominant in fire safety design in most European countries for a long time. Standards for the fire resistance of structural members were defined on the basis of the ISO standard temperature-time curve. Due to the increasing demand for objective-oriented fire safety concepts, the construction is more and more often designed using natural design fire scenarios and advanced calculation methods, that is

using fire safety engineering methods. Through the definition of the objectives it has to be ensured that the required safety level is not undermined. The Eurocodes were developed to enable the engineer, using the calculation methods on basis of a balanced safety concept, to perform the structural design for design fire scenarios.

In the creation of a safety concept, the aim is to allow for:

- different types of construction
- different occupations
- different design fire load densities based on natural fires
- different calculation methods

The concept will include steel, concrete, composite and wood construction.

The first step was to analyse existing safety concepts, especially the „Natural Fire Safety Concept" [3] which is part of Eurocode 1 part 1-2 annex E [1]. The next step involved an intensive literature research, in order to get the data basis for the safety concept. Of special interest are data concerning

- Ignition frequency
- Fire load
- Probability of fire spread
- reliability of fire protection installations
- reliability of the separating function or integrity of compartment separating elements
- reliability and time related effects on fire by the fire brigade
- reliability and time related effects on fire by sprinklers or other installations for fire extinguishing

Since statistics on fires are not available for all of Germany, and are only rarely collected (but not published) for individual states, data from international sources have to be used. Of special importance are publications containing data with fire loads, ignition frequencies, etc. for different occupancies that can be used for fire safety engineering methods. The data are used to derive area dependant pyrolysis rates or heat release rates. There exist only sparse data on the stochastic variations of the input variables and further model uncertainties. It is the same case for the effectiveness and reliability of installations and fire fighting measures in case of demand.
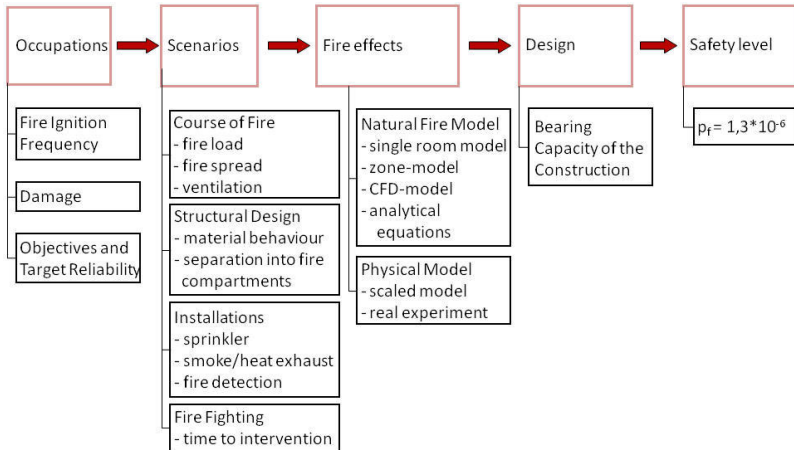
Figure 1: Approach for the design of the safety concept

The approach for the creation of the safety concept is presented in Figure 1 and is explained in more detailed below.

In those parts of the Eurocodes without temperature actions for „accidental actions" partial safety factors on the side of the material resistances are defined as $\gamma_M = 1,0$.

In adjusting the parts 1-2 to this design concept of the other material-related Eurocodes it seems reasonable also in case of fire to use a partial safety factor of 1,0 for material resistance.

The safety concept now part of Eurocode 1 part 1-2 appendix E [1] is based on the between 1994 and 1998 developed „Natural Fire Safety Concept" (NFSC [3]). The safety factors can principally be applied as in NFSC on the fire load density, on the amplitude of the rate of heat release, on the duration of the heat release, and thereby on the plateau of the rate of heat release, as well as the amplitude of the room temperature. For massive building elements, the integral under the curve of heat release, i. e. the sum of the energy induced into the building element, is the most important factor. For building elements with high thermal conductivity the maximum of the room temperature is most important, whereas e. g. for wooden building elements the point of inflammation and the total duration of the fire are the dominant factors. It is to be expected that for different construction types the safety factors have to be applied on different parameters. However, the design format is going to be the same for all types of constructions.

It follows that a large number of calculations are necessary in order to calibrate the safety level for the different constructions. Fortunately the Eurocodes allow a certain tolerance.

2 Required data

2.1 Determination of the target reliability

As safety level for structural elements in EN 1990 [4] in the informative appendix B the following minimum values for β is prescribed

Table 1: Definition of consequences classes EN 1990 [4] annex B

Consequences Class	Description	Examples of buildings and civil engineering works
CC3	**High** consequence for loss of human life, or economic, social or environmental consequences **very great**	Grandstands, public buildings where consequences of failure are high (e. g. a concert hall)
CC2	**Medium** consequences for loss of human life, economic, social or environmental consequences **considerable**	Residential and office buildings, public buildings where consequences of failure are medium (e. g. an office building)
CC1	**Low** consequence for loss of human life, an economic, social or environmental consequences small or **negligible**	Agricultural buildings where people do not normally enter (e. g. storage buildings), greenhouses

Table 2: Recommended minimum values for reliability index β (ultimate limit states) according to the classes for resulting damage

Reliability Class	Minimum values for β	
	1 year reference period	50 years reference period
RC 3	5,2	4,3
RC 2	4,7	3,8
RC 1	4,2	3,3

2.2 Ignition frequency

Table 3: Number of fires from 1996 until 1999 and areas of different building categories according to Statistics Finland [5]

Name	Occupancy	Fires	Total area [m2]
A	Residential buildings	4361	231 565 978
C	Commercial buildings	356	18 990 450
D	Office buildings	140	16 354 516
E+L	Transport and fire fighting and rescue service buildings	123	10 627 751
F	Buildings for institutional care	197	8 780 942
G	Assembly buildings	112	7 379 199
H	Educational buildings	122	15 801 759
J	Industrial buildings	1038	40 321 357
K	Warehouses	405	7 434 710
N	Other buildings	2650	2 437 960
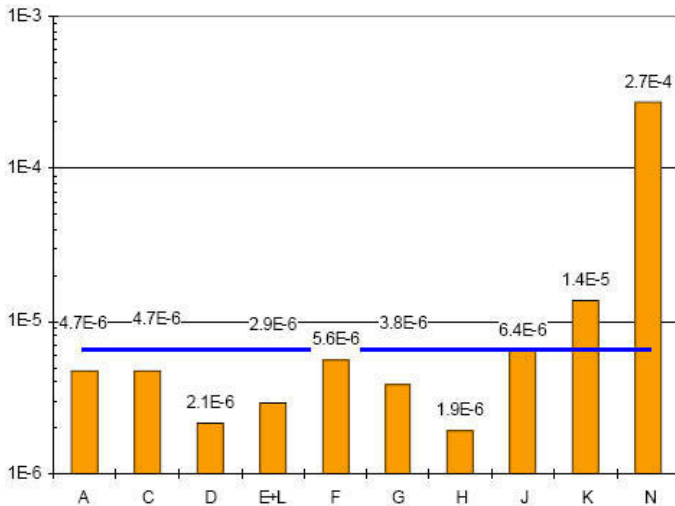
Figure 2: Average ignition frequency in $[/(m^2 \times a)]$ of different building categories from 1996-99. The horizontal line represents the average value of all categories, for the definition of categories (see table 2) [6]

The target reliability of a structural member or structure is derived from both loads and resistances. The division of the total reliability between loads and resistances is only possible if these factors are independent. For the calculation of the total reliability, the external loads are the basic variables. In cases of fire, the room temperature also has to be considered.

For the calculation of room temperature caused by a natural fire, the usual procedure is the derivation of a heat release rate based on the fire load in the compartment, the ventilation conditions, possible installations for fire detection and/or extinguishment and fire fighting measures.

This curve of time-dependant heat release taking failure probabilities or the reliability of the impacting basic variables is called „design rate of heat release". The derivation of an adequate fire scenario and a heat release rate or alternatively of a temperature-time curve determines the design safety level.

A design fire is the description of the development of a fire taking time and space into account. The design fire includes the influence of the building or room geometry, of installations, such as fire detection systems, smoke and heat exhausts, sprinkler systems, etc. and fire fighting measures. It can factor in the delay before arrival of the fire brigade at the site, and whether or not the fire has spread so much in this time that it can no longer be fought within the compartment. The design fire also takes into account the velocity of fire spread, the exchange of the fire with the surrounding building elements and the time of

activation of fire protection installations by smoke or heat or the destruction of objects such as windows by heat and thereby the change of ventilation conditions. A fire scenario together with the derived rate of heat release is the idealization of a natural fire, that can take place in the building in question.

The total failure probability per unit area and year is derived from the probability of fire activation per unit area and year and the failure probability of the construction. Fortunately a fire is a relatively uncommon phenomenon in a single building. The mean frequency of fires within a year and the calculation of the total area of all buildings enables the derivation fire ignition density for certain occupancies. Industrial buildings typically have one of the highest fire ignition densities, followed by dwellings. However, due to the size greater of the rooms/halls or compartments in industrial buildings fully developed fires occur with far lower frequency than in dwellings.

2.3   Characteristic values for materials

The failure probability of the construction can be calculated based on the material properties with their stochastic deviation. This includes the mechanical properties such as compressive strength and yield limit, as well as the thermal properties such as thermal conductivity, heat capacity and temperature-dependant density, and geometric properties e. g. the burning rate for wood constructions. For this project it was necessary to document numerous material properties from the literature for use in the safety analyses.

2.4   Fire loads

The number of data sources for fire loads is limited. Because of the vast variation in industrial buildings, fire loads are usually counted or calculated individually. Many literature sources cite the fire load densities given in CIB W14 Workshop Report [8], as do the BSi PD 7974 [7] and the Natural Fire Safety Concept [3].

Table 4: Excerpt from table 19 BS 7974-1:2003 [7] and NFSC [3] fire load densities

Occupancy	Fire load density [MJ/m2]			
	Average	Fractile		
		80 %	90 %	95 %
Dwellings	780	870	920	970
Hospital (room)	230	350	440	520
Hospital storage	2000	3000	3700	4400
Hotel (room)	310	400	460	510
Office	420	570	670	760
Shops	600	900	1100	1300
Manufacturing	300	470	590	720
Manufacturing and storage	1180	1800	2240	2690
Libraries	1500	2250	2550	-
Schools	285	360	410	450

3   Reliability analysis

In this research project both FORM/SORM-methods and Monte-Carlo-simulations are used for the calculation of the limit state function and the resulting β-values. Due to the specific properties of the building materials the use of FORM/SORM is limited. For the example with a steel member presented in the following section 4, the use of FORM was possible because all loads and resistances could be described completely by analytical equations.

Unfortunately this is not possible for structural members of reinforced concrete or composite concrete-steel constructions. For the heating of concrete, both the level of room temperature as well as the duration of the fire are of prime importance, due to the low thermal conductivity of concrete, its high heat capacity and mass. The heating of the structural member over time during natural fires cannot be calculated by hand. In these cases finite-element-models have to be used and therefore also Monte-Carlo-simulations.

In this project a program-package has been developed, and is subject to further development, that enables the user to calculate the room temperature according to ISO-standard-temperature-time curve, or using the zone model CFAST [9], or according to the parametric temperature-time curves from ZEHFUß [10]. The stochastic basic variables are generated by the program MCSim [11] based on Monte-Carlo-methods that also analyses the results of the complete program-package execution and with regard to the safety index β.

The FE-program Staba-F is integrated into the program package and enables the calculation of single temperature loaded structural elements made of reinforced concrete, composite concrete-steel, protected and unprotected steel and wood constructions.
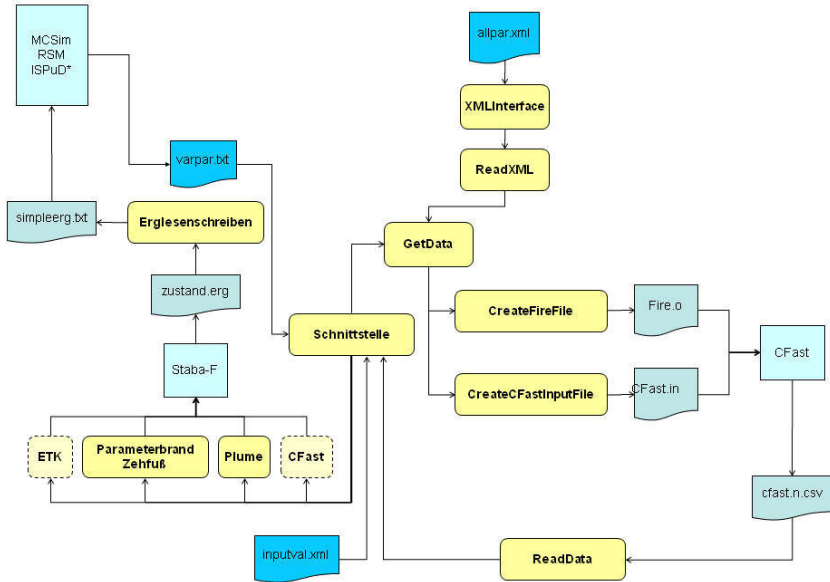
Figure 3: Program structure of the program package from A. WEILERT and C. KLINZMANN

In addition to the structural analyses, it is necessary to perform analyses of system failure probability with regard to fire protection installations and fire fighting measures. In this case, the reliability of the installations and the nature and timing of their response to the design fire is of special interest. The impact of failure of a component for the system also has to be taken into account. For example, if the fire has reached a certain size when the fire brigade arrives, it will no longer be possible to fight the fire within the compartment and efforts will instead be invested in the prevention of spread of the fire to other compartments or buildings. The relative importance of a failure path also depends on the resulting increase in damage. Sprinkler systems function properly far more often than they fail, but the increase in damage resulting from the failure of a sprinkler system is large.

For this reason, different scenarios require a vast number of calculations for the derivation of the system failure probability. In Figure 4 a section of the event tree for any scenario is presented. In case of the lack of a component, e. g. there is no fire detection system installed at this point, there is no ramification and the probability is 1.0.
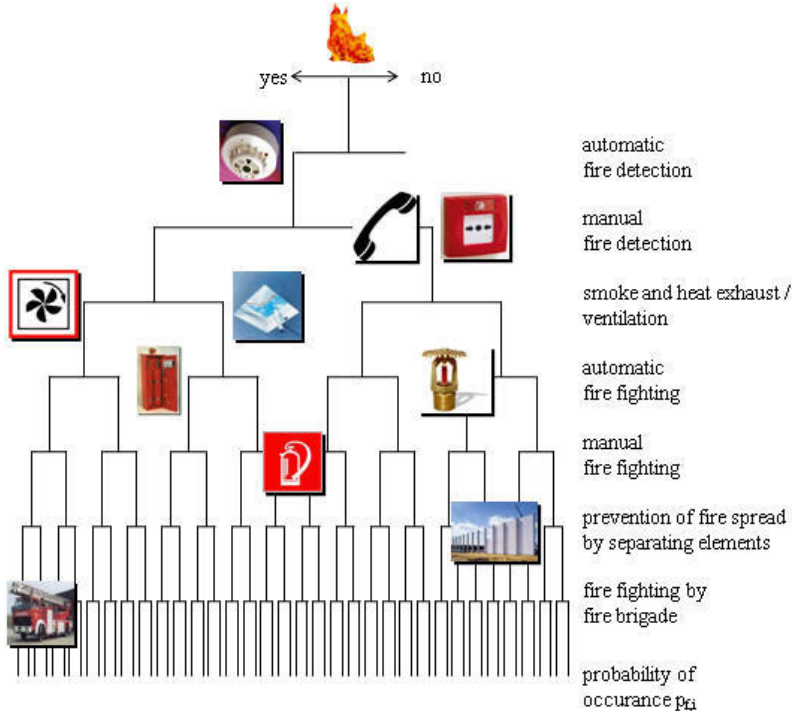
Figure 4: Event tree for any fire scenario

If the failure of a component causes the failure of the next in the hierarchy the ramification at this point is cancelled.

4   Example

In this section a short example for the calculation of the safety index β for a structural element exposed to fire is presented. An office building as steel construction is chosen. A comparison between the temperature development in the structural member dependant on the development of the room temperature with the critical temperature is presented. This method can only be used if the building member is not subject to stability problems.

- Fire load q for office buildings: $\mu = 420$ MJ/m2, $\sigma = 126$ MJ/m2

- Compartment area: $A = 1600m^2$

- Ignition frequency: $p_B = 2.1 \cdot 10^{-6}/(m^2 a)$ Finland

- Fire activation risk for the defined compartment:
$$p_{BA} \approx p_B \cdot A = 2.1 \cdot 10^{-6}/(m^2 a) \cdot 1600 m^2 = 3.36 \cdot 10^{-3}/(a) \qquad (1)$$

- Target reliability according to EN 1990: $p_{\tilde{s}} = 1.3 \cdot 10^{-6}/(a)$

- Target reliability in case of fire for this compartment and occupancy:

$$p_{F,BA} \leq 1.3 \cdot 10^{-6}/3.36 \cdot 10^{-3} = 3.87 \cdot 10^{-4} \tag{2}$$

- Safety index:

$$p_{F,BA} = 3.87 \cdot 10^{-4} = 1 - \Phi(\beta_{BA}) \tag{3}$$

$$\Rightarrow \beta_{BA} = 3.35 \tag{4}$$

- Structural Member: unprotected steel HEA 500 with $A_m/V = 111.6$ m^2/m^3

According to [12], the parametric temperature-time curves of Eurocode 1 Part 1-2, appendix A [1] do not refer to a design fire or documented physical principles. Some of these curves are derived from empirical evidence, calibrated by experiments. These curves do not describe the time-dependent behaviour of a natural fire.

On the other hand, within its application limits, the parametric fire model proposed by ZEHFUß [10] is well suited describing the behaviour of a fire depending on the fire load. The advantage of parametric temperature-time curves in general is the possibility of a very quick calculation of the thermal load induced to structures. Especially in case of simple compartment geometries, the user does not have to have special qualifications for the use zone models.

Compartment temperature following ZEHFUß [10] depending on the fire load:

A_F Area of the compartment

t_g time needed to reach a rate of heat release of 1 MW

For a reference fire load of q = 1300 MJ/m^2:

$$\dot{Q}_{max,B} = 0.25 \cdot A_F \tag{5}$$
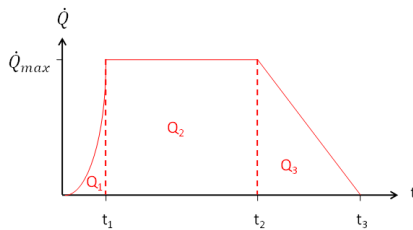
Figure 5: Qualitative representation of the time-dependant rate of heat release

Rate of heat release controlled by fire load:

$$T_1 = 24000 \cdot k + 20\,[°C] \quad f\ddot{u}r\ k \leq 0{,}04\ und\ f\ddot{u}r\ T_1 = 980°C\ f\ddot{u}r\ k > 0{,}04 \tag{6}$$

$$T_2 = 33000 \cdot k + 20\,[°C] \quad f\ddot{u}r\ k \leq 0{,}04\ und\ f\ddot{u}r\ T_2 = 1340°C\ f\ddot{u}r\ k > 0{,}04 \tag{7}$$

$$T_3 = 16000 \cdot k + 20\,[°C] \quad f\ddot{u}r\ k \leq 0{,}04\ und\ f\ddot{u}r\ T_3 = 660°C\ f\ddot{u}r\ k > 0{,}04 \tag{8}$$

with

$$k = \left(\frac{Q_{max}^2}{A_w \sqrt{h_w \cdot A_T \cdot b}}\right)^{1/3} \tag{9}$$

where:

$\dot{Q}$ Rate of heat release [MW]

b Mean of thermal properties of the enclosing building elements [J/($m^2 s^{0,5}$K)]

A_T Total area of the enclosing building elements without openings [m^2]
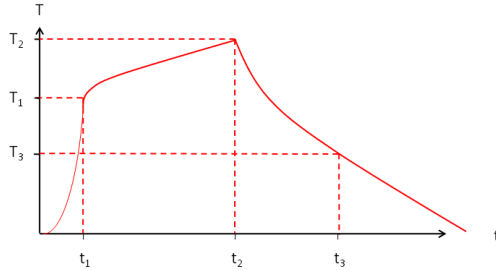
Figure 6: Qualitative representation of the time-dependant room temperature on basis of the parametric calculation of the temperature-time-curve according to ZEHFUß [10]

For fire load densities q ≤ 1300 MJ/m^2:

$$t_{2,x} = t_1 + \frac{(0,7 \cdot Q_x) - (t_1^3/(3 \cdot t_g^2))}{Q_{max}} \tag{10}$$

In case of very small fire load densities $Q_1 \geq 0,7 \cdot Q_x$ the decrease of the heat release already appears during the phase of rising temperature and the plateau of the heat release is not reached due to the lack of fire load (see Figure 5) - $t_{2,x}$ has to be calculated as:

$$t_{2,x} = \sqrt[s]{0,7 \cdot Q_x \cdot 3 \cdot t_g^2} \tag{11}$$

The related temperature $T_{2,x}$ is derived by inserting $t = t_{2,x}$ into equation (11):

$$T_{2,x} = (T_2 - T_1) \cdot \sqrt{(t_{2,x} - t_1)/(t_2 - t_1)} + T_1 \tag{12}$$

$$t_{3,x} = \frac{0,6 \cdot Q_x}{Q_{max}} + t_{2,x} \tag{13}$$

$$T_{3,x} = (T_3/\log_{10}(t_3 + 1)) \cdot \log_{10}(t_{3,x} + 1) \tag{14}$$

For q_x < 1300 MJ/m^2, the decreasing part of the natural fire curve can be calculated as:

$$T = (T_{3,x} - T_{2,x}) \cdot \sqrt{(t - t_{2,x})/(t_{3,x} - t_{2,x})} + T_{2,x} \tag{15}$$

In this example, the temperatures of the structural members have been calculated using the simple calculation model of EC 3-1-2 [13] for structural members not subjected to stability

problems. Subsequently, the temperatures of the structural members were compared with the critical temperature following [13] with $\mu_{Fi} = 0.65$.

For unprotected steel members:

$$\Delta\theta_{a,t} = \frac{A_m/V}{c_a/\rho_a} \cdot \dot{h}_{net,d} \cdot \Delta t \tag{16}$$

A_m/V section factor for unprotected steel members (envelope surface area/volume)

c_a specific heat of steel [J/(kg K)]

$\dot{h}_{net,d}$ the design value of the net heat flux per unit area [W/m2]

Critical temperature:

$$\theta_{a,cr} = 39{,}19 \cdot \ln\left[\frac{1}{0{,}9674 \cdot \mu_0^{3,833}} - 1\right] + 482 \tag{17}$$

In order to consider the stochastic deviation of the mechanical properties for the FROM and Monte-Carlo-simulations for the β-curve in Figure 8 the critical temperature was set to a mean of 540°C with a standard deviation of $\sigma_{Tkrit} = 54$°C. Furthermore the deviation in the room-temperature curve was taken into account by using a mean of 35 m^2 for the fire compartment area A_F with a standard deviation of $\sigma_{AF} = 5$ m^2. Following ZEHFUß [10] the fire compartment area A_F according to formula (6) determines the maximum of rate of heat release.
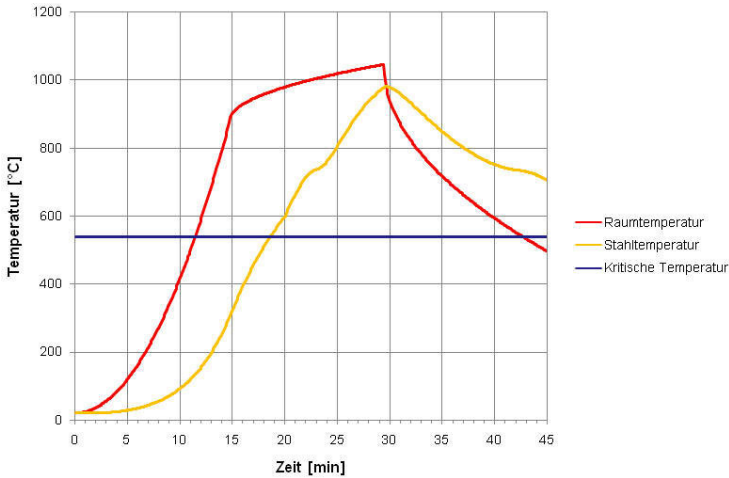
Figure 7: Comparison of the inner temperature of the structural element caused by the room temperature according to ZEHFUß [10] to the critical temperature

The calculation of the safety index based on FORM- and Monte-Carlo-methods was executed using the program COMREL.
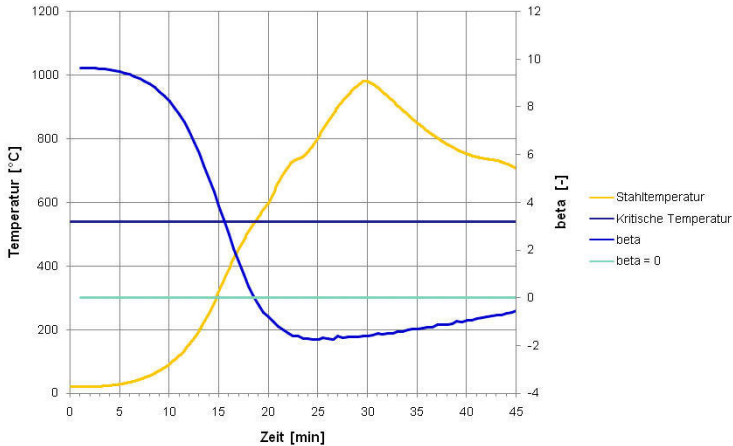
Figure 8: Development of safety index β over time depending on the inner temperature of the structural member and comparing with β_{krit} and $\beta = 0$

According to Figure 8, an unprotected steel construction with HEA 500 under full load is does not achieve the objective of "Preservation of bearing capability within the course of a natural fire". Therefore some protection or intumescent coating has to be applied or the building type has to be changed.

This example shows a simple calculation of the safety index β of a structure exposed to fire. In the course of this project, algorithms will be refined and extended to other building types.

5   Conclusion

The work on the design of a new safety concept for fire hazards, required data of parameters with influence on the development of a natural fire and the behaviour of structural elements in fire. This data was acquired during an intensive literature research. Since the behaviour of structural elements under thermal loads can only be described with numerical models. A program package using finite element models for the usage with simulation methods has been developed. Part of the ongoing work in this project is the definition of event trees for different fire scenarios and the determination of the dominant failure paths.

6   Literature

[1]   pr EN 1991-1-2: Eurocode 1: Einwirkungen auf Tragwerke; Teil1-2: Allgemeine Einwirkungen, Brandeinwirkungen auf Tragwerke; September 2003

[2]   Leitfaden Ingenieurmethoden des Brandschutzes, Hrsg.: Vereinigung zur Förderung des Brandschutzes in Deutschland e. V. (vfdb), Technisch Wissenschaftlicher Beirat (TWB), Referat 4, Hosser, D., vfdb TB 04/01, 1. May 2006

[3]   Competitive Steel Buildings through Natural Fire Safety Concept, Final Report, RPS Report n°32, CEC-Agreement 7210-SA/125,126,213,214,323,423,522,623,839,937, Profil Arbed, Centre de Recherches, march 1999

[4]   DIN EN 1990: Eurocode: Grundlagen der Tragwerksplanung. Ausgabe Oktober 2002

[5]   Rahikainen, J.; Keski-Rahkonen, O.; Statistical Determination of Ignition Frequency of Structural Fires in Different Premises in Finland; Fire Technology 40; p.335-353; 2004

[6]   Tillander, K.; Keski-Rahkonen, O.; The Ignition Frequency of Structural Fires in Finland 1996-99; Fire Safety Science – Proceedings of the seventh international symposium; 2003; ISBN 0-9545348-0-8; S. 1051-1062

[7]   BSi; PD 7974-1:2003; Application of fire engineering principles to the design of buildings; Part 1: Initiation and development of fire within the enclosure of origin

[8]   CIB W 14 Workshop Report, A Conceptual Approach towards a Probability Based Design Guide on Structural Fire Safety, 1983

[9]   Jones, W. W.; Peacock, R. D.; Forney, G. P.; Reneke, P. A.; CFAST – Consolidated Model of Fire Growth and Smoke Transport (Version 6), Technical Reference Guide; NIST Special Publication 1026; December 2005

[10]   Zehfuß, J.: Bemessung von Tragsystemen mehrgeschossiger Gebäude in Stahlbauweise für realistische Brandbeanspruchung, Dissertation 2004, TU Braunschweig, ISBN 3-89288-155-3

[11]   Klinzmann, C.; MCSim, SFB 477, Braunschweig, unpublished

[12]   Hosser, D.; Kampmeier, B.; Zehfuß, J.: Überprüfung der Anwendbarkeit von alternativen Ansätzen nach Eurocode 1 Teil1-2 zur Festlegung von Brandschutzanforderungen bei Gebäuden, Abschlussbericht im Auftrag des DIBt, Berlin, Aktz. ZP 52-5-3.83-1041/03 Dezember 2004

[13]   DIN EN 1993-1-2:2006-10; Eurocode 3: Bemessung und Konstruktion von Stahlbauten - Teil 1-2: Allgemeine Regeln - Tragwerksbemessung für den Brandfall; German edition

[14]   Reliability Consulting Programs (RCP) 2004. STRUREL, a Structural Reliability Analysis Program-System, COMREL & SYSREL: Users Manual. Munich: RCP Consult

Reliability-based Decision making for Steel Connections on Seismic Zones

David De Leon
Engrg. Department, Ciudad Universitaria, Toluca, México,
Univ. Aut. del Estado de México, 50130, México,

Abstract: The findings about the fragile behaviour of steel welded connections after the Northridge 1994 earthquake, specially for frames designed to withstand lateral force, has brought an amount of new attention to the design and safety issues of the welded connections for structures located on seismic zones. In México, practitioners and designers are wondering about the seismic effectiveness of the several kinds of connections as used in steel structures. A decision must be made to balance the safety required with the costs incurred after exceeding the serviceability limit state. Structural reliability techniques provide the proper framework to include the inherent uncertainties into the design process. Registered motions after the 1985 Mexico City earthquake are properly scaled according to the seismic hazard curve for soft soil in Mexico City. Earthquake occurrence is modelled as a Poisson process and the costs are expressed as a function of the damage level. The proposed formulation may support designers and builders for the decision making process about the selection of the convenient connection type for the seismic zones with soft soil in Mexico City.
Key words: Steel connections, reliability, life-cycle costing, decision making, seismic design.

1 Introduction

Steel buildings are a common design solution for seismic zones. However, the selection of the appropriate connection type is still an issue in Mexico, especially after the amount of damages experienced due to the Northridge earthquake (BRUNEAU, et al., 1998) occurred in California in 1994. The SAC Project (SAC project, 1994), developed in the US under FEMA´s coordination, provides some insight to improve the understanding of the seismic behavior of welded connections.

Usually the collapse limit state is emphasized to provide design recommendations but, given the character and extension of the damage produced by some earthquakes and the time the structure is off-service during repairs, the serviceability condition is also a concern.

Structural reliability and life-cycle costing serve as the measuring tools to weigh the cost/benefit relevance of the various connection alternatives and to balance the trade-off between required safety and costs of the damage consequences.

A seismic hazard curve, previously developed for Mexico City (ESTEVA and RUIZ, 1989) is used with scaling factors to assess the seismic vulnerability of the structures.

Throughout Monte Carlo simulation, statistics of the maximum acceleration demands are obtained at the connection location for typical buildings and, with these statistics and the connection model, statistics of the maximum responses are obtained. With these statistics and the state limit function, for a given connection type, probabilities of failure and damage are obtained for both demand levels: extreme and operational earthquakes. These probabilities are introduced into the life-cycle cost/benefit relationship for several connection types and the optimal type is obtained by comparing the expected life-cycle costs. The minimum value corresponds to the optimal connection type.

Damage costs include the repair cost and losses related to the potential fatalities, injuries and business interruption.

The results may also be used, after further refinements, to update the design specifications for seismic zones in Mexico.

2 Formulation of the Decision Criteria

The expected life-cycle cost is usually calculated to assess the economic effectiveness of potential structural solutions and come up to optimal decisions under uncertain loading conditions (NEVES, FRANGOPOL and HOGG, 2003; ANG and DE LEÓN, 2005).

Two alternative connection types are proposed and their performances are compared under the viewpoints of structural reliability and costs.

The expected life-cycle cost $E[C_L]$ is composed by the initial cost C_i and the expected damage costs $E[C_D]$:

$$E[C_L] = C_i + E[C_D]$$
(1)

The expected damage costs include the components of damage cost: expected repair $E[C_r]$, injury $E[C_{inj}]$ and fatality $E[C_{fat}]$ costs and each one depends on the probabilities of damage and failure of the structure.

These component costs of damage are defined as:

$$E[C_r] = C_r(PVF)P_r \tag{2}$$

where:

C_r = average repair cost, which includes the business interruption loss, $C_{bi,}$

PVF = present value function (ANG and DE LEÓN, 2005).

$$PVF = \sum_{n=1}^{\infty} [\sum_{k=1}^{n} \Gamma(k, \gamma L)/\Gamma(k, \upsilon L)(\upsilon/\gamma)^k](\upsilon L)^n / n! \exp(-\upsilon L) \tag{3}$$

where υ = mean occurrence rate of earthquakes that may damage the structure, γ = net annual discount rate, and L= structure life.

And P_r = probability of repair, defined in a simplified way, as a factor of the failure probability.

Similarly, the business interruption cost, $C_{bi,}$ is expressed in terms of the loss of revenue due to the repairs or reconstruction works after the earthquake, assumed to last T years:

$$C_{bi} = L_R(T) \tag{4}$$

where:

L_R = loss of revenues per year

The expected cost of injuries is proposed to be:

$$E[C_{inj}] = C_{IL}(N_{in})P_f \tag{5}$$

where:

C_{II} = average injury cost for an individual

N_{in} = average number of injuries on a typical steel building in Mexico given an earthquake with a mean occurrence rate υ.

For the expected cost related to loss of human lives, the cost corresponding to a life loss, C_{IL}, and the expected number of fatalities, N_D are considered. The cost associated with a life loss may be estimated in terms of the human capital approach, which consists in the calculation of the contribution lost, due to the death of an individual, to the Gross Domestic Product during his expected remaining life. The details of this calculation are explained in previous works (ANG and DE LEÓN, 1997). The expected number of fatalities is estimated from a curve previously developed for typical buildings in Mexico, in terms of their plan areas, given an earthquake with a mean occurrence rate υ.

$$E[C_L] = C_{1L}(N_D)P_f \tag{6}$$

In the next section, all the figures are estimated for typical costs in Mexico.

A typical geometry of a building, see Fig. 1, located on the soft soil of Mexico City is selected to analyze its critical frame under seismic loads. Statistics of its maximum response, at critical joint level, are obtained from the frame analyses subjected to Poissonian earthquakes (with mean occurrence rate ν) as scaled from the seismic hazard curve for Mexico City (ESTEVA and RUIZ, 1989).

The above described response statistics are used as an input to the FEM models of the alternative connections and a Monte Carlo simulation process is performed for each connection model in order to get the statistics of maximum shear force and moment. With these statistics and the limit state function of each connection, the corresponding failure probabilities are calculated. As an example, g_1 and g_2 are the state limit functions for maximum moment and for each one of the two alternative connections.

$$g_1 = 5.39 - M_1 \tag{7}$$

$$g_2 = 3.38 - M_2 \tag{8}$$

where M_1 and M_2 are the maximum moments for the alternative connections.

With the calculated failure probabilities, and Eqs. (1) to (6), the expected life-cycle cost of each connection is obtained. The connection type to be recommended is the one with the minimum life-cycle cost.

3   Application to a Steel Building in Mexico

The calculation process described in the last section is performed to the frame shown in Fig. 1 and the statistics of seismic spectral information is shown in Table 1. The mean $E[C_s]$ and coefficient of variation CV_{Cs} of the seismic coefficient are considered to generate random seismic excitations.
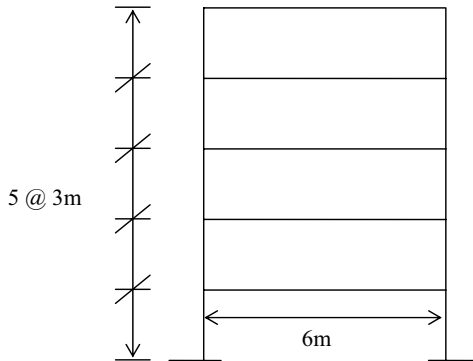
Fig. 1: Typical frame for a steel building in Mexico

Table 1. Seismic information for Mexico City

$E[C_s] =$	0.45
$CV_{Cs} =$	0.3
$\nu =$	0.142

The critical joints were found to be the first floor connections.

The costs data are shown in Table 2.

Table 2. Costs data (pesos)

C_i	10000
C_r	8000
γ	0.142
L_R	20000
C_{Ii}	10000
C_{IL}	80000
N_{in}	0
N_D	60
L	50 years

The first proposed connection is a bolted joint with 2 angles and A325 7/8" bolts. The angles join the beam web with the column flanges. The second one is a welded set of 2 fillets with 15cm length and ¼" thickness with electrodes E70 to join the beam web to the column flanges. A general view of the alternative connections is shown in Fig. 2.
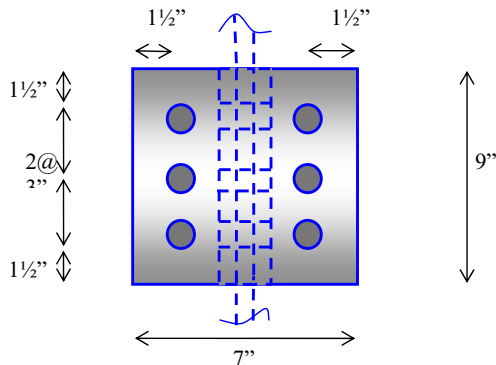
(a) Front view of bolted connection
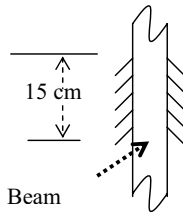
(b) Front view of welded connection

Fig. 2: Alternative connections (a) bolted, (b) welded

The distribution of the critical forces at the joints, for the alternative connections, are shown in Figs. 3 and 4.
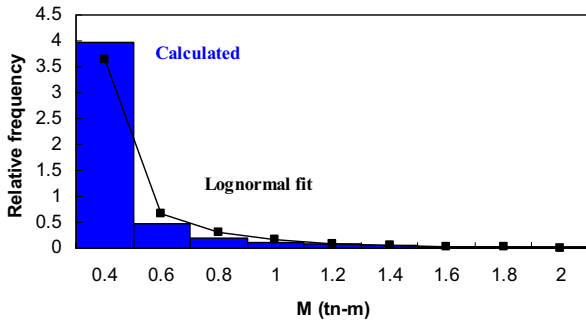
Fig. 3 Distribution of maximum moments at critical joint
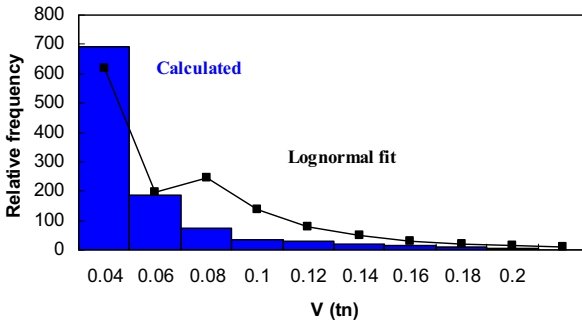
Fig. 4 Distribution of maximum shear forces at critical joint

The bending mode was found to govern the connection failure. A sample of the simulation process is shown in Table 3.

Table 3. Repair and failure probabilities for alternative connections

Random number uniform	Random number LN	M_1 (tn-m)	g_1	g_2
0.0044	-2.617	0.024	0	0
0.4713	-0.071	0.222	0	0
0.5094	0.023	0.242	0	0

$\xi_M=$	0.863
$\lambda_M=$	-1.438

The repair and failure probabilities, for the alternative connections, are shown in Table 4.

Table 4. Repair and failure probabilities for alternative connections

Pr_{1M}	Pr_{2M}
0.069	0.004
Pf_{1M}	Pf_{2M}
0.001	0.001

With the above obtained failure probabilities, the expected life-cycle costs are calculated and the results are shown in Table 5.

Table 5 Expected life-cycle costs for alternative connections

Alternative	$E[C_r]$	$E[C_{fat}]$	$E[C_{inj}]$	C_i	$E[C_D]$	$E[C_T]$
1	14490	96096	0	10000	110586	120586
2	840	96096	0	10000	96936	106936

4   Discussion of results

From the results obtained in the previous section, it is observed that the optimal connection type is the second one, the welded connection from beam web to column flanges.

The bending effect is the one that governs the connection design for the case treated here and for the seismic conditions illustrated.

Regarding the costs, the only difference between the two alternatives was the repair cost. This is due to the fact that the repair probability is different for these cases; it is more probable the repair for the bolted connection, where part of the work is made onsite, than the welded one which makes use of a more qualified workmanship.

Two simple options were included here for exemplification purposes. The decision tool may be extended to compare a wide variety of connections and details where the cost-benefit analysis is justified.

The results are useful for the hazard and site considered. Other conditions require an adaptation of data like, hazard type, seismicity and costs.

5   Conclusion and Recommandations

A risk-based decision tool has been presented to select potentially feasible connection types in a steel building under seismic loads.

For the case considered here, a welded connection is preferred, from the cost effectiveness point of view, over a bolted one.

Further research may lead to a wider range of applications in order to compare design, construction and retrofit alternative schemes.

Also, with additional work, the criteria may be used to update the Mexican code for design and retrofit specifications.

6   Acknowledgements

Mexican construction engineers suggested the connection types, as a common practice on the region. Their contributions are acknowledged and thanked.

7   References

[1] Ang, A. H-S. and De León, D., (1997), "Determination of optimal reliabilities for design and upgrading of structures", *Structural Safety*, Vol. 19, 1, pp. 91-103.

[2] Ang, A. H-S. and De León, D., (2005), "Modeling and analysis of uncertainties for risk-informed decisions in infrastructures engineering", *Journal of Structure and Infrastructure Engineering,* Vol. 1, 1, pp. 19-31.

[3] Bruneau, M.; Whitakker, A., and Uang, Ch. M. (1998) *"Ductile Design of Steel Structures"*. McGraw Hill.

[4] Esteva, L. and Ruiz, S., (1989) "Seismic failure rates of multistory frames". *Journal of Structural Engineering, ASCE*, Vol. 115, No. 2, pp. 268-284.

[5] Neves, L. C.; Frangopol, D. M. and Hogg, V. (2003). *"*Condition-reliability-cost interaction in bridge maintenance". *ICASP9*, San Francisco, CA, pp. 1117-1122

[6] SAC project (1994): *http://quiver.eerc.berkeley.edu:8080/library/index.html*

Optimal Safety Level of Acceptable Fatigue Crack

Martin Krejsa & Vladimír Tomica
Faculty of Civil Engineering, VSB - Technical University Ostrava,
Ostrava – Poruba, Czech Republic

Abstract: Limit criterion of stability fatigue crack propagation on building structures is not defined. Procedure leading to brittle fracture is known theoretically. Its application to practical building structures is unused. The paper focuses on probabilistic assessment of acceptable fatigue crack and theoretical critical crack. Risk of damage proceeds load effect. Fatigue crack growth is related to traffic load effect, acceptable fatigue crack to probability of extreme probabilistic load effect.

1   Introduction

The load-carrying capacity of the bearing structure has been significantly influenced by degradation resulting, in particular, from the fatigue of the basic materials. Wöhler's curves are used when designing such structures. The service life can be limited until a failure occurs. The failure is however very difficult to be determined. For purposes of the modeling, the amplitude oscillation is considered to be constant, and a certain number of load cycles is taken into account. The method has been developed to provide procedures describing real conditions, all this making the work of design engineers easier. As fatigue cracks appear randomly on existing structures (in crane rails and bridges), it is believed that the designing method is imperfect to a certain extent. Methods are under development that would be able to reveal potential defects and damage resulting from initiation cracks that accelerate considerably the propagation of fatigue cracks. Linear fracture mechanics is among alternative methods. Machinery experts, in particular, have been dealing with such issues for many years. Results have been gradually taken over and implemented into designs of the loading structures in buildings. It is typically used for the determination of times of inspection and analyses of inspection results. If cracks are not found, a conditional probability exists that they might appear later on.

2   Probabilistic approach to the propagation of fatigue cracks

The velocity of propagation of the fatigue crack is governed by principles of the widely known Paris-Erdogan law ([4]):

$$\frac{da}{dN} = C \cdot \Delta K^{m} \tag{1}$$

with a magnitude (length) of cracks
           N number of cycles
           C, m material characteristics
           ΔK oscillation of the stress intensity factor

When the oscillation of the stress peaks ($\Delta\sigma$) is known, the amplitude swing can be determined as follows:

$$\Delta K = \Delta\sigma . \sqrt{\pi . a} . F_{(a)} \tag{2}$$

The calibration function $F_{(a)}$ represents the course of propagation of the crack. After the change of the number of cycles from N_1 to N_2, the crack will propagate from the length a_1 to a_2. Having rearranged (1) with (2), the following formula will be achieved:

$$\int_{a_1}^{a_2} \frac{\mathrm{d}a}{\left(\sqrt{\pi . a} . F_{(a)}\right)^{m}} = \int_{N_1}^{N_2} C.\Delta\sigma^{m}.\mathrm{d}N \tag{3}$$

If the length a_1 of the crack equals to the initial length a_0 of the crack and a_2 equals to the final (critical) length a_{cr} of the crack, the left side of the equation (3) can be regarded as the resistance of the structure - R:

$$R_{(a_{cr})} = \int_{a_0}^{a_{cr}} \frac{\mathrm{d}a}{\left(\sqrt{\pi . a} . F_{(a)}\right)^{m}} \tag{4}$$

Similarly, it is possible to define the cumulated effect of loads that is equal to the right side (3):

$$S = \int_{N_0}^{N} C.\Delta\sigma^{m}.\mathrm{d}N = C.\Delta\sigma^{m}.\left(N - N_0\right) \tag{5}$$

with N total number of oscillations of stress peaks ($\Delta\sigma$)
                     for the change of the length from a_0 to a_{cr}
           N_0 number of oscillations in the time of initialization
                     of the fatigue crack

It is possible to define a reliability function. The analysis of the reliability function gives a failure probability P_f:

$$G_{fail(Z)} = R_{(a_{cr})} - S \tag{6}$$

with Z vector of random physical properties such as
mechanical properties, geometry of the structure,
load effects and dimensions of the fatigue crack

The failure probability equals to:

$$P_f = P\big(G_{fail(Z)} < 0\big) = P\big(R_{(a_{cr})} < S\big) \tag{7}$$

The probability can be calculated using the available software based either on DDFPM [3] (see below) or Monte Carlo simulation method.

3   Direct Determined Fully Probabilistic Method (DDFPM)

The Direct Determined Fully Probabilistic Method ("DDFPM") was originally developed as a Monte Carlo alternative to SBRA the development of which started in the mid of 1980's. Both for SBRA and DDFPMM, input random quantities (such as the load, geometry, material properties, or imperfections) are applied. The description of the random quantities is expressed by the non-parametric distribution in histograms. This technique can be also used for parametric distributions (see below). DDPFM is based on general terms and procedures used in probabilistic theories (such as [51]). DDFPM applications are processed in ProbCalc – this software is being improved all the time. It is rather easy to implement an analytical transformation model of the specific probabilistic application into ProbCalc. The reliability function under analysis can be expressed in ProbCalc analytically as a sign arithmetic expression (using the so-called calculator) or can be expressed using data from the dynamic library (DLL files) where the library can be created in any programming language. DDPFM can be used now to solve a number of probabilistic computations. The number of variables that enter the failure probability computation is however limited by capabilities of the software to process the application numerically. If there are too many random variables, the application is extremely time demanding - even if high-performance computers are used. For that reason, ProbCalc includes a number of optimizing techniques extending considerably the applicability options, maintaining, at the same time, the reliable results. The random nature of quantities entering the probabilistic calculation is often expressed by the histogram created on the basis of monitoring and, frequently long-lasting measurements. Those histograms are used then to assess the reliability of structures. Then, histograms of the input values are used in SBRA and DDPFM can be created for discrete or purely discrete quantities. The quantities used in static calculations (such as the load, material properties, or cross-section parameters) can be regarded as continuous quantities. Basic material operations can be carried out with the histograms in the probabilistic calculations. For instance, in case of a combined load, the histograms of the individual types of load will be summed up. The both histograms are summed up in program cycles where the quantities (on the horizontal axis) will be summed up first and their probabilities will be multiplied and added within a corresponding interval of the resulting histogram. The principle of the numerical solution is best evident on Fig. 1.
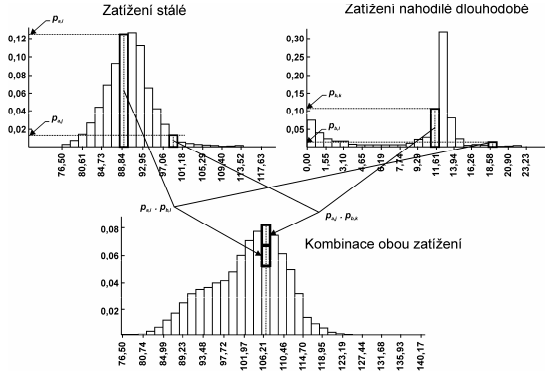
Fig. 1: Calculation Principles - Combination of the Permanent
and Random Long-termed Load

If general principles of the probabilistic theory are taken into account, arithmetic operations can be carried out with the histograms. It is possible to use any histogram expressing any random variable that enters the calculation. Let the histogram B be an arbitrary function f of histograms A_j, where j ranges from 1 to n. Then:

$$B = f(A_1, A_2, A_3, \ldots, A_j, \ldots A_n) \tag{8}$$

Each histogram A_j consists of i_j interval where each interval is limited with $a_{j,i}$ from below and $a_{j,i+1}$ from above. This means, that for the interval $i_j = 1$, the values will be as follows:

$$a_{j,1} \leq a_j \angle a_{j,2} \tag{9}$$

with $a_{j,2} = a_{j,1} + \Delta a_j \tag{10}$

$$\Delta a_j = \frac{a_{j,\max} - a_{j,\min}}{i_j} \tag{11}$$

In i_j, the following formula is valid:

$$a_{j,i} \leq a_j \angle a_{j,i+1} \tag{12}$$

Let us express a_j in that interval as $a_j^{(ij)}$. Similar relations are valid for the B histogram. if there are i intervals, the values of the histogram in the ith interval range from b_i to b_{i+1}, this means $b^{(i)}$). They can be expressed as follows:

$$b^{(i)} = f(a_1^{(i1)}, a_2^{(i2)}, \ldots, a_j^{(ij)}, \ldots a_n^{(in)}) \tag{13}$$

for the specific combination of arguments: $a_1^{(i1)}, a_2^{(i2)}, \ldots, a_j^{(ij)}, \ldots a_n^{(in)}$. The same value - $b^{(i)}$ can be derived for other values too (or at least for some values too) - $a_j^{(ij)}$. If the potential combination of values $a_j^{(ij)}$ is marked as l, the following general formula can be derived:

$$b^{(i)} = f(a_1^{(i1)}, a_2^{(i2)}, \ldots, a_j^{(ij)}, \ldots a_n^{(in)}) \tag{14}$$

The probability $(p_{bl}{}^i)$ of occurrence of $b^{(i)}$ is the product of $p_{aj}{}^{(ij)}$ (probabilities of occurrence of a_j^{ij} values). Then:

$$p_{bl}{}^i = (p_{aj}{}^{(i1)} \cdot {}_{aj}j^{(i2)} \cdot {}_{aj}j^{(i3)} \cdot \ldots \cdot {}_{aj}j^{(ij)} \cdot \ldots \cdot {}_{aj}j^{(in)}) \tag{15}$$

The probability of occurrence of all potential combinations $(a_1^{i1}, a_2^{i2}, \ldots, a_j^{ij}, \ldots a_n^{in})_l$, of f with the result of $b^{(i)}$ is:

$$p_b^{(i)} = \sum_{l=1}^{l} p_{pl}^{(i)} \tag{16}$$

The number of intervals (i_j) in each histogram (A_j) can vary similarly as the number of i intervals in the histogram (B). The number of intervals is extremely important for the number of needed numerical operations and required computing time. On top of this, the accuracy of the calculation depends considerably on the number of intervals. If Monte Carlo is used for the same calculation, the results will be always slightly different even if a relatively high number of simulations (1,000,000) are used. The reason is generation of random numbers, or to be more specific – pseudo-random numbers. This generation is always limited and slightly different for each series of simulations. If the directly probabilistic calculation is used and same intervals are chosen, the result is always the same.

4 Example of DDPFM calculation

Fatigue cracks appear most frequently in decks of railway or road bridges. The fatigue cracks may appear easily because each normal force represents one loading cycle. The loading effects are more evident if the construction element is located close to the point of loading application. An example of the probabilistic calculation will be shown in a longitudinal beam of a railway bridge. The construction connection is imperfect because effects of the moment of bending are neglected in the place of connection. The load carrying part is only the wall of the longitudinal beam. The propagation of the fatigue crack from the edge can be expressed in (2) by means of a calibration function:

$$F_{(a)} = 1{,}12 - 1{,}39 \cdot \frac{a}{b} + 7{,}32 \cdot \left(\frac{a}{b}\right)^2 - 13{,}8 \cdot \left(\frac{a}{b}\right)^3 + 14{,}0 \cdot \left(\frac{a}{b}\right)^4 \tag{17}$$

with a length of the crack
       b height of the wall (400 mm in this case)

Other input data include the random quantities – they are expressed by means of the parametric division (see Table 1). The deterministically set input values are the material characteristics $C = 2{,}15 \cdot 10^{-13}$ and $m = 3$.

Tab. 1: Overview of Variable Input Quantities

Quantity	Type of Distribution	Parameters	
		Mean Value	Standard Deviation
Oscillation of stress peaks	Normal	30	2
Total number of oscillation of stress peaks per year N [-]	Normal	2.10^6	10^5
Initial size of the crack a_0 [mm]	Lognormal	0,1	0,02
Smallest measurable size of the crack a_d [mm]	Normal	10	0,6
Critical size of the crack a_{cr}=200 mm	Normal	200	2

Within the probabilistic calculation of the critical fatigue crack (DDPFM) in ProbCalc, the structure reliability $R_{(acr)}$ (4) is to be determined first. Another quantity that is important for the reliability of the structure is the loading effect S (5). When calculating the loading effect, two deterministically material characteristics and two histograms (the oscillation of stress peaks $\Delta\sigma$ [MPa]) and the number of oscillations of stress peaks N) are used. Fig. 2 shows the histogram of the loading effects for S and for the set number of the stress peak oscillations in 14 years of operation.
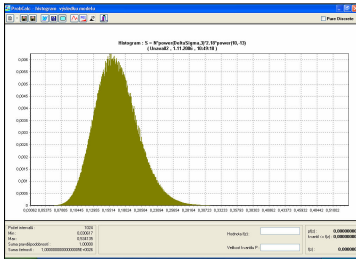
Fig. 2: Histogram – Loading Effects S for the total number of stress peaks oscillations in 14 years
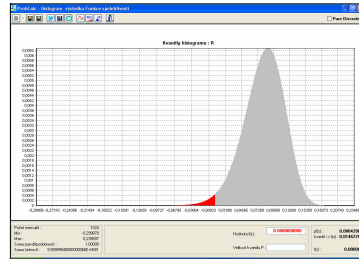
Fig. 3: Histogram - Reliability Function G_{fai} with the marked fractile where G_{fail}<0, P_f is 0.01462766

The resulting probability of failure P_f can be calculated from (6). The probability corresponds to the fractile of the histogram of the reliability function located in the interval where $G_{fail} < 0$ (see Fig. 3). The failure probability P_f can be calculated for individual years of operation of the bridge. On the basis of that calculation, it is possible to determine the dependence of the failure probability P_f on years of operation of the bridge. When the limit reliability (for instance $P_d = 2,3. 10^{-2}$) is known, it is possible to determine the time of first inspection of the bridge. Fig. 4 shows such dependence for a steel bridge. According to the probabilistic calculation, the first inspection of the bridge is required after 14 – 15 years of the operation. In case of crack propagation is possible to define random events, which can be in time t structure durability:

$U(t)$ … crack is not detected in time t – fatigue crack size $a(t)$ is less than detectable   size, so it applies:

$$a_{(t)} < a_d \tag{18}$$

with $\quad a_d \quad$ minimal detectable crack size

$D(t)$ … crack detection in time t – fatigue crack size $a(t)$ don't extend tolerable size, so it applies:

$$a_d \leq a_{(t)} < a_{cr} \tag{19}$$

$F(t)$ … crack detection in time t – fatigue crack size $a(t)$ extend tolerable size a_{cr}, so it applies:

$$a_{(t)} \geq a_{cr} \tag{20}$$

Using fully probabilistic calculation is possible to solve probability of these defined events:

- Probability of crack non-detection in time t :

$$P\big(U_{(t)}\big) = P\big(a_{(t)} < a_d\big) \tag{21}$$

with $\quad a_d \quad$ minimal detectable crack size

- Probability of crack detection in time t, crack size $a(t)$ is less than tolerable size a_{cr}:

$$P\big(D_{(t)}\big) = P\big(a_d \leq a_{(t)} < a_{cr}\big) \tag{22}$$

- Probability of crack detection in time t, crack size $a(t)$ is equal or greater than tolerable size a_{cr} :

$$P\big(F_{(t)}\big) = P\big(a_{(t)} \geq a_{cr}\big) \tag{23}$$

All of these three events create full space of events, which can occur in time t, it can be applied:

$$P\big(U_{(t)}\big) + P\big(D_{(t)}\big) + P\big(F_{(t)}\big) = 1 \tag{24}$$

5 Using Conditioned Probability to Determine Inspections of Construction

Probabilities mentioned in the relations (21) through (23) can be calculated in any time t using DDPFM (see Chapter 3). The calculation is carried out in time steps equal to one year of the service life of the construction. The inspection of the construction is proposed in the time when the probability of the F phenomenon exceeds the designed P_{fd} probability representing the probability of a fatigue crack in a structural element. The inspection provides information about real conditions of the construction. Such conditions can be taken into account when carrying out further probabilistic calculations. The inspection in the t_I time can result in one of following three alternatives:

$$P(U(t_I)) = P(a(t_I) < a_d)$$ (25)

$$P(D(t_I)) = P(a_d \leq a(t_I) < a_{cr})$$ (26)

$$P(F(t_I)) = P(a(t_I) \geq a_{cr})$$ (27)

Using the inspection results, it is possible to define the probability of the mentioned phenomena in another times: $T > t_I$. For that purpose, the conditioned probability should be taken into consideration. Let us assume that the U phenomenon occurred in the t_I time during the inspection:

$$
\left.
\begin{aligned}
P(U(T)/U(t_I)) &= \frac{P(U(T) \cap U(t_I))}{P(U(t_I))} = \frac{P(U(T))}{P(U(t_I))} \\
P(D(T)/U(t_I)) &= \frac{P(D(T) \cap U(t_I))}{P(U(t_I))} \\
P(F(T)/U(t_I)) &= \frac{P(F(T) \cap U(t_I))}{P(U(t_I))}
\end{aligned}
\right\} \sum = 1
$$ (28)

Let us assume that the D phenomenon occurred in the t_I time during the inspection, then:

$$
\left.
\begin{aligned}
P(U(T)/D(t_I)) &= \frac{P(U(T) \cap D(t_I))}{P(D(t_I))} = \frac{0}{P(D(t_I))} \\
P(D(T)/D(t_I)) &= \frac{P(D(T) \cap D(t_I))}{P(D(t_I))} \\
P(F(T)/D(t_I)) &= \frac{P(F(T) \cap D(t_I))}{P(D(t_I))}
\end{aligned}
\right\} \sum = 1 \right\} \sum = 1
$$ (29)

It follows from (29) that if the D phenomenon occurs in t_I, the phenomenon U cannot occur in T and $P(U(T)/D(t_I))$ must equal to 0. Let us assume that the F phenomenon occurred in the time t_I during the inspection:

$$
\left.
\begin{aligned}
P(U(T)/F(t_I)) &= \frac{P(U(T) \cap F(t_I))}{P(F(t_I))} = \frac{0}{P(F(t_I))} = 0 \\
P(D(T)/F(t_I)) &= \frac{P(D(T) \cap F(t_I))}{P(F(t_I))} = \frac{0}{P(F(t_I))} = 0 \\
P(F(T)/F(t_I)) &= \frac{P(F(T) \cap F(t_I))}{P(F(t_I))} = \frac{P(F(t_I))}{P(F(t_I))} = 1
\end{aligned}
\right\} \sum = 1
$$ (30)

It follows from (30) that if the F phenomenon occurs in t_I, it cannot occur in any other time. In order to propose the T time for the next inspection it is desirable to determine the conditioned probabilities. $P(F(T)/U(t_I))$ and $P(F(T)/D(t_I))$ can be determined using following formula:

$$P(F(T)/U(t_I)) = \frac{P(F(T) \cap U(t_I))}{P(U(t_I))} = \frac{P(F(T)) - P(F(t_I)) - P(D(t_I)).P}{P(U(t_I))}$$ (31)

$$P\big(F(T)/D(t_I)\big) = \frac{P\big(F(T) \cap D(t_I)\big)}{P\big(D(t_I)\big)} = \frac{P\big(F(T)\big) - P\big(F(t_I)\big) - P\big(U(t_I)\big).P\big(F(T)/}{P\big(D(t_I)\big)} \tag{32}$$

The mentioned relations (31) and (32) were used for further inspections. See Fig. 4.
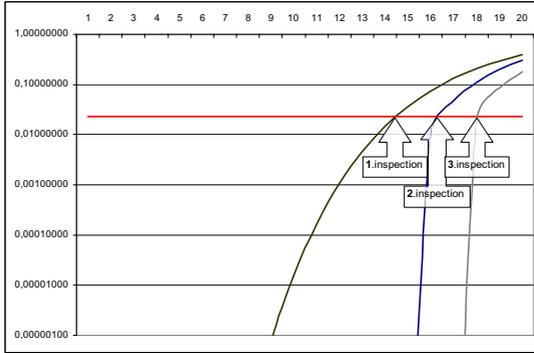
Fig. 4: Determining inspection times

6 Influence of Probabilistic Dimensions of Cracks with Different Parametric Distribution on Resistance of Construction

Resistance of the construction ranks among important quantities used in the probabilistic assessment of fatigue reliability of steel structures. Limits a_1 and a_2 in the formula (4) are typically expressed by means of a parametric distribution. A parametric study was carried out. The purpose was to find out the influence of input distribution parameters on the final resistance and to determine the optimum parametric distribution for the mentioned case.

Tab. 2: Overview of input parameters and quantilles for the final resistance (R) and variable standard deviation (a_0)

$a_1 = a_0$ Initial size of the crack [mm]			$a_2 = a_{cr}$ Critical size of the crack [mm]			R – resistance of the structure		
Type of distribution	Mean Value	Standard Deviation	Type of distribution	Mean Value	Standard Deviation	5% quantille	50% quantille	99% quantille
Lognorm	0.1	**0.01**	Norm	200	2	**0.239536**	**0.262418**	**0.299071**
Lognorm	0.1	**0.02**	Norm	200	2	**0.238220**	**0.260961**	**0.297357**
Lognorm	0.1	**0.04**	Norm	200	2	**0.235615**	**0.258073**	**0.294025**
Lognorm	0.1	**0.08**	Norm	200	2	**0.230500**	**0.252393**	**0.287475**
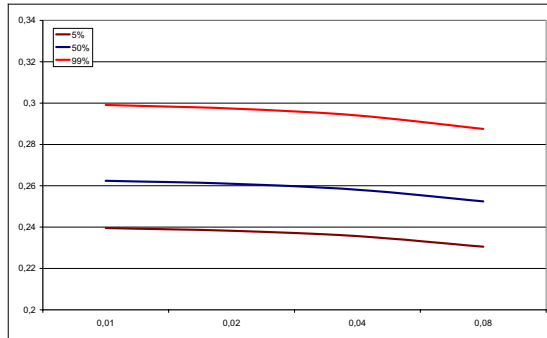
Fig. 5: Chart with R resistance quantilles for a_0 variable standard deviations (0,01 mm; 0,02 mm; 0,04 mm and 0,08 mm). Input parameters for the calculation of R: a_0 = lognormal distribution, mean value = 0.1 mm, a_{cr} = normal distribution, mean value = 200 mm, standard deviation = 2 mm.

It the first study the R resistance was determined using the a_0 variable standard deviation. Table 2 shows resulting quantilles for 5%, 50% and 99%. For graphic values see Chart on Fig. 6. When the a_0 standard deviation increases, the resistance goes down. From the point of view of calculation, the standard deviation influences the R final resistance. Then, the variable mean value of a_{cr} was used for determination of the R resistance. Table 3 shows resulting quantilles for 5%, 50% (see Fig. 7) and 99%. When the a_{cr} mean value increases, the resistance goes up. From the point of view of calculation, this parameter also influences the R final resistance.
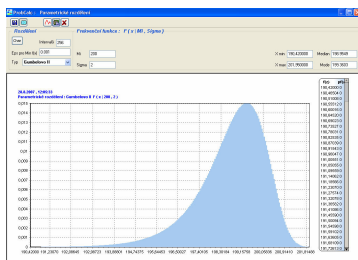
Fig. 6: a_{cr} histogram with Gumbel's distribution (II) and following input parameters: mean value = 200 mm, standard deviation = 2 mm
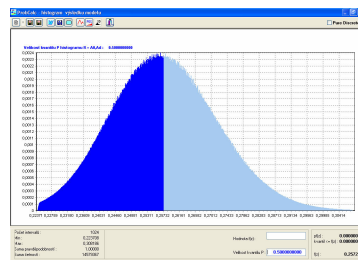
Fig. 7: R resistance histogram (a_0 = lognormal distribution, mean value = 0.1 mm, standard deviation = 0.02 mm, a_{cr} = normal distribution, mean value = 160 mm, standard deviation = 2 mm), 50% quantille

For the next calculation of the R resistance, variables changes in the a_{cr} standard deviation were used. Table 4 shows resulting quantilles for 5%, 50% and 99%. When the a_{cr} standard deviation increases, the R resistance almost does not change. From the point of view of calculation, this parameter seems to be less significant. In the next calculation, efforts were made to express the variable value of the initial size of the crack (a_0) with other than lognormal distribution. Considering the parameters of the quantity (mean value = 0.1 mm and standard deviation = 0.02 mm), we have failed to identify another suitable type of the parametric distribution. There were considerable differences in the distribution quantilles.

Tab. 3: Overview of input parameters and quantilles for the final resistance (R) and variable mean value (a_{cr})

$a_1 = a_0$ Initial size of the crack [mm]			$a_2 = a_{cr}$ Critical size of the crack [mm]			R- resistance of the structure		
Type of distribution	Mean Value	Standard Deviation	Type of distribution	Mean Value	Standard Deviation	5% quantille	50% quantille	99% quantille
Lognorm	0.1	0.02	Norm	160	2	0.235575	0.257269	0.292301
Lognorm	0.1	0.02	Norm	180	2	0.236709	0.259199	0.295126
Lognorm	0.1	0.02	Norm	200	2	0.238220	0.260961	0.297357
Lognorm	0.1	0.02	Norm	220	2	0.239532	0.262519	0.299382
Lognorm	0.1	0.02	Norm	240	2	0.240701	0.263932	0.301258

Tab. 4: Overview of input parameters and quantilles for the final resistance (R) and variable standard deviation (a_{cr})

$a_1 = a_0$ Initial size of the crack [mm]			$a_2 = a_{cr}$ Critical size of the crack [mm]			R - resistance of the structure		
Type of distribution	Mean Value	Standard Deviation	Type of distribution	Mean Value	Standard Deviation	5% quantille	50% quantille	99% quantille
Lognorm	0.1	0.02	Norm	200	1	0.238230	0.260941	0.297281
Lognorm	0.1	0.02	Norm	200	2	0.238220	0.260961	0.297357
Lognorm	0.1	0.02	Norm	200	4	0.238212	0.260958	0.297372
Lognorm	0.1	0.02	Norm	200	8	0.238182	0.260942	0.297390

Tab. 5: Overview of input parameters and quantilles for the final resistance (R) and variable type of distribution (a_{cr})

$a_1 = a_0$ Initial size of the crack [mm]			$a_2 = a_{cr}$ Critical size of the crack [mm]			R – resistance of the structure		
Type of distribution	Mean Value	Standard Deviation	Type of distribution	Mean Value	Standard Deviation	5% quantille	50% quantille	99% quantille
Lognorm	0.1	0.02	Constant	200		0.237815	0.260708	0.296833
Lognorm	0.1	0.02	Norm	200	2	0.238220	0.260961	0.297357
Lognorm	0.1	0.02	Gumbel I	200	2	0.238243	0.260937	0.297311
Lognorm	0.1	0.02	Gumbel II	200	2	0.230811	0.260855	0.297169
Lognorm	0.1	0.02	Raised cosine	200	2	0.238201	0.260939	0.297256
Lognorm	0.1	0.02	Cauchy	200	2	0.238148	0.260917	0.297376
Lognorm	0.1	0.02	Logistic	200	2	0.238214	0.260958	0.297371

Alternative types of the parametric distribution have proved to be a good approach when trying to express the width of the critical crack size. It follows from the resulting quantilles in Table 5, the wide range of parametric distributions can be used for calculation of the R resistance. Whatever parametric distribution is used, the R final resistance does not differ too much and this factor can be regarded as less significant for purposes of the calculation.

7 Conclusion

The example above shows possible applications of the software ProbCalc that is being developed now for probabilistic calculations of the critical fatigue cracks. The method described above provides always an unambiguous and comparable result (this differs from results achieved on the basis of the Monte Carlo method). The only error in this result is given by discretisation of input quantities. The available software and method can be also used to model and solve by means of the probabilistic method even considerably complex tasks that can be defined within the dynamic library - DLL. In the future, all those advantages should be used for an exact determination of the probability of failures in bridge structures caused by the propagation of fatigue cracks (such as a parametric study investigating into influences of the initial crack on propagation of the crack from the edge/surface and sensitivity of the critical crack on input parameters).

Notification

Literature

[1] Gocál, J.: *Fatigue Assessment of Steel Bridges by Means of Linear Fracture Mechanics and Probabilistic Method*. In: Steel Structures and Bridges, Present Situation and Lookout of Progress. (2000) (In Slovak).

[2] Janas, P.; Krejsa, M.: *Use of Direct Determinate Probabilistic Solutions in SBRA*. In: proceedings if scientific works of VSB - Technical University Ostrava. 1 (2003) p.57-62 (6 pages), ISBN: 80-248-0572-3, ISSN 1213-1962 (In Czech).

[3] Janas, P.; Krejsa, M.; Krejsa, V.: *Structural Reliability Assessment Using Direct Determined Fully Probabilistic Calculation*. In: proceedings of 3rd International ASRA-Net Colloquium 2006. Glasgow (2006), ISBN 0-9553550-0-1/978-0-9553550-0-4.

[4] Tallin, A. G.; Cesare, M.: *Inspection Based Reliability Updating for Fatigue of Steel Bridges*. In: proceedings of Bridge Management Conference. London (1990).

[5] Tomica, V.; Gocál, J.: *Probabilistic Approach to Fatigue Cracks*. Journal Steel Structures 2 (2001) (In Czech).

[6] Tomica, V.; Krejsa, M.: *Solution of Fatigue Crack Propagation without Using Monte Carlo Simulation Technique*. In: Actual Trends in Highway and Bridge Engineering 2006. Iaşi, Romania (2006). ISSN 1842-628X

Reliability Analysis of Anti Symmetric Laminated Composite Plates by Response Surface Method

B. Chakraborty[1] & A. Bhar[2]

[1] Dept. of Civil Engg., Haldia Institute of Technology, West Bengal; India
[2] Dept. of Ocean Engg. & Naval Architecture, Indian Institute of Technology Kharagpur, West Bengal; India

1 Introduction

The use of laminated composite panels or plates in fabricating the structures has resulted in a significant increase in payload, weight reduction, speed and durability. Composite inherently possess high variability in material and geometric properties and involve a lot of uncertainties. These uncertainties result in dispersion in the material properties of the composite laminates. Accurate prediction of failure of composite structures has become more challenging to designers in the presence of inherent scatter in the material properties.

Most of the composite structure reliability analysis papers deals with in-plane direction loadings such as tension and compression [1-3]. ENGELSTAD et al. [4] and KAM et al. [5] studied the reliability of linear and nonlinear laminated composite plates subjected to transverse loading. REDDY et al. [6] and KAM et al. [7] studied the linear and nonlinear failure load based on MINDLIN's hypothesis deterministically. KAM et al. [8] studied the reliability formulation taking the strength parameters as random. JEONG and SHENOI [9] used KIRCHOFF's theory & direct simulation method to do reliability analysis of mid plane symmetric laminated plates. LIN and KAM [10] proposed probabilistic failure analysis of transversely loaded laminated composite plates using FOSM JEONG and SHENOI [11] used Monte Carlo Simulation to find out the probability of failure of anti symmetric rectangular FRP composite plates. Sensitivies of each basic random variable is also obtained by MCS. LIN [12] used stochastic finite element method for predicting the reliability of laminated composite plates by taking material properties as random. ONKAR et al. [13] studied the probabilistic failure of laminated composite plates using the stochastic finite element method.

In the present work a probabilistic analysis method has been adopted in order to predict the reliability based on the uncertainty of the random variables. The random variables are the anisotropic material properties of ply, ply thicknesses, length and width of the plate, loads, and lamina strengths. There is significant randomness in the material properties of composites. Another source of variation is the loading. The exact load distribution, its variation in

time, and its effect on composites for structural applications, are seldom deterministic. The proposed method combines (1) Structural Failure Analysis by FEM and (2) Probabilistic analysis in order to develop a reliability prediction algorithm for composite plates.

2   Composite Plate Theory

Consider a laminated composite plate of in-plane dimensions A and B and constant total thickness h, composed of thin orthotropic layers bonded together as in Fig. 1. The displacement field is assumed to be of the form

$$U(x, y, z) = u(x, y) + z\theta_x(x, y)$$

$$V(x, y, z) = v(x, y) + z\theta_y(x, y)$$

$$W(x, y, z) = w(x, y) \tag{1}$$

where U, V and W are the displacements in the x, y and z-directions at any point and u, v, w are the associated mid-plane displacements and θ_x and θ_y are the rotations about the y and x axes respectively.
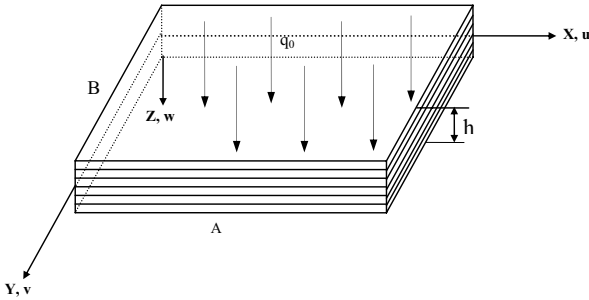
Fig. 1. Geometry of a laminated composite plate.

The strain-displacement for a plate using first order shear deformable theory can be expressed in the form

$$\begin{Bmatrix} \varepsilon_1 \\ \varepsilon_2 \\ \varepsilon_6 \\ \varepsilon_4 \\ \varepsilon_5 \end{Bmatrix} = \begin{Bmatrix} \dfrac{\partial U}{\partial x} \\ \dfrac{\partial V}{\partial y} \\ \dfrac{\partial U}{\partial y}+\dfrac{\partial V}{\partial x} \\ \dfrac{\partial V}{\partial z}+\dfrac{\partial W}{\partial y} \\ \dfrac{\partial W}{\partial x}+\dfrac{\partial U}{\partial z} \end{Bmatrix} = \begin{Bmatrix} \dfrac{\partial u}{\partial x} \\ \dfrac{\partial v}{\partial y} \\ \dfrac{\partial u}{\partial y}+\dfrac{\partial v}{\partial x} \\ \dfrac{\partial w}{\partial y}+\theta_y \\ \dfrac{\partial w}{\partial x}+\theta_x \end{Bmatrix} + z \begin{Bmatrix} \dfrac{\partial \theta_x}{\partial x} \\ \dfrac{\partial \theta_y}{\partial y} \\ \dfrac{\partial \theta_x}{\partial y}+\dfrac{\partial \theta_y}{\partial x} \\ 0 \\ 0 \end{Bmatrix} \tag{2}$$

or

$$\begin{Bmatrix} \varepsilon_1 \\ \varepsilon_2 \\ \varepsilon_6 \\ \varepsilon_4 \\ \varepsilon_5 \end{Bmatrix} = \begin{Bmatrix} \varepsilon_1^0 \\ \varepsilon_2^0 \\ \varepsilon_6^0 \\ \varepsilon_4^0 \\ \varepsilon_5^0 \end{Bmatrix} + z \begin{Bmatrix} \kappa_1 \\ \kappa_2 \\ \kappa_6 \\ 0 \\ 0 \end{Bmatrix} \tag{3}$$

where ε_1^0, ε_2^0, ε_4^0, ε_5^0 and ε_6^0 are the mid plane strains and κ_1, κ_2 and κ_6 are the curvatures of the laminated plate. The stress and the moment resultants defined by

$$(N_i, M_i) = \int_{-h/2}^{h/2} (1,z)\sigma_i dz$$

$$(Q_1, Q_2) = \int_{-h/2}^{h/2} (\sigma_5, \sigma_4) dz \tag{4}$$

Here $\sigma_i (i = 1,2....6)$ denote the stress components in the laminate coordinates $(\sigma_1 = \sigma_x, \sigma_2 = \sigma_y, \sigma_4 = \sigma_{zy}, \sigma_5 = \sigma_{xz}, \sigma_6 = \sigma_{xy})$.

3   Finite Element Formulation

The formulation of plate element has been carried out using eight-noded isoparametric quadratic elements with five degrees of freedom ($u, v, w, \theta_x, \theta_y$) per node.

The constitutive equation for the plate can be expressed as

$$\{\sigma\} = [D]\{\varepsilon\} \tag{5}$$

where D is the rigidity matrix of the plate given by $[D] = \begin{bmatrix} A_{ij} & B_{ij} & 0 \\ B_{ij} & D_{ij} & 0 \\ 0 & 0 & \bar{A}_{ij} \end{bmatrix}$;

$$(A_{ij}, B_{ij}, D_{ij}) = \sum_{k=1}^{N} \int_{z_{k-1}}^{z_k} \bar{Q}_{ij}^{(k)}(1, z, z^2)dz, \quad i, j = 1, 2, 6 \text{ and } \bar{A}_{ij} = \sum_{k=1}^{N} \int_{z_{k-1}}^{z_k} K_s \bar{Q}_{ij}^{(k)} dz, \quad i, j = 4, 5$$

where N is the number of layers of the laminate; z_k denotes the distance from the mid-plane to the lower surface of the kth layer; K_s is the shear correction coefficient and is equal to 5/6. $\bar{Q}_{ij}^{(k)}$ are the off-axis elastic constants of an individual lamina.

The derivation of stiffness matrix for a plate element has been done using standard finite element method [14] and finally we obtain the following

$$[K]\{\delta\} = \{P\} \tag{6}$$

Here δ is the column vector of the global displacements, K is the overall stiffness matrix of the P is the column vector of the force contributions. For details refer [14-16].

4 Computation of Layer-wise Stresses

The finite-element procedure described in the preceding section can be used to determine the stresses at any point of the laminate. The strain components at the mid-plane of the plate can be determined using

$$\{\varepsilon\} = [B]\{\delta\}_e \tag{7}$$

where $[B]$ and $\{\delta\}$ are the strain-displacement matrix and nodal-displacement vector for the plate element, respectively. The off-axis strains of individual lamina can be obtained using eq. (3). The strain components with respect to material axis system for the kth lamina are expressed by

$$\begin{Bmatrix} \varepsilon_1' \\ \varepsilon_2' \\ \varepsilon_6' \\ \varepsilon_4' \\ \varepsilon_5' \end{Bmatrix}^{(k)} = \begin{bmatrix} m^2 & n^2 & mn & 0 & 0 \\ n^2 & m^2 & -mn & 0 & 0 \\ -2mn & 2mn & m^2 - n^2 & 0 & 0 \\ 0 & 0 & 0 & m & -n \\ 0 & 0 & 0 & -n & m \end{bmatrix}^{(k)} \begin{Bmatrix} \varepsilon_1 \\ \varepsilon_2 \\ \varepsilon_6 \\ \varepsilon_4 \\ \varepsilon_5 \end{Bmatrix}^{(k)} \tag{8}$$

where $m = \cos \Phi$ and $n = \sin \Phi$ with Φ as the fiber orientation in the kth lamina. The on axis stresses at the kth lamina are calculated from the constitutive relationship

$$
\begin{Bmatrix} \sigma_1' \\ \sigma_2' \\ \sigma_6' \\ \sigma_4' \\ \sigma_5' \end{Bmatrix}^{(k)} = \begin{bmatrix} Q_{11} & Q_{12} & 0 & 0 & 0 \\ Q_{12} & Q_{22} & 0 & 0 & 0 \\ 0 & 0 & Q_{66} & 0 & 0 \\ 0 & 0 & 0 & Q_{44} & 0 \\ 0 & 0 & 0 & 0 & Q_{55} \end{bmatrix}^{(k)} \begin{Bmatrix} \varepsilon_1' \\ \varepsilon_2' \\ \varepsilon_6' \\ \varepsilon_4' \\ \varepsilon_5' \end{Bmatrix}^{(k)} \tag{9}
$$

here Q_{ij} (i,j = 1,2,4,5,6) denote the on axis elastic constants of kth lamina.

5 Method of Deterministic Failure Analysis

Initial failure of a layer within the laminate of a composite structure can be predicted by applying an appropriate failure criterion based on first-ply failure theory. There are various failure criteria two of which are discussed below.

5.1 Maximum Stress criterion

Failure of the material is assumed to occur if any one of the following conditions is satisfied:

$$
\sigma_1 > X_T ; \sigma_2 > Y_T ; \sigma_3 > Z_T ; \sigma_4 > R ; \sigma_5 > S ; \sigma_6 > T \tag{10}
$$

where σ_1, σ_2, σ_3 are the normal stress components; σ_4, σ_5, σ_6 are the shear stress components; X_T, Y_T, Z_T are the lamina normal strengths in the x, y and z directions respectively; R, S, T are the shear strengths in the yz, zx, xy planes respectively. When σ_1, σ_2, σ_3 are of compressive nature, then they should be compared with X_C, Y_C, Z_C, the normal strengths in compression in the x, y and z directions.

5.2 The Tsai-Wu criterion

The Tsai-Wu criterion can be expressed as

$$
F_i \sigma_i + F_{ij} \sigma_i \sigma_j \geq 1 \tag{11}
$$

where

$$
F_1 = \frac{1}{X_T} - \frac{1}{X_C}; \quad F_2 = \frac{1}{Y_T} - \frac{1}{Y_C}; \quad F_3 = \frac{1}{Z_T} - \frac{1}{Z_C}; \quad F_{11} = \frac{1}{X_T X_C}; \quad F_{22} = \frac{1}{Y_T Y_C};
$$

$$
F_{33} = \frac{1}{Z_T Z_C}; \quad F_{44} = \frac{1}{R^2}; \quad F_{55} = \frac{1}{S^2}; \quad F_{66} = \frac{1}{T^2}; \quad F_{12} = -\frac{1}{2\sqrt{X_T X_C Y_T Y_C}};
$$

$$
F_{13} = -\frac{1}{2\sqrt{X_T X_C Z_T Z_C}}; \quad F_{23} = -\frac{1}{2\sqrt{Y_T Y_C Z_T Z_C}}
$$

6 Reliability Analysis by Response Surface Method

The limit state equation or safety margin for a structural member can be defined by using strength and load parameters as follows, [17-19]

$$M = STRENGTH - LOAD = g(x_1, x_2, ...x_n) \qquad (12)$$

The failure of a structural member is defined when $M \le 0$ and the survival of structural member is defined when $M > 0$ as shown in Fig 2. Structural reliability estimation in the time-invariant domain therefore requires procedures for the evaluation of the n-dimensional integral for the failure probability P_f :

$$P_f = \int_{g(x)<0} p_x(x)dx \qquad (13)$$

where x is the vector of basic random variables described by the joint probability density function $p_x(x)$.
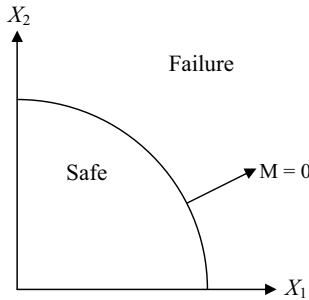
Fig. 2: Schematic Diagram of Failure and Safe Regions

There are number of methods in reliability analysis. These include Monte Carlo Simulation, First and Second Order Reliability Methods. In the implementation of FORM and SORM, the gradient of limit state function is required. In those cases where gradient is not easy to obtain their performance is affected. Monte Carlo simulation can be an alternate solution when the function is implicit but have a prohibitive computational cost in large structural systems.

The Response Surface method emerges as an alternative. Basically, the principle consists in the substitution of the real limit state function by approximate simple functions only at the neighbourhood of the design points so that the computational operations cost can be reduced with respect to the cost required when the real limit state function is used. Wong [20] proposed a response surface function, which has the polynomial form $g(x) = y = a_0 + \sum_{i=1}^{k} a_i x_i + \sum_{j<i=2}^{k} \sum a_{ij} x_i x_j$. FARAVELLI [21] used factorial designs and regression methods to obtain least square estimates of the unknown coefficients. To improve the

accuracy of the response surface method, BUCHER [22] proposed an adaptive interpolation scheme to arrive at the response surfaces. This procedure requires $4n + 3$ evaluations of $g(x)$. RAJASHEKHAR and ELLINGWOOD [23] showed that using a constant value of h may not always yield good solutions, particularly when g(x) is highly nonlinear. They demonstrated how a better fit of the response surface can be obtained by subsequent updating of the centre point and by lowering the value of the parameter h in subsequent cycles of updating. KIM and NA [24] proposed a sequential approach to response surface method MELCHERS and AHAMMED [25] proposed a method in which numerical results from a Monte Carlo reliability estimation procedure are converted to a form that will allow the basic ideas of the first order reliability method to be employed. Using these allows sensitivity estimates of low computational cost to be made.

The limit state function subjected to a given condition is defined in eq.

$$g(x) = g(x_1, x_2, x_3, ..., x_n) = 0 \qquad (14)$$

in which x are the set of basic random variables.

When $g(x)$ is described by only implicit form, the response surface method may be applied. Here the original implicit limit state is replaced by an approximate explicit function in terms of basic random variables. The response surface model can be of linear, linear with cross terms, quadratic and quadratic with cross terms. Depending on the nature of problem the type of model is chosen. Since the failure function is not highly nonlinear, a linear response surface model sufficiently gives good results. The response surface, approximated by a linear polynomial without cross terms may be written as

$$g(x) = y = a_0 + \sum_{i=1}^{k} a_i x_i \qquad (15)$$

Here the constants are determined by evaluating $g(x)$ at certain specified sampling points. Various techniques have been explored to select the sampling points and determine the coefficients. Saturated design method is one of these. It requires only the minimum runs for fitting a response surface model. The total number of the sample points for fitting a first order model is $p = k + 1$ and the total number of runs is $n = 2k + 1$ where k is the number of random variables taken. The points chosen are μ_i (mean values of the random variable x_i) and $\mu_i \pm h_i \sigma_i$. Here the center point is taken as μ_i and the corner points are taken as ($\mu_i \pm h_i \sigma_i$). h_i is taken as 1.0.

The equation (15) can be written in matrix form

$$\{y\} = [x]\{a\} \qquad (16)$$

where, y is a (n x 1) vector of the observations (responses); x is a (n x p) matrix of the independent variables; a is a (p x 1) vector of the regression coefficients

Least square technique is used to calculate the regression coefficients and the coefficients are obtained as

$$\{a\} = \left([x]^T[x]\right)^{-1}[x]^T\{y\} \tag{17}$$

Once the response surface has been adjusted a search is performed in order to find the minimum distance from the origin to this approximated limit state function. This distance gives the reliability index β and the corresponding point on the limit state function is the design point x_D. The position of the design point may be improved through interpolation of a new central point for the samples to be generated using the eq.

$$x_{Mi}^{j+1} = x_i^j + (x_{Di}^j - x_i^j)\frac{G(x^j)}{G(x^j) - G(x_D^j)} \tag{18}$$

Thus new $2k+1$ samples are generated in each iteration, centered on the new central point. Thus a total number of $(2k+1)j$ samples are generated, where j is the total number of iterations. This is continued till convergence. The final central point is taken as the design point. The Response Surface is constructed and finally we get an approximated $g(x)$ explicitly. The mean and the standard deviations of the newly constructed limit state function, when the random variables are normally distributed and independent can be expressed as

$$\mu_G = a_0 + a_1\mu_{x1} + a_2\mu_{x2} + \ldots + a_k\mu_{xk} \tag{19}$$

$$\sigma_G = \left[\sum_{i=1}^{k}(a_i\sigma_{xi})^2\right]^{1/2} \tag{20}$$

The probability of failure can be expressed as

$$P_f = 1 - \phi(\beta) = 1 - \left(\mu_G/\sigma_G\right) \tag{21}$$

For the non normal variables an equivalent normal means and standard deviations should be taken and the rest is similar to the case of normal variables.

7   Sensitivity Analysis

Sensitivity analysis has been carried out in order to identify the relative importance of parameters on failure probability. GUPTA and MANOHAR [26] propose global measures of sensitivity of failure with respect to the basic random variables by performing Monte Carlo Simulation. Because all input random variables do not have equal influence on the statistics of the output, a measure called the sensitivity index can be used to quantify the influence of each basic random variable [27]. α is the unit direction cosine vector and the elements of the vector are directly related to β with respect to the standard normal variables and given by

$$\frac{\partial\beta}{\partial u_i} = \alpha_i = \frac{a_i\sigma_{xi}}{\sigma_G} \tag{22}$$

These are related to the original variables and their statistical variation a unit sensitivity vector can be derived as

$$\gamma = SB^t \alpha \tag{23}$$

Here, S is a diagonal matrix of the standard deviations of the input variables or equivalent normal standard deviations for the non-normal random variables, B is a diagonal matrix of reciprocals of the standard deviations or equivalent normal standard deviations. If the variables are statistically independent, the product of SB^t will be a unit diagonal matrix. Therefore,

$$\gamma = \alpha \tag{24}$$

The elements of the vector γ are referred to as sensitivity indices of the individual variables.

8 Algorithm of the Proposed Method

The algorithm for the proposed method consists of six stages. (i) Selection of the basic random variables. (ii) Computation of maximum stresses in each layer by composite laminated plate theory and finite element analysis. (iii) Development of the limit state function based on the failure criteria. (iv) Construction of Response Surface and estimating the failure probability. (v) Computation of sensitivity indices of basic random variables. (vi) Reduction of random variables and estimating the final probability of failure.

9 Results and Discussions

In the present failure study of laminated composite plates, it is assumed that the ply is composed of laminate, which possess the same material properties throughout the thickness. The ply numbering is shown in Fig 3. The laminates considered for generating the results are made of glass/epoxy material with properties as listed below:

$E_{11} = 55.0$ GPa; $E_{22} = 18.0$ GPa; $G_{23} = 3.0$ GPa; $G_{12} = G_{13} = 8.0$ GPa; $\upsilon_{12} = 0.25$

The ultimate strengths for the above material which are used to calculate the strength parameters are defined as

$X_T = 1500.0$ MPa; $X_C = 1250.0$ MPa; $Y_T = 50.0$ MPa; $Y_C = 200.0$ MPa; $R = 75.0$ MPa; $S = T = 100.0$ MPa.

The coefficients of variation of the basic random variables are as: load = 0.25; material properties = 0.05; ultimate strengths = 0.125; geometric properties = 0.01.
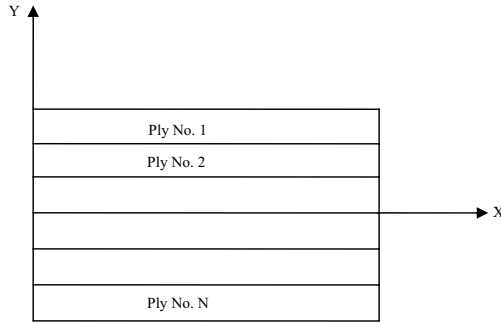
Fig 3. The Ply Numbering System of Laminated Composite Plate

9.1 Eight layer anti-symmetric laminated composite plates with various boundary conditions

Two different laminated plates of size 100 x 100mm with the following lay-ups schemes are used to illustrate the present method. These are

Ply scheme 1: [(0/90)$_4$]

Ply scheme 2: [(-45/45)$_4$]

Two different types of boundary conditions SSSS and CCCC (Fig. 4) are used to study the probabilistic failure of the laminates. Plate thickness ratio b/h = 100 has been used in this study.
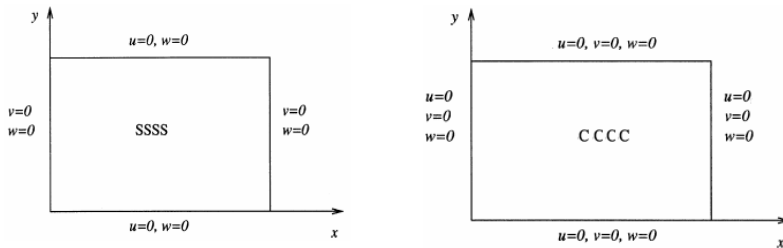
Fig. 4. Boundary conditions of a laminated composite plate.

The mean failure load predicted by Max. Stress and Tsai-Wu criteria for different ply lay-ups and boundary conditions are listed in Table 1. The results for the ply by ply failure analysis by max. Stress criterion for different ply lay-ups and different boundary conditions are presented in Table 2. The sensitivity analysis is carried out and sensitivity indices

are calculated for each basic random variable in case of both the ply schemes with different boundary conditions by the present method. These are compared with those obtained by FORM and presented in Table 3.

Table 1 Mean Failure load with different lay ups and boundary conditions

Ply lay-ups	Failure Criteria	Mean Failure load for boundary conditions (MPa)	
		SSSS	CCCC
$[(0/90)_4]$	Max. Stress	0.03964	0.05585
	Tsai-Wu	0.04062	0.05598
$[(-45/45)_4]$	Max. Stress	0.05092	0.08207
	Tsai-Wu	0.05218	0.08254

Table 2 Ply by ply failure analysis for different lay ups and boundary condition

Ply lay-ups	Ply No.	Probability of Failure	
		SSSS	CCCC
$[(0/90)_4]$	1	0	0.49985
	2	0	2.3168×10^{-2}
	3	0	7.4619×10^{-4}
	4	0	0
	5	0	0
	6	4.6831×10^{-4}	0
	7	4.385×10^{-2}	0
	8	0.49985	4.929×10^{-4}
$[(-45/45)_4]$	1	7.5817×10^{-4}	0.4999
	2	0	4.587×10^{-2}
	3	0	4.639×10^{-4}
	4	0	0
	5	0	0
	6	4.242×10^{-4}	0
	7	5.03×10^{-2}	1.1324×10^{-6}
	8	0.4992	1.0324×10^{-4}

Table 3(a) Sensitivity indices for different lay ups with SSSS boundary conditions

Sensitivity Indices	SSSS			
	$[(0/90)_4]$		$[(-45/45)_4]$	
	Present	FORM	Present	FORM
Failure Load	-0.8980	-0.8924	-0.8958	-0.8936
E_{11}	0.07915	0.0786	0.1226	0.1221
E_{22}	-0.1293	-0.1314	-0.1252	-0.1241
υ_{12}	-0.0209	-0.0203	-0.0319	-0.0318
G_{12}	0.04943	0.0486	0.0494	0.0489
G_{13}	1.312×10^{-6}	1.323×10^{-5}	9.993×10^{-7}	9.875×10^{-7}
G_{23}	3.5×10^{-6}	3.47×10^{-5}	2.665×10^{-6}	2.584×10^{-6}
Y_t	0.3992	0.413	0.3983	0.3942
A	-0.0127	-0.0132	-0.0357	-0.0348
B	-0.0585	-0.0574	-0.0357	-0.0353
h	0.0687	0.0683	0.0679	0.0674

Table 3(b) Sensitivity indices for different lay ups with CCCC boundary conditions

Sensitivity Indices	CCCC			
	$[(0/90)_4]$		$[(-45/45)_4]$	
	Present	FORM	Present	FORM
Failure Load	-0.8973	-0.8965	-0.8958	-0.8957
E1	0.1080	0.1074	0.0937	0.0934
E2	-0.1234	-0.1229	-0.1277	-0.1273
ν_{12}	0.0031	0.0025	-0.0232	-0.0228
G_{12}	0.0130	0.0123	0.0320	0.0315
G_{13}	0.0002	0.0002	0.0002	0.0001
G_{23}	0.0006	0.0006	0.0006	0.0006
Y_t	0.3987	0.3984	0.3984	0.3979
A	-0.0644	-0.0642	-0.0675	-0.0674
B	-0.0061	-0.0056	-0.0675	-0.0674
h	0.0676	0.0671	0.0676	0.0676

9.2 Effect of simultaneous variation of coefficients of variation of all random variables

The effects of material properties on reliability index of composite laminated plates under transverse random loading are now presented. The variations of reliability index with the

change in coefficients of variation of all basic random variables for all the plates with SSSS and CCCC boundary conditions are presented in Fig 5.

It is found that symmetric cross ply has more reliability index than the anti-symmetric cross ply and angle ply. The reliability index in case of simply supported plate is more than that of clamped.
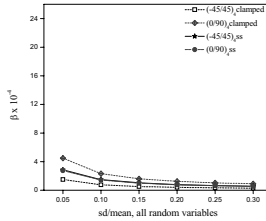
Fig 5. Influence of c.o.v. of all basic random variables simultaneously on β

9.3 Effect of variation of individual random variables

It is desirable to obtain the sensitivity of individual random variables on the reliability of plate. The influence of each basic random variable on probability of failure for all the ply schemes with SSSS and CCCC boundary conditions has been depicted in Figs. 6(a) – (i). From these figures we observe that:

(i) The variation of probability of failure is most affected by change in failure load. It is also significant for change in Y_T, E_{22} and E_{11}.

(ii) The least affect is due to the change in G_{12}, G_{13}, v_{12} and G_{23}.

(iii) The failure load, E_{22}, v_{12}, plate length and width have negative sensitivity whereas Y_T, E_{11}, G_{12}, G_{13}, G_{23} and plate thickness have positive sensitivity.
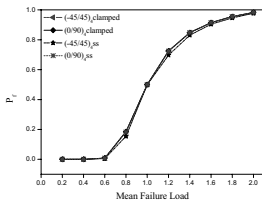
(a)
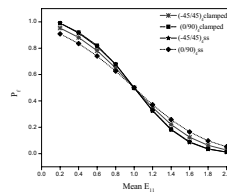
(b)
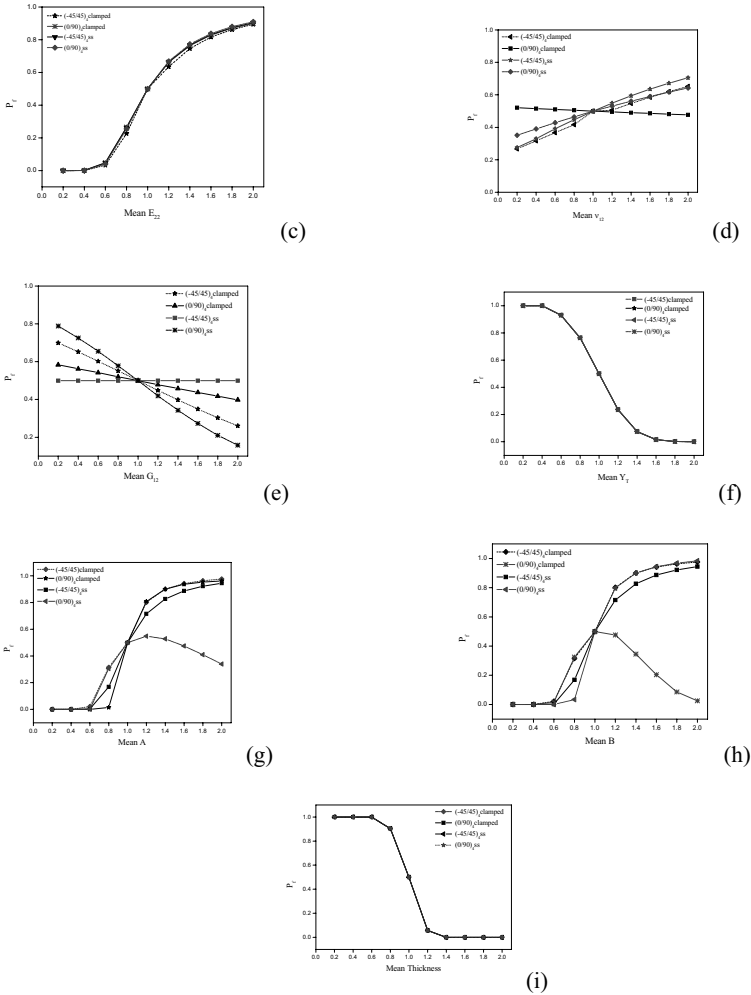
Fig. 6 Influence of individual basic random variable on P_f. Variation in (a) load, (b) E_{11}, (c) E_{22}, (d) υ_{12}, (e) G_{12} (f) Y_T, (g) Length, (h) Width, (i) Thickness

10   Conclusions

A probabilistic static failure analysis of composite laminates has been investigated with the help of response surface method. The approach has been validated by comparison with the results available in the literature. Applications of the proposed procedure has been demonstrated for the composite laminates with different lay ups and different boundary condi-

tions under transverse random loading. The conventional methods of reliability calculation for composite structures are FORM and MCS. MCS requires 10000 times run of the finite element program which is very cumbersome and in case of FORM finding gradient is very complicated. In response surface approach the finite element program will run only 70 times. This will save lot of computational time. In all the cases it is found that at the failure load the probability of failure of the laminate is 50% irrespective of the lay ups and boundary conditions. The approach can also be used to predict the sensitivity indices of the basic random variables. It has been shown that among all random variables the failure load has the greatest effect on the probability of failure. The failure load, E_{22}, υ_{12}, length and the width have negative sensitivity whereas E_{11}, Y_T and the thickness have positive sensitivity. Rest of the basic design variables have very less or no sensitivity at all. Variables with low sensitivity indices can be treated as deterministic at their mean values for subsequent reliability analysis. This will save a lot of computational time. It is expected that response surface approach would lead to fast and efficient estimation of probability of failure. Consequently, for the reliable and economic design of composite plates, it is important to reduce the computational time and selecting the random variables that have significant effect on the safety of the plate.

11   References

[1]   Cassenti BN. Probabilistic Static Failure of Composite Material. AIAA 1984; 22(1): 103-10.

[2]   Cederbaum G, Elishakoff I, Librescu L. Reliability of Laminated Plates via The First-Order Second Moment Method. Compos Struct 1990; 15: 161-7.

[3]   Guvrich M.R. and Pipes R.B. Probabilistic Strength Analysis of Four Directional Laminated Composites, Composite Science and Technology, 1996; 56: 649-656.

[4]   Engelstad SP, Reddy JN. Probabilistic Nonlinear Finite Element Analysis of Composite Structure. AIAA 1992; 31(2): 362-9.

[5]   Kam TY, Lin SC, Hsiao KM. Reliability Analysis of Nonlinear Laminated Composite Plate Structures. Compos Struct 1993; 25: 503-10.

[6]   Reddy YSN, Reddy JN. Linear and Nonlinear Failure Analysis of Composite Laminates with Transverse Shear. Compos Sci Technol 1992; 44: 227-45.

[7]   Kam TY, Sher HF, Chao TN, Chang RR. Predictions of Deflection and First-Ply Failure Load of Thin Laminated Composite Plates via the Finite Element approach. Int. J. Solids Struct 1996; 33(3): 375-98.

[8]   Kam TY and Chang ES, Reliability Formulation for Composite Laminates subjected to First Ply Failure, Composite Structures, 1997; 38: 447-452.

[9] Jeong HK, Shenoi RA. Reliability Analysis of Mid-Plane Symmetric Laminated Plates using Direct Simulation Method. Compos Struct 1998; 43: 1-13.

[10] Lin SC, Kam TY. Probabilistic Failure Analysis of Transversely Loaded Laminated Composite Plates using First-Order Second Moment Method. J. Engg. Mech ASCE 2000; 126(8): 812-20.

[11] Jeong HK, Shenoi RA. Probabilistic Strength Analysis of Rectangular FRP Plates using Monte Carlo Simulation. Computers & Struct 2000;76: 219-35.

[12] Lin Sc. Reliability Predictions of Laminated Composite Plates with Random System Parameters. Prob Engg Mech 2000; 15: 327-338.

[13] Onkar AK, Upadhyay CS, Yadav D. Probabilistic Failure of Laminated Composite Plates using the Stochastic Finite Element Method. Compos Struct; Article in press.

[14] Reddy JN, Pandey AK. A First-Ply Failure Analysis of Composite Laminates. Computers & Struct 1987; 25(3): 371-393.

[15] Reddy JN, Mechanics of Laminated Composite Plates and Shells; Theory and Analysis; Second Edition; CRC Press.

[16] Mukhopadhyaya M. Mechanics of Composite Materials and Structures; University Press; 2004.

[17] Ranganathan R. Reliability Analysis and Design of Structures. Tata Mcgraw-Hill Co. Ltd. 1990.

[18] Ditlevsen O. and Madsen H. Structural Reliability Methods. John Wiley & Sons, 1996.

[19] Ang AHS, Tang W. Probability Concepts in Engg. Planning and Design; Vol II. John Wiley & Sons. 1984.

[20] Wong FS. Slope reliability and response surface method. J Geo Eng ASCE 1989; 111: 32-53.

[21] Faravelli L. Response surface approach for reliability analysis. J Engg. Mech ASCE 1989; 115 (12): 2763-81.

[22] Bucher CG, Bourgund U. A fast and efficient response surface approach for structural reliability problems. Structl Safety 1990; 7: 57-66.

[23] Rajashekhar MR, Ellingwood BR. A new look at the response surface approach for reliability analysis. Structural Safety 1993; 12: 205-20.

[24] Kim SH, Na SW. Response surface method using vector projected sampling points. Structural Safety 1997; 19(1): 3-19.

[25] Melchers RE, Ahammed M. A fast approximate method for parameter sensitivity estimation in monte carlo structural reliability. Computers & Struct 2004; 82: 55-61.

[26] Gupta S, Manohar CS. An Improved Response Surface Method for the Determination of Failure Probability and Importance Measures. Structural Safety 2004; 26: 123-39.

[27] Haldar A, Mahadevan S. Reliability assessment using stochastic finite element analysis, John Wiley & Sons, 2000.

Robustness of externally and internally post-tensioned bridges

Bernard von Radowitz, Matthias Schubert and Michael Havbro Faber
Institute of Structural Engineering, ETH Zurich, Switzerland

Abstract: The quantitative assessment of the robustness of structures has been widely discussed in the recent decades. This paper starts out with an outline of a recently developed risk based methodology for the quantification of the robustness of structures which explicitly accounts for different damage states, the characteristics of the structure in regard to redundancy and for all consequences, direct and indirect. The framework is then applied to assess the robustness of an externally and internally post-tensioned highway bridge designed according to present best practice. The significance of different damage states on the robustness is investigated and the potential of the framework is highlighted through parameter studies. Finally different measures to increase the structural robustness are discussed.

1   Introduction

Robustness is widely discussed in the field of structural engineering; the ultimate aims are to concept and maintain structures such that these perform safely under both normal operational load conditions as well as under exceptional loads. The variety of different exposures is very large and also not always known; therefore not all possible loading conditions can be taken into account in practical codified design procedures. There are several experience based suggestions on how a sufficient robustness may be ensured through design provisions, however, there is so far no consensus among structural engineers in regard to how the effect of these design provisions may be quantified on the structural robustness. Present best practice design codes prescribe that structures must be robust but effectively we have not yet synthesized the attribute "robustness" in a manner where we quantify it in a standardized format. Since robustness is related to a variety of different system characteristics a methodology for the quantification of robustness has to account for such characteristics explicitly.

Design codes address primarily the design of individual structural components; if structural components are designed according to the design codes we can assume that the reliability

of the components is sufficient. However, the significance of the individual components for the integrity of the overall structural system is not addressed explicitly.

Recently a new risk based framework was developed by BAKER et al. [1], which differentiates between damage states and failure states in the system; correspondingly the consequence model differentiates between direct consequences and indirect consequences which are sometimes also denoted with follow-up consequences. The framework facilitates the incorporation of different human actions such as inspection and repair. Different system configurations can be assessed and compared according to their effect on the structural robustness.

The present paper focuses on the application of this framework to a realistic structure – a post-tensioned highway bridge of a type presently frequently applied in the development of the German roadway network. The main emphasis here is to investigate the effect of different deterioration caused damage states (such as stress-corrosion cracking, chloride induced corrosion as well as creep and shrinkage) on the structural robustness. The philosophy being that if we understand the effect of degradation on the robustness of structures then we may also in a more efficient manner make design provisions and strategically plan inspection and maintenance activities to ensure and maintain a sufficient structural robustness over the life time of the structure. Finally examples are provided to illustrate the various aspects of the robustness; different measures with the potential to increase the robustness are assessed and discussed.

The Eurocode (CEN [4]) specifies the requirement to structural robustness through the following provision; *the consequences of structural failure should not be disproportional to the effect causing the failure*. This provision does, however, not directly facilitate an assessment whether a design is robust or not. Implicitly, the provision includes system characteristics which are not yet accounted for in the codes. However, the formulation does give some guidance in regard to how risk based assessments may help to quantify the robustness of the structure.

Accidental exposures, such as impact, explosion and fire, are of special interest when assessing the robustness of structures; these exposures are generally rare and it would be incorrect to say that there exists a generally applicable and well tested design philosophy for such loads. Some of the exposures can surely be accounted for directly in the design procedures but for others this is not practical; they are either unknown, their effects cannot be accurately measured and in general accounting for these would make ordinary design very complicated. What is needed is a framework which facilitates that:

1) the robustness for specific exceptional structures not covered by normal design codes can be assessed

2) more ordinary different structural concepts can be assessed in regard to robustness such that simple provisions may be formulated and implemented in the ordinary design codes.

Such a framework has been proposed in BAKER et al. [1] and this will be outlined in the subsequent.

1.1 Event tree formulation

According to the generic risk assessment framework presently proposed by the Joint Committee on Structural Safety (JCSS) a system can be represented as a spatial and temporal representation of all constituents required to describe the interrelations between all relevant exposures and their consequences (FABER et al. [9]). The representation of a system can be modeled in an event tree as shown in Figure 1 .
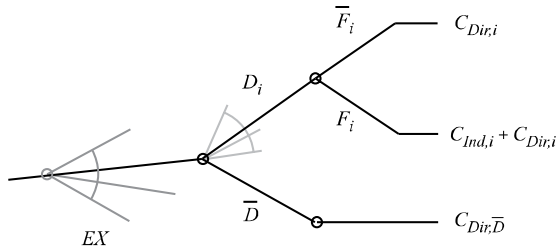
Figure 1: Event tree formulation.

First, an undamaged structure is considered, which is designed according to the design codes and requirements of the owner. During the lifetime the structure is subjected to different endogenous or exogenous exposures such as dead loads, life loads, deterioration processes and also accidental actions. Each exposure has the potential to cause damage to the components of the structural system. Exposure events can be either discrete or continuous over time. In Figure 1 the exposure is denoted by EX. After an exposure event occurs the components of the structural system can be either damaged D or undamaged $\overline{D}$. In general, no consequences are associated with undamaged states of the structure. However, in case of clearly observable exposure events such as accidents or extraordinary environmental loads, a reassessment of the structural components might be initiated to verify that the structure is still in an acceptable condition. In this case the event causes direct consequences ($C_{Dir,\overline{D}}$).

Direct consequences are defined as all consequences associated with damage of the structural components individually; thus not including consequences associated with the failure of the structural system. Indirect consequences are all consequences beyond the direct consequences (FABER and MAES [8]); thus only considering consequences due to the loss of the functionality of the structural system.

Apart from the situation, where all components of the structural system remain undamaged, different damage states are possible. These damage states are denoted with D_i (Figure 1). The damage state D_i may result in the failure of the entire structure (F_i). This failure mode may impose direct ($C_{Dir,i}$) and indirect consequences ($C_{Ind,i}$).

The case where the system sustain the damage state D_i without structural system failure is denoted by $\overline{F}_i$. By calculating the probabilities of all possible events in the event tree, the total risk can be calculated.

1.2   Risk calculation and the index of robustness

The total risk is defined as the expected value of the total consequences in a given time period. For the consistent assessment and management of risks in the built environment, all risks should be expressed as annual risks (RACKWITZ [19]).

The direct risk is calculated by the consideration of all events which lead to direct consequences:

$$R_{Dir} = \int\limits_{EX} \int\limits_{D} C_{Dir}(D)\, p(D\,|\,EX)\, p(EX)\, dEX\, dD \tag{1}$$

The indirect risk can be calculated analogously:

$$R_{Ind} = \int\limits_{EX} \int\limits_{D} C_{Ind}(F)\, p(F\,|\,D,EX)\, p(D\,|\,EX)\, p(EX)\, dEX\, dD \tag{2}$$

By summing up the direct and the indirect risk the total risk R_{Tot} is obtained. The index of robustness is then defined by:

$$I_{Rob} = \frac{R_{Dir}}{R_{Dir} + R_{Ind}} = \frac{R_{Dir}}{R_{Tot}} \tag{3}$$

The index accounts not only for the characteristics of the structural performance but also for the behavior of the system after damage and all relevant consequences. Furthermore, all measures (decision alternatives), which can be implemented either to improve the structural performance in regard to robustness or to decrease the vulnerability (increasing component reliability), are explicitly accounted for.
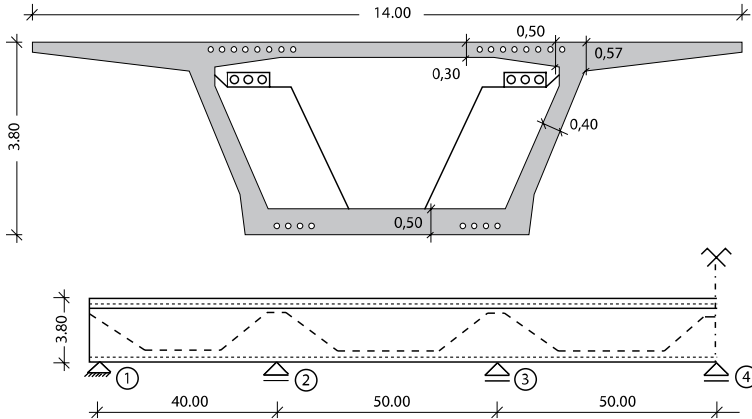
Figure 2: Cross section and longitudinal section of the considered post-tensioned bridge.

2   Application of the framework

In the present paper the introduced framework is applied to a general type of post-tensioned box girder bridge typically used in the German roadway network. Considering the high construction costs and the high consequences of failure, a robust design is of utmost importance.

The portfolio of infrastructural buildings in Europe contains many post-tensioned concrete beam bridges. Different pre-stressing and post-tensioning systems are applied. Post-tensioning systems can be differentiated in systems with bonded tendons and tendons without bond. The considered bridge is shown in Figure 2. It consists of six spans with 40 m and 50 m lengths. 16 bonded internal post-tensioning tendons are located inside the top and eight tendons in the bottom flange with a cross-sectional area of $1800\ mm^2$ each. In the longitudinal section in Figure 2 the internal tendons are illustrated by a dotted line. The dashed line in Figure 2 shows the alignment of the six external post-tensioning tendons without bond inside the box girder. They have a cross-sectional area of $1680\ mm^2$ per tendon. The box girder is constructed using a C 30/35 concrete according to Eurocode 2 (CEN [3]). In general the internal post-tensioning is built-in for different limit states during the construction phase and to carry dead loads. The external tendons are designed for live loads. The advantage of external tendons is easy maintenance and replacement if necessary.

This type of bridge can be considered as a generic type of bridge. It reflects the characteristics of most of the existing bridges. Its slenderness, e.g. the ratio of the span length and height, is close to the statistical average for this type of bridges in Germany (VON RADOWITZ [26]).

One assumption underlying the proposed index of robustness is that the design of the structure is conducted according to existing codes which implies that the direct risks are already acceptable by society; the individual members are designed to fulfill component

reliability requirements. In the design the considered load cases are dead loads, traffic loads, temperature loads and loads due to post-tensioning. Those loads are generally decisive for the design. Furthermore, the influences due to creep and shrinkage of the concrete and relaxation of the post-tensioning tendons are taken into account. The bridge is designed according to the Eurocodes for the Ultimate Limit State (ULS) and Serviceability Limit State (SLS), as well as for decompression aiming at an un-cracked concrete during the bridge's design lifetime of 100 years. All calculations for the design are performed using the finite element code SOFiSTiK AG [23].

In order to provide a sufficient robustness the Eurocode requires minimum structural reinforcement which aims to provide enough structural capacity to prevent brittle failure. In the case of sudden post-tensioning losses cracks are often not visible and failure occurs without any warning. The minimum required reinforcement ensures ductility and helps to prevent unwarned failure. This facilitates emergency and evacuation actions to prevent fatal losses of life and thereby to minimize the consequences. The design codes denote this type of reinforcement as robustness reinforcement.

Engineering modeling problems usually are associated with uncertainties; models and parameters involved in the models may be subject to natural variations but also lack of knowledge and insufficient data may add to uncertainty. In recent design codes it is attempted to incorporate these uncertainties directly into the design concept using principles of reliability based code calibration, see e.g. FABER and SORENSEN [10].

Explicit reliability analysis and risk calculations require the consideration of the variations of all variables and models used in the assessment. In the following the modeling of all uncertain parameters and models for the considered bridge is outlined in accordance with the Probabilistic Model Code of the Joint Committee on Structural Safety (JCSS [12]): The risk analysis is performed according to FABER et al. [9].

2.1 Modeling of the system exposures

2.1.1 Dead and live loads

In the following the modeling of the system exposures is presented. The dead loads are assumed to be uncertain represented by Gaussian distributed random variables. They include loads from the parapet, rim beam, railing, wearing surface and the self weight of the box girder including reinforcement and the post-tensioning strands. According to STEWART et al. [24] it is assumed that the resulting dead load is Gaussian distributed with a coefficient of variation of $CoV = 0.1$. Loads due to temperatures and settlements are modeled explicitly and the associated uncertainties are incorporated in the model uncertainties. The live traffic loads are also assumed uncertain and modeled probabilistically according to MEHLHORN [14]. Here it is assumed that the left lane of the two lane bridge is restricted to passenger cars. The effects due to creep and shrinkage of the concrete are calculated according to DAFSTB-525 [5] taking into account non-linear creep effects. The methodology and the assumed boundary conditions are shown in detail in VON RADOWITZ [26]. Expected stress losses due to relaxation of the post-tensioning wires at time t are assumed to be Gaussian distributed with $CoV = 0.3$ according to JCSS [12].
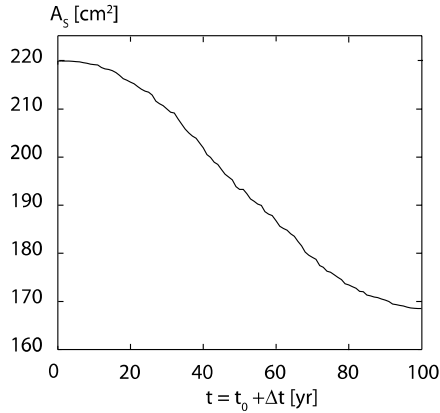
Figure 3: Expected value of the remaining reinforcement over time t.

2.1.2   Chloride induced corrosion

Most Europe bridges are subjected to chlorides either due to the usage of de-icing salt or due to their near shore location. It can be seen as one of the main deterioration inducing exposures of bridges. The chloride induced corrosion can be modeled in two separate phases; an initiation phase and subsequently a damage propagation phase. The transport process of the chlorides through the concrete cover to the reinforcement is modeled as being diffusion; this process may thus be described by Fick's law (DURACRETE – BRITE EURAM III [6]).

When the chloride concentration reaches a critical value C_{crit} at time t_0, the initiation phase is over and the corrosion of the reinforcement starts to propagates. A Monte-Carlo-Simulation (MCS) (see e.g. MELCHERS [15]) is applied to determine the probability of chloride propagation at time t_0. The velocity of the corrosion process is modeled according to DURACRETE – BRITE EURAM III [6]. The expected value of the remaining reinforcement area at time $t_0 + \Delta t$ including all uncertainties, is shown in Figure 3. Details of the used model are given in FABER and GEHLEN [7] , GEHLEN [11] and in DURACRETE – BRITE EURAM III [6].

2.1.3   Stress corrosion cracking

For the considered type of structure stress corrosion cracking under high post-tensioning stresses has been found to be of significant importance (PETERSEN [18]). MAES et al. [13] uses a model to calculate the time to micro crack propagation to estimate the corrosion progress. This model is based on a damage parameter D which is dependent on the material, the environment and the stress. A detailed description of the applied methodology

can be found in VON RADOWITZ [26]. The highest tensile stresses occur in the top flange of the box girder above support 2 (see Figure 2). In VON RADOWITZ [26] it is shown that only those 16 tendons in the top flange are affected to stress corrosion cracking in the considered lifetime of the structure. Each of the 16 strands in one tendon is comprised of seven wires with a diameter of $15,7\,mm$ each. For simplicity, a wire is considered as failed when half of its diameter is corroded. The strand is assumed to be failed if four of its wires are failed. In Figure 4 the expected number of failed strands at time t is shown.
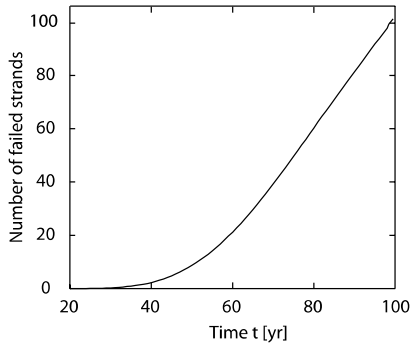
Figure 4: Expected value of the number of failed strands over time t.

2.2 Modeling of the system vulnerability

For the probabilistic modeling of the structural system performance each considered material resistance has to be represented in accordance with its assumed density function. All random variables related to the applied material resistances are summarized in Table 1.

Table 1: Material characteristics.

Type of material resistance	Mean Value	Distribution	CoV	Reference
Concrete capacity	38 MN/m²	ND	0.128	MÜLLER [16]
Reinforcement capacity	560 MN/m²	ND	0.038	JCSS [12]
Post-tensioning (PT) steel capacity	1630 MN/m²	ND	0.025	JCSS [12]
Internal PT steel area	0.0018 m²	ND	0.025	JCSS [12]
External PT steel area	0.00168 m²	ND	0.025	JCSS [12]

The presented corrosion exposures are assumed to act simultaneously and independently from each other. The probability for a corrosive environment is dependent on the location. In this study generic values are chosen to calculate the probability of corrosion. At the same time effects due to creep and shrinkage are considered and exposures due to loads are applied. The damage states are integrated in the analysis by using the calculated loss of post-tensioning wires and the corroded reinforcement area, whereas the probability of

failure includes the probability of each damage state. This approximation reduces the amount of simulations necessary to estimate the robustness. The approximation is given in SCHUBERT [22]:

$$I_{Rob} = \frac{\sum_i P_{D,i} \cdot C_{Dir,i}}{\sum_i P_{D,i} \cdot C_{Dir,i} + P_F \cdot C_{Ind}} \approx \frac{P_{D,1} \cdot C_{Dir,1}}{P_{D,1} \cdot C_{Dir,1} + P_F \cdot C_{Ind}} = \frac{C_{Dir,1}}{C_{Dir,1} + \frac{P_F}{P_{D,1}} \cdot C_{Ind}} \tag{4}$$

where $P_{D,i}$ is the probability for the damage state i, P_F the probability of failure of the structural system, $C_{Dir,i}$ is the direct consequence associated with the damage state i and C_{Ind} is the indirect consequence. This approximation holds if one damage state dominates the risk calculation. Using this approximation only the direct consequences for the relevant damage states are estimated.

Based on cost estimates for a bridge in Germany (VOCKROD and FEISTEL [25]) the consequence model is established. The expected values of the different kinds of consequences are given in Table 2.

Table 2: Summary of the considered direct consequences.

Type of the consequences	Expected value [10^3 €]
Administrative costs and planning	42
Traffic organization	200
Safety precautions	50
Repair and maintenance costs	940

The expected value of the total direct consequences for planning, traffic organization, safety measures and repair maintenance costs sum up to 1,203,800 €.

2.3   Modeling of the system robustness

For the risk based analysis the specific probabilities of failure depending on the considered damage states at any given time are calculated. For this analysis the limit state function is formulated for the cross section at a location just above the second support (see Figure 2).

A failure state is reached if the internal moment due to exposures exceeds the internal moment of the resistance. Here, the probability of failure at each point in time is calculated using MCS. The model uncertainties are approximated by a lognormal distributed random variable with a mean value of 1 and a CoV of 0.2. The indirect consequences are defined as all consequences beyond the direct consequences which are associated with the failure state. One type of indirect consequences is the number of possible fatalities in the case of bridge failure. Taking into account all failure modes where evacuation action could be performed, the expected number of fatalities given failure in this example is estimated to 2.62.

A consistent basis to include aspects of life safety into the decision making is provided by the Life Quality Index (NATHWANI et al. [17]). The underlying idea of the LQI is to model the preferences of a society as an indicator comprised by a relationship between the GDP per capita, the expected life at birth and the proportion of life spend for earning and living. Using the LQI the value of a statistical live can be derived for the society and it can be included in the risk analysis (RACKWITZ [20]). Using the LQI for Germany the value of a life is estimated to be 3.38 million € according to RACKWITZ [21] assuming an interest rate of 3%.

Another type of the indirect consequences is the user costs for the highway user. These consequences are taken from the provisions of the BRD [2] and summarized in Table 3. Additionally the costs for the reconstruction have to be taken into account. Those costs contain costs for deconstruction, planning and design of the new bridge, traffic organization, safety precautions and new construction for an assumed construction time of one year.

Table 3: Summary of the considered indirect consequences.

Type of the consequences	Expected value [10^3 €]
User costs	24,013
Operational costs	15,386
Administrative costs and planning	318
Safety precautions	10
Deconstruction	2,000
Reconstruction	6,800

Table 3 illustrates the large contribution from the user costs. They are calculated on the basis that the bridge is closed for one year in case of failure. This type of consequences has a large impact on the decision making and the assumptions underlying their quantification should be a subject for further research.

2.4   Results

The result of the MCS for the annual probability of failure is shown in Figure 5. The values of the annual probability of failure ranges between 10^{-6} and $6 \cdot 10^{-2}$. The time evolution of the probability of failure can be divided into three periods. It can be observed that in the first 20 years the increase of the probability of failure is quite high. The main effects leading to this development is creep and shrinkage of the concrete. After 20 years both effects can be regarded insignificant. In the second period the increase of the failure probability is mainly driven by chloride corrosion. This period ends after about 80 years with a maximum probability of failure of about $5 \cdot 10^{-3}$. After 80 years approximately 60 % of the internal post-tensioning wires in the top flange are ruptured. The failure probabilities seem to be very high but they are comparable with results obtained by MAES et al. [13] and reported by MELCHERS [15] for similar conditions assuming no maintenance. However, MELCHERS [15] recommends to perform maintenance action in cases where the failure probability exceeds a range between 10^{-3} and 10^{-4}. In this example this level is reached after 20 years which corresponds to a normal interval for maintenance actions.

In the last period, between 80 and 100 years the failure probability increases significantly. Until this point in time the strands can be regarded as a parallel system with the potential to redistribute the loads to different wires. After 80 years the post-tensioning wire losses and reinforcement losses are too high to provide reserve capacity to prevent a failure of the system; the system fails as a series system. A failure of additional wires leads directly to a progressive failure. At the end of the design lifetime 102 of the 196 wires of the internal post-tensioning tendons in the top flange are ruptured and approximately 23 % of the reinforcement is corroded.
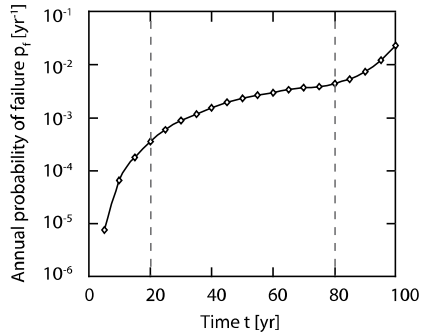
Figure 5: Annual Probability of failure of the system.

Based on calculations of the probability of failure under consideration of the different damage states and the direct and indirect consequences the index of robustness can be calculated. The result is shown in Figure 6.
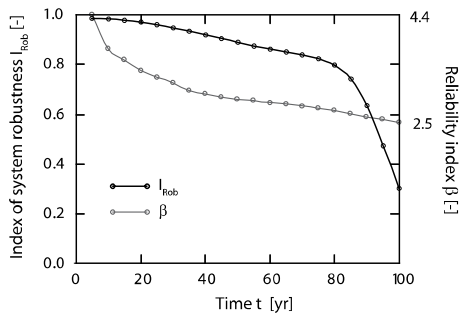
Figure 6: Index of robustness (black line) and the reliability index for the system without consideration of the damage states (grey line).

The index of robustness reflects the significant influence of post-tensioning wire losses after about 80 years. That indicates that the expected value of the indirect consequences

increases faster than the expected value of the direct consequences. Especially the user costs contribute significantly to the indirect risks. Under consideration of the system definition and the applied consequence model a strong decrease of the index of robustness after 80 years indicates that additional damage in the structure lead to progressive collapse with a high probability. In Figure 6 the corresponding reliability index β for the system is shown. The reliability index is calculated for the cross-section of the bridge without taking system effects and damage states into account. It is based on the code regulations and it underestimates the situation at hand in the last 20 years of the lifetime of the structure. That illustrates that damage states and system effects contribute significantly to the total risk.

2.4.1   Measures to increase the robustness

Apart from proposed actions in the design process like additional alternative load paths providing redundancy or specific means of construction like monolithic connections avoiding critical joints or bearings two further options are discussed for the bridge structure to provide additional robustness.

Especially the bonded post-tensioning wires are subject to stress corrosion cracking. Whereas external tendons can be maintained, post-tensioned in the case of post-tensioning losses and exchanged if necessary or further tendons can be added. Thus effects due to stress corrosion cracking can be avoided. However, due to higher construction costs exclusively external tendons inside the box girder are not generally applied, but in order to take advantage of post-tensioning wires in the flanges the tendons are constructed as wires in pipes without bond located inside the flanges. Chloride induced reinforcement corrosion can not be neglected. Such a structural system is investigated and the effects on the robustness are illustrated in Figure 7.
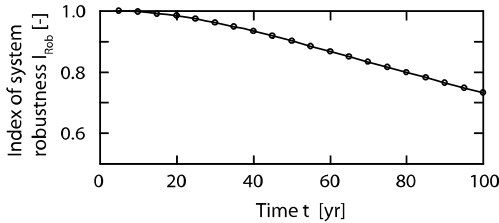
Figure 7: Index of robustness for a system using external post-tensioning tendons.

Obviously in the range up to 80 years the effects due to the corrosion of the reinforcement dominate and the effects due to stress corrosion cracking are compensated by the robustness reinforcement. After 80 years further reinforcement corrosion reduces the robustness, but the robustness can be improved by up to approximately 50 %. The strong effect on the index after 80 years due to progressive failure can be avoided.

3 Conclusions

In this paper a recently developed framework for the quantification of robustness is summarized and applied to a generic type of externally and internally post-tensioned box girder bridge. Different aspects of the reliability of such bridges are discussed and the robustness is quantified.

It is observed that the damage states in the internal tendons have a large influence on the failure probability and on the robustness of the system. If the loss of post-tensioning wires and reinforcement bars increase, the system acts as a series system and any additional damage states can lead to progressive failure of the bridge. The explicit consideration of the damage states of the structural system facilitates the assessment of the performance of different system configurations. Here, different types of post-tensioning, namely external post-tensioning and internal post-tensioning are investigated and it is shown that these configurations lead to large differences in the robustness over the life-cycle of the structures. By changing the post-tensioning system the corrosion effects can be minimized and the structural robustness is improved.

It is shown that the robustness decreases rapidly if the conditional probability of failure $P(F \mid D, EX)$ increases in the system. One measure to increase the robustness is therefore to decrease this conditional failure probability. Other measures – which lead to the same result – could aim to reduce the indirect consequences. Redundancy in the roadway network would significantly reduce the user costs. Such measures directly increase the index of robustness. The index of robustness, proposed by BAKER et al. [1], can be seen as a measure for the performance of the whole considered system, including damage states and all consequences. The index of robustness is therefore more a characteristic of the system than a characteristic of the structure.

The present paper focuses on the application of the proposed framework for assessment of structural robustness to a specific type of structure being part of a larger system. Further research is thus still needed to develop a general basis for the codification of provisions for robust design. To proceed in this task different relevant and representative structure classes with specified consequences should be considered and the indexes of robustness should be calculated. This would provide more general insights on the efficiency of different provisions for robust design for different classes of structures and thus facilitate an improvement of present date design codes.

4 References

[1] Baker, J. W., Schubert M.; Faber M. H: *On the assessment of robustness*. Journal of Structural Safety, in press. 2007

[2] BRD. *Bundesverkehrswegeplan: Grundlagen für die Zukunft der Mobilität in Deutschland*. Bundesministerium für Verkehr Bau- und Wohnungswesen. Bonn, Germany. 2003

[3] CEN. *Eurocode 2 - design of concrete structures*, European Committee for Standardization. European Prestandard ENV 1992-1-6. 1992

[4]   CEN. *Eurocode 1 - actions on structures part 1 - basis of design*. , European Committee for Standardization. European Prestandard ENV 1991-1: 250. 1994

[5]   DAfStb-525.   *Erläuterungen   zu   DIN   1045-1*. Deutscher Ausschuss für Stahlbetonbau, Beuth Verlag. 525. 2003

[6]   DuraCrete – Brite EuRam III: *DuraCrete, Final Technical Report*. DuraCrete: Probabilistic Performance based Durability Design of Concrete Structures, The European Union; Contract BRPRCT95-0132, Project BE95-1347. 2000

[7]   Faber M.H.; Gehlen M.A.: *Probabilistischer Ansatz zur Beurteilung der Dauerhaftigkeit von bestehenden Stahlbetonbauten*, Beton- und Stahlbetonbau 97(8): 421-429. 2002

[8]   Faber M.H.; Maes M.A.: Modeling of Risk Perception in Engineering Decision Analysis. *Proceedings 11th IFIP WG7.5 Working Conference on Reliability and Optimization of Structural Systems*, Banff, Canada. 2003

[9]   Faber, M. H., Maes M. A., Baker J. W., Vrouwenvelder T.; Takada T.: Principles of Risk Assessment of Engineered Systems. *10th International Conference on Applications of Statistics and Probability in Civil Engineering*, The University of Tokyo, Kashiwa Campus, Japan. 2007

[10]   Faber, M. H., Sørensen, J. D.: Reliability based code calibration - the JCSS approach. *Proceedings to the 9th International Mechanisms for Concrete Structures in Civil Engineering ICASP*, University of Berkley, Berkley, USA. 2003

[11]   Gehlen, C.: *Probabilistische Lebensdauerbemessung von Stahlbetonbauwerken Zuverlässigkeitsbetrachtungen   zur   wirksamen   Vermeidung   von Bewehrungskorrosion*. PhD Thesis, RWTH Aachen, 2000

[12]   JCSS: *Probabilistic Model Code*, The Joint Committee on Structural Safety, online available: www.jcss.ethz.ch. 2001

[13]   Maes, M. A., Wei X.; Dilger W. H.: Fatigue reliability of deteriorating prestressed concrete bridges due to stress corrosion cracking. *Canadian Journal of Civil Engineering* 28: 673-683. 2001

[14]   Mehlhorn, G.: *Tragwerkszuverlässigkeit, Einwirkungen. Berlin*, Ernst & Sohn. 1996

[15]   Melchers, R. E.: *Structural Reliability Analysis and Prediction*, John Wiley & Sons. 2002

[16]   Müller, H: *Skriptum Baustoffkunde und Konstruktionsbaustoffe*. Institut für Massivbau und Baustofftechnologie Karlsruhe, Germany, University of Karlsruhe. 2006

[17]   Nathwani, J. S., Lind N. C.; Pandey M. D.: *Affordable Safety by Choice: The Life Quality Method*. Waterloo, University of Waterloo. 1997

[18]   Petersen, C.: *Stahlbau : Grundlagen der Berechnung und baulichen Ausbildung von Stahlbauten*. Braunschweig, Vieweg. 1993

[19]   Rackwitz, R.: Optimization - the basis of code-making and reliability verification. *Structural Safety* 22(1): 27-60. 2000

[20]   Rackwitz, R.: Optimization and risk acceptability based on the Life Quality Index. *Structural Safety* 24(2-4): 297-331. 2002

[21]   Rackwitz, R.: The effect of discounting, different mortality reduction schemes and predictive cohort life tables on risk acceptability criteria. *Reliability Engineering & System Safety* 91(4): 469-484. 2006

[22]   Schubert, M.: Probabilistic Assessment of the Robustness of Structural Systems. *6th International PhD Symposium in Civil Engineering*, Zurich, Switzerland. 2006

[23]   SOFiSTiK AG: *SOFiSTiK Structural Desktop - SSD; FEM & CAD Software für den Ingenieurbau*. Nürnberg, Germany. 2007

[24]   Stewart, M. G., Rosowsky D. V.; Val D. V.: Reliability-based bridge assessment using risk-ranking decision analysis. *Structural Safety* 23(4): 397-405. 2001

[25]   Vockrod, H.-J.; Feistel D.: *Handbuch Instandsetzung von Massivbrücken Untersuchungsmethoden und Instandsetzungsverfahren*. Basel, Switzerland, Birkhäuser. 2003

[26]   von Radowitz, B.: *Robustheit von Balkenbrücken mit externer und interner Vorspannung*. Institut für Massivbau und Baustofftechnologie, Abteilung Massivbau. Karlsruhe, Universität Karlsruhe: 103. 2007

Traffic load effects in prestressed concrete bridges

D.L. Allaix [(1)], A.C.W.M. Vrouwenvelder [(2)] & W.M.G. Courage [(3)]
[(1)] Polytechnic of Turin, Turin, Italy
[(2)] Delft University of Technology, Delft, The Netherlands.
[(3)] TNO Built Environment and Geosciences, Delft, The Netherlands.

Abstract: The traffic load effect in a two-span prestressed concrete bridge with two traffic lanes is analyzed in this paper. The design value of the resulting bending moment in some prescribed sections is estimated by means of a Monte Carlo simulation. The model for the vehicular loads is derived from a set of measurements done in The Netherlands in 2004. A two dimensional dynamic model is adopted and the interaction between the vehicles and the bridge is considered in the evaluation of the dynamic amplification factor. The structure is modelled by 2D beam elements and the spatial variability of the material stiffness properties is described by a random field. A numerical technique, based on the Karhunen-Loeve expansion, is used to represent the random field by a finite set of random variables. The influence of the spatial variability is also investigated.

1   Introduction

The research in the area of bridge engineering has been focused mainly on the modelling of the structural behaviour and a limited number of investigations have been carried out in the field of the traffic load modelling. Recently, the safety evaluation of the road bridges built during the past decades became an important topic due to its economical relevance. Due to the deterioration and damage, an existing structure may not satisfy the safety requirements included in the actual safety codes. Consequently, a better knowledge of the real loads applied to the bridge and of the structural resistances is desirable to evaluate the reliability of the structure and to define decision criteria. A refined traffic load model, based on recent measurements done in The Netherlands, is presented. The gross weight, axle loads and axle distances of the lorries are described by random variables, whose parameters are estimated from the observed data. The modelling of the gross weight requires particular care in the upper tail of the distribution, which is dominant for the ultimate states. The coupling of the Monte Carlo method with a structural solver is used to simulate a stochastic traffic flow approaching a two-span prestressed concrete bridge and to evaluate the traffic induced bending moment by a static and dynamic analysis. The design value of the bending moment in two cross sections of the structure are extrapolated from the dis-

tribution of the maximum daily bending moment. The geometrical and material properties of the bridge are described by a probabilistic approach, involving random variables and random fields. A numerical procedure for the discretization of continuous random fields is employed. The results of the aforementioned simulations are compared with the corresponding design stress calculated according to the Eurocodes.

2   Recent measurements

In the following, a summary of the analysis of a set of measurements conducted by the Rijkswaterstaat, Dienst Weg-en Waterboukunde (RWS DWW) from the 25th of April 2004 to the 31st of October 2004 [1]. The data were collected by a Weigh-In-Motion (WIM) system on the highway A16 in the neighbourhood of the Moerdijk bridge in The Netherlands. The database contains 1,301,163 records, each one describing a truck passage. The size of the database is large if compared, for example, to the measurements used in the background documents of the EN 1991, *Eurocode 1: Actions on structures – Part 2: Traffic loads on bridges* [2]. The length of the measurement period and the significant amount of data can be considered as representative of heavy traffic present in The Netherlands. The date, time, velocity axle loads and relative axle distances were registered for each vehicle. The accuracy of the system of weighing the trucks travelling on the highway is stated in probabilistic terms as follows: in at least 95% of the cases, the relative deviation between the measured and the static loads is not larger than 15%. This statement can be formulated as follows:

$$P[L_{static}(1-\delta) \leq L_{measured} \leq L_{static}(1+\delta)] \geq 1-\alpha \qquad (1)$$

where:

- $L_{measured}$ is the measured axle load;

- L_{static} is the corresponding static load;

- δ is half of the width of the confidence interval centred on L_{static} at the confidence level *(1-α)*, where $\alpha = 0.05$.

The value of $\delta = 15\%$ is in agreement with the recommendation of the European research project COST 323 [3] to meet the required accuracy with respect to the static loads. It is questionable if the accuracy of the measurements has implications on the assessment of traffic loads effects. Recently, an investigation of the influence of the aforementioned accuracy of the WIM data on the prediction of extreme load effects has been exploited [4]. The conclusion of the investigation was that the accuracy of the WIM data plays an important role only for short span lengths, where the axle load governs the prediction of the extreme load effects. On the contrary, as the span length increases, the importance of the vehicular load increases with respect to the axle load. The inaccuracy of the measured data has not a significant influence on the predicted extreme load effects. Therefore, the difference between the static and the measured loads is negligible for the span length chosen for this paper. Nevertheless, the measured data can, in principle, contain other errors. Three

filtering criteria were applied to the collected data to exclude unreasonable data before further analysis and modelling:

- the vehicles have at least two axles;

- the vehicles with an axle load greater than 300 kN are deleted (this criterion was suggested by DWW);

- the minimum relative distance between two consecutive axles is 0.75 m.

After applying the filtering criteria, the database was reduced to 1,295,211 records. A wide range of vehicle types were registered including buses, single and articulated lorries and lorries with a trailer. The number of axles varies between two (small lorries) and ten (road trains and special vehicles). The percentage composition of the traffic with respect to the number of axles is listed in table 1.

Tab.1: Traffic composition

Number of axles	Frequency [%]
2	10.53
3	5.81
4	23.32
5	51.99
6	5.50
7	0.49
8	0.21
9	0.09
10	0.05

The lorries with five axles, made up of a truck with two axles and a semi-trailer with three axles represent approximately half of the measured traffic flow. This percentage is in agreement with the heavy traffic composition in other european countries. For each class, the minimum and maximum observed vehicular loads are listed in table 2. Regarding the minimum weight, it is clear that also passages of unloaded vehicles with two, three and four axles were registered. The column of the maximum weight shows that extremely over-loaded lorries of each class were present on the roadway. In the case of lorries with six or more axles, it is believed that the maximum weights belong in some cases to special transports.

Tab. 2: Vehicular loads

Number of axles	W_{min} [kN]	W_{max} [kN]
2	13	550
3	13	757
4	22	508
5	57	886
6	48	1500
7	70	1430
8	102	1130
9	154	1220
10	188	1380

3   Traffic models

The traffic models concern the following aspects:

- traffic flow;

- static properties of the vehicles (weight, axle loads, axle distances);

- dynamic properties of the vehicles (tyre and suspension stiffness and damping).

For the traffic flow, a model developed previously at TNO has been applied [5]. Although, this model should be updated considering the measured data, it is believed that the prediction of the extreme traffic load effects is much more influenced by the vehicular model rather then the traffic flow model. For the vehicle models, a finite set of thirty-one representative types of lorries was recognized. The number of vehicle types is a compromise between the homogeneity of properties within each type and the simplicity in handling the vehicular model for practical applications. The description and frequency of observation of each type are listed in table 3.

Tab. 3: Representative vehicle types

Number of axles	Type	Description	Frequency
2	1	Buses and lorries with two single axles.	10.53%
3	2	Buses and lorries with a front tandem axle and a rear single axle.	0.17%
	3	Buses and lorries with a front single axle and a rear tandem axle.	1.59%
	4	Buses and lorries with three single axles.	0.05%
	5	Buses and lorries with a trailer.	0.25%
	6	Trucks with a semi-trailer.	3.75%
4	7	Lorries with a front single axle and a rear tridem axle; Lorries with a front single and three rear single axles; Lorries with four single axles.	0.51%
	8	Lorries with a front single axle and a single plus a tandem axles in the rear.	1.21%
	9	Lorries with a front tandem axle plus two single axles in the rear; Lorries with two couples of tandem axles; Lorries with a front tridem axle and a rear single axle; Lorries with a group of four axles.	0.31%
	10	Lorries with two single axles and a trailer with two single axles.	3.18%
	11	Lorries with two single axles and a trailer with a tandem axle.	1.43%
	12	Trucks with two single axles and a semi-trailer with two single axles.	7.92%
	13	Trucks with two single axles axles with a semi-trailer with a tandem axle.	10.67%

	14	Trucks with a three axles and a semi-trailer with a single axle.	0.09%
	15	Lorries with two axles and a trailer with three axles.	0.72%
	16	Lorries with three axles and a trailer with two axles.	3.91%
5	17	Trucks with two axles and a semi-trailer with three axles.	46.41%
	18	Trucks with three axles and a semi-trailer with two axles.	0.66%
	19	Other vehicles with five axles.	0.29%
	20	Lorries with three axles and a trailer with three axles.	1.21%
	21	Lorries with two tandem axles and a trailer with two axles.	0.01%
	22	Trucks with two single axles with a semi-trailer with four axles.	0.01%
6	23	Trucks with a front single axle and a rear tandem axle with a semi-trailer with three axles.	3.89%
	24	Trucks with a front tandem axle and a rear single axle with a semi-trailer with three axles.	0.02%
	25	Other vehicles with six axles.	0.36%
	26	Lorries with two tandem axles and a trailer with three axles.	0.46%
7	27	Trucks with three axles with a semi-trailer with four axles.	0.02%
	28	Other vehicles with seven axles.	0.01%
8	29	Vehicles with eight axles.	0.21%
9	30	Vehicles with nine axles.	0.09%
10	31	Vehicles with ten axles.	0.05%

In the following, the models for the gross weight, the axle loads and the axle distances of each lorry type are derived directly from the collected data. Regarding the gross weight, its empirical distribution could show, in general, two peaks due to the fact that loaded and unloaded lorries are present in the traffic. The model discussed in this paper concerns only the loaded part, because the complete traffic model is adopted to estimate the extreme traffic induced effects in concrete bridges. The modelling of the weight distribution required the following steps:

- selection of a limited number of candidate distribution functions;

- estimation of the distribution parameters by fitting the data from the top value w_{top} of the PDF to the upper tail;

- formulation of the criteria used to assess the goodness of fit of the model;

- choice of the distribution function that fits better the data.

The truncated Weibull, lognormal, Frechet and Gumbel distribution are used to model the tail of the distribution. Their CDFs are listed in table 4.

Tab. 4: Distribution functions

Distribution	Distribution parameters	CDF
Weibull	u, k	$F_W(w) = 1 - P_2 \dfrac{\exp\left[-\left(\dfrac{w-\delta}{u}\right)^k\right]}{\exp\left[-\left(\dfrac{w_0-\delta}{u}\right)^k\right]}$
Lognormal	λ, ς	$F_W(w) = 1 - P_2 \dfrac{1 - \Phi\left[\dfrac{\ln(w-\delta)-\lambda}{\varsigma}\right]}{1 - \Phi\left[\dfrac{\ln(w_0-\delta)-\lambda}{\varsigma}\right]}$
Frechet	a, b	$F_W(w) = 1 - P_2 \dfrac{1 - \exp\left[-\left(\dfrac{a-\delta}{w-\delta}\right)^b\right]}{1 - \exp\left[-\left(\dfrac{a-\delta}{w_0-\delta}\right)^b\right]}$
Gumbel	a, b	$F_W(w) = 1 - P_2 \dfrac{1 - \exp[-\exp(-a(w-b))]}{1 - \exp[-\exp(-a(w_0-b))]}$

The terms P_2 and w_0 are, respectively, the probability of having a loaded vehicle and the truncation weight that separates the unloaded and loaded parts of the distribution of the weights. First, the truncation weight w_0 is chosen arbitrarily as a local minimum of the empirical PDF of the weights. Then the probability P_2 is calculated as the relative frequency of the vehicles heavier than the truncation weight. Ten values of the shift parameter δ between 0.0 and w_0 are tested and the value leading to the best fit is chosen. The values of the distribution parameters are calculated to fit the range of values bigger than the top value w_{top}, defined as the weight corresponding to the peak of the empirical distribution. The least square method (LSM) is applied to fit the univariate distributions listed in table 4, minimizing the sum of the square errors between the theoretical model and the empirical data. For each distribution the expression of the error is listed in table 5. The mathematical expressions of the distribution functions are manipulated, in order to have a linear relationship between a function of the CDF and a function of the weight. If the data come from a selected distribution, a linear behavior should be observed in the probability paper if the empirical CDF and the observed weights are used in the derived relationship.

Tab. 5: Error functions minimized by the least square method

Distribution	Error minimized by the LSM	Constant c
Weibull	$\varepsilon = \sum_{i=1}^{n}\left[\ln\left(-\ln\left(c\left(1-F_W\left(w_i\right)\right)\right)\right) - k\ln\left(w_i - \delta\right) + k\ln(u)\right]^2$	$c = \dfrac{\exp\left[-\left(\dfrac{w_0 - \delta}{u}\right)^k\right]}{P_2}$
Lognormal	$\varepsilon = \sum_{i=1}^{n}\left[\Phi^{-1}\left(1 - c\left(1-F_W\left(w_i\right)\right)\right) + \dfrac{\lambda}{\zeta} - \dfrac{\ln\left(w_i - \delta\right)}{\zeta}\right]^2$	$c = \dfrac{1 - \Phi\left[\dfrac{\ln\left(w_0 - \delta\right) - \lambda}{\zeta}\right]}{P_2}$
Frechet	$\varepsilon = \sum_{i=1}^{n}\left[\ln\left(-\ln\left(c\left(1-F_W\left(w_i\right)\right)\right)\right) - b\ln(a) + b\ln\left(w_i - \delta\right)\right]^2$	$c = \dfrac{1 - \exp\left[-\left(\dfrac{a-\delta}{w_0 - \delta}\right)^b\right]}{P_2}$
Gumbel	$\varepsilon = \sum_{i=1}^{n}\left[\ln\left(-\ln\left(c\left(1-F_W\left(w_i\right)\right)\right)\right) + aw_i - ab\right]^2$	$c = \dfrac{1 - \exp\left[-\exp\left(-a\left(w_0 - b\right)\right)\right]}{P_2}$

Regarding the judgment criteria of the goodness of fit of the model, it should be mentioned that usually the chi-square and the Kolmogorov-Smirnov tests are used for this purpose. Both tests are applied to the hypothesis H_0 that the empirical data come from a selected distribution. The disadvantages of chi-square statistical test are:

- the value of the chi-square statistics depend on how the data is binned;

- it requires a sufficient sample size for the chi-square approximation to be valid (it affects the tail of the distribution);

- when a large amount of data is available, the test detects soon deviation from the selected distribution and the hypothesis H_0 is rejected.

The most important disadvantage of the Kolmogorov-Smirnov statistical test is that it is more sensitive near the center of the distribution than at the tails. Due to the aforementioned remarks, the results of the statistical tests can not be considered as a decisional tool to judge the goodness of the model in the tail. The analysis of the probability papers and the diagram of the probability of exceedance has to be considered as the primary criteria. The aforementioned fitting procedure gave satisfactory results for a good number of lorry types. For some types of lorries, a multimodal behavior is observed also in the upper tail. It is believed that the reason is the merge of non strictly homogeneous data in one single representative lorry type. In this case, a two sided truncated distribution is used to fit the loaded part and a left-truncated distribution is chosen for the tail of the empirical pdf. The truncated Weibull, lognormal, Frechet and Gumbel distribution are used to model these parts of the distribution. The CDFs of the two sided truncated distributions are listed in table 6, where w_L and w_U are the lower and upper bounds of the two sided truncated distribution. The probability P_1 and P_2 are defined as follows: P_1 is the probability that the weight is smaller than the upper bound w_U, while the probability P_2 is the probability that the weight is between the lower and the upper bounds.

Tab. 6: Two sided truncated distributions functions

Distribution	Distribution parameters	CDF
Weibull	u, k	$F_W(w) = P_1 - P_2 \dfrac{\exp\left[-\left(\dfrac{w-\delta}{u}\right)^k\right]}{\exp\left[-\left(\dfrac{w_L-\delta}{u}\right)^k\right] - \exp\left[-\left(\dfrac{w_U-\delta}{u}\right)^k\right]}$
Lognormal	λ, ς	$F_W(w) = P_1 - P_2 \dfrac{1 - \Phi\left[\dfrac{\ln(w-\delta)-\lambda}{\zeta}\right]}{\Phi\left[\dfrac{\ln(w_U-\delta)-\lambda}{\zeta}\right] - \Phi\left[\dfrac{\ln(w_L-\delta)-\lambda}{\zeta}\right]}$
Frechet	a, b	$F_W(w) = P_1 - P_2 \dfrac{1 - \exp\left[-\left(\dfrac{a-\delta}{w-\delta}\right)^b\right]}{\exp\left[-\left(\dfrac{a-\delta}{w_U-\delta}\right)^b\right] - \exp\left[-\left(\dfrac{a-\delta}{w_L-\delta}\right)^b\right]}$
Gumbel	a, b	$F_W(w) = P_1 - P_2 \dfrac{1 - \exp[-\exp(-a(w-b))]}{\exp[-\exp(-a(w_U-b))] - \exp[-\exp(-a(w_L-b))]}$

Given the model of the gross weight, the axle loads are derived by means of the following linear relationship:

$$Q_i = \alpha_i W + \beta_i \tag{2}$$

where:

- Q_i is the i-th axle load;

- W is the vehicular weight;

- α_t and β_t are constants.

The assumption of full correlation between the weight and the axle loads is adopted. The accuracy of the model is sufficient for the purpose of the paper. The relative axle distances are modeled by Gaussian random variables, whose statistical parameters are estimated from the collected data. Regarding the dynamic properties of the lorries, three different dynamic models were formulated: simple, double and articulated lorries. The axle mass and the tyre and suspension stiffness of each axle are described by Gaussian random variables with a coefficient of variation of 0.10. The values are randomly generated in such way that the axle frequencies belong to the range [7-12] Hz and the body frequencies belong to the range [1-3] Hz.

4   Description of the bridge

A two-span post-tensioned concrete bridge has been designed according to the relevant Eurocodes. Each span is 40 m long and the roadway is made up of two traffic lanes in one direction. The 90% of the traffic flow is on the slow lane, while the 10% is on the fast lane. The box-girder concrete cross-section is shown in figure 1. On the action side, the self weight of the concrete deck, the dead loads of the pavement and safety barriers and the traffic load model 1 (LM1) are considered. Two anchorage zones, located at the beginning and end of the bridge, are considered. The design takes in account the immediate and time dependent prestress losses, according to the design codes. For the immediate losses, the losses due to friction, losses at the anchorages and the losses due to elastic deformation of concrete are taken in account. For the time dependent losses, the contributions of creep, shrinkage and relaxation losses have been estimated. Ten tendons are used in the design. The areas of each tendon are listed in table 7. The layout of each tendon consists of three parabolas, whose parameters are obtained by solving a system of equation considering the constraints on the vertical position of the tendon. The tendons layout of half structure is shown in figure 2. The effect of prestress on structural concrete is computed using a system of equivalent forces to the prestress action, based on the equilibrium of 1 m long segments of the bridge.
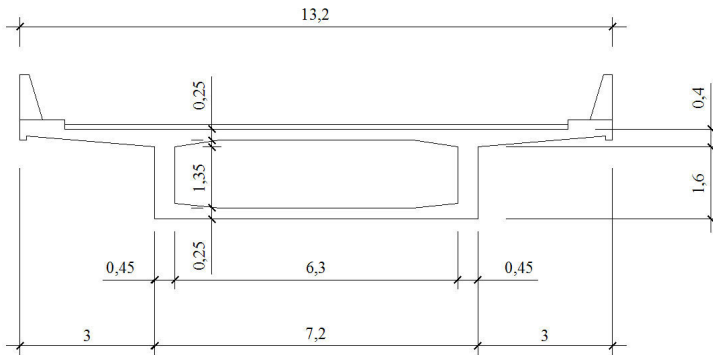

Fig. 1: Cross section

Tab. 7: Data of the tendons

| Tendons	Number of strands	Strand diameter [mm]	Area [mm^2]
1, 2, 3, 8, 9 and 10	19	16	2850
4, 5, 6 and 7	15	16	2085
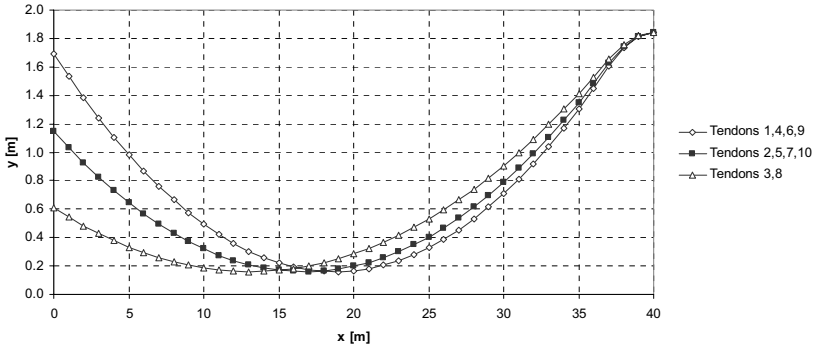
Fig. 2: Tendons layout

Beside the model for the traffic load, a probabilistic model is defined to describe the geometrical properties of the concrete section, the material properties of the concrete, the dead loads and the prestress action. The area and moment of inertia of the cross section are described by normal random variables and they are characterized by a small coefficient of variation. A correlation coefficient equal to 0.96 has been estimated between the area and the moment of inertia. For the concrete properties, the elastic modulus and the density are considered within the model. The elastic modulus has been described by a random field, taking into account the long term behaviour of concrete. The random field is discretized by applying a numerical technique based on the Karhunen-Loeve expansion, on the finite elements with Lagrange interpolation functions [6] and on the minimization of a discretization error estimator on the structural domain. A random field mesh consisting of twenty-one nodes and ten elements with three nodes each one is obtained. The discretized random field is defined by ten random variables. The density of concrete is described by a Gaussian random variable with a coefficient of variation of 0.03. For the dead loads a Gaussian distribution with a cov=0.04 is adopted, while the prestress force $P(x,\infty)$ at a distance x from the jacking section, is described by a normal random variable with mean value equal to the value obtained in the design and coefficient of variation equal to 0.09. Full correlation is assumed between the prestress force in different tendons and at different distances from the jacking end. The details of the probabilistic model are listed in table 8.

Tab. 8: Probabilistic model

Parameter	Distribution	Mean value	Std. dev.	C.o.v.	Number of r.v.
Area [m^2]	N	7.17	0.10	0.01	1
Inertia [m^4]	N	4.33	0.11	0.03	1
Elastic modulus [kN/m^2]	LN	35,332,370.0	5,567,050.1	0.16	10
Density [kg/m^3]	N	2400.00	72.0	0.03	1
Dead loads [kN/m]	N	229.00	9.16	0.04	1
Prestress force [kN]	N	var.	var.	0.09	246

5   Simulations

One static simulation of fifty years and a set of three dynamic simulations of ten days are performed. A linear elastic finite element model is used. The goal of the static simulation is to estimate the distribution of the maximum daily bending moment in the section located at 15 m from the left support (section A) and in the inner support section (section B) by a statistical treatment of the results of the simulations and to assess the design value of the chosen load effect, defined as the fractile of the distribution with a return period of 16000 years. The mechanical and geometrical properties of the bridge are assumed to be equal to the mean values of the corresponding distributions.
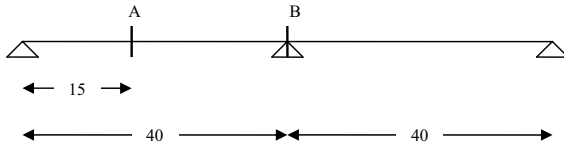
Fig. 3: Location of the sections A and B

The Weibull, Frechet and Gumbel distributions are selected as theoretical models of the tail of the results of the simulations. The statistical parameters of the proposed distributions are calculated by fitting with the least square method the results of the simulation from the top value of the PDF to the tail. For the section A, the probability of exceedance of the results of the static simulation and the theoretical models is plotted in figure 4.
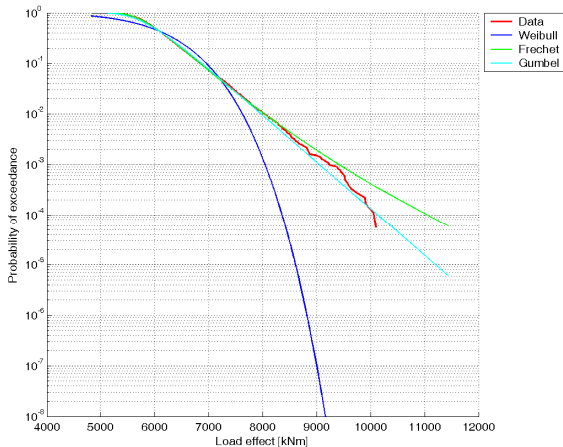
Fig. 4: Probability of exceedance vs load effect (section A)

The Gumbel model is adopted in the modeling of the tail of the distribution, while the Frechet distribution is considered to be too conservative. The fractiles of the distribution of the maximum bending moment are extrapolated for several return periods according to the Gumbel distribution, as shown in figure 5. The design value is equal to $M_d = 13110$ kNm.
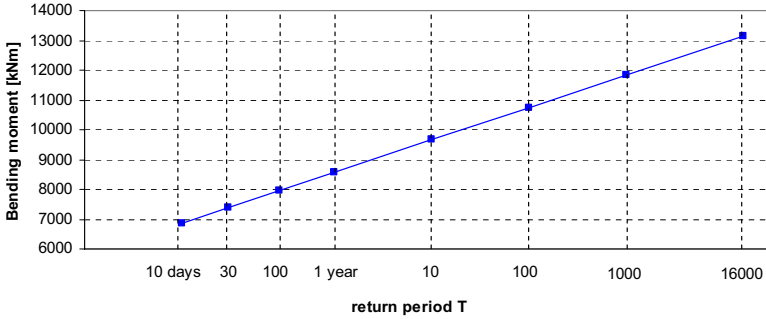
Fig. 5: Results of the extrapolation (section A)

For the section B, the probability of exceedance of the results of the static simulation and the theoretical models is plotted in figure 6, where the absolute value of the load effect is considered.
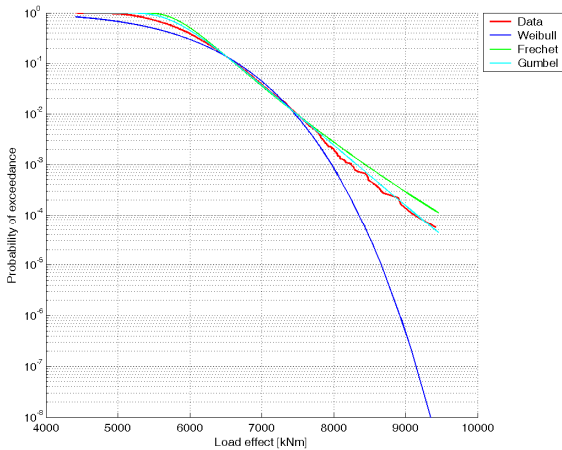
Fig. 6: Probability of exceedance versus load effect (section B)

In this case, a better fit in the upper tail is obtained by the Gumbel distribution. The fractiles of the distribution of the maximum bending moment are extrapolated according to the Gumbel model, as shown in figure 7. The design value is equal to $M_d = -11466$ kNm.
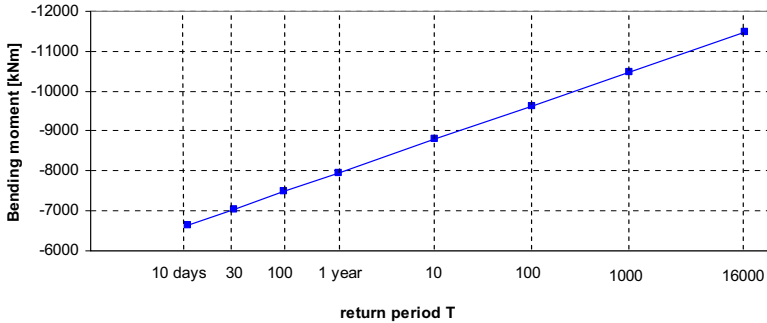
Fig. 7: Results of the extrapolation (section B)

By means of the three dynamic simulations, the dynamic amplification factor (DAF) is estimated as the ratio of the extreme dynamic and static bending moment on a relevant period of time of one day. In the first simulation, the properties of the bridge are considered as in the static case, while in the second simulation the aforementioned probabilistic model is adopted. Finally in the third simulation, the elastic modulus of the concrete is considered as a random variable. Due to the small number of outcomes of the dynamic simulations, it is not possible to have a reliable prediction of the extreme dynamic and static bending moment for a return period of 16000 years and to calculate the DAF as ratio between those extreme values. Then, the mean of the ten values of the DAF has been calculated for each dynamic simulation, leading to a value equal of 1.03. The randomness of the geometrical properties, dead loads, prestress action and material properties, as well as its spatial variability has not a significant effect on the value of the dynamic amplification factor. However, longer dynamic simulations are planned. A comparison between the extreme traffic load effects obtained by simulations and those obtained by the Load Model 1 of the Eurocode 1 is outlined. The design value of the bending moment according to the Eurocode 1 includes a load factor and the DAF. Therefore, it is reasonable for the comparison to consider the previously mentioned extrapolated design value of the bending moment obtained by static simulation multiplied by the DAF equal to 1.03 and a trend and uncertainty factor [7] equal to 1.40. For the section A, the Load Model 1 leads to a design value $M_d = 22434$ kNm. Applying the DAF and the trend and uncertainty factor to the extrapolated value $M_d = 13110$ kNm, the predicted design value by the model presented in this paper is equal to $M_d = 18905$ kNm. The relative difference respect to the value coming from the Eurocode is 16%. For the section B, the Load Model 1 leads to a design value $M_d = -19043$ kNm. Applying the same DAF and the trend and uncertainty factor to the extrapolated value $M_d = -11466$ kNm, the predicted design value by the model presented in this paper is equal to $M_d = -16694$ kNm. The relative difference respect to the value coming from the Eurocode is 13%.

6   Conclusions

A traffic load model based on a large amount of recent data is presented. The model concerns the vehicular load, the axle loads and distances and the dynamic properties of the vehicles. A probabilistic model is formulated also for the geometrical properties, material properties, dead loads and prestress action of a two-span post-tensioned concrete bridge. The Monte Carlo method in combination of a structural solver is employed to evaluate the stress in two sections of the bridge, induced by a random traffic flow. A statistical treatment of the results allows to predict the extreme traffic load effects with respect to the ultimate limit state. A comparison with the Eurocode 1 shows that the European design code is conservative also in the case of the traffic measurements in The Netherlands.

7   References

[1] Van der Wiel, W.D.; De Wit, M.S.: *Statistische analyse voertuiglasten Moedijkbrug*. Report 2005-CI-R0040. Delft: TNO Built Environment and Geosciences, 2005.

[2] Prat, M.: Traffic load models for bridge design: recent developments and research. *Progress in Structural Engineering and Materials* 3 (2001), p. 326-334.

[3] COST 323: *Collection and analysis of requirements as regards weighing vehicles in motion*: 1997.

[4] O'Connor, A.; O'Brien, E.J.: Traffic load modeling and factors influencing the accuracy of predicted extremes. *Canadian Journal of Civil Engineering* 32 (2005), p. 270-278.

[5] Vrouwenvelder, A.C.W.M.; Waarts, P.H.: *Traffic flow models*. Report B-91-0293. Delft: TNO Building and Construction Research, 1992.

[6] Ghanem, R.G.; Spanos, P.D.: *Stochastic finite elements: a spectral approach.* New York: Springer-Verlag, 1991.

[7] Vrouwenvelder, A.C.W.M.; Waarts, P.H.: Traffic loads on bridges. *Structural Engineering International* 3(1993), p. 169-177.

Statistical, Probabilistic and Decision Analysis Aspects related to the Efficient Use of Structural Monitoring Systems

Alfred Strauss[1] & Dan M. Frangopol[2]

[1] Institute of Structural Engineering, University of Natural Resources and Applied Life Sciences, Vienna, Austria

[2] Department of Civil and Environmental Engineering, ATLSS Center, Lehigh University, Bethlehem, PA, USA

Abstract: Structural reliability assessment as well as the lifetime planning of engineering structures can be affected by efficient designed monitoring systems. The design and selection of monitoring systems and their associated sensors are complex and need knowledge about the mechanical characteristics of the structure and the monitoring system. Since uncertainties are unavoidable in the design and planning of engineering systems, statistical and probabilistic methods are necessary for (a) the design of a monitoring system, (b) the determination of the necessary number of sensors, (c) the prediction of monitored physical quantities, and (d) the selection among monitoring alternatives. The objective of this paper is to discuss statistical and probabilistic aspects that allow a smart and effective design of monitoring systems.

1.   Introduction

In recent years, monitoring systems are becoming attractive for the reliability assessment of engineering structures. The objectives associated with the reliability assessment of structures can be manifold such as (a) to assure a reliability level above a prescribed threshold during the lifetime of a structure, (b) to determine the optimum time of interventions, and (c) to determine the duration of monitoring periods. Uncertainties have to be considered in order to provide reliable solutions to these objectives. Therefore, there is the demand for methods like acceptance sampling, as known in material conformity testing, for the systematic treatment of uncertainties. In addition, data obtained by monitoring systems provides also the basis for prediction of monitored physical quantities at defined time horizons or even at the end of the planned life time. The aim of this paper is (a) to review acceptance sampling based concepts and show their applicability to

monitoring systems, (b) to present extreme data concepts for the prediction of physical quantities of structures, and (c) to present decision-based concepts for the selection among monitoring alternatives.

2. Number of sensors based on sampling by attributes and variables

Reliability assessment of existing and new engineering structures based on monitoring systems demands an efficient placement of sensors and use of recorded data. The design of monitoring systems is associated with issues regarding the location and necessary number of sensors. These issues are treated by using engineering knowledge and assumptions regarding potential structural deteriorating locations. Statistical methods, until now hardly used in monitoring engineering structures, can assist in solving such problems. The methods are known as acceptance criteria and provide the required number of sensors n on selected structural components out of all components, necessary for reliable statements with respect to the condition of physical quantities. This kind of monitoring allows the assessment of the entire lot of selected structural members N by indicating a bad performance for defined r violations out of n sensors. The definition of the acceptable r violations [1], [2] for a given number of sensors n installed on selected structural members N and an accepted probability of f threshold violations can be based on the hyper-geometric distribution as follows[2]:

$$P(f) = \sum_{x=0}^{r} \frac{\binom{N \cdot f}{x}\binom{N \cdot h}{n-x}}{\binom{N}{n}} \qquad (1)$$

where $h = 1 - f$. This formulation is valid by assuming that each monitored component is recorded by only one sensor [2]. The lot will be accepted, if there are r or less sensors indicating a threshold violation. The hyper-geometric distribution, as indicated in Eq. (1), serves for (a) finding the probability $P(f)$ of accepting a lot of size N with an actual fraction of threshold violations f monitored by n sensors from which r indicate threshold violations, and (b) finding the necessary number of sensors n by limiting the probability of accepting an actual fraction f of threshold violations. The no threshold violation requirement, $r = 0$ out of n sensor measurements, yields to the probability of accepting a lot N with an actual fraction f of threshold violations as follows [3]

$$P(f) \approx \sum_{x=0}^{r=0} \frac{n!}{x!(n-x)!} \cdot f^x \cdot h^{n-x} \qquad (2)$$

Hence, for a given confidence level $C = 1 - h^n$, with $h = 1 - f$, the necessary number of sensors n can be computed as

$$n = \frac{ln(1-C)}{ln(h)} \tag{3}$$

The previous formulation (monitoring by attributes) does not take into account the quality of each monitored component or sensor measurement. The components or sensor measurements are classified simply as good or bad. A simply bad or good classification does not fully utilize the information that can be achieved from the monitoring results.

There is an alternative method, called monitoring by variables [2] that allows the consideration of distributed sensor data for accepting or not accepting a lot N. Monitoring by variables allows a significant reduction of the required number of sensors to achieve the same degree of quality control compared to monitoring by attributes. Acceptance criteria are based on the concept of minimizing both the probability κ that a good physical quantity $N(\mu_G, \sigma_G)$ will be rejected and the probability λ that a poor (bad) physical quantity $N(\mu_B, \sigma_B)$ will be accepted. These probabilities provide the basis for the determination of the threshold γ and the required number of sensors n. The probability κ that a sensor measurement will indicate a bad condition for no violation of the threshold γ by the mean $\overline{X}$ can be computed as:

$$P\left(\overline{X} < \gamma \middle| \mu_G\right) = \Phi\left(\frac{\gamma - \mu_G}{\sigma / \sqrt{n}}\right) = \kappa \tag{4}$$

Conversely, the probability λ can be computed as

$$P\left(\overline{X} > \gamma \middle| \mu_B\right) = 1 - \Phi\left(\frac{\gamma - \mu_B}{\sigma / \sqrt{n}}\right) = \lambda \tag{5}$$

These two equations serve for the computation of the necessary number of sensors n and the threshold γ for the given characteristics $N(\mu_G, \sigma_G)$, $N(\mu_B, \sigma_B)$, κ, and λ. It has to be emphasized that these computations are based on the assumption that the standard deviation σ of the measurements is known in advance (e.g., from experience) and the measurements are Gaussian distributed. Equations (4) and (5) provide also the basis for the extension to non-Gaussian considerations.

3. Extreme value distributions for monitoring-based predictions

Extreme values are associated with the largest and smallest values from a monitored sample of size n within a known population. Therefore, the largest and the smallest value are associated with a probability distribution. A monitored physical quantity recorded at defined locations of a structure can be considered as a random variable X (or population). The monitored sample of size n from this population will have a largest and a smallest value which are related to the probability density distribution (PDF) $f_X(x)$ or cumulative probability distribution (CDF) $F_X(x)$. These extreme values will also have their respective distributions which are related to the distribution of the initial variable X [4].

The monitored sample of size n can be considered as a set of observations $(x_1, x_2, ..., x_n)$ representing the first, second,…., nth observed values. Nevertheless, the monitored values are unpredictable, they are a specific realization, whichever underlies a set of random variables $(X_1, X_2, ..., X_n)$. Therefore, the interest is in the maximum and minimum of $(X_1, X_2, ..., X_n)$, which can be expressed as follows

$$Y^{max} = max(X_1, X_2, ..., X_n)$$
(6)

and

$$Y^{min} = min(X_1, X_2, ..., X_n)$$
(7)

Based on certain assumptions [4], it is possible to develop the exact probability distributions of Y^{min} and Y^{max}. These assumptions can be derived as follows [4]. Consider a specified value y, in case of Y^{max} lesser than y, all the sample associated random variables $X_1, X_2, ..., X_n$ must also be less, see Eq. (6). Assuming that $X_1, X_2, ..., X_n$ are statistically independent and identically distributed yields to the CDF [4]

$$F_{Y\max}(y) = [F_X(y)]^n$$
(8)

and the PDF

$$f_{Y^{max}}(y) = n \cdot [F_X(y)]^{n-1} \cdot f_X(y)$$
(9)

where $F_X(y)$ and $f_X(y)$ are, respectively, the CDF and PDF of the initial variable X. The same consideration can be performed for the minimum Y^{min} with the survival function, resulting in the CDF [4]

$$F_{Y^{min}}(y) = 1 - [1 - F_X(y)]^n$$
(10)

and the corresponding PDF

$$f_{Y^{min}}(y) = n \cdot [1 - F_X(y)]^{n-1} \cdot f_X(y)$$
(11)

Therefore, the exact distribution of the largest and smallest values from samples of size n is a function of the distribution of the initial variable.

There is the possibility to capture the exact solutions with asymptotic distributions. The following statements are valid according to ANG and TANG [4]: (a) the extreme value from an initial distribution with an exponential decaying tail (in the direction of the extreme) will converge asymptotically to a *Type I*, (b) the distribution of an extreme value of an initial variate with a PDF that decays with the polynomial tail will converge to a *Type II* (Eq. 12), (c) if the extreme value is limited, the corresponding extremal distribution will converge asymptotically to a *Type III* (Eq. 13),

$$\text{Type II}: \quad F_{Y^{max}}(y) = \exp[-(v_n/y)^k]$$
(12)

$$\text{Type III}: \quad F_{Y^{min}}(y) = 1 - \exp\left[-\left(\frac{y-\varepsilon}{w_1-\varepsilon}\right)^k\right]; \quad y \geq \varepsilon$$
(13)

where ν_n = most probable value of Y^{max}, k = shape parameter, which is an inverse measure of the dispersion of values Y^{max}, w_1 = most probable smallest value, and ε = lower bound value of y [4].

Numerical Example: Wisconsin Bridge

The previously described approaches are suitable to be directly applied to monitoring programs of existing structures. Fig. 1 shows the monitored data taken from the I-39 Northbound Bridge over the Wisconsin River [3]. This bridge was built in 1961 in Wausau, Wisconsin. The total length of the bridge is 196.04 m (643.2 ft). It is a five span continuous steel plate girder bridge. The monitoring of this bridge included the strain/stress behavior of specified structural components. Details are given in MAHMOUD et al. [5]. Fig. 1 shows the recorded extreme monitored data per day provided by the sensor CH15 (solid line) and a scenario simulating an increase of the extreme monitored data (dashed line) as follows

$$\xi_m = \xi_m^o \cdot \left(1 + a \cdot t + b \cdot t^2\right) \tag{14}$$

where ξ^o_m = existing monitoring data, ξ_m = modified monitored data, $a = 1/500$ and $b = 1/20$ (assumed changes in the monitoring process), and t = time (days)
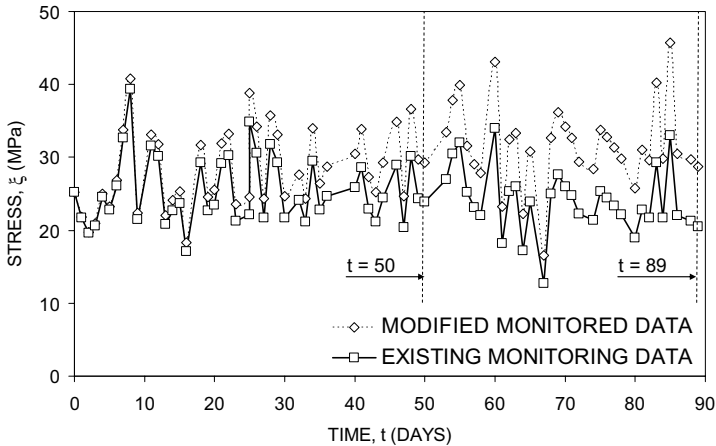
Fig.1: Recorded extreme monitored data per day provided by the sensor CH15
($a = 1/500$ and $b = 1/20$)

The application of the exponential distribution of Eq. (12) to the existing monitored extreme data ξ^o_m (see Fig. 1) yields the extreme value distributions as shown for different $n = t$ = time in days (solid lines) in Fig.2. For $n = t = 1000$ (equivalent to 1000 days monitoring) the median value of the extreme distributions associated with the monitored extreme data is $\xi^0_{t=1000}$ = 43.1 MPa.
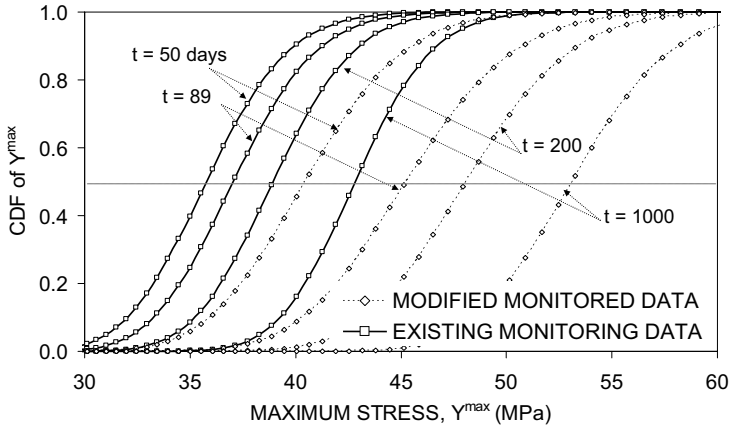
Fig.2: CDF of the extreme value Y^{max} based on the existing and modified monitored extreme values ξ^o_m and ξ_m ($a = 1/500$ and $b = 1/20$) of the Wisconsin Bridge
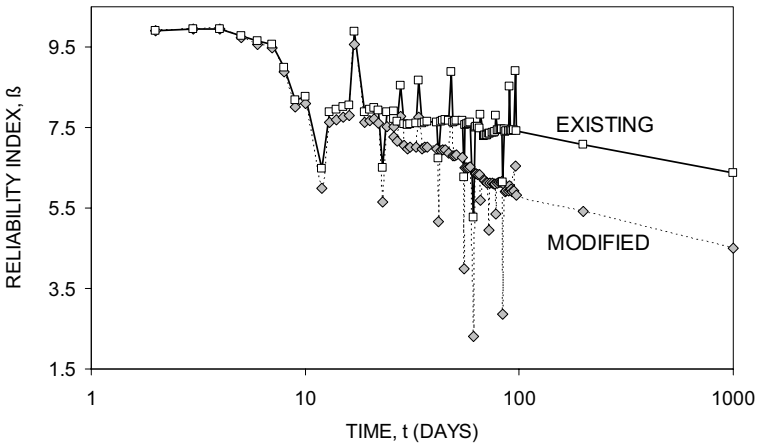
Fig.3. Computed reliability profiles based on the monitored and modified monitored data (see Eq. (14)) associated with the extreme value distributions of Eq. (12)

Assuming that there will be a change in the monitored extreme values process (see Eq.14), as shown in Fig. 1, this procedure yields to drastically changes in the extreme values, for instance for a size $t = 1000$ days the median value of the extreme monitored data will be 53.3 MPa instead of 43.1 MPa. In this manner, it is possible to (a) predict the characteristic values of the extreme distribution with increasing sample size, and (b) detect changing processes in the monitored structure. The detection can be based on the comparison of the extreme value distributions associated with different sample sizes n (where $n = t =$ number of monitored days). Additionally, the continuously provided extreme value exponential

distributions during monitoring and future predictions, associated to the sample sizes n, can be used to predict the time-dependent reliability index β and its expected value at the time horizon, (e.g., 89 days). The calculation of the reliability index, using FORM [6], was based on the yield strength f_y = LN(377 MPa, 30.16 MPa). Fig. 3 shows the reliability index profile and the effect of increasing extreme monitored data (see Eq. (14)).

4.   Decision Analysis in Monitoring

4.1   General Approach

There are various systems for monitoring of structures. In some cases, the benefit of a monitoring system for a defined task is clear. However, this is not usually the case. The decision analysis applied to monitoring systems is an useful tool. Consider the following example.

The reliability index of a given structure has to be predicted. There are two methods for assessing the reliability. Method (I) consists of visual inspection, and Method (II) is using a monitoring system. The reliability index using visual inspection is based on n = 10 indicators. The error is random with mean zero and standard deviation σ_I where σ_I is estimated with a mean = 1 and a coefficient of variation c.o.v. = 50%.

The monitoring system (II) consist of two sensors monitoring the physical quantity associated with the resistance. The error in each measurement has mean zero and standard deviation σ_{II} (σ_{II} is estimated with a mean = 0.7 and a c.o.v. = 60%). The costs of performing the required inspections are \$1,500 and \$2,000 with methods (I) and (II), respectively. The penalty of inaccurate inspection is proportional to the square of the total error, or

$$L = k \cdot \left(X_1 + X_2 + ... + X_n \right)^2 \tag{15}$$

where k = 100, and X_i is the error in each indicator. Which of the monitoring program should the inspector use based on the Maximum Expected Monetary Value (EMV) criterion [4]. The expected loss from inaccurate measurement based on the above quadratic penalty function can be expressed in terms of the standard deviation of the error in each segment as [4]

$$E(L|\sigma) = E\left[L = k \cdot (X_1 + X_2 + ... + X_n)^2 | \sigma \right] = k \left[\sum_{i=1}^{n} E(X_i^2|\sigma) + \sum_i \sum_{\neq j} E(X_i \cdot X_j|\sigma) \right] \tag{16}$$

If each measurement is assumed to be statistically independent and identically distributed,

$$E(L|\sigma) = k \cdot n \cdot E(X^2|\sigma) = k \cdot n \cdot \sigma^2 \tag{17}$$

and

$$E(L) = k \cdot n \cdot E(\sigma^2) = k \cdot n \cdot \left[Var(\sigma) + E^2(\sigma) \right] \tag{18}$$

where $Var(\sigma)$ = variance of σ. For method (I), the expected total cost, therefore is

$$E(C_I) = 1,500 + 100 \times 10 \times [0.5^2 + 1^2] = \$2,750 \qquad (19)$$

The corresponding total cost for method (II) is

$$E(C_{II}) = 2,000 + 100 \times 2 \times [0.42^2 + 0.7^2] = \$2,133 \qquad (20)$$

Consequently, on the basis of the maximum EMV criterion, the inspector should use method (II).

4.2   Additional Monitoring Information – Terminal Analysis

In maintenance engineering it is common to perform inspections or monitoring. These investigations provide a better final decision regarding the maintenance planning or performance prediction of a structure. In general, this approach is applied to structural members indicating unusual behavior or unexpected degradation processes, or for long term monitoring programs to detect time dependent structural processes of resistance or loading changes. The acquisition of additional information from e.g., monitoring systems, will require the expense of time, energy, and financial resources [4]. As indicated in ANG and TANG [4] "*in spite of these added costs, the additional information may be valuable and will generally improve the chance of making a better decision.*" Finally, a decision has to consider the added cost for the efforts necessary to obtain the new information. It has to be noted that even tremendously efforts cannot eliminate all uncertainties [4].

For example, the capability of engineering inspection methods applied on specified structures can be illustrated by a decision tree. Bayesian updating methods provide the possibility for updating past inspections with new inspection data obtained by e.g., (A) traditional methods or (B) novel monitoring systems. The decision can be based on traditional decision analysis or on decision analysis with additional information (commonly referred to as terminal analysis), which is similar to the prior analysis, except that the updated probabilities (probabilities conditional on the monitoring outcome) are used in the computation of the expected monetary value or utility [4]. Several examples according to decision analysis including monetary values are provided in ANG and TANG [4]. In general, terminal analysis can be considered as an efficient method for decision making under uncertainties.

Consider the following example. There is the demand for a reliability assessment of an existing structure. The designated engineering office considers two methods to obtain data for the assessment: (A) a traditional inspection method, and (B) a novel monitoring system. Method (B) would mean a large initial investment that may be wasted if the reliability level will be much larger than the allowed level and will show no significant degradation process. Fig. 4 shows the probabilities of detecting an unexpected failure mechanism associated with the proposed methods (A) and (B) and the monetary loss by not detecting the mechanism
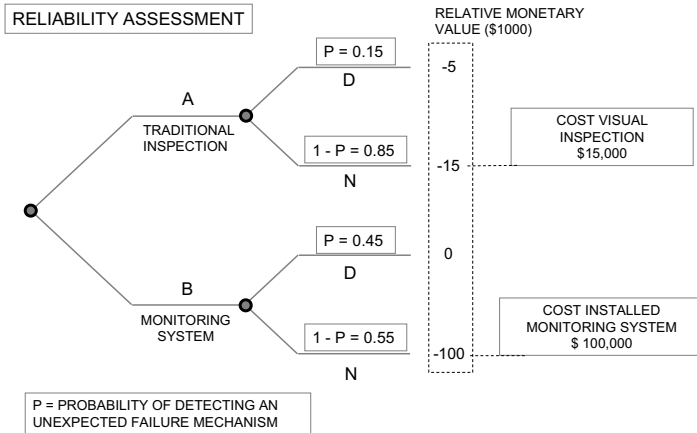
Fig.4. Prior Analysis: Decision tree for monitoring treatment system before the finite element investigation

Based on *prior analysis*, the expected monetary loss for the two methods are: $E(A) = 0.15 \times (-5,000) + 0.85 \times (-15,000) = -\$ 13,500$ and $E(B) = 0.45 \times (0) + 0.55 \times (-100,000) = -\$ 55,000$. With the given information, method (A) should be selected with the monetary loss of $-\$ 13,500$. The engineering office decided to find out more about the structural conditions and processes acting on the structure. A finite element modelling of the structure under given loading conditions was performed. The cost of finite element computation is $\$ 6,000$. The proposed monitoring layout based on the FEM shows the probability of detecting an unexpected failure mechanism $P\,(B_{FEM}|D) = 0.95$ and not detecting an unexpected failure mechanism of $P\,(B_{FEM}|N) = 0.05$ for the novel monitoring system and $P\,(A_{FEM}|D) = 0.60$ and $P\,(A_{FEM}|N) = 0.40$ for the traditional inspection method, where A_{FEM}, and B_{FEM} indicate the outcomes and D, and N denote detected or not detected failure mechanism, respectively. Bayesian theorem can be used to update the previous assumed probabilities P as follows:

$$P''(B \mid D) = \frac{P(B_{FEM} \mid D) \cdot P'(B \mid D)}{P(B_{FEM} \mid D) \cdot P'(B \mid D) + P(B_{FEM} \mid N) \cdot P'(B \mid N)} = \ldots$$

$$\ldots \frac{0.95 \times 0.45}{0.95 \times 0.45 + 0.05 \times 0.55} = 0.94 \qquad (21)$$

and

$$P''(A \mid D) = \frac{P(A_{FEM} \mid D) \cdot P'(A \mid D)}{P(A_{FEM} \mid D) \cdot P'(A \mid D) + P(A_{FEM} \mid N) \cdot P'(A \mid N)} = \ldots$$

$$\ldots \frac{0.60 \times 0.15}{0.60 \times 0.15 + 0.40 \times 0.85} = 0.21 \qquad (22)$$
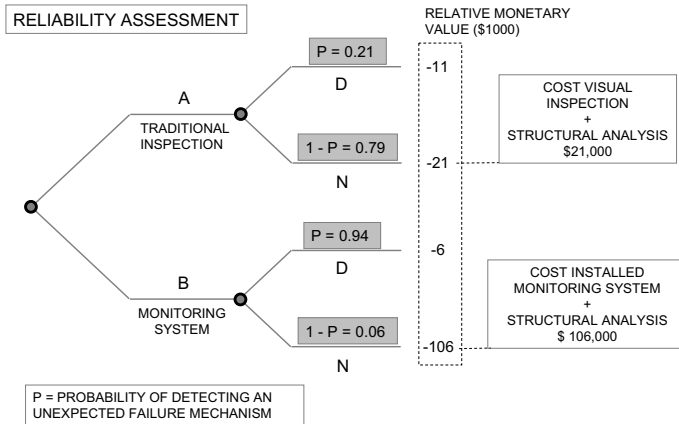
Fig.5: Terminal Analysis: Decision tree for monitoring treatment system after the finite element investigation

In other words, the probability of detecting unexpected failure mechanism is increased due to the finite element based layout of the monitoring system from $P(B|D) = 0.45$ to 0.94. The corresponding updated probability $P(B|N) = 0.06$. Probabilities for all the paths are revised accordingly.

Fig. 5 shows the revised probabilities of detecting an unexpected failure mechanism for both traditional inspection (Method A) and the planned monitoring system (Method B) based on the finite element investigations. Therefore, the expected monetary losses associated with the two methods are

$$E(A) = 0.21 \times (-11{,}000) + 0.79 \times (-21{,}000) = -\$18{,}900 \tag{23}$$

$$E(B) = 0.94 \times (-6{,}000) + 0.06 \times (-106{,}000) = -\$12{,}000 \tag{24}$$

The terminal analysis used in conjunction with the maximum expected monetary value criterion indicates that method (B) (monitoring system) should be selected. In this case, the finite element computation changes the solution. It is important to note that the expected failure cost was not included in the above computations.

5.   Conclusion

In conclusion, it is emphasized that statistical, probabilistic, and decision-based on terminal analysis are powerful tools for performing an efficient health monitoring of a structural system. However, much future effort has to be devoted to integrate these tools in an overall life-cycle management of civil infrastructure systems.

6.   Acknowledgements

References

[1]   Ang, A.H.-S. & Tang, W.H., Probability Concepts in Engineering Planning, 2nd Edition, John Wiley, 2007.

[2]   Frangopol, M., Strauss, A., Kim, S., "Sensor-based monitoring systems for performance assessment of engineering structures." submitted for publication, 2007.

[3]   Hald, A., "Statistical Theory with Engineering Applications." J. Wiley and Sons, New York, 1952.

[4]   Ang, A.H.-S. and Tang, W.H., Probabilistic Concepts in Engineering Planning and Design – Volume II: Decision, risk and reliability. New York, NY: John Wiley & Sons, 1984.

[5]   Mahmoud. H.N, Connor. R.J. and Bowman C.A., "Results of the fatigue evaluation and field monitoring of the I-39 Northbound Bridge over the Wisconsin Rever." Lehigh University, 2007.

[6]   Novák, D., Vořechovský, M. and Rusina, R. 2006. FREET - Feasible Reliability Engineering Efficient Tool, User's and Theory guides. Brno/Cervenka Consulting, Czech Republic.

Determination of fracture-mechanical parameters for reliability calculation

Zbyněk Keršner, David Lehký, Drahomír Novák & Jan Eliáš
Institute of Structural Mechanics, Brno University of Technology, Czech Republic
Alfred Strauss, Simon Hoffman, Roman Wendner & Konrad Bergmeister [2]
IKI, BOKU University, Vienna, Austria

Abstract: The knowledge of fracture-mechanical parameters is fundamental for virtual failure modelling of elements and structures made of concrete. A key parameter for nonlinear fracture mechanics modelling is certainly the fracture energy of concrete and its variability, being a subject of research of many authors. The paper describes the particular example of an experimental-numerical approach for the determination of fracture-mechanical parameters. Experimental results are used of 8 notched-beam concrete specimens subjected to three-point bending. Two basic approaches are applied to determine the fracture-mechanical parameters: (i) effective crack model / work-of-fracture method, (ii) inverse FEM analysis using nonlinear fracture mechanics based on virtual stochastic simulation. The utilization of stochastic training of neural networks appeared to be a promising tool to obtain material model parameters including theirs variability. The results presented in this paper are the mean values and variances of fracture-mechanical parameters based on a specific material model. They can be utilized for consequent deterministic and/or stochastic virtual computer modelling of a real structure.

1   Introduction

The knowledge of fracture-mechanical parameters is fundamental for virtual failure modelling of elements and structures made of concrete. A key parameter of nonlinear fracture mechanics modelling is certainly fracture energy of concrete and its variability, which is a subject of research of many authors, e.g. BAŽANT & PLANAS [1], BAŽANT & BECQ-GIRAUDON [2]. Within this paper experimental results from three-point bending tests on notched-beam specimens are analysed. Two basic approaches are applied to determine fracture-mechanical parameters from these tests: (i) effective crack model / work-of-fracture method, (ii) inverse FEM analysis using nonlinear fracture mechanics based on virtual stochastic simulation (NOVÁK & LEHKÝ [3], [4]; KUČEROVÁ et al. [5]; ČERVENKA et al. [6]).

The paper is focused on the determination of fracture-mechanical parameters of concrete used for damage identification experiments of continuous reinforced concrete beams performed at IKI, BOKU within the research project AIFIT (HOFFMANN et al. [13]).

2   Experiments

2.1   AIFIT – user orientated identification for infrastructure

For most developed countries infrastructure challenges will shift more and more from building new infrastructure to the maintenance of existing structures. The corresponding increase of inspections will cause additional demand for global identification methods and their simplification in practice. Therefore BOKU University proposed together with the industrial partners Schimetta Consult, and Maurer Söhne, as well as the bridge owner ÖBB (Austrian railway) for funding by the Austrian research foundation FFG of a research project called "AIFIT". The second work package of the project aims for the comparison and validation of different global identification methods, applied to several progressively damaged reinforced concrete beams. Based on the experimental data and identified stiffness non linear numerical models will be calibrated in the project's third work package and used for parameter studies including different scenarios of degradation and statistical spread of material parameters. The parameter analysis presented in this paper will be an important input to these studies. Following work packages address the specific further development of monitoring systems regarding the requirements of the identification methods. For the evaluation of the user orientation and feasibility of the identification methods a field test will be conducted at a 3 span bridge close to Vienna.

2.2   Three-point bending tests

All experimental load–deflection diagrams obtained from three-point bending tests of specimens with central edge notch are presented in Fig. 1.

Results of fracture test measurements show, that analysis of a measured time series of inner system parameters can serve for recognition of 'catastrophe' origination. During a selected time series of loading point displacement there can be visible irregularity in loading speed and first of all a sudden increase in displacement – see Fig. 2. Therefore, the time derivative of this displacement is a useful criterion of the origination and range of the fold catastrophe. The catastrophe is recognizable as extreme values of loading speed (Fig. 2). The corrected loading diagram and fold catastrophe have such properties, which can help discover the probable development of the diagram in the catastrophic part. As a first attempt to create an algorithmic development of this correction a third order polynomial was applied (Fig. 3).
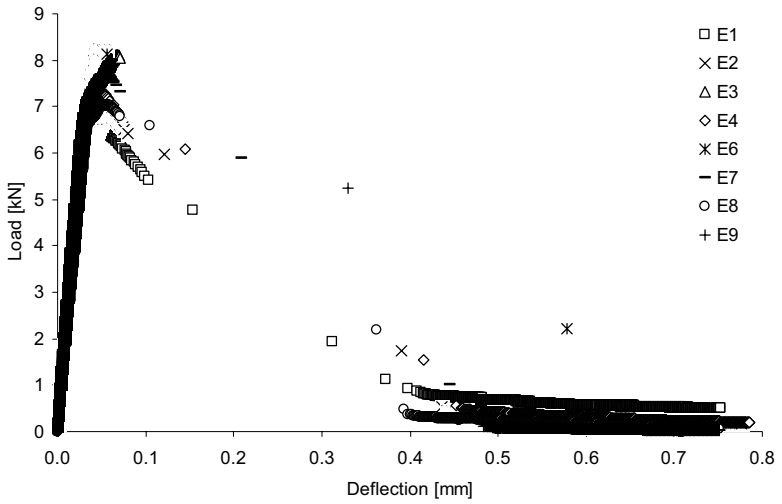
Fig. 1: Experimental load–deflection diagrams obtained from three-point bending tests
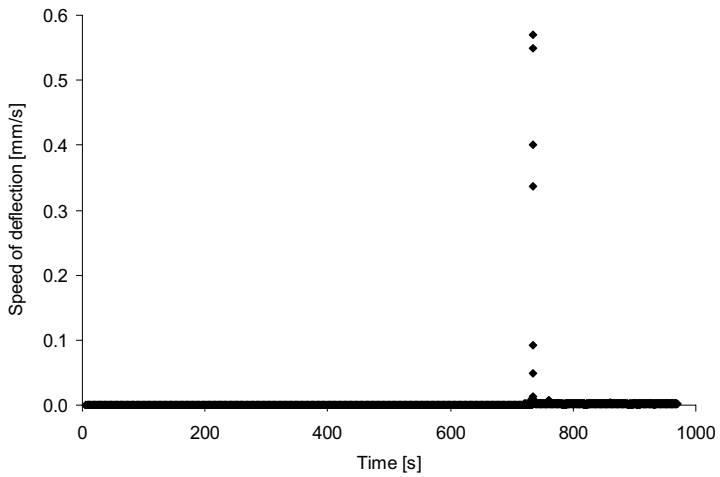
Fig. 2: Time derivative of measured time series of deflection (E4)
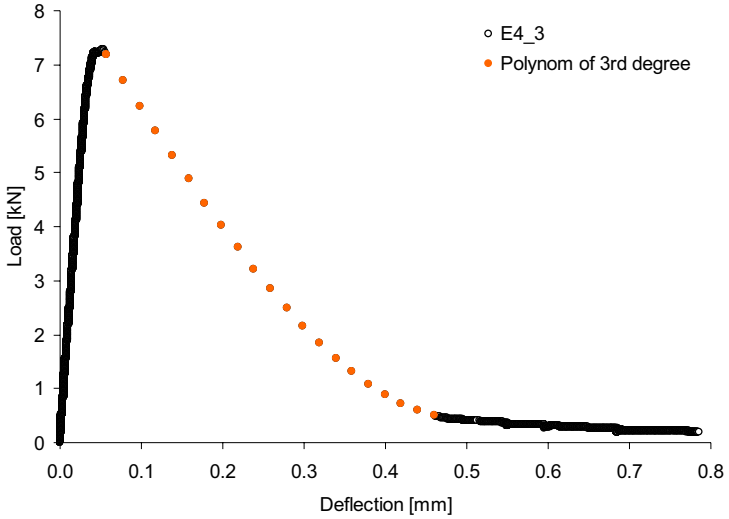
Fig. 3: Load–deflection diagram (E4) incl. approximated correction by 3rd degree polynom
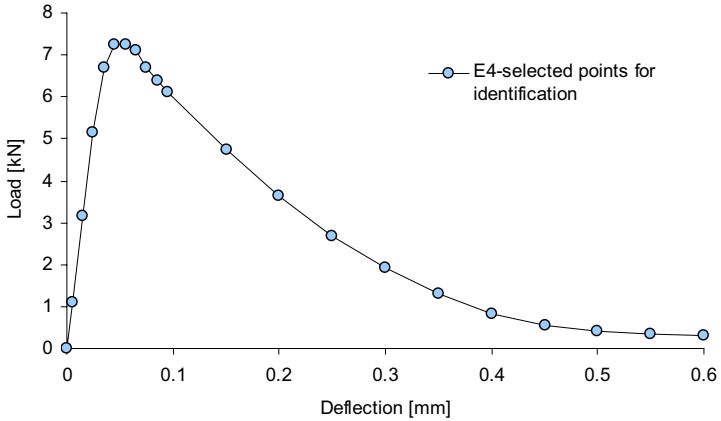
Fig. 4: Load–deflection diagram (E4) with selected points for identification
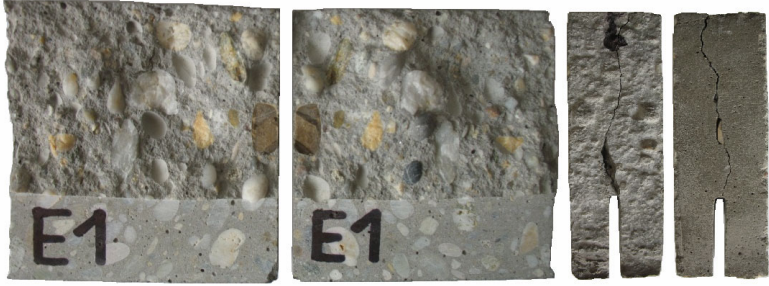
Fig. 5: Example of fracture surface and crack path for selected specimen E1
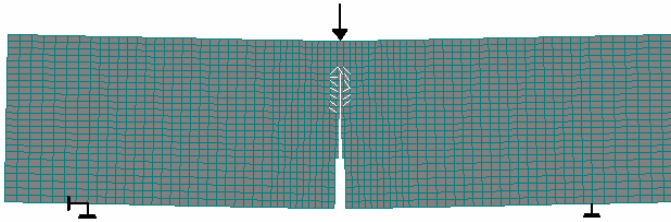
Fig. 6: Virtual testing of notched beams: numerical model in ATENA software

3 Fracture-mechanical parameters determination

3.1 Effective crack model / work-of-fracture method

Experimental load–deflection curves (*l–d* diagrams) after corrections were first used to determine fracture-mechanical parameters by standard techniques – two-parameter effective crack model (ECM-TPM) and work-of-fracture method, e.g. KARIHALOO [7]. Every curve was assessed separately, and the variability is described by the first two statistical moments (mean value and standard deviation), summarized in Table 1 and 2 for the conducted tests. The following main parameters of interest, quantifying brittleness/ductility of the composite are studied: effective crack length or effective crack elongation, effective fracture toughness, effective toughness and fracture energy.

In this contribution the fracture energy is determined in two variants – a) directly calculated from experimental *l–d* curves and b) using estimation of "whole" fracture work (e.g. KARIHALOO [7], STIBOR [8]). It can be noted that the calculated variability expressed by coefficient of variation is around 0.08.

Tab. 1: Selected results of fracture test: parameter value, mean value, standard deviation and coefficient of variation (COV) in %

Parameter	Symb.	Unit	Specimen	Value	Mean Value	Standard Deviation	COV [%]
Modulus of Elasticity	E_c	GPa	E1	35.4	34.6	2.9	8.3
			E2	30.1			
			E3	33.3			
			E4	34.1			
			E6	35.4			
			E7	39.3			
			E8	32.2			
			E9	37.0			
Effective Crack Elongation	a_e-a	mm	E1	9.0	12.4	3.5	28.4
			E2	14.0			
			E3	17.9			
			E4	8.3			
			E6	8.4			
			E7	15.3			
			E8	12.7			
			E9	13.9			
Effective Fracture Toughness	K_{Ice}	MPa.m$^{1/2}$	E1	1.195	1.498	0.233	15.6
			E2	1.392			
			E3	1.899			
			E4	1.288			
			E6	1.475			
			E7	1.614			
			E8	1.401			
			E9	1.720			
Effective Toughness	G_{ce}	J/m^2	E1	40.3	66.3	20.7	31.2
			E2	64.5			
			E3	108.4			
			E4	48.7			
			E6	61.5			
			E7	66.2			
			E8	61.1			
			E9	80.1			
Fracture Energy	G_F	J/m^2	E1	245.4	248.0	18.5	7.5
			E2	235.5			
			E4	263.3			
			E7	257.2			
			E8	218.8			
			E9	267.5			

Tab. 2: Results of compressive strength test (using fragments after fracture test): parameter value, mean value, standard deviation and coefficient of variation (COV) in %

Parameter	Symb.	Unit	Specimen	Value	Mean Value	Standard Deviation	COV %
Compressive Strength	f_c	MPa	E1a	58.9	55.9	4.4	7.9
			E1b	57.2			
			E2a	44.2			
			E2b	47.8			
			E3a	54.2			
			E3b	58.0			
			E4a	60.2			
			E4b	57.2			
			E6a	55.1			
			E6b	55.2			
			E7a	59.2			
			E7b	58.5			
			E8a	53.5			
			E8b	58.1			
			E9a	60.7			
			E9b	55.7			

3.2   Inverse analysis based on virtual stochastic simulation

The second possibility to obtain fundamental parameters is to perform virtual numerical simulation of the experiments and to adjust relevant parameters of the computational model to achieve a good agreement with the experimental *l–d* curves. Such a procedure is not trivial and needed a sophisticated approach of inverse analysis based on coupling of artificial neural network, software DLNNET (LEHKÝ [9]), nonlinear fracture mechanics FEM modelling, software ATENA (ČERVENKA & PUKL [10]) and probabilistic stratified simulation for training of artificial neural network, software FReET (NOVÁK et al. [11]). The procedure can determine the most suitable parameters of a computational model to get the best agreement with the experimental response (NOVÁK & LEHKÝ [3], [4]). The whole process can be itemized the following:

- First, the computational model for the given problem has to be developed using the appropriate software tools. The model has to be a heuristically "tuned" one using material model parameters; the initial calculation uses a set of initial material model parameters resulting in a rough agreement with experimentally measured data.

- The material model parameters are considered as random variables described by a probability distribution. For the given case a rectangular distribution is a "natural choice" as the lower and upper limits represent the bounded range of physical exis-tence. Subsequent the variables are simulated randomly based on the Monte Carlo type simulation, while for the small-sample simulation a LHS is recommended.

- A multiple calculation of deterministic computational model using random realizations of material model parameters is performed and a statistical set of the virtual structural response is obtained.

- Random realizations and the corresponding responses from the computational model serve as the basis for the training of an appropriate neural network. After the training the neural network is ready to solve the opposite task: To select the best material parameters in order the numerical simulation will result in the best agreement with the experiment. This is performed by means of the simulation of a network using measured response as an input. Finally it results in a set of identified material model parameters.

- The last step is the verification of the results by the calculation of the computational model using identified parameters. A comparison with the experiment will show to what extend the inverse analysis was successful.

SBETA material model implemented in the software ATENA was used for the modeling of three-point bending test. This material model consists of the following six main parameters: modulus of elasticity E, tensile strength f_t, compressive strength f_c, fracture energy G_f, compressive strain in uniaxial compressive test ε_c, critical compressive displacement w_d. Not all these parameters can be successfully identified from the three-point bending test. A sensitivity analysis was performed first to all eliminate non-dominant parameters. For the modeling of the cracked concrete a rotational crack approach was used.

The sensitivity analysis based on non-parametric rank order correlation (Spearman) used 100 simulations of a LHS type. The results showed that 3 out of the 6 parameters are dominant (E, f_t, G_f) and can be identified from the three-point bending test. All remaining parameters (f_c, ε_c, w_d) are not dominant (low sensitivity) and it is impossible to identified them without another type of experimental test.

4 Results

In the following subsections compare the values of selected material parameters obtained form the experimental testing and from inverse analysis.

4.1 Modulus of elasticity E

For the identification of the modulus of elasticity E the pre-peak part of the l–d diagram was used. The identification was based on inverse stochastic analysis using the SARA software package (PUKL et al. [12]). All resulting values for selected tests are introduced in Tab. 3. Both coefficients of correlation obtained from tests, as well as from identifications are equal 0.85.

Tab. 3: Values of modulus of elasticity E for each specimen plus mean value m
and coefficient of variation COV

E [GPa]	E1	E2	E4	E7	E8	E9	m	COV
Test	35.4	30.1	34.1	39.3	32.2	37.0	34.7	0.10
Identification	32.0	31.5	36.6	44.5	33.0	39.0	36.1	0.14

4.2 Fracture energy G_f

For the identification of the fracture energy G_f a neural network based identification method was used. First, the training set was prepared by randomization of all material parameters and following stochastic analysis using the SARA tool. One hundred ATENA analyses were carried out and then used for the training of the artificial neural network as well as for the sensitivity analysis mentioned above. The resulting values for selected tests are introduced in Tab. 4. Both coefficients of correlation obtained from tests as well as from identifications are equal 0.88.

Tab. 4: Values of specific fracture energy G_f for each specimen plus mean value m
and coefficient of variation COV

G_f [N/m]	E1	E2	E4	E7	E8	E9	m	COV
Test	245	236	263	257	119	268	248	0.08
Identification	225	210	212	215	190	220	212	0.06

4.3 Tensile strength f_t

For the identification of the tensile strength f_t the same procedure as for the fracture energy was used. The resulting values for selected tests are introduced in Tab. 5 (no experimental tensile tests were carried out).

Tab. 5: Values of tensile strength f_t for each specimen plus mean value m and coefficient of variation COV

f_t [N/m]	E1	E2	E4	E7	E8	E9	m	COV
Identification	3.80	4.08	4.50	4.60	4.73	5.00	4.45	0.10

4.4 Correlation

As for nonlinear stochastic modeling imposing of statistical correlation is sometimes convenient, both correlation coefficients for the experimentally obtained as well as for the identified parameters were calculated (Tabs. 6, 7).

Tab. 6: Correlation matrix for experimental parameters

	E_c	a_e-a	K_{Ice}	G_{ce}	G_F	f_c
E_c	1	0.036	0.321	0.202	0.657	0.75
a_e-a	0.036	1	0.667	0.81	-0.086	0
K_{Ice}	0.321	0.667	1	0.929	0.314	0.095
G_{ce}	0.202	0.81	0.929	1	0.371	0.024
G_F	0.657	-0.086	0.314	0.371	1	0.714
f_c	0.75	0	0.095	0.024	0.714	1

Tab. 7: Correlation matrix for identified parameters

	E_c	f_t	G_f
E_c	1	0.657	0.257
f_t	0.657	1	-0.2
G_f	0.257	-0.2	1

4.5   Load-deflection diagrams

With the sets of parameters obtained from the inverse analysis the numerical analysis was conducted. A comparison of the experimental and numerical results in form of load–deflection diagram for beam E4 is given in Fig 7.
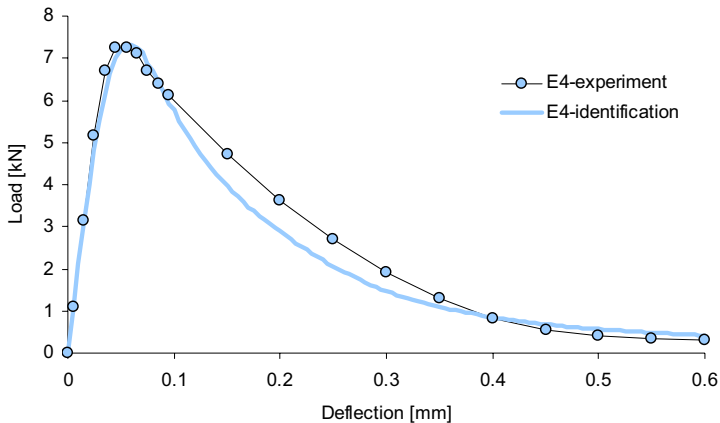

Fig. 7: Comparison of experimental a numerical *l–d* diagram for beam E4

5 Conclusions

Experimental results of notched-beam concrete specimens subjected to three-point bending are used in this contribution to obtain fracture-mechanical parameters. Two basic approaches were applied: effective crack model / work-of-fracture method and inverse FEM analysis using nonlinear fracture mechanics. The results are presented for the means and variances of fracture-mechanical parameters of a specific material model. In the case of fracture energy of concrete the results of the two variants provides close estimates and for the stochastic analysis. For structures made of this concrete the mean value from an interval 200–260 J/m^2 and a coefficient of variation 0.08 can be recommended. They will be utilized for consequent deterministic and/or stochastic virtual nonlinear fracture mechanics computer modelling of the reinforced concrete beams tested for dynamic damage identification purposes.

Acknowledgements

References

[1] Bažant, Z.P.; Planas, J.: *Fracture and size effect in concrete and other quasibrittle materials*. CRC Press, Boca Raton, Florida, 1998

[2] Bažant, Z.P.; Becq-Giraudon, E.: Statistical prediction of fracture parameters of concrete and implications for choice of testing standard. *Cement and Concrete Research*, 32 (2002), S. 529–556

[3] Novák, D.; Lehký, D.: Inverse analysis based on small-sample stochastic training of neural network. *9th Int. Conf. on Engineering Applications of Neural Networks*, EAAN2005, Lille, France, 2005

[4] Novák, D.; Lehký, D.: ANN Inverse Analysis Based on Stochastic Small-Sample Training Set Simulation. *Engineering Aplication of Artificial Inteligence*, 19 (2006), S. 731–740

[5] Kučerová, A.; Lepš, M.; Zeman, J.: Soft computing methods for estimation of microplane model parameters. In: *Computational Mechanics Conference, WCCM VI in conjunction with APCOM´04*, Beijing, China, Tsinghua University Press & Springer-Verlag, 2004

[6] Červenka, V.; Pukl, R.: ATENA Program documentation, Cervenka Consulting, Prague, 2004, http://www.cervenka.cz

[7]   Karihaloo, B.L.: *Fracture mechanics of concrete*, New York: Longman Scientific & Technical, 1995

[8]   Stibor, M.: *Fracture-mechanical parameters of quasibrittle materials and the methods for its determination*. Institute of Structural Mechanics, Faculty of Civil Engineering, Brno University of Technology, Brno, Czech Republic (in Czech), 2004 – Ph.D. thesis

[9]   Lehký, D.: *DLNNET – program documentation*. Theory and User's Guides, Brno, 2007 (in preparation)

[10]   Červenka, V.; Novák, D.; Lehký, D.; Pukl, R.: Identification of shear wall failure mode. In: *CD-ROM proc. of 11th International Conference on Fracture, ICF XI*, Torino, Italy, 2005

[11]   Novák, D.; Vořechovský, M.; Rusina, R.: *FReET – program documentation*. User´s and Theory Guides. Brno/Červenka Consulting, Prague, 2005, http://www.freet.cz

[12]   Pukl, R.; Červenka, V.; Strauss, A.; Bergmeister, K.; Novák, D.: An advanced engineering software for probabilistic-based assessment of concrete structures using nonlinear fracture mechanics. *9th Int. Conf. on Applications of Statistics and Probability in Civil Engineering* (ICASP9), San Francisco, California, USA, 2003, S. 1165–1171

[13]   Hoffmann, S.; Wendner, R.; Strauss, A.; Ralbovsky, M.; Bergmeister, K.: AIFIT – Anwenderorientierte Identifikation für Ingenieurtragwerke, Versuchsgestützte Steifigkeitsanalysen. In: *Beton- und Stahlbetonbau*, Edition 11/2007, Springer Verlag, Berlin, Germany (in German)

Novel Identification Methods for the Assessment of Engineering Structures

Roman Wendner, Alfred Strauss, Simon Hoffmann & Konrad Bergmeister
Institute of Structural Engineering,
University of Natural Resources and Applied Life Sciences, Vienna

Abstract: Damage in reinforced concrete structures generally results in cracking due to the materials non linear characteristics and thus leads to loss of stiffness within the region of this defect. Even with detailed monitoring data of a structure a localization or quantification of such stiffness loss still is very limited and difficult. Aiming at methods resulting in simple identification and localization of local bending stiffness reductions in reinforced concrete bridges, new approaches based on direct measurements of influence lines and dynamic identification procedures using sensitivity and modal bending lines based on model update were developed. For verification purposes in a first step laboratory beams were casted, progressively damaged and detailed static and dynamic surveys conducted at each damage state. The identified bending stiffness reductions of these beams were compared to the as far as possible undistorted crack pattern and width resulting only from the progressively increased load. Additionally a non-linear finite element model was created and calibrated using the recorded load-deflection curves as well as crack patterns. Considering the importance of the serviceability limit state for maintenance and use, one of the beams was evaluated in this respect using the identified stiffness distribution and working with the non- linear finite element model respectively.

1   Introduction

For most developed countries infrastructure challenges will shift more and more from building new infrastructure to the maintenance of existing structures. This will demand detailed knowledge of the structures' state not only to guarantee sufficient safety of the structures, but to economically optimize maintenance planning. Inspection methods should allow the identification at a very early damage state to enable the best preventive actions. Especially for concrete structures damage identification and localization is mostly limited

to damages visible at the surfaces of the structure. More sophisticated methods, giving an insight into the structure, are applied in most cases only as a result of this visual inspection or special incidences to the structure (e.g. fire or impact). The limited use of such insight giving methods is normally caused by their high cost and time efforts. Therefore simplified and inexpensive methods will be required, allowing at least general estimations of the structures health status. Global identification methods applied to structures can offer an attractive method for such estimations of the health status, including rough quantification and localization of damages, expressed by local stiffness changes.

Several methods serve to identify the stiffness of a structure by measuring static or dynamic parameters. Some of these methods determine the global stiffness of the structure by deformation or inclination measurements of single members. Other methods measure strain or stresses in confined areas. Both have the capability of very exact quantification of the stiffness, but are usually limited to the member or confined area. Therefore these methods require a large number of single sensors to cover an entire structure or allow localizations of the damages. Dynamic methods using eigenfrequencies, mode shape or damping allow for a considerable reduction of single sensors such as accelerometers, which are furthermore easy to install, as stated by CANTIENI [1]. These methods led to very promising results when applied to single span beams under laboratory conditions and in field on a progressively damaged bridge, see MAECK et al. [5] . Nevertheless this method requires very specific knowledge and substantial effort for the modeling of the structure and the interpretation of the measurements.

The need for global identification methods and their difficulties in practice and/or very specific engineering requirements demand their simplification. Therefore BOKU University proposed together with the industrial partners Schimetta Consult, and Maurer Söhne, as well as the bridge owner ÖBB (Austrian railway) for funding of a research project by the Austrian research foundation FFG. The proposal presents a project for user orientated identification systems for engineering structures, called "AIFIT". This contribution shows results of the second work package of the project, which aims for the comparison and validation of different global identification methods, applied to several progressively damaged reinforced concrete beams. Based on experimental data non linear models were calibrated in work package 3 and used for parameter studies including the assessment serviceability.

Following work packages address the further development of monitoring systems regarding the requirements of the identification methods. For the evaluation of the user orientation and feasibility of the identification methods a field test will be conducted at a 3 span bridge close to Vienna.

2   Identification Methods

Apart from the methods presented subsequently another dynamic approach by RALBOVSKY [8], arsenal research, Austria, and a neural network approach by NOVÁK et al. [6], University of Brno, Czech, used for comparison within the project, but could not be included in this contribution so far.

2.1   STRatified IDEntification (STRIDE)

STRIDE is a sensitivity factor based approach. In the first step suitable basic variables are selected by which the structural response can be captured - geometrical, mechanical and dynamical structural parameters, or any combination of these. In several iterations the basic variables are randomized, structural response is calculated by finite element or mathematical model and a sensitivity analysis is performed. Based on those results the variables are corrected until the difference between simulations and monitoring results is smaller than a predefined limit. Details about different search strategies, used randomization techniques and the correction process itself can be found in STRAUSS et al. [9].

2.2   Direct Stiffness Calculation (DSC)

DSC is a quasi-static identification method first developed by MAECK [5]. For this approach mode-shapes measured precisely and in a dense grid, as well as eigenfrequencies are necessary. In the first step inertia forces for every mode shape are calculated by (1).

$$q(x) = \omega_m^2 \rho(x) A(x) \varphi_m(x) \tag{1}$$

where ω_m is the measured eigenfrequency, $\varphi_m(x)$ denotes the measured mode shape and $\rho(x)A(x)$ is the mass of the structure at position x. Those inertia forces are applied onto a static model and the moment distribution $M(x)$ is calculated. Together with the curvature $\kappa_m(x)$ deduced as second derivative from the measured mode shape the stiffness distribution is determined individually for every mode shape, as follows

$$EI(x) = M(x) / \kappa_m(x) \tag{2}$$

Due to the high sensitivity of curvatures the measurement data has to be prepared in advance. This can be done by different tools – in this case fitting a high order spline to the derived curvatures to minimize the smoothing effect to a necessary degree.

2.3   MOdal BEnding Lines (MOBEL)

MOBEL too is a pseudo-static approach, in this case based on curve-fitting. Again inertia forces are calculated and applied onto a static model of the structure. Unlike DSC the pseudo-static bending line $\varphi_{c,j}(x)$ is calculated, which corresponds to the mode shape j. Using a curve-fitting algorithm the stiffness distribution along the structure can be optimized by minimizing the difference between $\varphi_{m,j}(x)$ and $\varphi_{c,j}(x)$ acc. to (3) in a least squares sense. This approach allows including several mode-shapes in the identification process and due to the over-determination and the curve-fitting algorithm does not necessitate preparation of the measurement data such as filtering or smoothing, see also HOFFMANN et al. [4].

$$\min_{K} \sum_j \sum_i \left(\varphi_{m,i} - \varphi_{c,i} \right)^2 \tag{3}$$

with i=number of measurement point and the j=number of mode shape

2.4   DEflection Line Function Identification (DELFI)

DELFI takes advantage of the known moment distribution of a loaded two-span beam. Just geometrical information and the load reactions at the bearings allow describing the deflection line by an analytical function or FEM model. A dense measurement grid for the experimental deflection gives the basis to fit this description by varying the stiffness of sections formulated in the model. The stiffness distribution resulting in the least square error represents smeared stiffness in sections along the beam. A detailed explanation and the application of DELFI to non linear FE models can be found in HOFFMANN et al. [2].

2.5   Influence Line Identification ASsessment (ILIAS)

ILIAS uses the change of influence lines of hyperstatic systems by their stiffness distributions. As this dependency is based solely on the relative stiffness distribution the algorithm can identify only relative stiffness along the system. A direct survey of the influence lines can be performed by measuring the bearing reactions, while knowing the position and magnitude of a traveling load. The use of this information in an optimization process, similar to the one used for DELFI, results in the identification of the relative stiffness distribution of the system. How this algorithm works in detail and might even use ambient traffic is described in HOFFMANN et al. [3].

3   Laboratory Tests

Early November 2006 a total of 9 reinforced concrete beams according to Fig. 1 were casted right in front of the test facility at BOKU University. Care was taken not only for the preparation and curing of the beams, but also all beams were lifted into the experimental rig by hand in order to prevent initial cracks in the test specimens, before they were damaged by applying load to one or both midspans.
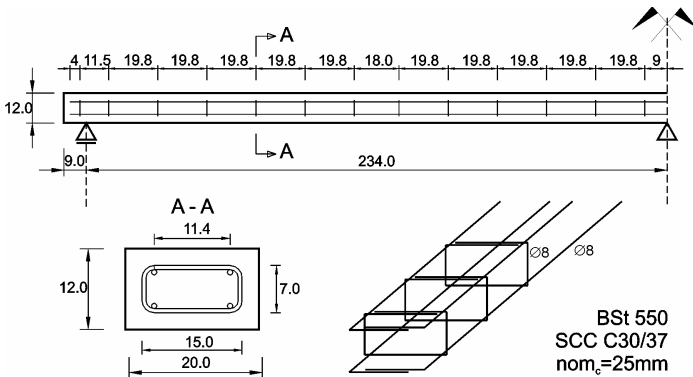

Fig. 1:   Reinforced concrete test beams [cm]

3.1   Measurements

At each load step the static deflection line of the full damaging load, first load step level and dead load are measured in a close grid by a vertical laser sensor mounted on linear guides underneath the beam. For the quasi-static influence line measurements precise force transducers are placed under each bearing recording the reaction forces while a constant load travels over the entire length of the beam. The position of this load is measured by a laser sensor. Large efforts were necessary for the precise survey of the modal behavior of the beams. Thanks to arsenal research in Vienna a laser vibrometer could be used which allows maximum precision for the direct measurement of the modal deflection of the beams. The laser vibrometer was placed outside the test rig, while holes in the bearings allowed adjusting the laser beam along the linear guides. A surface mirror mounted to the very stiff guides deflects the laser beam vertical to the concrete beam and back to the laser vibrometer (see Fig. 2), providing a precise measurement of deflection in a grid of optional density. During the test a distance of 9 cm between two measurement points, leading to a total of 50, showed to be sufficient.
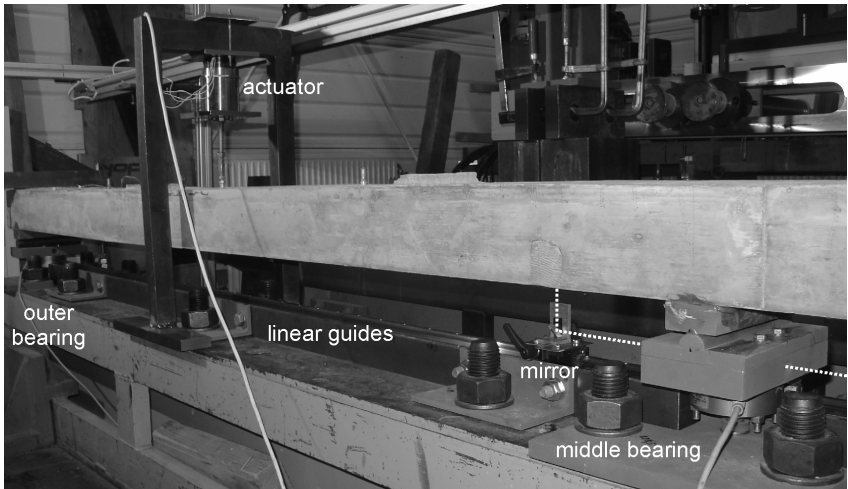
Fig. 2:   Test beam excited by moving coil actuators and measured by a laser vibrometer accelerometers and force transducers for the survey of its modal behaviour

In order to ensure a stable excitation during the measurement in each point two moving coil actuators were connected to the beam according to the specific modal shape and kept in resonance of the beam. Additionally accelerometers were placed on both sides of the beam underneath the connection to one actuator to control excitation and be able to capture torsion modal behavior of the beam. Using those as reference sensors the displacements obtained with the vibrometer could be corrected, if necessary. These dynamic measurements were conducted only for the first two eigenmodes as a realistic adjustment of the excitation to higher modes with only two available actuators turned out to be impossible. Finally yielding of the reinforcement was controlled by strain gages at 4 of the 8 beams.

3.2   Identified Stiffness

This contribution will concentrate on the analysis of one beam only, as results from the other beams lead to corresponding conclusions. During testing two scenarios were considered. Four beams were damaged in several steps by loading them in both midspans and four by applying load only to the first midspan, thus leading to different crack patterns and stiffness distributions. Since the resulting stiffness distributions for the asymmetrical case are more interesting, beam N°8 was chosen for this paper. In Tab. 1 the target of each load step is explained and the loads by which beam N°8 was damaged are given.

Tab. 1:   load-steps of beam N°8

N° of load step	Criteria	target load [N]	reached load [N]
1	first cracking	3500	3480
2	moderate loss of stiffness	4000	4020
3	finished crack initiation	5000	4980
4	design load	6500	6550
5	first cracks $\geq$ 0,3 mm	12000	12130
6	failure load	16000	15850

One important goal of this study is determine the relation between crack length, crack width, crack pattern and loss of stiffness. Consequently the complete crack pattern was noted and documented by photo for the undamaged beam as well as after each load step. With the help of ethyl alcohol, which was sprayed onto the surface and then evaporated except along cracks, and special magnifying glasses, cracks with width down to 0.01 mm could be detected. All cracks exceeding a crack width of 0.1 mm under load were labeled in steps of 0.1 mm.

The obtained crack pattern for beam N°8 as shown in Fig. 3 corresponds well to the moment distribution. Cracks which developed in a previous load step are shown in black, new ones in grey.
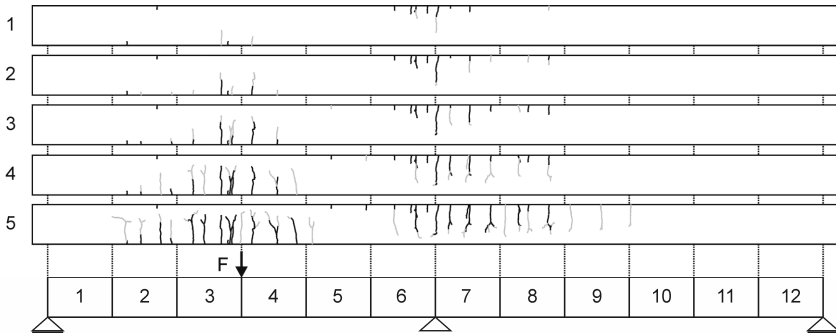

Fig. 3:   Crack pattern of test beam N°8 (view 2x heightened)

Fig. 4 shows the results for the sensitivity based model update STRIDE for all 5 load steps and the undamaged state of the beam. It reproduces the dominant influence of the crack length vs. density well, for instance resulting in significant higher stiffness loss in elements 3, 4 and 6 for the second load step. The crack development after load step 4 and 5 especially in the second span is detected too and finally leads to a total loss of bending stiffness of 75% of initial stiffness.
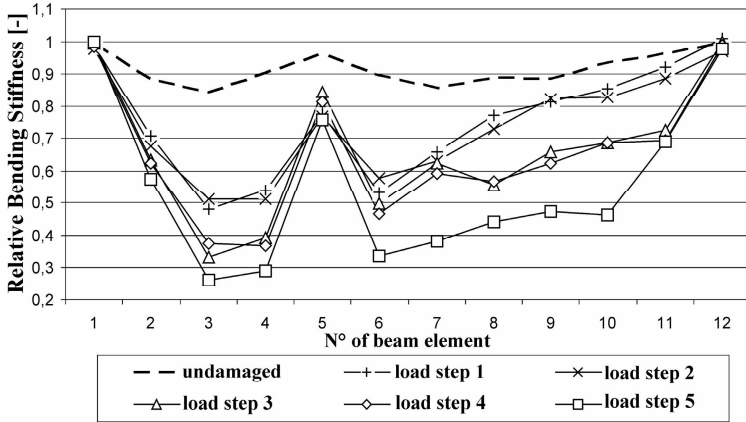
Fig. 4: Stiffness distribution of beam N° 8 identified by STRIDE

The results of MOBEL, as shown in Fig. 5, confirm this effect and offer moreover a better mapping of the crack distribution. However this method utilizes the entire data set available and was to be expected to return highly accurate stiffness distributions whereas the results presented for STRIDE were solely based on frequencies and modal displacements in 2 points of the second mode.
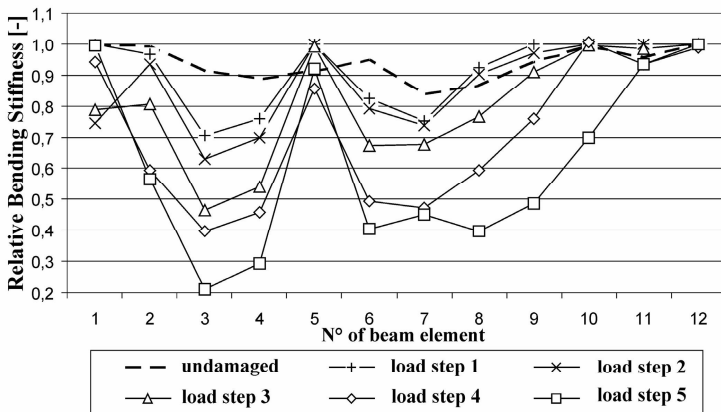
Fig. 5: Stiffness distribution of beam N° 8 identified by MOBEL

While the STRIDE and MOBEL results are standardized to the theoretical stiffness the identified absolute stiffness by the DSC is far of a theoretical model. Therefore all given results are standardized to the values of the identification of the undamaged state. Although DSC needs considerable engineering efforts and the method suffers from the influence of boundary conditions in the rear element 1 and 12, as little curvature is provided in this area, it still offers a valuable comparison, see Fig. 6.
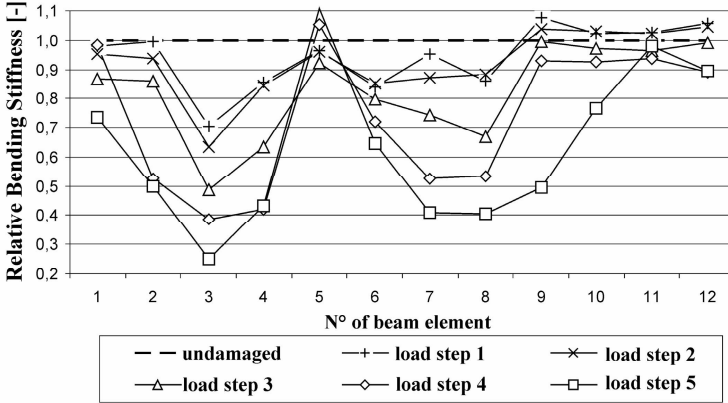
Fig. 6:   Stiffness distribution of beam N° 8 identified by DSC

In general DELFI permits the identification of absolute stiffness similar to STRIDE and MOBEL. Unlike the other approaches DELFI requires applying a significant load to the beam for identification. Furthermore the measurement of the statical deflection line is rather demanding, which makes DELFI for practical purposes unfeasible. Fig. 7 shows the relative loss of stiffness identified with DELFI, which is much graver as for the other methods, since stiffness under load is determined.
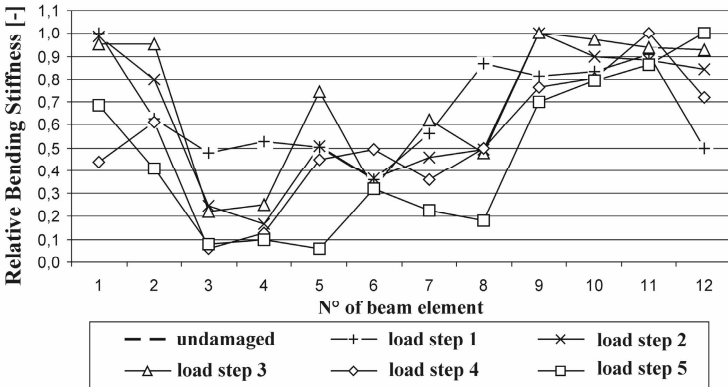

Fig. 7:   Stiffness distribution of beam N° 8 identified by DELFI

The results for DELFI in Fig. 7 and ILIAS in Fig. 8 are standardized to the maximum of each damage state. Identification with ILIAS is based on the measurement of relative changes in the bearing reactions. Thus it is not possible to identify absolute stiffness. Stiffness identified by DELFI as well as ILIAS follows the moment distribution quite well and corresponds to the documented crack pattern. The results of ILIAS match those of the dynamic approaches although the measured influence line data is of comparably lower quality than the modal data used, which is made possible by the high over-determination.
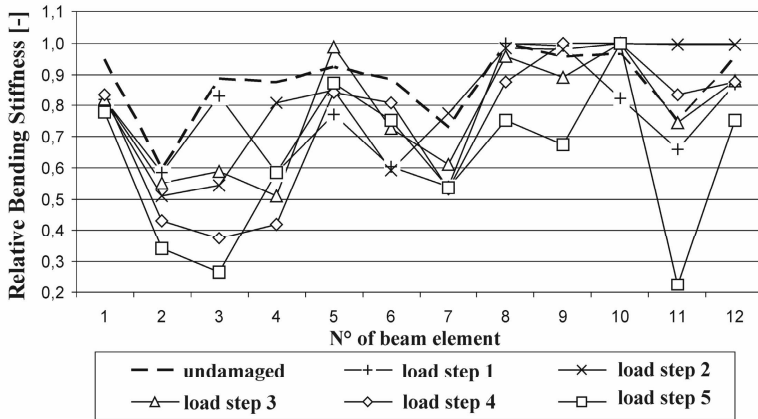
Fig. 8:   Stiffness distribution of beam N° 8 identified by ILIAS

Results from beam N°8 as well as from other test beams lead to the conclusion that basically all tools are capable of identifying and to a certain extent localizing damage. Especially the dynamic approaches result in very similar stiffness distributions which correspond well with the output from ILIAS and DELFI. Of course there are system immanent differences. ILIAS can only identify relative stiffness and DELFI only stiffness under load. Furthermore differences between static and dynamic stiffness have to be kept in mind when working with absolute values. Considering the goal of the research project – robust, user-orientated identification tools – DSC has to be eliminated due to its high engineering effort. The necessary measurements of DELFI make this approach also unfeasible for practical purposes. Since MOBEL was developed as reference tool, it was designed to use all available data. Consequently its applicability for user orientated identification still has to be determined, although very little engineering effort is necessary.

4   Assessment of deflection - SLS

For several years, the relevance of monitoring and identification to efficient maintenance planning have become more and more apparent and common knowledge. However most commercially available solutions for monitoring and identification provide the system operator only with raw data or at least with qualitative interpretations of the data. The opera-

tor on the other hand is in need of some kind of assessment index, by which a structures condition can be evaluated with respect to codes and necessary maintenance steps planned. Since especially the serviceability limit state (SLS) among others is of interest to the operator an approach was proposed to obtain an assessment index based on available material data or identified stiffness respectively.

Based on the assumption that only the basic material properties and geometry of the test beam are known a non-linear finite element model was developed in ATENA. The design load according to codes serves for the computation of the mean value of the variable action force S_Q. The non-linear finite element analysis was performed several times by SARA, a nonlinear safety and reliability assessment analysis software, with different sets of input variables taking into account material uncertainties as well as the unknown load history, described by the variables statistical properties according to Tab. 2. So the statistical properties of maximum deflection due to varying stiffness distributions can be determined and a failure probability by the usage of Freet (NOVAK et. al [7]) can be calculated considering an allowable deflection $w_{lim} = L/300$.

Tab. 2: variables for SARA calculation

variable	unit	mean value	coefficient of variation	type of distribution function
E	N/mm²	30 000	0.15	Lognormal
f_t	N/mm²	1.8	0.18	Weibull min
f_c	N/mm²	-50	0.10	Lognormal
G_f	MN/m	4e-5	0.20	Weibull min
$f_{y,i}$	N/mm²	360/ 560/ 730	0.05	Lognormal
$S_{Q,01}$	N	4827	0.10	Normal
$S_{Q,02}$	N	4827	0.20	Normal

Due the expected computational demands of non-linear calculation only 45 samples were generated using Latin hypercube sampling, see STRAUSS et al. [10]. During sampling a correlation of 0.9 was considered between the values $f_{y,i}$ building the multilinear law of the reinforcement and correlations between the concrete parameters were included acc. to [10].

Comparing the returned maximum elastic deflections with the admissible limit w_{lim} leads to a failure probability of $p_f = 5.14 \times 10^{-3}$ for a coefficient of variation for the variable action force S_Q of 10% and $p_f = 4.59 \times 10^{-2}$ for 20% in contrast to the demanded value of 10^{-3} per year, see Tab. 3. The rather high failure probability is mainly caused by the high uncertainties of the input variables describing the resistance. Thus the need to identify the proper material properties with higher certainty arises, which would decrease failure probability to an acceptable level and improve the quality of assessment; see NOVAK et al. (submitted paper to this conference). Calculated sensitivities confirm the dominant influence of input variables related with cracking such as tensile strength f_t and fracture energy G_f followed by Young's modulus E. This proves the high influence of cracking on the stiffness distribution and its relevance especially to the serviceability limit state.

In a second step the identified stiffness distribution should be evaluated and used to determine a safety index with respect to the allowable deflection. Since DELFI identified the

highest loss of stiffness and provides absolute values those results were used for the following study, considering an error in identification of 5% and 10% respectively. The elastic deflections resulting from the same variable action force $S_{Q,01}$ and $S_{Q,02}$ (see Tab. 2) were calculated using a small finite element tool programmed in MATLAB for the obtained stiffness distribution after load step 3 and 4 respectively.

Tab. 3: elastic deflection w_{elast} in first midspan and resulting failure probability p_f

version	mean value of w_{elast}	coefficient of variation	resulting failure probability
ATENA, COV_{SQ}=0.1	3.82 mm	0.37	5.14e-03
ATENA, COV_{SQ}=0.2	3.90 mm	0.52	4.59e-02
linear, LS3, COV_K=0.1, COV_{SQ}=0.1	3.19 mm	0.11	~0
linear, LS3, COV_K=0.1, COV_{SQ}=0.2	3.19 mm	0.21	8.02e-12
linear, LS4, COV_K=0.1, COV_{SQ}=0.1	5.15 mm	0.11	1.43e-05
linear, LS4, COV_K=0.1, COV_{SQ}=0.2	5.15 mm	0.21	9.00e-03

Since the mean value of the variable action force S_Q used in the SARA calculation lies in between the attained load of load step 3 and 4 of laboratory beam N° 8, so do the resulting experimental and numerical stiffness distributions and consequently the elastic deflections in the first midspan, see Tab. 3. The further decrease of stiffness after load step 4 leads to a sizable loss of safety with respect to load step 3, but still lies above the estimated level of the SARA calculation, since the uncertainties involved in the input variables are far less when identification results are used. The evaluation of sensitivities shows the dominant influence of those elements with the highest loss of stiffness and most impact on deflection. Those are elements 3 and 4 – around the first midspan – and element 7 – the element just after the middle support. In Tab. 3 the statistical descriptors of the elastic deflection associated with the different calculations are summarized and for each the failure probability is listed. Concentrating on the estimated mean value similar results are obtained for the non-linear and the linear calculations – in both cases far below the admissible w_{lim} = 7.8 mm. Consequently better information about the material properties supports a very good estimation of the performance concerning the SLS. However the most accurate assessment could be reached by using identified stiffness, information which currently is only rarely available. In this respect it must be mentioned that stiffness e.g. of a cross-section results from a set of several physical properties, whose single influence might be estimated using SARA.

5   Conclusion

Future demands will enforce the need for global identification systems to ease the inspection of our aging infrastructure and make its maintenance more efficient. The research project "AIFIT" aims for the enhancement of well known or new approaches to make them more user-orientated. Based on laboratory tests all methods could be validated and in their capabilities evaluated. In spite of their ability to identify stiffness some of the methods presented are not feasible for practical application due to high engineering effort or diffi-

culty to obtain the necessary input data. However STRIDE and ILIAS proved to be promising and can show their potential during a field test, as can MOBEL, which might prove to be applicable too. The concept for assessing a structure under SLS demonstrated the need for accurate information about material properties and proves the benefit of global identification tools for assessment, when available. In addition the significant influence of cracks on structural stiffness and SLS was shown – both experimentally and numerically, which challenges existing codes especially regarding the accounted deformation.

Acknowledgement

References

[1] Cantieni, R.: Experimental techniques in dynamics of bridges. In: *Proceedings of 4th European Conference on Structural Dynamics: Eurodyn '99*, Prague, Czechia, 1999, pp 13-22

[2] Hoffmann, S.; Bergmeister, K.; Strauss, A.; Preslmayr, M.: Identifying Stiffness Distributions by Direct Influence Measurements. In: *10th International Conference on Applications of Statistics and Probability in Civil Engineering (ICASP10)*, Tokyo, Japan, 2007

[3] Hoffmann, S.; Bergmeister, K.; Strauss, A.: Damage identification by influence line measurements. In: *Structural Engineering Conferences (SECON) and Croatian Society of Structural Engineers (CSSE): Bridges. International Conference on Bridges*, Dubrovnik, Kroatia, 2006 , pp 1029-1034

[4] Hoffmann, S.; Wendner, R.; Strauss, A.; Bergmeister, K.: Comparison of stiffness identification methods for reinforced concrete structures. In: *Proceedings of the 6th International Workshop on Structural Health Monitoring*, Standford, USA, 2007

[5] Maeck, J.: Damage Assessment of Civil Engineering Structures by Vibration Monitoring. Katholieke Universiteit Leuven., Heverlee, Belgium. 2003 - Phd thesis.

[6] Novák, D.; Lehky, D.: Inverse analysis based on small-sample stochastic training of neural network. In: *9th International Conference on Engineering Applications of Neural Networks, EAAN 2005*, Lille, France, 2005, pp. 155-162

[7] Novák, D.; Vořechovský, M.; Rusina, R.: *FReET – program documentation*. User´s and Theory Guides. Brno/Červenka Consulting, Prague, 2005, http://www.freet.cz

[8] Ralbovsky, M.: Damage Detection in Concrete Structures Using Modal Force Residual Method, University of Technology, Bratislava, Slovakia. 2007 - Phd thesis (tendered)

[9] Strauss, A.; Bergmeister, K.; Lehky, D.; Novak, D.: Inverse statistical nonlinear FEM analysis of concrete structures. In: *Euro-c 2006. Computational Modelling of Concrete Structures*, G. Meschke, R. de Borst, H. Mang and N. Bicanic, Mayrhofen, Austria, 2005, p. 897.

[10] Strauss, A.; Hoffmann, S.; Wendner, R.; Bergmeister, K.: Structural Assessment and Reliability Analysis for Existing Concrete Structures, Application on Real Structures. In: Structure and Infrastructure Engineering, Taylor & Francis, 2007, ISSN 1573-2479

Risk-orientated planning of structural health monitoring

Christoph Klinzmann & Dietmar Hosser
Institute for Building Materials, Concrete Constructions and Fire Protection,
Technical University of Braunschweig

Abstract: The Collaborative Research Centre (CRC) 477 at the Braunschweig University of Technology investigates and optimizes innovative methods for structural health monitoring (SHM). Its main target is the development and optimization of monitoring technologies and strategies. In project field A1 of the CRC, a framework for risk-orientated planning of SHM is developed. Its objective is the reduction of the SHM measures to a minimum required level. The basis of the framework are probabilistic models of the concerning structure, which are analysed with reliability methods. Recommendations for the monitoring process and its amount can be derived from the results of the analyses. Vice-versa data from SHM is used to assess the safety of the structure anytime during its usage and to refine the monitoring process. This paper describes the methodology of the framework which is currently implemented in a program system called PROBILAS. It will assist engineers in the assessment of structures and the planning of monitoring measures.

1   Introduction

Accidents, natural phenomena or ageing processes are often followed by damages in structures. This can have significant economical and environmental consequences, e. g. if the structure is not useable for a certain time. In a later state, even the users are endangered when the amount of damage increases to a level, which can lead to a critical limit state and eventually to a collapse. In Germany, most elements of the traffic infrastructure are investigated for damages during regular inspections, which are carried out in a normal manner every 3 years and more intensively every 6 years. In cases where damage is growing rapidly or after heavy accidents extraordinary inspections and rehabilitation measures are carried out. The actual procedure is rather static and inflexible. It would be an improvement, if the structure itself would be able to signal whether it has reached a state that would require an inspection and eventually rehabilitation. In addition, the amount of money needed for

restoration measures could be reduced, when damages would be detected earlier and before they reach critical extents. Structural health monitoring (SHM) is one to possibility to improve the situation, because it enables the finding of damages shortly after the occurrence or initiation.

The work of the collaborative research centre (CRC) 477 at the Braunschweig University of Technology addresses many questions and problems regarding SHM. The CRC explores and develops innovative methods for SHM and optimizes monitoring technologies and strategies. In project field A1 of the CRC, a framework for the risk-orientated planning of SHM measures was developed. It bases on the idea that the necessary amount of monitoring depends on the actual state of the structure. Young structures that show no significant errors or damages should not be monitored continuously, but periodically in suitable time intervals. The amount of monitoring shall be increased, when the structure starts to show signs of significant damages. There exist the possibilities to increase the amount of placed sensors in sensible areas, to shorten the time intervals between periodic monitoring phases or to increase the measurement frequency.

The framework developed utilizes the methods of reliability analysis for the assessment of structures and is therefore able to consider different failure modes, spatial variability and natural uncertainty. All available information about a structure, including already identified weak points or hot-spots, is summarized in a risk-orientated probabilistic model of the structure, which is ideally developed prior to the begin of the construction process. The results of the analyses with reliability methods are used to develop a first monitoring strategy. The framework covers the identification of trends and the determination of stochastic information from the measured data. This information is used to update the reliability level of the structure and to evaluate necessary changes of the monitoring strategy. The procedure has advantages over classic approaches, because the actual state of the structure can be estimated independently of predefined inspection intervals at any point in time.

The topic of the assessment of structures under consideration of effects of uncertainty is becoming more and more important. A very active field of research is the determination of optimal inspection and maintenance intervals, shown by FABER et al. in [3]. These technologies are especially interesting for building management systems (BMS), which were based on deterministic approaches for a long time. Actually, the consideration of probabilistic models within BMS is increasing steadily and with the current trend for cost saving and optimization they will become a widely used technique. The methodology described in this article follows this trend, but investigates possible simplifications of exact probabilistic models, in order to ensure the applicability of the methods in practical cases. The idea was to develop a computer program to assist users in the design and calculation of these simplified models and to make suggestions where and to which extent the structure should be monitored on their basis.

2 The framework for risk-orientated planning of SHM

The first step in the application of the framework is to formulate the risk-orientated probabilistic model, based on a thorough anamnesis of the structure. Depending on its age, the sources of information for the anamnesis are different. In the optimal case, when the structure is not yet built, all relevant points in the structural design should as well be included in the probabilistic model. As long as no significant faults occur during the construction process, this information is sufficient. Further action is necessary, if the object of concern is an already existing structure because they usually show signs of deterioration and degradation. When these damages have been identified in the necessary inspection they are considered in addition to the standard probabilistic model. In every case, the probabilistic model is created on the basis of the actual level of knowledge about the structure. Obviously it can only include foreseeable failure modes. It is impossible to predict every type of failure which can occur in a structure throughout its lifetime, e. g. damage due to heavy accidents and extreme natural phenomena. The reliability index which results from the analyses must be seen in this context. It can only give an indication of the actual safety level of the structure. In case new deteriorations are found during the lifetime, the probabilistic model must be extended. After the model has been created, it should be calibrated using measured data from inspections and/or quality control. Usually, the stochastic information in the model is derived from the assumptions and definitions in the structural design. For important parameters, these assumptions should be verified. This is done in the calibration process, where the stochastic model is updated with data from inspections or quality control. After that, the continuous evaluation procedure of the framework with repeated assessments, refinements of the model and modifications of the monitoring strategy can be started. Figure 1 gives an overview of the sequence of the necessary steps.
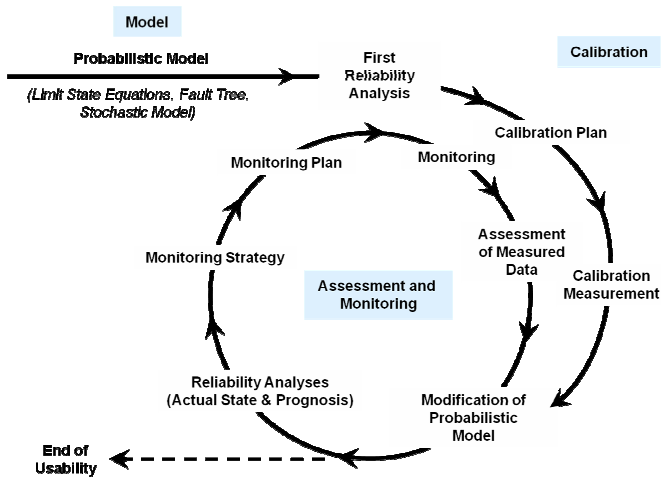

Fig. 1: Structural evaluation process according to the framework

In the assessment and monitoring phase, the necessary level of monitoring is derived from the results of reliability analyses. The framework distinguishes between periodic and continuous monitoring. The choice between both possibilities depends on the actual state of the structure and its predicted performance in the future. The necessary analyses are carried out repeatedly in the predefined time intervals and on the basis of data from SHM if it is available. The usability of the structure ends when the reliability of the structure falls below a pre-chosen target reliability level.

The following chapters explain the procedure from the definition of the special type of probabilistic model required for the analyses to the different types of analyses and the possible decisions arising from the results.

2.1   Probabilistic model

The probabilistic model summarises all information which is required to carry out the reliability analyses. It consists of the stochastic model of all parameters, a fault tree and limit state equations.

2.1.1   Definition of the stochastic model of parameters

The stochastic model summarizes information about deterministic (constant) and random parameters. The variability of a random parameter compared to its target value has large influences on the reliability calculation. There are multiple causes of this variability. The most important is the natural randomness or inherent variability of a parameter that cannot be influenced by technical means. Examples are most material properties and time-dependant loads. The model uncertainty, which naturally exists every time when a model is used to describe natural phenomena and the statistical uncertainty due to sparse information are other sources of variability.

When defining a stochastic model, it has to be decided whether the uncertainty of a parameter is taken into account or neglected. Parameters that show only very small variations over their lifetime can be treated as deterministic. Typical examples are dimensions like length, height or width of structural elements. Usually, these parameters do not require long-term monitoring, but eventually a simple control after the construction phase.

Parameters, which incorporate a natural uncertainty, are treated as simple basic variables. They are defined with stochastic distribution functions and their describing moments or parameters. In most cases, the necessary information can be taken from literature, e.g. from standards or alternative sources like the *Probabilistic Model Code* [4]. In addition, it is possible to estimate stochastic information from measurements.

If the time-dependant behaviour of a parameter has to be considered in addition to a natural variation, the problem gets more complex. These parameters have to be treated as functions of basic variables with the help of stochastic processes that are able to consider both types of variation. The computation of the reliability is even more complex and often only possible for special cases and under certain assumptions. For practical appliances it is useful, to transfer the time dependant reliability problem to a time independant case, e. g. by

using extreme value distributions. In cases, where only the tendencies of the reliability are of interest, this approach is sufficient.

2.1.2   Definition of the fault tree

The correct description of the behaviour of the system has a large influence on the calculated reliability level. Most structural systems consist of redundant elements. These systems usually collapse only, when a failure mechanism has been reached. This means that failure has to occur in multiple elements at the same time or shortly after another. Usually, there exist multiple failure mechanisms, which each consist of different failure modes.

The application of event tree analysis (ETA) is an appropriate method to find all possible combinations of failure modes. In simple cases, the most probable combinations are predictable by engineering experience. However, the total amount of possible mechanisms increases with the complexity of a structure and therefore a systematic analysis should include the ETA.

The calculation of the probability of failure of a system of failure modes and mechanisms requires a fault tree, which can be derived from the findings in the ETA. The fault tree summarizes all causes for system failure by regarding all possible causal sequences of component and subsystem failures. Originally, this procedure was limited to technical systems, but was later adapted for the description of structural systems.

The design of fault trees is relatively complex and for that reason, the framework provides a simplified scheme for their definition. This assists engineers, which are usually not familiar with the methodology. At first, so-called "points of failure" are defined. These points are the hot-spots of the structure, where the occurrence of a failure is very likely. Examples are areas with a high utilisation or special points in which degradation can be expected. Points of failure establish a relation between the real structure and the abstract failure modes in the fault tree. Failure modes can often be described with single components using a simple mechanical model. A failure mode needs more components, when conditional probabilities have to be modelled. This can be the case, when the probability of failure of a component is dependant on the initiation of a deterioration process. The next higher level within the schematized fault tree is the so-called "failure mechanism", which describes the redundancies of a system by a combination of failure modes. A failure mode can become a failure mechanism, when it is the single reason for the collapse of the system.

The described scheme has the advantage that the fault tree is well structured and it enables computer programs to set up the complete fault tree automatically with the least amount of user input. The user only has to provide knowledge about eventual conditional probabilities within the failure modes and which failure modes can together lead to a system failure. For further details, please see KLINZMANN & HOSSER [5]. An example for a typical fault tree is shown in figure 2.

The necessity to include all important hot-spots in the probabilistic model was already explained. This makes sense, when deterioration is very likely to occur and if it will affect the reliability of the structure. In case of potential deteriorations this is different. Deterioration
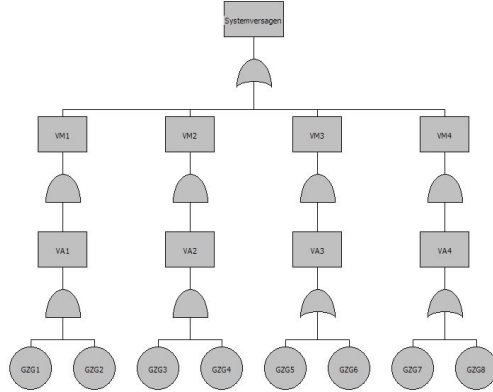
Fig. 2: Typical fault tree

processes are often monitored preventatively. Examples are durability sensors, which are installed in places of concrete structures, where the ingress of chloride is highly probable. As long as the deterioration process has not yet initiated or has reached a critical extent, the reliability of the system in terms of an ultimate limit state is not yet affected. Its consideration from the beginning would make the model more complex, because it would have to be modelled as a conditional probability for a mechanical failure triggered by the deterioration process. The framework provides so-called "indicatory components" to avoid the usage of such complex probabilistic models. The indicatory component consists of a single limit-state equation, which describes the process that leads to the deterioration, e. g. the mentioned chloride ingress into the concrete structure. The reliability of the indicatory component is calculated separately to the model of the system. The reliability index or respectively the probability of failure of the component indicates the probability that the mechanical model of the structure is affected by the special deterioration process. If the computed reliability exceeds a pre-defined threshold, the deterioration should be included directly in the more complex probabilistic model of the system. Alternatively, the structure can be restored at this point. The described procedure helps to keep the fault tree simple without making significant mathematical errors.

2.1.3   Definition of the limit state equations

The failure or survival of a component in the fault tree is calculated with the help of limit state equations. The general form of such an equation for a time invariant case can be written as

$$Z = R - S \tag{1}$$

The component fails when Z is smaller than zero, which happens when the resistance parameter (R) is smaller than the action parameter (S). In more complex situations, R and S must not necessarily be parameters, but can be functions of different basic variables, which

describe the resistance (R) and/or the stress (S) quantities with any type of model. For the time variant case, one or both quantities are functions of time.

In cases where the monitoring process shall be concentrated on the ultimate limit state, well known and established mechanical models can be used for the definition of limit state equations. This is a fast and transparent way to create models for the use with the framework. If it is kept in mind that a typical structure under normal loading should not show nonlinear behaviour, models according to elastic theories are sufficient to formulate limit state equations for the usage with the framework. Nevertheless, an increasing amount of structural designs makes use of numerical models, which leads to the problem that such a simple methodology is not always applicable. In these cases, analytical equations can be created with the help of the response surface method. For a discussion of the method see BUCHER et. al. [1].

The general procedure is explained with an example. Figure 3 shows a steel truss bridge and some marked hot-spots. Ideal truss bridges are statically determinate and their load bearing members are only loaded with longitudinal forces. This has advantages when the limit state equations are defined. Taking into account that only elastic deformations shall be allowed, the yield strength f_y is a suitable resistance quantity for tensile forces. In case of mainly compressive forces, the yield strength f_y should be attenuated to avoid stability failures. A reduction factor χ can be calculated e. g. via the model column method. The stress quantity can be represented by the stress σ in the bars.

Fig. 3: Typical truss bridge with marked hot-spots

Using equation 1, these definitions lead to two simple limit state equations for the cases of compressive (Equation 2) and tensile (Equation 3) loading.

$$Z = \chi * f_y - \sigma \tag{2}$$

$$Z = f_y - \sigma \tag{3}$$

In their present formulation these limit state equations have the disadvantage that none of the parameters within them is measurable. For that reason the structure cannot be assessed based on measured data. To overcome this problem, the stress in the bars is formulated in dependence of measurable response parameters. Taking into account the stress-strain relationship, the limit state equations 2 and 3 can be formulated in dependence of the measurable strain (Equations 4 and 5).

$$Z = \chi * f_y - E * \varepsilon \tag{4}$$

$$Z = f_y - E * \varepsilon \tag{5}$$

This modification allows the determination of the actual safety level of the structure every time when new data from the monitoring process is available.

2.2   Methodology of the reliability analyses

The reliability analyses are carried out using first and second order reliability methods (FORM / SORM) on the basis of the STRUREL software [6]. The main results of the calculation procedure are the probability of failure p_f or respectively the safety index β of the system $[\beta=-\Phi^{-1}(p_f)]$. In addition, the calculation yields sensitivity factors (α_i) for all random variables x_i of the system, which indicate the influence of all variables x_i on the reliability index.

At first, the calculated reliability level of the system is compared to a pre-defined target reliability level. If the calculated reliability index falls below the target reliability level, a further usage of the structure cannot be recommended. The target reliability level can be defined according to Eurocode 1 [2] in dependence of the level of hazardousness which emanates from the structure. This target reliability level does not consider structures that are monitored. Possible reductions of the target reliability to consider that a structure is monitored level shall be discussed in the future.

The framework distinguishes between two different levels of reliability analysis. The first type evaluates the actual state of the system and considers data from SHM when it is available. The future development of the reliability of the system should be considered when the monitoring strategy is developed. This is a time dependant reliability problem, which can be solved using stochastic processes and the calculation of outcrossing rates. They determine the most probable point in time when the resistance quantity is first exceeded by the stress quantity. The corresponding calculation method is relatively complex and as already mentioned is only valid if certain requirements are met. In addition, the planning of monitoring measures requires only an approximation of the future reliability level. The literature shows different approaches to this problem. Global concepts, e. g. described by STRAUSS [7], make use of degradation functions for the reliability index β depending on a Weibull formulation. They provide time-dependant reliability curves without a special reliability calculation.

The framework presented in this paper makes use of similar functions, here called modification functions. In contrast to the described global approach, these functions describe the

time dependant behaviour of single parameters within the probabilistic model. This approach has the advantage that different effects, like structural deterioration and the increase or decrease of loads, can be considered at the same time. They can be defined for any basic variable as well as for constant parameters and are calibrated with measured data. The change of the parameter in the future is estimated via an extrapolation of its development in history to a time interval in the future. This is done by fitting linear or nonlinear models to the measured data. In the prognosis calculation the probabilistic model is evaluated in a time-step procedure. Prior to every calculation step, the functions are evaluated for each parameter and the current time step. The stochastic model of parameter is modified accordingly. Figure 4 shows a typical reliability index profile from the prognosis calculation (light grey curve), calculated with linear modification functions.
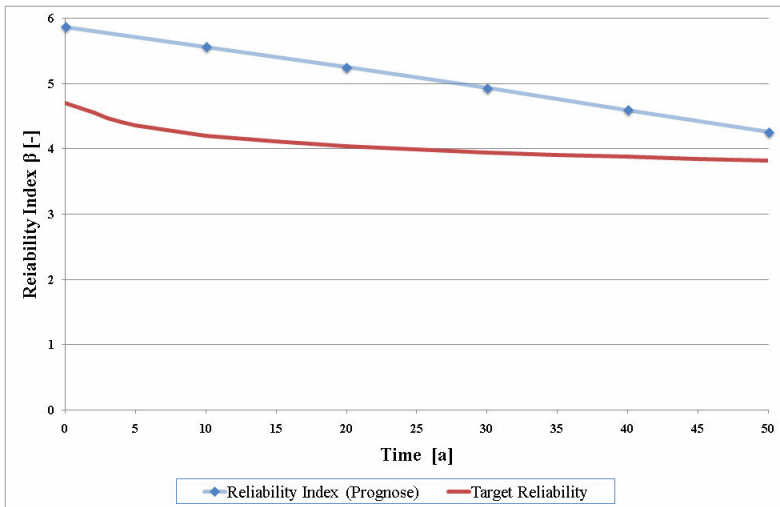

Fig. 4: Typical development of reliability index in the prognosis calculation

In the prognosis calculation, the target reliability level decreases with time and the length of the reference period. This is illustrated by the dark grey curve in Figure 4.

In contrast to the mentioned global approaches, this procedure has the advantage that deterioration can be modelled more realistically and that the functions improve the more data from SHM is available. Nevertheless, due to the lack of data in the first years of assessment, their formulation during this time must be based on experience.

2.3   Monitoring Concept and Monitoring Plan

The monitoring strategy defines which parameter(s) in the probabilistic model should be monitored. It is a decision aid for users, who want to set up a monitoring plan for the special structure. It utilizes the results of the reliability calculations to give hints about the necessary amount of monitoring. The following passages explain the procedure.

First of all, all parameters with a time-dependant nature and a high significance are included in the strategy. Time independent parameters can have a significant influence on the reliability as well, but due to their nature it is sufficient to measure them during the calibration phase and to update the stochastic model afterwards.

The sensitivity factors α_i show the contribution of each parameter to the reliability of the system. In general, all parameters with a high sensitivity factor should be monitored more often than a parameter with a low factor. Figure 5 shows typical results for sensitivity factors of some parameters resulting from a FORM / SORM evaluation of a probabilistic model. Further knowledge about a parameter must be considered in addition to the absolute value of the sensitivity factor.
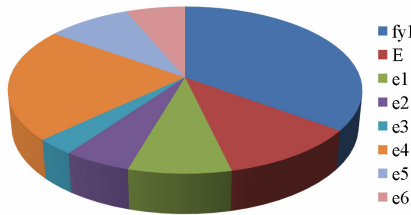

Fig. 5: Sensitivity factors of parameters

Eventually, different parameters describe different phenomena with different speeds of variation, which cannot be considered by the FORM / SORM calculation. An algorithm working directly with the sensitivity factors would suggest the identical amount of monitoring measures for a phenomenon with a high (e. g. action effect) and low (e. g. deterioration) speed of variation. The framework proposes a decision aid to overcome this problem. The "intensity of monitoring" is determined directly from the sensitivity factors and a relative safety index β, which is calculated according to equation 6.

$$\beta_{rel} = \min (\beta_t - \beta_{target,t}) \qquad (6)$$

Tab. 1: Intensity of monitoring

β_{rel}	Intensity of Monitoring [MI]		
	$\alpha < 0.33$	$\alpha < 0.66$	$\alpha \leq 1.00$
≤ 0.0	High	High	High
< 0.5	Medium	High	High
< 1.0	Low	Medium	High
< 1.5	Very low	Low	Medium
> 1.5	None	Very low	Low

The value for β_{rel} is calculated in all time steps of the prognosis calculation. The minimum value is used in conjunction with the sensitivity factor α of each parameter to determine

the intensity of monitoring (Table 1). When the reaction speed of the phenomenon which has to be monitored is known, the intensity of monitoring can be taken as indication for the necessary amount of monitoring. Table 2 shows suggestions for possible monitoring intervals in dependence of the intensity of monitoring. These values are examples only and should be determined specifically for each structure. The examples are given for a high and slow reaction speed (e. g. monitoring of live loads on a bridge vs. monitoring of chloride ingress into a concrete structure).

If the reliability analyses suggest a low monitoring intensity for certain parameters, it does not necessarily mean, that it should not be included in the monitoring plan. Especially en engineering experience suggests that deterioration is very likely to happen in the related hot-spot, it may be useful to monitor it preventatively. In addition, such parameters can be useful in the deterministic assessment procedures of the data.

Tab. 2: Intensity of monitoring in dependence of sensitivity factors

MI	Speed of variation of monitored phenomenon	
	Fast (e. g. Live load)	Slow (e. g. Deterioration)
High	Continuous	High frequency (1x / month)
Medium	High frequency (1 day / week)	Medium frequency (1x / half year)
Low	Medium frequency (1 day / month)	Low frequency (1x / year)
Very low	Low frequency (1 day / half year)	Very low frequency (1x/ 2 years)

2.4   Assessment of measured data

The measured data is analysed with deterministic and probabilistic methods. Usually, reaction speeds in structures are slow. For that reason is not necessary to carry out a probabilistic assessment every time when new data is available. The first analyses utilize deterministic methods. Their purpose is to identify negative trends in the measured data. This is necessary, because only the most likely failure modes are included in the probabilistic model of the structure. This means, that if a failure occurs which has not been considered in the model before, the calculated reliability level of the structure can be overestimated. Most failures do not happen suddenly and can be identified before they reach a critical threshold. Three simple algorithms are provided by the framework to find problems which can lead to new failure modes. The analyses are carried out at the end of the monitoring phase when the structure is monitored periodically and in pre-defined intervals if it is monitored continuously.

Normally, the probabilistic assessments are carried out in fixed time intervals (usually 1 year). In case a negative trend is indicated, the structure has to be inspected to identify the cause for the change. The model has to be updated with the findings prior to the next assessment.

Before the reliability analyses can be carried out, the necessary stochastic information about the basic variables has to be extracted from the measured data. If the data does not

follow a known stochastic model or in case the underlying model it is unknown, the data is analysed for conformity with typical stochastic distributions and the goodness-of-fit is confirmed with statistic tests. If no fit can be achieved or if not enough data is available, an alternative method is the utilisation of one of the asymptotic extreme value distributions (e. g. the Gumbel(max) distribution for system responses). This has numerical advantages and guarantees that the result of the probabilistic assessment lies on the safe side as long as no extraordinary loads will be applied to the structure.

3   Conclusion

This article provides an overview of the framework developed to help engineers to plan optimal structural health monitoring (SHM) measures. The framework provides help to set up the required probabilistic model and gives decision aids for the necessary amount of monitoring. Additionally, it includes a possible procedure for the integration of data from the SHM process into the probabilistic model. The complete integration of the methodology into the computer program PROBILAS (PRObabilistic Building Inspection and Life ASsessment) and its tests with real world data is the task for the last remaining funding period of project field A1 of CRC 477.

Acknowledgements

References

[1] Bucher, C. G., Bourgund, U. 1987. "Efficient use of response surface methods". *Technical Report 9-87*, Universität Innsbruck, Innsbruck, pp 6-9.

[2] EN 1990 2002. Eurocode: Basis of structural design.

[3] Faber, M. H. (ed.) 2001. "Risk Based Inspection and Maintenance Planning". Institute of Structural Engineering, *Report Nr. 266*, Swiss Federal Institute of Technology, Zurich

[4] Joint Committee on Structural Safety (JCSS): Probabilistic Model Code, 12th draft. http://www.jcss.ethz.ch, 17.05.2002

[5] Klinzmann, C. & Hosser, D. 2005. "Probabilistic Building Inspection and Life Assessment – a computer program for reliability based system assessment". *Proceedings of 22nd CIB-W78 Conference Information Technology in Construction,* Dresden. pp. 441-448

[6] Reliability Consulting Programs (RCP) 2004. STRUREL, a Structural Reliability Analysis Program-System, COMREL & SYSREL: Users Manual. Munich: RCP Consult.

[7] Strauss, A. 2003, "Stochastische Modellierung und Zuverlässigkeit von Betonkonstruktionen", Institut für konstruktiven Ingenieurbau, Universität für Bodenkultur, Vienna, Austria

Probability based updating for the assessment of existing timber beams

Tino Bretschneider

Chair for Steel and Timber Structures, Brandenburg University of Technology, Cottbus (Germany)

Abstract: Within the framework of this paper, dependent probability considerations will be applied to the load bearing properties of timber beams. This will be done by proof loading and finally by a simulation approach.

A strong variance reduction technique is especially advantageous in applications to timber structures. Here large variances even within graded lumber have a strong negative influence on research procedures and on the assessment of structural reliability of existing beams.

As basis of the simulation approach, the Karlsruher-Simulation-Model will be used. Using new data from experiments the Karlsruher Simulation Model will be confirmed. Additional and new consideration on the precision of the predicting process will be added.

Demonstrated examples will present the advantage and application fields of the improved prediction of the load bearing capacities. At first additional considerations to the effect on safety calculations will be made. This will be followed by an adoption of accelerated research procedures for timber structures.

1 Introduction

1.1 Influences on strength properties of timber

Since centuries the influencing parameters on timber strength are discussed. The following ones are found to be significant:

| kind of wood | density | knots | fibre direction | moisture content | size | other defects |

| growth conditions | **Timber Strength** | harvest and preparation conditions |

| load duration | load kind | climate during use | maintenance | decay | MANY OTHERS |
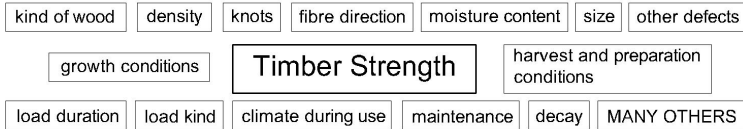
Fig. 1: Influence parameters on timber strength

Caused by the fact that strengths can not be received by full size testing for every combination of parameters, reference strengths were defined. Historically these reference strengths were derived testing small, defect free test specimens. Later also beams in a reference size were tested. Derivations from the derived reference strengths were described by correlations. Based on this, reduction factors for structural design were received.

With the usage of wood as an industrial traded material, grades were introduced and the limited influencing parameters for each grade. Also in-grade-testing and finally quality control programs were developed.

1.2 Quality of in-grade property prediction

During the calibration of the LRFD design codes, the data of in-grade-testing and quality control programs were intensively analyzed. Target was a sufficient description of the distribution type and the distribution parameters within a grade. Beneath many others RUG [10] described his experience with the data from the former German Democratic Republic quality control program. His experience about the distribution within a grade are summarised in the following table.

Tab. 1: Quality of property prediction within a grade

Modulus of Rupture (MOR)	Distribution type	Coefficient of variation
Graded Glued Laminated Timber	2 parametric Weibull	22 percent
Graded Structural Lumber	2 parametric Weibull	28 percent

Depending on the (over the complete market) practised efficiency of the grading system, the coefficients of variation are sometimes a little bit lower. Target of this paper is to analyze different possibilities to receive a better degree of believe for single beams, in the sense of a lower coefficient of variation, by taking into account additional information.

1.3   Mathematical structure for additional information

Additional information can be from different kinds. DITLEVSEN [2] proposed the definition of three different information types based on their mathematic effect. The definition was made in the multidimensional probability space of the influencing parameters. The following three information types were defined:

Type A: Additional information in the sense of new sampling information about one ore more parameter becomes available. The usual procedure is to use standard Bayesian updating for the calculation. It is widely used for sampling the material properties of wood. The "difference" is the informative priors now may be used.

$$\Omega = \left\{ x \in R^n \mid x_i = a_i \right\}$$

(1)

R^n sample space; a_i additional test values

Type B1: The sample space is divided into a valid and a non-valid part by measurement. So a certain variable is larger or smaller than a certain value.

$$\Omega = \left\{ x \in R^n \mid h(x) \leq 0 \right\}$$

(2)

h(x) hypothetic limit state function

Type B2: The space is reduced about dimension(s) trough measure (nearly) fixed value (s) for one ore more variables. A possibility is the usage of additional introduced strong correlations between the variables.

$$\Omega = \left\{ x \in R^n \mid \phi(x) = Z \right\}$$

(3)

$\phi(x)$ represents the hyperplane of the residual sample space

Of course, mixed information from those mentioned before, are also possible. Some of this shall also work for timber. Within the following sections, two approaches for timber beams were assessed.

2   Proof loading for timber structures

2.1   Probabilistic effect

Proof loading seems to be the simplest method to receive additional information about the load carrying capacity of a building component. The risk of structural failure during the proof loading process is usually limited by self securing loading equipment. Considerations for practical proceeding are described by QUADE [9]. After the proof loading process a truncated distribution for the resistance is received, if the structure survives (and the measurement uncertainty is neglected). An example therefore is given in Figure 2.

2.2 Additional consideration for timber structures

An additional effect has to be taken into account if proof loading is applied to timber structures. A great effort was made by many researchers to assess the possibility of undetected damage caused by the proof loading process. According to the original application field in timber structures, the focus was on very low proof loads used within grading procedures. In this case the major aim was to pick out mavericks.

Proof loading for reassessment will need relative high proof loads for sufficient efficiency. It will not be concerned here how the risk of wracking a timber structure is limited in absence of yielding. But relative high proof loads may lead also to reasonable undetected damage. To answer this question it is useful to derive a (deterministic) damage function for a single high load pulse based on the extensive dataset published by MADSEN [7].

$$R'' = R' - 0.2 \cdot R' \cdot \left(\frac{R' - \text{proof load}}{\text{proof load}} + 1 \right)^{-10}$$

(4)

R' prior resistance / R'' posterior resistance

If this information is included in Figure 2, it can be recognized, that the positive effect of proof loading is significant reduced. Until now there is no possibility available to limit or detect this damage.
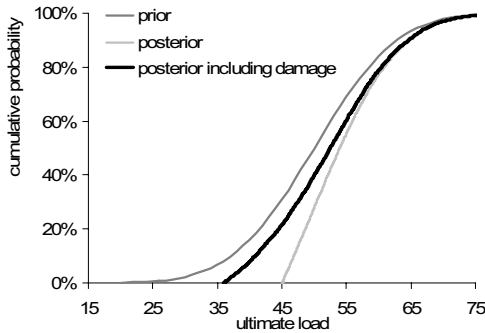

Fig. 2: Truncated distribution after survived proof load

Therefore this negative influence has to be reduced by additional research. Promising seems the control of ultrasonic sound emission. This shall be under further investigation to limit this effect in future. If sound emission control is possible, this will also be a method to limit structural failure during the proof loading process. Until this point the effect of possible undetected damage shall be included in safety assessment on timber structures using proof loading.

3 Updating by a simulation approach

Simulation models for timber

Through the last decades multiple models were developed for predicting the properties of future grades. The aim was in all cases the improvement in efficiency of usage of the raw material. Figure 3 [1] represents some approaches.
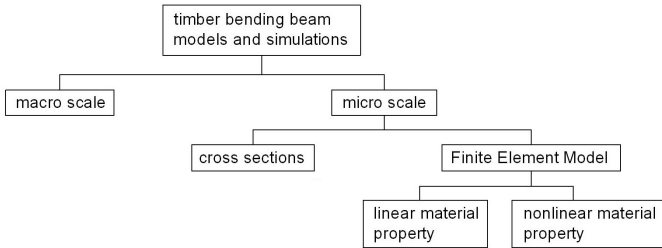

Fig. 3: Different simulation approaches

The models can be distinguished at first by the size of the chosen reference volume size. The second differentiation can be made according to the assumed material properties assumption linear or non-linear. The easiest models are working with an effective cross section modulus (Cross section as reference volume), were all cross section parts, probable covered by knots, are neglected. Something more promising seemed the development of small reference volume Finite-Element-Models with a Monte-Carlo based sampling routine for the material properties. Herein the beam is divided into small reference volumes to see in Figure 4.
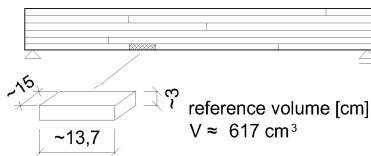
Fig. 4: Beam and reference volume

Within such a volume the material properties are assumed homogenous, but depending on influencing parameters like Knot per Area Ratio (KAR), density (RHO) and in some cases additional information. The dependency is described by a set of correlations. Due to the relatively small reference volumes, a plenty amount of tests were possible to derive these necessary correlations with sufficient confidence. The advantage of these models seems there adaptability to different size and loading condition. Of course disadvantages remain, for some models major influence parameters are not taken into account, because for the original application field they found to be not significant.

Experimental reference tests and updating dataset

Target was to proof an extended use of a simulation model for updating. Therefore additional tests and a reference volume wise data acquisition were necessary. 24 glued laminated beams were tested in a 4-point bending tests. Afterwards the knot per area ratio (KAR), density (RHO), and finger joints (FJ) were documented.

Layer		1			2			3			4		
Cell		KAR	RHO	FJ	KAR	RHO	FJ	KAR	RHO	FJ	KAR	RHO	FJ
1	-0.30 - -0.15	0.00	453	0	0.00	437	0	0.00	390	0	0.00	581	0
2	-0.15 - 0.00	0.00	453	0	0.00	437	0	0.00	390	0	0.00	581	0
3	0.00 - 0.15	0.24	453	0	0.17	437	0	0.00	390	0	0.21	581	0
4	0.15 - 0.30	0.00	453	0	0.00	437	0	0.68	390	0	0.10	581	0
5	0.30 - 0.45	0.00	453	0	0.38	437	0	0.00	390	0	0.00	581	0
6	0.45 - 0.60	0.29	453	0	0.16	437	0	0.47	390	0	0.37	581	0
7	0.60 - 0.75	0.00	453	0	0.04	437	0	0.00	390	0	0.09	581	0
8	0.75 - 0.90	0.05	453	0	0.00	437	0	0.12	390	0	0.08	581	0
9	0.90 - 1.05	0.05	453	0	0.71	437	0	0.11	390	0	0.04	581	0
10	1.05 - 1.20	0.00	453	0	0.04	437	0	0.00	390	0	0.00	462	1
11	1.20 - 1.35	0.21	453	0	0.25	437	0	0.39	390	0	0.05	462	0
12	1.35 - 1.50	0.00	453	0	0.15	437	0	0.25	390	0	0.08	462	0
13	1.50 - 1.65	0.00	453	0	0.17	437	0	0.12	390	0	0.16	462	0

Fig. 5: Example for reference volume data

The complete dataset was published by BRETSCHNEIDER [1], where the Glued-Laminated-Beams were cut to Boards. This information may be alternative derived by non-destructive testing. The work done by HASENSTAB [5] may serve as a reference therefore.

Updating with the Karlsruher-Simulation-Model

For the updating calculation the Karlsruher-Simulation-Model [3] was used in an extended way. In the original application of the model the input parameters (KAR, RHO, FJ) were scattering values within the range of future grades. The result of a couple of simulation iterations is a prediction for the reference properties of a future grade.

Now these values were fixed, according to the assessed additional data as shown in Figure 5. If updating is possible, every simulation loop gives a prediction for the beam, were the data was from. The curves of 10 simulation iterations as a prediction for a single beam are represented in Figure 6. If the model is usable for updating the predictions shall be similar to the real beams behaviour (in average for a couple of beams and iterations).

Also similar should be the simulated geometric position of the failure point. In most of the cases the observed failure position shall be equal to the simulated one. Usually 2 to 3 failure points are occurring in the iterations for a single beam, of course with different probability. This will lead to a posterior distribution type similar to those assumed for the residuals in regression formulas.
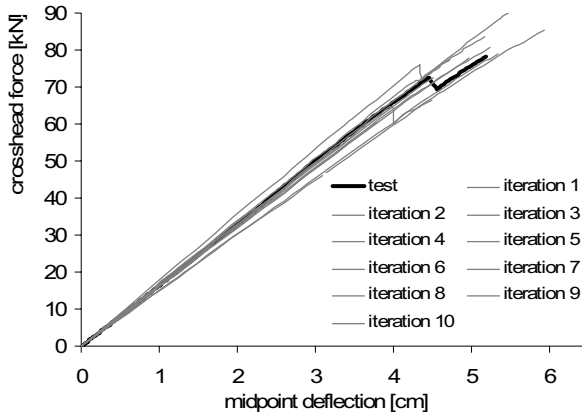
Fig. 6: Different simulation iteration as prediction for a single beam

If updating with this approach is possible, these predictions shall be correct when averaged over a couple from decision situations. This was done for 24 beams. On the axis of abscissa the test values are given. On the axis of ordinate the mean and the standard deviation of the simulated values are marked.
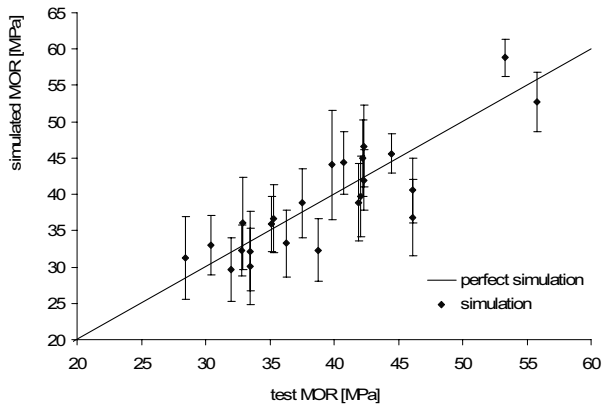

Fig. 7: Different simulation iteration as prediction for a single beam

The predicted modulus of ruptures variation coefficient is in average 12 percent. This is a reasonable reduction compared to the 22 percent given in Table 1. The use of this model has still a disadvantage; it is not applicable to solid beams. The reason therefore is that a major influence parameter, grain derivation, which is not included in the input correlations until now.

4 Effect of updated resistance distribution in safety calculations

Proof loading in safety calculation

The question arises, whether the received truncated resistance distribution is sufficiently covered by common level I and II safety calculations. Depending on the origin of the author's until now as well as level I, II or III calculations were proposed. The effect is most efficiently demonstrated by a short example with the limit state function:

$$k_{mod} \cdot R - E_{Dead\,load} - E_{Live\,load} = 0 \qquad (5)$$

The input is summarized in the following table (unit free):

Tab. 2: Safety assessment after proof loading: example input data

	distribution type	mean	coefficient of variation
Resistance	Normal	50	0.2
$E_{Dead\,Load}$	Normal	5	0.05
$E_{Live\,Load}$	Logarithmic Normal	5	0.1
k_{mod}	0.8		
Proof Load	45		
Result	Structure survives		

Compared is the safety assessment according to DIN 1055-100 (level I), a FORM analysis as described e.g. by NOWAK [8] (level II), and a closed solution for the direct failure probability calculation (level III).

Tab. 3: Safety assessment after proof loading: example result:

	before proof load	after proof load	quotient
Level I	R_d=20.6	R_d=27.3	1.33
Level II	β=3.3 → $\Phi(-\beta) = P_f = 5 \cdot 10^{-4}$	β=3.9 → $\Phi(-\beta) = P_f = 5 \cdot 10^{-5}$	11.7
Level III	$P_f = 7 \cdot 10^{-4}$	$P_f = 3.8 \cdot 10^{-5}$	18.4
(E_d=26.3	β_{target}=3.8	$P_{f,target}$=7.3 10^{-5})	

As expected, truncated distributions are not really sufficiently covered by traditional level I analysis. Such a proceeding, which is still proposed in many textbooks covering proof loading (e.g. QUADE [9]), needs an extension with the considerations made in the example.

Effect of a prediction with reduced coefficient of variation

Using the simulation approach a variation coefficient of 12 percent was received. Similar to the previous section the question arises, weather the partial safety factors for timber are still the correct choice if safety assessment is performed with these values. The simplest solution approach is to refer to the values given in the Background Documentation of

Eurocode 1 (EC 1), Table 4 [4]. Additional it is possible to perform for the common application field a calibration calculation as done by BRETSCHNEIDER [1].

Tab. 4: γ_M values given in EC 1

COV_{model}	$COV_{geometry}$	$COV_{Material}$	γ_M
0.05	0.05	0.05	1.20
0.05	0.05	0.10	1.23
0.05	0.05	0.15	1.29
0.05	0.05	0.20	1.37
0.05	0.05	0.25	1.46
0.10	0.05	0.05	1.33
0.10	0.05	0.10	1.34
0.10	0.05	0.15	1.38
0.10	0.05	0.20	1.45
0.10	0.05	0.25	1.53

5 Application to accelerated research procedures

Extension of the matched sample technique

A common technique to reduce "noise" parameters is the matched sample technique. With this technique, positively correlated "pairs" of test specimen from one mixture are produced, assuming that, within one pair (set), there is originally nearly no difference with respect to the surveyed parameters. After performing any process with one member of a pair (set), the members are tested and the statistics are then performed only with values of difference between the members of the pairs (sets). The usage of a reassessment process, e.g. the Karlsruher-Simulation-Model, for predicting the bending properties of a single beam makes it possible to set up a similar procedure. Additionally, it has to be considered that the prediction is not perfect, that means it is still a random variable. Taking this into account, the following procedure can be proposed on the basis of the performed tests and updating calculations.

(a) Pair: Experimental Result - Simulation   (b) Scaled pair: Experimental R. - Simulation
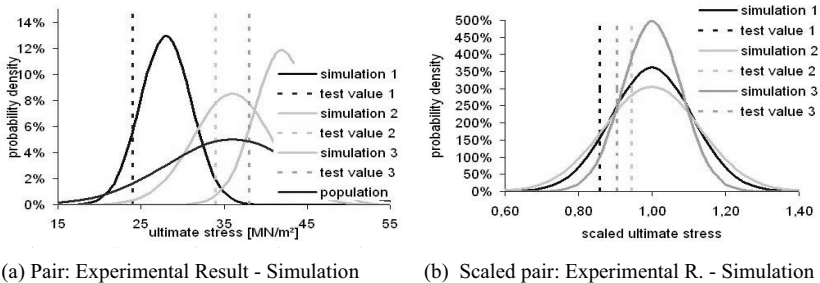
Fig. 8: Extended matched sample technique

The possible reduction in experimental tests will be similar to the reduction of the coefficient of variation in the updating process. So, depending on the research aim, approximately 50 percent of the physical tests are saved [6].
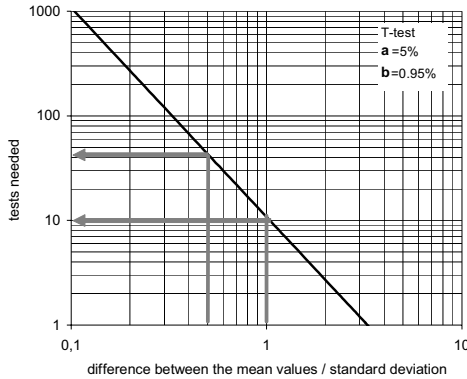

Fig. 9: Number of required tests

Application of sampling with unequal probabilities

Some research questions for timber design are observing effects on 5 per cent cumulative probability values. Reason for this research may be the effect on strength of a new chemical treatment, questions to damage accumulation and so on. It may be advantageous to use sampling with unequal probabilities for this problem, so to sample more beams in the interesting area (in most cases "bad" ones).
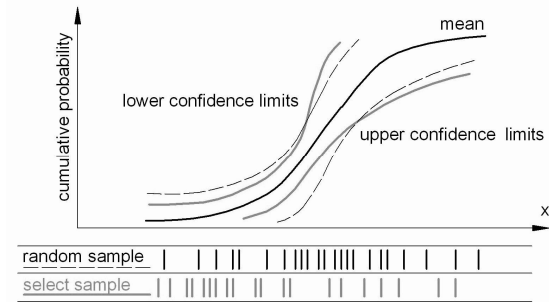

Fig. 10: Sampling with unequal probabilities

This shall lead with less physical tests to closer confidence borders around this point. To perform such sampling, two things are necessary. First, raff estimation about good and bad beams must be possible. Even a good craftsman shall be able to do this by his experience (Figure. 10). Second, this raff estimation must be numerical verified. The updating process seems to be one possibility to achieve this.

The updating process results in a prediction for the modulus of rupture of a beam. The beams which are under consideration can be sorted according to the predicted modulus of rupture. Every single beam may be also taken as a representative of a class. The original classes' probabilities result from the observed grades distribution (Figure 11a).

After the modification with chemical treatment, load accumulation the real test of the modified beams was performed. The resulting cumulative density function can be set up, using the real test results and the probability values from the reassessment process (Figure 11b).

(a) weight value   (b) set up of a cdf function
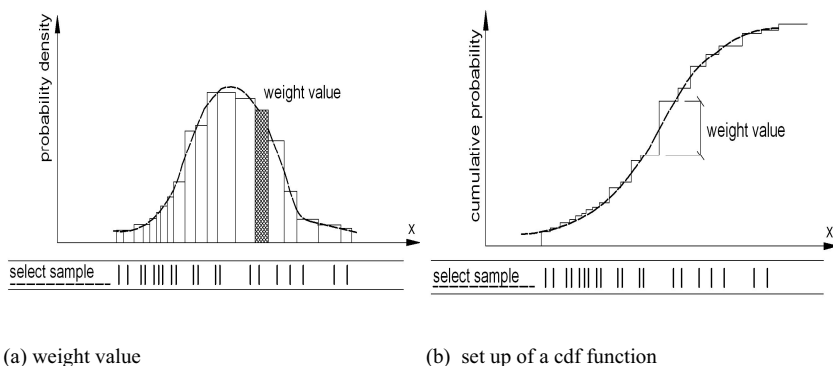
Fig. 11: Sampling with unequal probabilities

If this process is done by a Monte-Carlo-Simulation multiple times the confidence borders can be plotted. Also reduction factors can be derived this way. For the example in Table 5 the target was a characteristic value from about 10.4. The prediction is given, including a confidence from 85 per cent. The calculation was performed for different sample sizes and for different updating uncertainties.

Tab. 5:   Efficiency of sampling with unequal probabilities

characteristic value real: 10.4		sample size			
		20	30	50	100
traditional statistics		7.2	7.5	8.5	9.1
updating uncertainty	0 %	9.1	9.3	9.6	9.8
	5 %	9.0	9.2	9.5	9.7
	10 %	8.9	9.1	9.3	9.5
	15 %	8.7	8.8	9.1	9.4

It can be recognized, that sampling with unequal probabilities makes sense, because closer confidence borders are reached around the interesting points. The highest effect is reached for a medium sample size of 30 to 50.

6   References

[1]   Bretschneider, T.: Assessment of existing glued laminated beams by probability based updating. BTU Cottbus: Der Andere Verlag, 2007 – Dissertation

[2]   Ditlevsen, O.; Madsen, H. O.: *Structural Reliability Methods*. Chichester: John Wiley & Sons, 1996

[3]   Ehlbeck, J.; Colling, F.: Biegefestigkeit von Brettschichtholz in Abhängigkeit von den Eigenschaften der Brettlamelle im Hinblick auf Normungsvorschläge. Stuttgart: IRB Verlag, 1992

[4]   Eurocode 1.1 Project Team: *Background Documentation Part 1 of EC 1, Basis of Design.* Eurocode 1.1 Project Team, 1995

[5]   Hasenstab, A. G. M.: Integritätsprüfung von Holz mit dem zerstörungsfreien Ultraschallechoverfahren. BAM: 2006 – Dissertation

[6]   Kühlmeyer, M.; Kühlmeyer, C.: *Statistische Auswertungsmethoden für Ingenieure*. Berlin: Springer, 2001

[7]   Madsen, B.: *Structural Behaviour of Timber*. Vancouver: Timber Engineering Ltd, 1992

[8]   Nowak, A. S.; Collins, K. R.: *Reliability of Structures*. Boston: Mc Graw Hill, 2000

[9]   Quade, J.; Tschötschel, M.: *Experimentelle Baumechanik*. Düsseldorf: Werner Verlag, 1993

[10]   Rug, W.; Badstube, M.: Development of a GDR Limit State Design Code for Timber Structures. 20th CIB W 18 Conference. Dublin: 1987

Cost and Safety Optimization for Load Factor Based Reliability Analysis

Armagan Korkmaz & Engin Aktas
Suleyman Demirel University, Civil Engineering Department, Isparta, Turkey
Izmir Institute of Technology, Civil Engineering Department, Urla, Izmir, Turkey

Abstract: The main aim of design specifications is to produce safe and economic structures. Reliability based Load and Resistance Factor Design codes accomplish target safety levels inferred from previous versions of these codes. This approach often leads to different target safety indices for each load case such as live, wind, earthquake and snow. A dilemma also arises as to which target safety index should be used in calibrating load factors for load combination cases. In the present study, cost and safety optimization approach is used to consistently calibrate the load factors for each load combination case. The total cost utilizes construction cost and uniform failure costs inferred from previous versions of codes. Codified load factor tables for dead, live and wind effects are optimized using cost values obtained from a range of designs. The analyses propose discounted present worth for annual failure costs, separation of time dependent and independent load variables. The come up to provides consistent load factors calibrated to provide an optimum balance between structural safety and the expected total cost for the load combination being considered.

Key Words: Load Factor Based Design, Reliability Analysis, Cost and Safety Optimization.

1 Introduction

The quality of human life and economic progress depend on the quantity, quality, and efficiency of structures and infrastructures and their networks. Buildings and associated structures play an important role in the economical system. For this an effective design code is essential.

Mainly in the United States and partially in the rest of the world, the great expansion in new technology construction from the 1970s to now has resulted in a modern structural network. However, the structures built during this period have aged over 30 years and many require major maintenance interventions. A great amount of money has been already spent to keep these structures in an operative condition [1].

The issue of prescribing target safety levels for structural design codes has been the center of debate since the publication of the American National Standard Institute (ANSI) A-58 document on Minimum Design Loads in Buildings [2]. The A-58 document and subsequent updates have played an important role in developing procedures to calibrate structural design codes based on probability concepts. The ANSI model uses previous codes to fix a sample of satisfactory designs. Load and resistance factors for a new code are calibrated according to the level of satisfaction that the engineering experts have with the safety implicit in previous codes. Since absolute safety is impossible to reach, the decision of determining an acceptable risk level plays a definitive role in code developments. A trade-off exists between the level of safety that a structure meets and the cost of the structure. Thus, an ideal code must provide an optimum balance between safety and cost. Although the approach used by ANSI and other code developments does not explicitly address this trade-off, code committees have implicitly accounted for the construction costs while deciding on the target safety levels that are used to calibrate the load and resistance factors. This paper proposes a method to consistently calibrate load and resistance factors based on a uniform cost optimization algorithm. The goal is to develop a procedure that explicitly accounts for the additional costs that would results from increasing the target reliability levels.

The total cost of a structure is the combination of the initial construction cost, maintenance, damage and failure costs. In order to illustrate the problem, only initial and failure costs are considered in this paper. The failure of a structure may occur at any time during its design life, therefore, to express the total expected cost, the individual annual costs must be discounted to their present worth value. Annual failure probabilities are calculated throughout the design life for the time dependent loads including live, wind, etc. Load combination techniques including Turkstra's Rule and the Ferry Borges method are proposed to combine two or more time dependent load effects [3, 4]. The annual maximum environmental and other load events are assumed to be independent from year to year. Actually, because of modelling uncertainties and structural parameters which are same throughout the design life, the annual maximum load effects as well as resistance are correlated. Therefore, the uncertainties of the yearly load effects are separated into constant uncertainties and time dependent variables. Cost optimization is carried out for different load combinations and a load factor table that minimizes the total cost over the design space is illustrated.

2   Cost Function

In reliability-based structure management systems, system performance is decided by the reliability index. As mentioned earlier, it is assumed herein that the initial and failure costs

are the only cost affecting the total cost. The present worth cost function can be expressed as,

$$C_T = C_1 + C_f \sum_{i=1}^{n} \frac{P_{f1}}{e^{ij}} \qquad (1)$$

C_T is the total cost, C_I is the initial cost, e^{ij} is the discount factor, "j" is the discount percentage rate (real rate=nominal-inflation), P_{fi} is the annual failure probability for year "i", and C_f is the failure cost, n is the total number of years in the design life of the structure. The discount rates in developed countries are between 2% to 4%, and assuming that rate equal to 3% throughout the design life is sufficient to represent the trend. It is also assumed that the annual failure costs in real terms are constant throughout the design life. The initial and failure costs must cover the whole possible range of applications, and generally represent the overall design space such as the different structural types, sizes and geometries covered by the code. For purposes of calibration, these costs will be normalized.

Fig. 1 shows a maintenance scenario associated with two interventions and corresponding deterministic cost components over lifetime [1]. The application times for these interventions are denoted as t_1 and t_2. It is assumed that the total cumulative maintenance cost is the same for all possible combinations of interventions. Then cost is normalized to make comparisons easy. Therefore, $C_f=C_1+C_2=1.0$. The effects of interventions on point in time reliability improvement, reduction of reliability deterioration rate, and system reliability are considered separately.
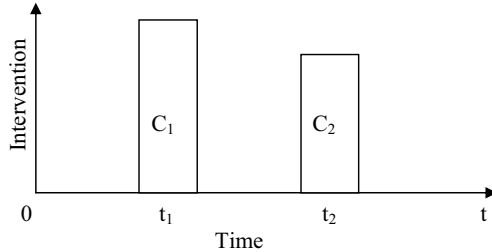

Fig. 1. Two interventions and associated normalized cost

2.1 Initial Cost

Given a structural configuration and size, the initial cost of a structure is a function of its safety level. The initial cost can be represented by the following formula [5],

$$C_1 = C_c \left(1 + K_D \left(\frac{\gamma_D}{\gamma_{DO}} - 1 \right) + K_L \left(\frac{\gamma_L}{\gamma_{LO}} - 1 \right) + K_W \left(\frac{\gamma_W}{\gamma_{WO}} - 1 \right) + \cdots \cdots \right) \qquad (2)$$

C_o is the base cost which is the construction cost of the structure associated with the use of the reference load factors (g_{a0}, a={D, L, W, ...}), and K_a is the normalized cost factor for

the respective load effects. Equation 2 is a general form of the initial cost function and assumes a linear relationship between the load factors and the cost; it is adjusted for the load combinations in question. For most structures, the cost slope for lateral loading such as wind or earthquake can significantly exceed that of gravity loads. The parameters in the initial cost function for the specific types of structures covered by a code are obtained from information on construction costs. Designing for different load factors and observing the change in the initial cost will help determine the normalized cost factors. Each gravitational and environmental load effect may have different cost contributions; therefore they are represented with different terms. The reference load factors affect only slightly the value of the cost factors, so the reference load factors may be either set at unity or may be chosen to correspond to the load factors of current codes.

2.2   Failure Cost

A challenging part of the process is the determination of the failure cost, CF. This cost should include the economic costs incurred from the failure and other intangible costs including the cost to the engineering industry and disruption to society. The value of CF in Eq. (1) reflects the importance of the structure. An increase in CF implies that the consequences of failure are more drastic, and reflects the importance of keeping that structure functional. The determination of CF is especially difficult when the loss of life is to be included. The choice of an appropriate failure cost is often a political issue. Since there is no absolute safety, the risk level that a type of structure must satisfy should be decided by society. According to DITLEVSEN, some fixed reference point from the current code should be used as a basis for determining the failure cost. As an example, one load case such as dead load alone can serve as a reference [6]. The failure cost deduced from that situation can then be used to consistently calibrate other load combinations. Due to the correlation of some variables over time, such as resistance and load modeling variables, the probability of failure changes annually, therefore the failure probability throughout the design life has to be calculated in order to apply Eq. (1).

A FORM reliability analysis is usually sufficient to calculate the safety index, b and the annual probability of failure. The separation of the time independent uncertainties in the load effects becomes important during the calculation of the reliability. Assume that an environmental load effect, Y_1 can be represented as follows:

$$Y_1 = X_m Q_1 \tag{3}$$

where X_m is the structural modeling factor including modeling uncertainty, and Q_1 is the annual maximum load intensity. Although the Q_1 are independent from year to year, X_m does not vary each year. The maximum environmental load effect, Y_k in k years can be expressed as;

$$Y_k = X_m Q_k \tag{4}$$

where $FQk(Q^*) = [FQ1(Q^*)]k$, which is used to calculate the distribution in k years during the calculation of reliability index b. The annual probabilities are calculated for each year of design life as:

$$P_{fak} = P_{f(k+1)} - P_{fk} \qquad (5)$$

where P_{fak} is the probability of failure for year k, $P_{f(k+1)}$ is the probability of failure for a period of $k+1$ years, and P_{fk} is the probability of failure for a period of k years.

2.3   Cost Normalization

The code calibration includes a range of designs and therefore must be generalized. The total cost function (Eq. (1)) is normalized by the base cost C_0, and a total cost factor, *TCF* is expressed as;

$$TCF = \frac{C_T}{C_0} = \left(1 + K_D\left(\frac{\gamma_D}{\gamma_{DO}} - 1\right) + K_L\left(\frac{\gamma_L}{\gamma_{LO}} - 1\right) + K_W\left(\frac{\gamma_W}{\gamma_{WO}} - 1\right) + \ldots\ldots\right) + g\sum_{i=1}^{n}\frac{P_{fai}}{e^{ij}} \qquad (6)$$

where $g = C_F / C_0$ is the ratio of failure cost to reference initial cost. As mentioned one load combination case can be selected to deduce the failure cost factor, g.

3   Reliability Based Cost Optimization

The optimization of the total cost gives the balanced solution between safety and cost. the optimal solution for the total cost is at the point where the slope of the initial cost is equal to the negative of the failure cost curve's slope. In order to illustrate the proposed procedure a highway bridge code will be used. AASHTO's basic load combination for bridge strength, namely *Rn>gDDn+gLLn*, is used as the reference case, with the target safety index, $b_T=3.5$ selected for the new AASHTO LRFD code. The statistical data for the loads are given in Table 1. The load factors are 1.25 and 1.75 for dead and live load, respectively. The total cost factor, *TCF* can be stated as,

$$TCF = 1 + \left(K_G\left(\frac{\gamma_D + \alpha\gamma_L}{\gamma_{DO} + \alpha\gamma_{LO}} - 1\right)\right) + g\sum_{i=1}^{n}\frac{P_{fi}}{e^{ij}} \qquad (7)$$

where K_G is the normalized cost factor for gravitational load, and *a* is the nominal live load to nominal dead load ratio in the range of 0.5 to 2.0. P_f is calculated from limit state function *G=R-D-L*. A study conducted on bridges by MOSES showed that 25% change in g_L produce a change of 2% in initial cost of bridges [7]. The K_G can be calculated by Eq. (8) with this information for different *a* values. Averaged along the range of *a*, the factor K_G is calculated as 0.14.

$$\frac{\Delta C_1}{C_0} = \left(K_G\left(\frac{\gamma_{Do} + \gamma_{Lo}\left(1 + \frac{\Delta\gamma_L}{\gamma_{LO}}\right)\alpha}{\gamma_{DO} + \alpha\gamma_{LO}} - 1\right)\right) \qquad (8)$$

Then differentiating *TCF* with respect to load factors about the target safety index and equating to zero will give the failure cost ratio, *g* as

$$g = -\frac{\left[\sum \frac{\partial}{\partial \gamma_D}\left(\frac{P_{fi}}{e^{ij}}\right)\right]^{-1}}{\gamma_{DO} + \alpha\gamma_{LO}} K_G = -\alpha\frac{\left[\sum \frac{\partial}{\partial \gamma_L}\left(\frac{P_{fi}}{e^{ij}}\right)\right]^{-1}}{\gamma_{DO} + \alpha\gamma_{LO}} K_G \qquad (9)$$

g values deduced using Eq. (9) along with the code specified $g_{D0}=1.25$ and $g_{L0}=1.75$ are averaged along the *a* values and found equal to 27. The load combination cases $n>g_{DDn}$, $R_n>g_{WWn}$ and $R_n>g_{DDn}+g_{WWn}$ are next studied using this value of *g*. Optimized load factors are calculated for different ratios of normalized cost factors of wind and gravitational load. This process is repeated with *g* increased by two, namely *g*=54 to illustrate the effect of failure cost factor. The analyses were run with an optimization process to optimize the sum of the total cost factors along the design space. The dead load alone case gives an optimum safety index of 3.50 and load factor of 1.43, which are equal to 3.68 and 1.46 when *g* is increased by a factor of 2. the results of the wind load and dead and wind load are tabulated as in Table 2 and 3, respectively. In Table 3 safety indices are the average values along the W_n/D_n range. Procedure will be extended to $R_n>g_{DDn}+g_{LLn}+g_{WWn}$ case using Ferry Borges Method.

Table 1. Load and Resistance Statistical Data

	Time Dependent			Time Independent		
	TYPE	BIAS	COV	TYPE	BIAS	COV
R	--	--	--	LOGN	1.12	0.1
D	--	--	--	NORM	1.03	0.08
L	LOGN	1.00	0.13	NORM	1.00	0.12
W	EXTR1	1.02	0.10	NORM	0.85	0.25

Table 2. Wind Load Alone

	g=27		g=54	
K_w/K_G	β	γ_W	β	γ_W
0.5	3.05	2.15	3.24	2.32
1.0	2.84	1.99	3.05	2.15
2.0	2.63	1.84	2.84	1.99
3.0	2.50	1.75	2.72	1.90

Table 3. Dead and Wind Loads

	g=27			g=54		
K_w/K_G	β	γ_D	γ_W	β	γ_D	γ_W
0.5	3.03	1.18	2.08	3.23	1.20	2.23
1.0	2.85	1.22	1.86	3.06	1.24	2.01
2.0	2.71	1.29	1.66	2.93	1.31	1.81
3.0	2.70	1.39	1.54	2.91	1.40	1.68

4   Conclusions

It is important to attain a balance between safety and economy. In this study reliability based cost optimization is used to achieve this goal. A single consistent value for the cost of failure is used which is deduced from previous code experience. The cost of failure is adopted as a target for optimizing the load factors for different load cases. The input to the optimization includes the marginal initial load slope for a given load type. The output includes the corresponding load factors and safety indices. Tables 2 and 3 show that with increasing wind load cost factor the optimum safety index, b decreases. This observation is consistent with experience in codes such as building and offshore structures where computed safety indices for gravity loads are higher than for environmental loads such as wind. That is the natural result of the trade off; as the marginal cost to upgrade the structure increases the optimum safety level decreases. Optimized safety index values for the dead and wind load combined case fall between the dead and wind load alone cases, except the case of *KW/KG=0.5*.

5   References

[1]   Kong, JS.; Frangopol, DM.: Cost–Reliability Interaction in Life-Cycle Cost Optimization of Deteriorating Structures. *ASCE, journal of Structures,* 2004, 0733-9445.

[2]   Ellingwood, B.; Galambos T.V.; MacGregor, J.G.; Cornell C.A.: Development of a Probability Based Load Criteria for American National Standard A58. *NBS Special Publication N0.577,* 1980.

[3]   Melchers, R.E.: Structural Reliability Analysis and Prediction*,* 2nd ed., *Wiley*, New York, NY, 1999.

[4]   Thoft-Christensen, P.; Baker M.J.: Structural Reliability and Its Applications, *Springer Verlag,* NewYork, N, 1982.

[5]   Ellingwood, B.; Kanda J.: "Formulation of Load Factors Based on Optimum Reliability," *Structural Safety*, 1991, 9, 197-210.

[6]   Ditlevsen, O.: Structural Reliability Codes for Probabilistic Design – A Debate Paper Based on Elementary Reliability and Decision Analysis Concepts, *Structural Safety*, 1997, 19(3), 253-270.

[7]   Moses F.: Effects on Bridges of Alternative Truck Configurations and Weights, *Final Report, TRB, National Research Council,* Washington DC, 1989.

Global Safety Format for Nonlinear Calculation of Reinforced Concrete

Vladimir Cervenka
Cervenka Consulting, Prague

Abstract: The safety format suitable for design of reinforced concrete structures using non-linear analysis requires a global approach. The performance of various safety formats is compared on four examples ranging from statically determinate structures with a bending mode of failure up to indeterminate structures with a shear failure.

1   Introduction

Non-linear analysis is becoming a frequent tool for design of new and assessment of existing structures. This development is supported by the rapid increase of computational power as well as by new capabilities of the available software tools for numerical simulation of structural performance.

On the other hand the code provisions provide very little guidance how to use the results of non-linear analysis for structural assessment or design. The safety formats and rules that are usually employed in the codes are tailored for classical assessment procedures based on beam models, hand calculation, linear analysis and local section checks. The non-linear analysis is by its nature always a global type of assessment, in which all-structural parts, or sections interact. Until recently the codes did not allow applying the method of partial safety factors for non-linear analysis, and therefore, a new safety format was expected to be formulated. Certain national or international codes have already introduced new safety formats based on overall/global safety factors to address this issue. Such codes are, for instance, German standard DIN 1045-1 [6] or Eurocode 2 EN 1992-2 [7]. This paper will try to compare several possible safety formats suitable for non-linear analysis: partial factor method, global format based on EN 1992-2, and fully probabilistic method. A new alternative safety format was proposed by CERVENKA [5], which is based on a probabilistic estimate of the coefficient of variation of resistance.

A standard assessment procedure based on partial safety factors usually involves the following steps:

(1) Linear elastic analysis of the structure considering all possible load combinations. Results are actions in some critical sections, which could be referred as *design actions* and can be written as

$$E_d = \gamma_{S1} S_{n1} + \gamma_{S2} S_{n2} + \ldots\ldots \gamma_{Si} S_{ni} \tag{1}$$

They include safety provisions, in which the nominal loads S_{ni} are amplified by appropriate partial safety factors for loading γ_{Si}, where index i stands for load type, and their combinations.

(2) *Design resistance* of a section is calculated using design values of material parameters as:

$$R_d = r(f_d, \ldots), f_d = f_k / \gamma_m \tag{2}$$

The safety provision for resistance is used on the material level. The design value of material property $f_d = f_k / \gamma_m$ is obtained from the characteristic value f_k by its reduction with an appropriate partial safety factor γ_m. The random variability of material properties is covered by the partial safety factors individually for each material.

(3) Safety check of limit state is performed by *design condition*, which requires, that design resistance is greater then design action:

$$E_d < R_d \tag{3}$$

Note, that in the partial factor method the safety check is ensured in local material points. However, the probability of structural failure, i.e. the probability of violation of the design criteria (3) is not known.

In the above outlined procedure, the non-linear analysis should be applied in step 1) to replace the linear analysis. Following the current practice an engineer will continue to steps 2), 3) and perform the section check using the internal forces calculated by the non-linear analysis. This is a questionable way since in non-linear analysis material criteria are always satisfied implicitly by the constitutive laws. Instead, a global check of safety should be performed on a higher level and not in local sections. This is the motivation for the introduction of new safety formats for non-linear analysis.

The final step of the verification process often involve assessment of serviceability conditions, i.e. deflections, crack width, fatigue, etc. In certain cases, these serviceability conditions might be the most important factors affecting the assessment conclusions.

Another important point is that a non-linear analysis becomes useful when it is difficult to clearly identify the sections to be checked. This occurs in structures with complicated geometrical forms, with openings, special reinforcement detailing, etc. In such cases, usual

models for beams and columns are not appropriate, and non-linear analysis is a powerful alternative.

The above discussion shows that it would be advantageous to check a global structural resistance to prescribed actions rather than checking each individual section. This approach can bring the following advantages:

(a) The nonlinear analysis checks automatically all locations and not just those selected as critical sections.

(b) The global safety format gives information about the structural safety, redundancy and robustness. This information is not available in the classical approach of section verification.

(c) The safety assessment on global level can bring more economic solution by exploiting reserves due to more comprehensive design model and a risk of unsafe design is reduced.

However, the above enthusiastic statements should be accepted with caution. There are many aspects of the assessment process, which require engineering judgment. Also many empirical criteria must be met as required by codes. Therefore, the global safety assessment based on non-linear analysis should be considered as an additional advanced tool, which should be used, when standard simple models are not sufficient.

The non-linear analysis offers an additional insight into the structural behaviour, and allows engineers to better understand their structures. It is often referred as a virtual testing. On the other hand, non-linear analysis is usually more demanding then a linear one, therefore an engineer should be aware of its limits as well as benefits. Other disadvantage is that the force super-position is not valid anymore. The consequence is that a separate non-linear analysis is necessary for each combination of actions.

Finally, a note to terminology will be made. The term for *global* resistance (*global* safety) is used here for assessment of structural response on higher structural level then a cross section. In technical literature, the same meaning is sometimes denoted by the term *overall*. The term *global* is introduced in order to distinguish the newly introduced check of safety on global level, as compared to local safety check in the partial safety factor method. This terminology has its probabilistic consequences as will be shown further in the paper. The proposed global approach makes possible a reliability assessment of resistance, which is based on more rational probabilistic approach as compared to partial safety factors. The presented study is based on the paper by CERVENKA [5].

2 Safety formats for non-linear analysis

2.1 Design variable of resistance

Our aim is to extend the existing safety format of partial factors and make it compatible with nonlinear analysis. First we introduce a new design variable of resistance $R=r(f, a, ...,$

S). Resistance represents a limit state. In a simple case this can be a single variable, such as loading force, or intensity of a distributed load. In general this can represent a set of actions including their loading history. We want to evaluate the reliability of global resistance, which is effected by random variation of basic variables f - material parameters, a – dimensions, and possibly others.

Random variation of resistance is described by a statistical distribution which can be characterized by following parameters: R_m - mean value of resistance, R_k - characteristic value of resistance, (corresponding to the probability 5%), R_d - design value of resistance. For our further derivations it is important to realize, that the characteristic and design values reflect the random scatter of the resistance, which in probabilistic terms means that they reflect distribution function of resistance and its parameters, namely the standard deviation.

The resistance is determined for a certain loading pattern, which is here introduced by the symbol of actions *S*. It is understood that unlike material parameters and dimensions, which enter the limit state function *r* as basic variables, the loading is scalable, and includes load type, location, load combination and history. The objective of the resistance *R* is to determine the load magnitude for a given loading pattern of *S*.

In general, action E_d and resistance R_d, which appear in design equation (3), can include many components (for example vertical and horizontal forces, body forces, temperature, etc,) and can be described by a point in a multi-dimensional space. It is therefore useful to define a resistance scaling factor k_R, which describes safety factor with respect to the considered set of design actions. In the simplified form, considering one pair of corresponding components it can be described as:

$$k_R = \frac{R}{E_d} \tag{4}$$

Then, the design condition (3) can be rewritten as:

$$\gamma_R < k_R \tag{5}$$

Where γ_R is required global safety factor for resistance. Factor k_R can be used to calculate the relative safety margin m_R for resistance

$$m_R = k_R - 1 \tag{6}$$

It remains to determine the design resistance R_d. The following methods will be investigated and compared:

(a) Proposed method ECOV, i.e. estimate of coefficient of variation for resistance.

(b) EN 1992-2 method, i.e estimate of R_d using the overall safety factor from Eurocode 2 EN 1992-2.

(c) PSF method, i.e. estimate of R_d using the partial factors of safety

(d) Full probabilistic approach. In this case R_d is calculated by a full probabilistic non-linear analysis.

Furthermore, the limit state function **r** can include some uncertainty in model formulation. However, this effect can be treated separately and shall not be included in the following considerations. It should be also made clear, that we have separated the uncertainties of loading and resistance (and their random behaviour). Our task is reduced to the calculation of design resistance R_d to be used in Eq.(3).

2.2   ECOV method – estimate of coefficient of variation

This method was inspired by the global safety analysis by HOLICKY [8]. It is based on the idea, that the random distribution of resistance, which is described by the coefficient of variation V_R, can be estimated from mean R_m and characteristic values R_k. The underlying assumption is that random distribution of resistance is according to lognormal distribution, which is typical for structural resistance. In this case, it is possible to express the coefficient of variation as:

$$V_R = \frac{1}{1.65} \ln\left(\frac{R_m}{R_k}\right) \tag{7}$$

Global safety factor γ_R of resistance is then estimated as:

$$\gamma_R = \exp(\alpha_R \beta V_R) \tag{8}$$

where α_R is the sensitivity (weight) factor for resistance reliability and β is the reliability index. The above procedure enables to estimate the safety of resistance in a rational way, based on the principles of reliability accepted by the codes. Appropriate code provisions can be used to identify these parameters. According to Eurocode 2 EN 1991-1, typical values are $\beta = 4.7$ (one year) and $\alpha_R = 0.8$. In this case, the global resistance factor is:

$$\gamma_R \cong \exp(-3.76 \, V_R) \tag{9}$$

and the design resistance is calculated as:

$$R_d = R_m / \gamma_R \tag{10}$$

The key steps in the proposed method are to determine the mean and characteristic values R_m, R_k. It is proposed to estimate them using two separate nonlinear analyses using mean and characteristic values of input material parameters, respectively.

$$R_m = r(f_m,...) , \ R_k = r(f_k,...) \tag{11}$$

It can be argued, why not to calculate R_d directly from Eq.(2) as we do in partial factor method. One of the reasons is the fact that design material values f_d are extremely low and do not represent a real material. A simulation of real behaviour should be based on mean material properties and safety provision should be referred to it. Analysis based on extremely low material properties may result in unrealistic redistribution of forces, which may not be on the conservative side. It may also change the failure mode. Therefore, the characteristic value f_k, which is not so far from a mean, but well reflects the scatter is preferred for analysis. Then a transformation within estimated distribution function is performed as described by Equations (7), (8), (9).

The method is general and reliability level β and distribution type can be changed if required. It reflects all types of failure. Its sensitivity to random variation of all material parameters is automatically included. Thus, there is no need of special modifications of concrete properties in order to compensate for greater random variation of certain properties. However, the method requires two separate non-linear analyses.

2.3   EN1992-2 method

Design resistance is calculated from

$$R_d = r(\tilde{f}_{ym}, \tilde{f}_{cm}..., S) / \gamma_R \tag{12}$$

Material properties used for resistance function are considered by mean values. The mean steel yield strength $\tilde{f}_{ym} = 1.1 f_{yk}$. For concrete the mean strengths is reduced to account for greater random variation of concrete properties $\tilde{f}_{cm} = 1.1 \dfrac{\gamma_s}{\gamma_c} f_{ck}$, where γ_s and γ_c are partial safety factors for steel and concrete, respectively. Typically this means that the concrete compressive strength should be calculated as $\tilde{f}_{cm} = 0.843 f_{ck}$. This method allows to treat the steel and concrete failure models in a unified way. The global factor of resistance shall be $\gamma_R = 1,27$. The evaluation of resistance function is done by nonlinear analysis assuming the material parameters according to the above rules.

2.4   PSF method – partial safety factor estimate

Design resistance R_d can be estimated using design material values as

$$R_d = r(f_d,..., S) \tag{13}$$

In this case, the structural analysis is based on extremely low material parameters in all locations as was already mentioned in the end of Section 2.2. This may cause deviations in structural response, e.g. in failure mode. It may be used as an estimate in absence of a more refined solution.

2.5 Full probabilistic analysis

Probabilistic analysis is a general tool for safety assessment of reinforced concrete structures, and thus it can be applied also in case of non-linear analysis. A limit state function can be evaluated by means of numerical simulation. In this approach the resistance function $r(\mathbf{r})$ is represented by non-linear structural analysis and loading function $s(\mathbf{s})$ is represented by action model. Safety can be evaluated with the help of reliability index β, or alternatively by failure probability P_f taking into account all uncertainties due to random variation of material properties, dimensions, loading, and other. More about the probabilistic analysis is presented in the paper by NOVAK et al [9] and here we shall only briefly outline this approach. The probabilistic analysis is more general, but can be used only for determination of design value of resistance function $r(\mathbf{r})$ expressed as R_d. It involves random sampling includes following steps:

(1) Numerical model based on non-linear finite element analysis. This model describes the resistance function $r(\mathbf{r})$ and can perform deterministic analysis of resistance for a given set of input variables.

(2) Randomization of input variables (material properties, dimensions, boundary conditions, etc.). This can also include some effects of actions, which are not in the action function $s(\mathbf{s})$ (for example pre-stressing, dead load etc.). Random properties are defined by random distribution type and its parameters (mean, standard deviation, etc.). They describe the uncertainties due to statistical variation of resistance properties.

(3) Probabilistic analysis of resistance and action. This can be performed by numerical method of Monte Carlo-type, such as LHS sampling method. In this an array of resistance values is generated, which represents a distribution function of global resistance by a set of points. Based on this the distribution function of resistance can be calculated including type, mean, standard deviation, etc. This fully describes the random properties of resistance and can be used as a ration basis for safety verification.

(4) Evaluation of safety using reliability index β or probability of failure.

Probabilistic analysis is so far an ultimate tool for safety assessment. It can reveal reserves, which can not be discovered by conventional methods. However, it is substantiated mainly in cases, where real random properties of material or other parameters can be exploited.

2.6 Nonlinear analysis

Examples in this paper are analysed with program ATENA for non-linear analysis of concrete structures. ATENA is capable of a realistic simulation of concrete behaviour in the entire loading range with ductile as well as brittle failure modes as shown in papers by CERVENKA [3], [4]. The numerical analysis is based on finite element method and non-linear material models for concrete, reinforcement and their interaction. Tensile behavior of concrete is described by smeared cracks, crack band and fracture energy, compressive behavior of concrete is described by damage model with hardening and softening. In the

presented examples the reinforcement is modelled by truss elements embeded in two-dimensional isoparametric concrete elements. Nonlinear solution is performed incrementally with equlibrium iterations in each load step.

3   Examples of application

The performance of presented safety formats will be tested on several examples ranging from simple statically determinate structures with bending failure mode up to statically indeterminate structures with shear failure modes.

Example 1 : Simply supported beam in bending.

Simply supported beam is uniformly loaded as shown in Fig.1. The beam has a span of 6m, rectangular cross-/section of h=0.3m, b=1m. It is reinforced with 5⌀14 along the bottom surface. The concrete type is C30/37 and reinforcement has a yield strength of 500 Mpa. The failure occurs due to bending with reinforcement yielding.
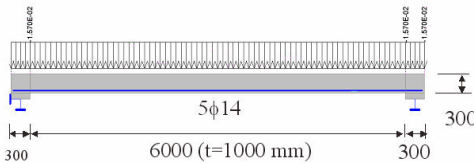
Fig. 1. Beam geometry with distributed design load for example 1.

Example 2 : Deep shear beam

Continuous deep beam with two spans is shown in Figures 2 and 3. It corresponds to one of the beams tested at Delft University of Technology by ASIN [1]. It is a statically indeterminate structure with a brittle shear failure.
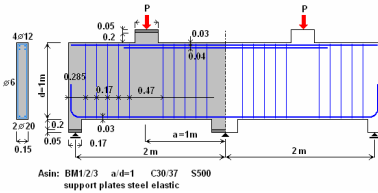
Fig. 2. Deep beam in Example 2.   Fig. 3. Laboratory test of deep beam.

Example 3 : Bridge pier

This example is chosen in order to verify the behavior of the various safety formats in the case of a problem with second order effect (i.e. geometric nonlinearity). It is adopted from a practical bridge design in Italy that was published by Bertagnoli et. al. (2004). It is a bridge pier loaded by normal force and moment in the top, Figure 4.
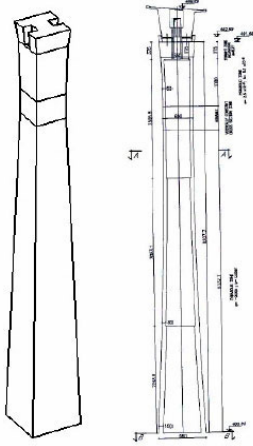

Fig. 4. Bridge pier in Example 3.   Fig. 5. Railway bridge in Example 4. Top
– model, bottom real structure.
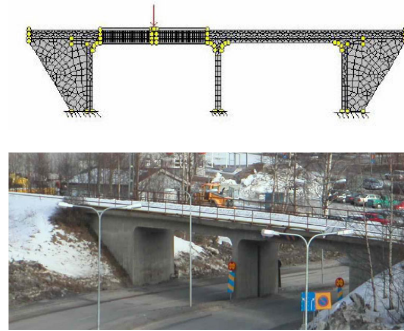
Example 4 : railway bridge frame structure

The bridge frame structure in Sweden shown in Figure 5 fails by a combined action of bending and shear. It is an existing bridge that was subjected to a field test up to failure by a single load in the middle of the left span.

In the non-linear analysis, the load is gradually increased up to failure. Typical results are illustrated on the case of simple supported beam of Example 1. Figure 6 shows the beam response for increasing load using various safety methods described in Section 2. The straight dashed line denoted as ENV1992-1 represents the load-carrying capacity given by standard design formulas based on beam analysis by hand calculation and critical section check by partial factor method. The curve denoted as PSF, thus corresponds to the partial factor method from Section 2.4, in which the used material parameters are multiplied by the corresponding factors of safety. These two methods are based on the same safety format, PSF, and the differences are only due to different analysis models used: cross section analysis with zero tensile strength of concrete (hand calculation) and FE analysis utilizing real tensile strength. The other curves correspond to the analyses with different material properties as specified by the safety format approaches that are presented in Section 2.

The response curve EN1992-2 is obtained from an analysis, where the material parameters are given by Section 2.3. For the ECOV method (Section 2.2), two separate analyses are needed: one using mean material properties, and one with characteristic values. The results from these two analyses are denoted by the labels "Mean" and "Char." respectively.

For each example, a full probabilistic analysis was also performed. Each probabilistic analysis consisted of several (at least 32 to 64) non-linear analyses with randomly chosen material properties. The design resistance is then obtained by a probabilistic analysis of randomly generated resistances.

Calculated design resistances for all examples and various methods are compared in table 1. The design resistances are normalized with respect to the values obtained for PSF method to simplify the comparison. This means that the design method based on partial factors – PSF, which is the current design practice is taken as a reference.
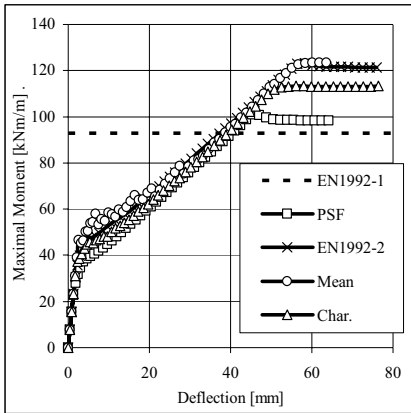
Figure 6. Load-displacement diagrams for beam in Example 1.

Table 1: Comparison of various safety formats.

	R_d / R_d^{PSF}			
	PSF	ECOV	EN 1992-2	Probabilistic
Example 1 Bending	1.0	1.00	0.95	0.96
Example 2 shear beam	1.0	1.02	0.98	0.98
Example 3 bridge pier	1.0	1.06	0.98	1.02
Example 4 bridge frame	1.0	0.97	0.93	1.01
average	1.0	1.01	0.96	0.99

4   Concluding remarks

The paper presents a comparison of several safety formats for the safety assessment based on non-linear analysis. A new method called ECOV (Estimate of Coefficient Of Variation) of ultimate state verification suitable for non-linear analysis of reinforced concrete structures is described. The proposed method can capture the resistance sensitivity to the random variation of input variables, and thus it can reflect the effect of failure mode on safety. It requires two non-linear analyses with mean and characteristic values of input parameters, respectively. Other safety formats suitable for non-linear analysis that are based on global resistance are also presented. They are: the global approach proposed by EN 1992-2, fully probabilistic analysis and a simple approach based on design values of input parameters, i.e. characteristic parameters reduced by partial safety factors. The last approach is usually not recommended by design codes, but practicing engineers often overlook this fact, and use this approach if a non-linear analysis is available in their analysis tools. The consequences are investigated in this paper.

The discussed safety formats are tested on four examples. They include ductile as well as brittle modes of failure and second order effect (of large deformation). For the investigated range of problems, all the methods provide quite reliable and consistent results.

Based on the limited set of examples the following conclusions are drawn:

(a) The differences between all methods are not significant. None of the simple methods, PSF, EN 1992-2 and ECOV is superior to others.

(b) EN 1992-2 method using a fixed global factor $\gamma_R = 1,27$ gives more conservative results comparing to other methods.

(c) The proposed ECOV method gives results consistent with PSF and Probabilistic method.

(d) The PSF method, gives results consistent with Probabilistic analysis. It is a natural extension of the conventional PSF approach to the design based on non-linear analysis.

Fully probabilistic analysis is sensitive to the type of random distribution assumed for input variables. It offers a rational safety assessment in which real random properties of materials and other parameters can be utilized. The presented study was too limited to draw generally valid conclusions. However, it supports the authors experience that nonlinear analysis can be applied using any of the presented safety formats. The choice of the safety format depends on the specific situation (design of new structure, assessment of existing structure, knowledge of specific material data). The methods are currently subjected to further validation by authors for other types of structures and failure modes.

5 References

[1] Asin, M. (1999) The Behaviour of Reinforced Concrete Continuous Deep Beams. Ph.D. Dissertation, Delft University Press, The Netherlands, 1999, ISBN 90-407-2012-6

[2] Bertagnoli, G., Giordano L., Mancini, G. (2004), Safety format for the nonlinear analysis of concrete structures. STUDIES AND RESEARCHES –V.25, Politechnico di Milano, Italy.

[3] Cervenka V. (1998): Simulation of shear failure modes of R/C structures. In: Computational Modeling of Concrete Structures (Euro-C 98), eds. R. de Borst, N. Bicanic, H. Mang, G. Meschke, A.A.Balkema, Rotterdam, The Netherlands, 1998, 833-838.

[4] Cervenka V. (2002). Computer simulation of failure of concrete structures for practice. 1st fib Congress 2002 Concrete Structures in 21 Century, Osaka, Japan, Keynote lecture in Session 13, 289-304

[5] Cervenka J., Cervenka, V., Janda, Z., Safety Assessment in Fracture Analysis of Concrete structures, Proceedings of the 6th International Conference on Fracture Mechanics of Concrete Structures, FRAMCOS-6, Catania, Italy, June 2007, Taylor&Francis Group, ISBN 978-0-415-44616-7, pp.1043-1049.

[6] DIN 1045-1 (1998), Tragwerke aus Beton, Stahlbeton und Spannbeton, Teil 1: Bemessung und Konstruktion, German standard for concrete, reinforced concrete and pre-stressed concrete structures

[7] EN 1992-2, (2005), Eurocode 2 – Design of concrete structures – Concrete bridges – Design and detailing rules

[8] Holický, M.(2006) Global resistance factors for reinforced concrete members. ACTA POLYTECHNICA 2006, CTU in Prague.

[9] Novák, D., Vořechovský, M., Lehký, D. & Rusina, R., Pukl, R. & Červenka, V. Stochastic nonlinear fracture mechanics finite element analysis of concrete structures. Proceedings of 9th Int. conf. on Structural Safety and Reliability Icossar, Rome, Italy, 2005

Global resistance factor for reinforced concrete beams

Diego Lorenzo Allaix, Vincenzo Ilario Carbone and Giuseppe Mancini
Department of Structural and Geotechnical Engineering, Politecnico di Torino, Torino

Abstract: A procedure for the specification of global resistance factors, based on probabilistic analysis of concrete members has been proposed recently. The global resistance factors are related to the coefficient of variation of the resistance of a cross section of the structure, the reliability index and the resistance sensitivity factor for the Ultimate Limit States. The resisting bending moment of reinforced concrete beams is considered in this paper. The reinforcement is designed according to the Eurocode 2, taking into account the ductility requirements. A probabilistic model describing the material properties of concrete and reinforcement steel, the reinforcement area, the uncertainty in the resisting model and the geometrical dimensions of a rectangular reinforced concrete section is outlined. The Monte Carlo method is adopted to estimate the coefficient of variation of the distribution of the resisting bending moment. The result of the statistical treatment of the outcomes of the simulations is used directly to estimate a global resistance factor defined as the ratio between the mean value and the design value of the distribution of the resisting bending moment. The influence of the reinforcement ratio on the global resistance factor is studied by a parametric analysis.

1   Introduction

A procedure for the specification of global resistance factors, based on probabilistic analysis of beams, slabs and columns, has been proposed recently [1]. The hypothesis of the proposal are:

1. the probabilistic relationship recommended by the EN1990 [2] to determine the design value R_d of a resistance R:

$$\text{Prob}(R \leq R_d) = \Phi(-\alpha_R \beta) \tag{1}$$

where $\Phi(\cdot)$ is the cumulative distribution function of the standard normal distribution, α_R is the resistance sensitivity factor and β is the reliability index. For the Ultimate Limit States, the values $\alpha_R = 0.8$ and $\beta = 3.8$ for an intended design life of fifty years are recommended.

2. the resistance of reinforced concrete members can be described by a two-parameter lognormal distribution. In general, the coefficient of variation is small ($V_R < 0.25$), then the design value R_d is approximated by:

$$R_d = \mu_R \exp(-\alpha_R \beta V_R) \tag{2}$$

The global resistance γ_G is defined in the proposal as the ratio between the mean value and the design value of the distribution of the resistance:

$$\gamma_G = \frac{\mu_R}{R_d} = \frac{\mu_R}{\mu_R \exp(-\alpha_R \beta V_R)} \approx \exp(3.04 V_R) \tag{3}$$

The behaviour of the global safety factor is plotted in figure 1.
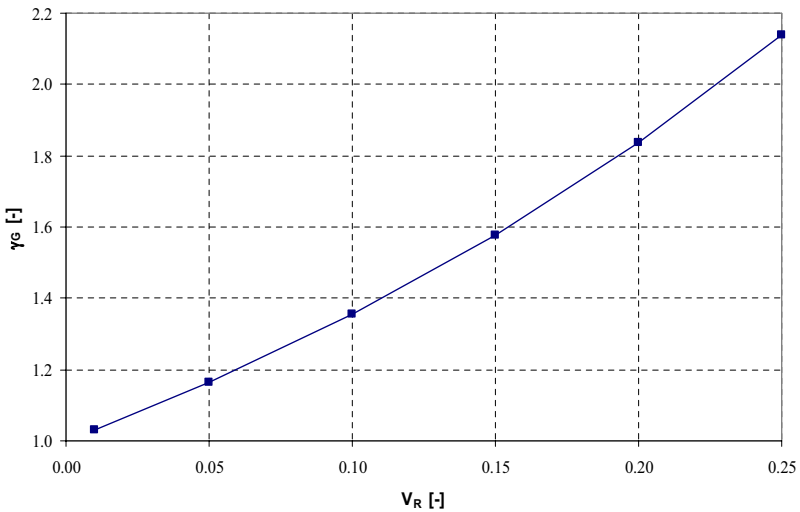
Fig. 1: Global resistance factor

In this paper, a global resistance factor is estimated for a rectangular cross-section of a reinforced concrete beam. The reinforcement is designed according to the EN 1992-1-1 [3] and the ductility requirements are considered in terms of maximum relative depth of the neutral axis. Several values of the reinforcement ratio between 0.25 % and 3 % are consid-

ered at the design stage to investigate the sensitivity of the aforementioned global resistance factor with respect to the amount of reinforcement present in the cross-section.

2 Probabilistic approach

A probabilistic model is derived from [4] for the compressive strength of concrete, the yielding stress of steel, the geometrical dimensions of the concrete section, the reinforcement area and the resisting model uncertainty. Each of these parameters is described by a single random variable. The Monte Carlo method is employed for the uncertainty analysis of the model. One thousand samples are used for this purpose. For each randomly generated sample, corresponding to a set of model parameters, the resisting bending moment M_R of the reinforced concrete section is calculated, considering the parabola-rectangle constitutive law for the concrete in compression and the elastic-plastic diagram for the reinforcement steel [3]. The mean value μ_R and the standard deviation σ_R of the resisting bending moment, obtained by simulation, are estimated. The coefficient of variation V_R of the distribution is derived and used to calculate the global resistance factor γ_G by means of equation (3). Due to this relationship, the global resistance factor increases with the coefficient of variation. The behaviour of the coefficient of variation V_R can be explained as follows. The bending moment M_R is a linear combination of the contributions M_C of the concrete, M_F and $M_{F'}$ of the bottom and top reinforcements respectively. This information is useful to decompose the mean value μ_R in a linear combination of the mean values of M_C, M_F and $M_{F'}$ and the variance σ_R^2 in a linear combination of the variances and covariances of the aforementioned terms. Then the mean value μ_R and the variance σ_R^2 are:

$$\mu_R = \mu_{MC} + \mu_{MF} + \mu_{MF'} \tag{4}$$

$$\sigma_R^2 = \sigma_{MC}^2 + \sigma_{MF}^2 + \sigma_{MF'}^2 + 2Cov[M_C, M_F] +$$

$$+ 2Cov[M_C, M_{F'}] + 2Cov[M_F, M_{F'}] \tag{5}$$

The analysis of each single term listed in equations (4) and (5), considered as functions of the reinforcement ratio, gives a detailed knowledge about the coefficient of variation V_R.

3 Application example

The aforementioned procedure is applied to a reinforced concrete beam. The steel class S500 and the concrete class C20/25 are used in the design. The cross-section is rectangular with base b = 0.30 m and height h = 0.45 m. The vertical positions of the bottom and top reinforcements are described, respectively, by the quantities d_{bottom} = 0.045 m and d_{top} = 0.405 m (see figure 2).
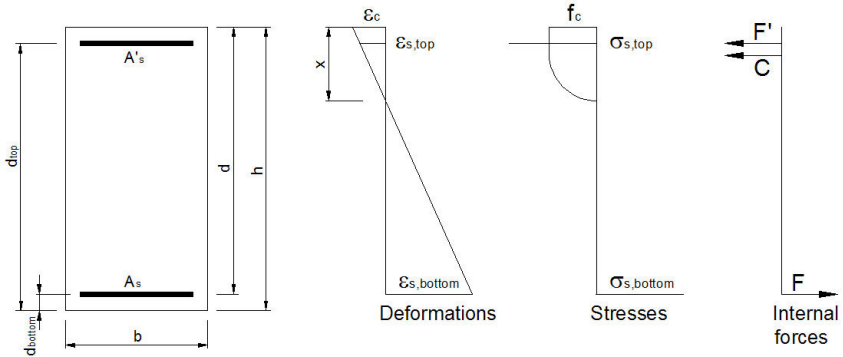
Fig. 2: Cross-section

The ductility requirements adopted in the design lead to the following values of the maximum relative depth of the neutral axis:

- case A: $\left(\dfrac{x}{d}\right)_{lim} = 0.45$

- case B: $\left(\dfrac{x}{d}\right)_{lim} = 0.62$

where d is the distance of the bottom reinforcement from the top fibre of the cross-section. The first value is required by the Eurocode 2 to ensure enough ductility for hyperstatic structures. The second value is adopted to achieve the yielding of the reinforcement at the ULS and could be assumed for isostatic beams. Seven values of the reinforcement ratio $\rho = A_s / (bd)$ varying between 0.25 % and 3 % are considered in the design. The reinforcement areas are listed in tables 1 and 2.

Tab. 1: Reinforcement areas for $(x/d)_{lim} = 0.45$

ρ [%]	$A_{s,bottom}$ [mm^2]	$A_{s,top}$ [mm^2]
0.25	315	-
0.50	630	-
1.00	1260	-
1.50	1890	536
2.00	2520	1166
2.50	3150	1796
3.00	3780	2426

Tab. 2:   Reinforcement areas for $(x/d)_{lim} = 0.62$

ρ [%]	$A_{s,bottom}$ [mm^2]	$A_{s,top}$ [mm^2]
0.25	315	-
0.50	630	-
1.00	1260	-
1.50	1890	37
2.00	2520	667
2.50	3150	1297
3.00	3780	1927

The probabilistic model [4] is presented in table 3. The concrete compressive strength, the steel yielding stress, the area of the rebars and the resisting model uncertainty are described by log-normal random variables. The normal distribution is chosen to describe the geometrical dimensions of the cross-section. Full correlation is assumed for the area of the top and bottom rebars, while a correlation coefficient of 0.12, as suggested in [4], is considered between the base and the height of the concrete section. The vertical positions of the rebars are assumed to be deterministic.

Tab. 3:   Probabilistic model

Variable	Description	Distribution	Mean value	Std. dev.	C.o.v.
$f_{c\,20/25}$ [MPa]	Concrete compression strength	Log-normal	30.0	5.5	0.18
f_y [MPa]	Yielding stress	Log-normal	560.0	30.0	0.05
b [m]	Base of the concrete section	Normal	0.30	0.006	0.02
h [m]	Height of the concrete section	Normal	0.45	0.007	0.02
$A_{s\,bottom}$ [mm^2]	Area of the bottom reinforcement	Log-normal	var.	var.	0.02
$A_{s\,top}$ [mm^2]	Area of the top reinforcement	Log-normal	var.	var.	0.02
K_R [-]	Resisting model uncertainty	Log-normal	1.1	0.077	0.07

First, the behaviour of the coefficient of variation, the mean value and the standard deviation of the distribution of the resisting bending moment is explained for the ductility requirements for hyperstatic structures (case A). Then, the case of isostatic beams (case B) is considered for a comparison. The coefficient of variation V_R is plotted in figure 3.
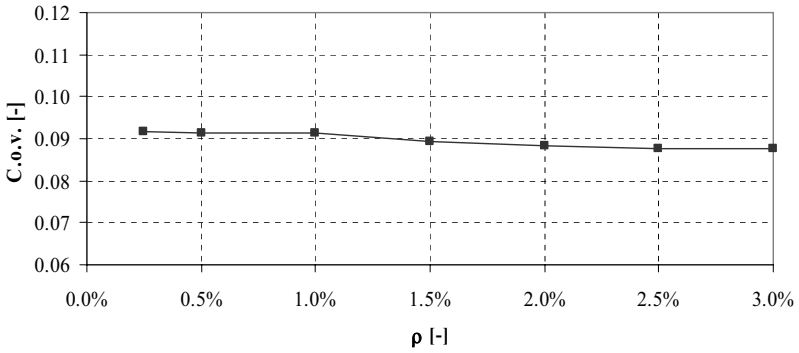
Fig. 3: Coefficient of variation V_R

The relative variation of the coefficient of variation V_R is about 4.7 %. It induces a decrement of the global resistance factor γ_G of 1.4 %, which is considered negligible. The reason of the nearly constant behaviour of V_R is that the standard deviation and the mean value of the distribution increase with the reinforcement ratio approximately with a constant slope, as shown in the figures 4 and 5.
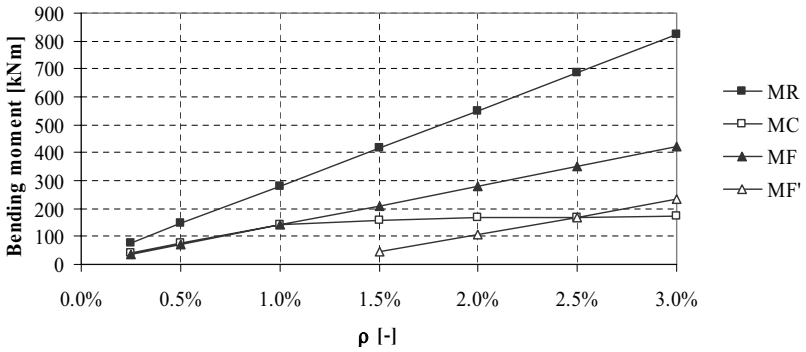

Fig. 4: Mean value of the components of the resisting bending moment
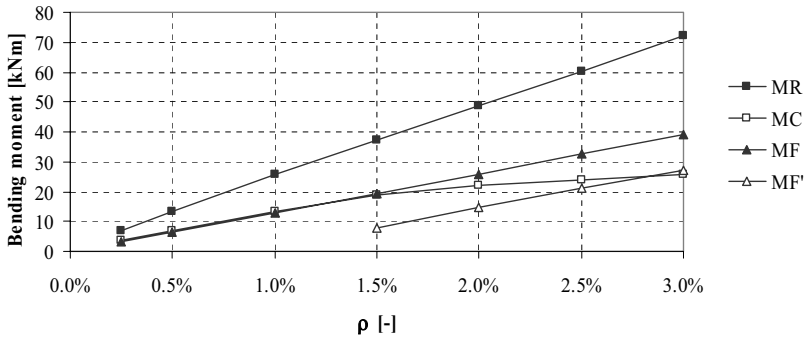
Fig. 5: Standard deviation of the components of the resisting bending moment

The contribution M_C of the concrete in compression is equal to the product of the resultant C of the stress in the concrete by the distance b_c of this resultant from the centre of gravity of the cross-section. The mean value of the compressive resultant C increases in absolute value from $\rho = 0.25$ % to $\rho = 1.0$ % with the same rate of increment of the resultant F of the bottom reinforcement, in order to satisfy the equilibrium of internal forces, as shown in figure 6. If a reinforcement ratio equal or bigger than 1.5 % is adopted, an increasing part of the concrete section in compression reaches the peak stress f_c. Hence, the small increment of C observed in the case of $\rho = 3.0$ % is due to the gradual broadening of the area of the cross section with a concrete deformation smaller than -0.2 %. Moreover, the distance b_c decreases in the mean value for the same reason.
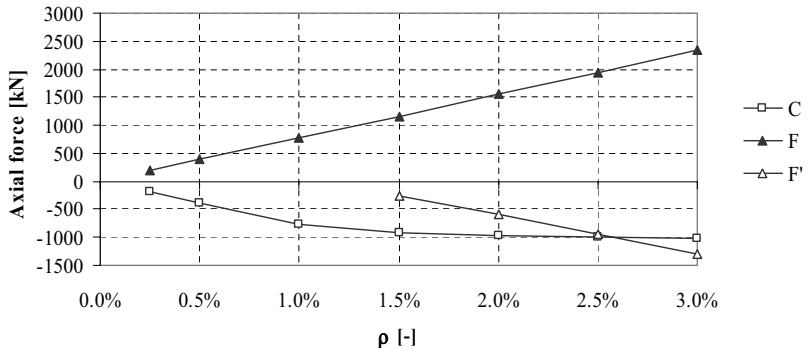

Fig. 6: Mean value of the internal forces

In terms of standard deviation of the resultant C, a more significant increment can be observed (nearly 38 %) between the reinforcement ratios $\rho = 1.5$ % and $\rho = 3.0$ % (see figure 7).
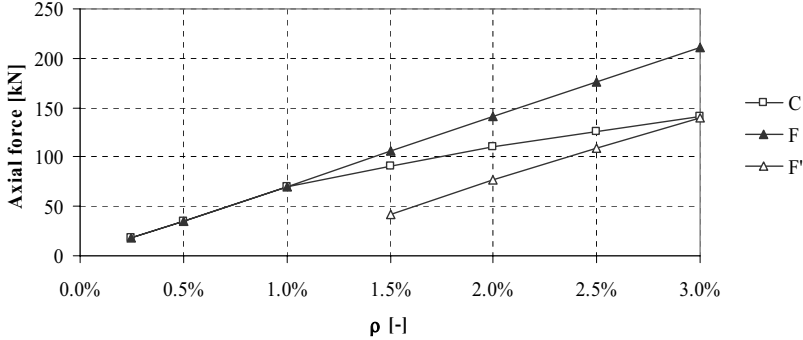

Fig. 7: Standard deviation of the internal forces

As previously mentioned, an increment of the reinforcement ratio leads to a larger number of fibres with a stress equal to the compressive strength f_c. Consequently, the standard deviation of C increases. An increment in the standard deviation of the distance b_c is observed at the same time. The coupling of the behaviour of the standard deviation of the resultant C and the distance b_c explains the increment of the standard deviation of the contribution M_C to the resisting bending moment. The contribution M_F of the bottom reinforcement is a linear function of the reinforcement area and the steel stress. While the reinforcement ratio ρ varies between 0.25 % and 3 %, the bottom steel is always yielded. Then, the increment of the reinforcement area leads to a linear increment of both the values μ_{MF} and σ_{MF}, due to the constant value of the coefficient of variation of the distribution of the area of the rebars. The contribution $M_{F'}$ of the top reinforcement is an increasing function of the reinforcement ratio. In almost 99 % of the outcomes of the Monte Carlo simulations, the top rebars are in the elastic range. The increment of the reinforcement ratio leads to a increment of the strain in the top rebars in order to satisfy the equilibrium of the axial forces acting in the cross section. Therefore, the stress in the rebars increases in absolute value. If the mean value of the stress in the top rebars is considered, it is noticeable that it increases due to the increment of the strain. On the contrary, the standard deviation is a decreasing function of the reinforcement ratio. The distributions of the stress in the top rebars are shown in figure 8.
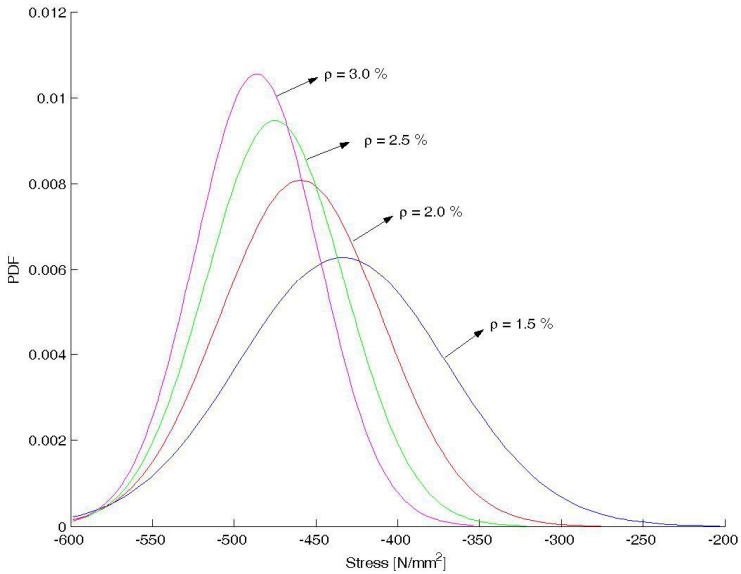
Fig. 8: Stress in the top reinforcement

The behaviour of the covariances of M_C, M_F and $M_{F'}$ depends on the correlation coefficients and the standard deviations of the involved terms. The correlation coefficients are shown in figure 9. The correlation coefficient between M_C and M_F has a value bigger than 0.90 when the top reinforcement is not present. Otherwise, the increment of M_C is significantly lower with respect to the increment of the contributions of the bottom and top rebars to the overall resisting bending moment. Hence the correlation between M_C and M_F decreases. For the same reason the correlation between M_C and $M_{F'}$ decreases in absolute value and the correlation between M_F and $M_{F'}$ increases.
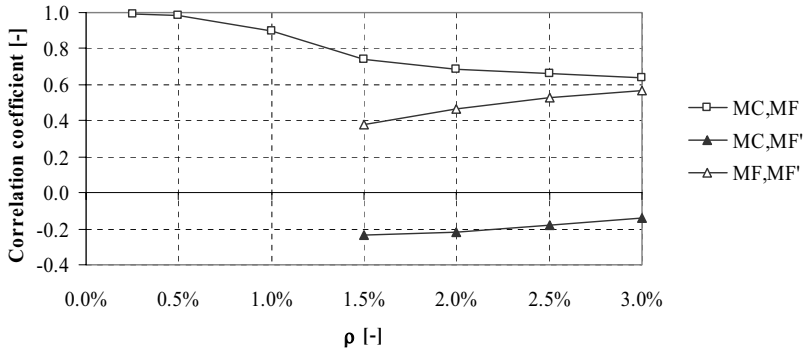
Fig. 9: Correlation coefficients

Taking into account the behaviour of the standard deviations and the correlation coefficients, the covariances are shown in figure 10. The covariance $Cov[M_C, M_F]$ increases due to the increment of the standard deviations and $Cov[M_C, M_{F'}]$ decreases due to the increment of the standard deviations and the sign of the correlation coefficient. The term $Cov[M_F, M_{F'}]$ has the same increasing behaviour of the standard deviations and the correlation coefficient.
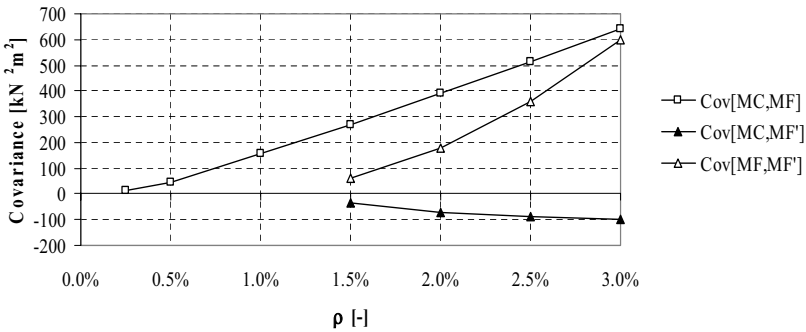

Fig. 10: Covariances

In the case B of the design of isostatic structures, the same values of the coefficient of variation V_R shown in figure 3 are obtained. It can be observed in the figure 11, that the difference, due to the choice of the limit value of the relative depth of the neutral axis, in terms of mean value and standard deviation of the resisting bending moment is not significant. In the case of the design for isostatic structures, the concrete in compression is able to give an higher contribution to the resisting bending moment, while a decrement in the internal force and consequently in the bending moment is observed in the top reinforcement.

This situation is well shown in figure 12, in terms of mean values of the contributions M_C and $M_{F'}$. The same conclusion can be drawn for the standard deviation. Due to the variation of the standard deviations, a similar change in the covariances $Cov[M_C , M_{F'}]$ and $Cov[M_C , M_{F'}]$ is observed (figure 13).
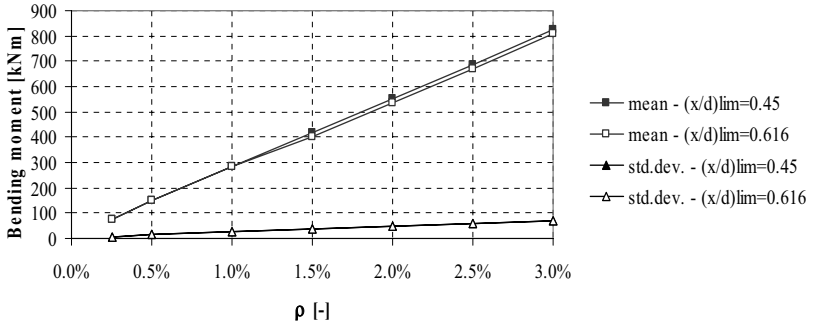

Fig. 11: Comparison of the mean value μ_R and standard deviation σ_R
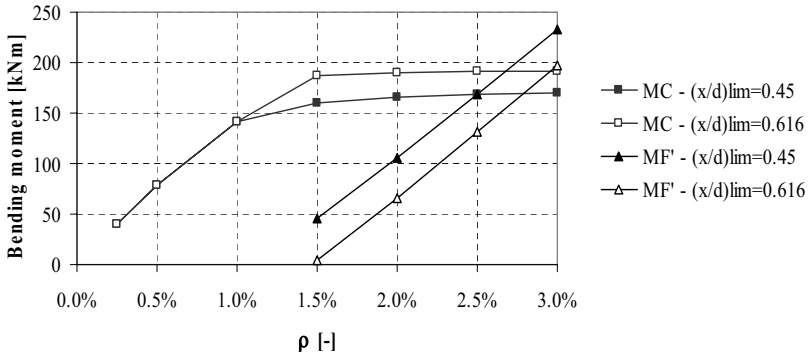
Fig. 12: Comparison of the mean value of M_C and $M_{F'}$

The global resistance factor assumes values between 1.32, when $\rho = 0.25$ %, and 1.30 when $\rho = 3.0$ %. The percentage variation is negligible. The value of $\gamma_G = 1.32$ is proposed for the selected reinforced concrete section.
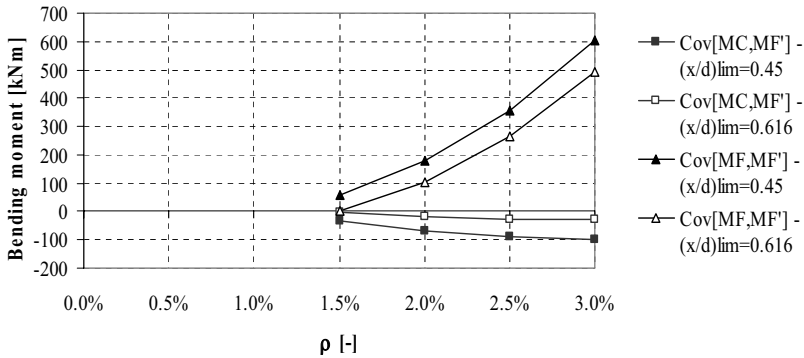
Fig. 13: Comparison of the covariances

4 Conclusions

A global resistance factor for reinforced concrete beams, designed according to the Eurocode 2, is estimated by a probabilistic approach. The global resistance factor, defined as the ratio between the mean value and the design value of the distribution of the resisting bending moment of a cross section of the structure, is related to the coefficient of variation V_R of the distribution, the reliability index and the resistance sensitivity factor for the Ultimate Limit States. A probabilistic model describing the mechanical properties of concrete and reinforcement steel, the reinforcement area, the geometrical properties of the concrete section and the model uncertainty is adopted. The coefficient of variation V_R is estimated from the statistical treatment of the outcomes of a Monte Carlo simulation. The behaviour of V_R is explained by the analysis of the mean value and standard deviation of the contributions of the concrete in compression, bottom and top reinforcements to the overall resisting bending moment. The percentage variation of V_R is not significant when the reinforcement ratio varies between 0.25 % and 3 % in both cases of hyperstatic and isostatics structures. The global resistance factor assumes an approximately constant value and the value $\gamma_G = 1.32$ is proposed for the selected concrete section.

5 References

[1] Holicky, M. Global resistance factors for reinforced concrete members. *FIB-SAG5 New Model Code*, 2006.

[2] CEN. *EN 1990: Eurocode: Basis of structural*, 2002.

[3] CEN. *EN 1992-1-1: Eurocode 2 - Design of concrete structures. Part 1-1: general rules and rules for buildings*, 2003.

[4] Joint Committee on Structural Safety. *Probabilistic Model Code*, Internet publication, 2001, www.jcss.ethz.ch

Probabilistic approach to the global resistance factors for reinforced concrete members

Milan Holický

Klokner Institute, Czech Technical University in Prague

Abstract: The design value of structural resistance can be determined directly from the mean or the characteristic value of the resistance using appropriate factors, called here global resistance factors. The concept of global resistance factors may enable non-linear structural analysis and significantly simplify the reliability verification of reinforced concrete structures. The submitted proposal for the specification of global resistance factors is based on probabilistic analyses of selected reinforced concrete members (slab, beam and column). It appears that the global resistance factors are dependent on the type of concrete members and on their reinforcement ratio. Similarly defined global load factors are strongly dependent on load ratio of variable and total actions. The total factors of safety may be then derived as products of the global resistance and the global load factors.

1   Introduction

Available European documents for the design of structures (Eurocodes) [1, 2] are primarily focused on structures exposed to static loads and the linear dependence between load effect and deformations. Then it is possible to analyse and verify structural reliability using the design values of basic variables. For structures with non-linear behaviour Eurocodes provide simplified rules and recommendations only. One of the general rules introduced in the basic document EN 1990 [1] suggests an alternative procedure for determining design resistance using the characteristic value (determined from the characteristic values of basic variables) and an appropriate partial factor called here the global resistance factor. However, this approach may not be satisfactory in case of dynamic actions or significantly non-linear behaviour of structures, when the mean values of basic variables including the resistance need to be considered [3].

The submitted study is an extension of a previous contribution [4] that attempts to derive the global resistance factors for determining the design value of resistance taking into ac-

count the general rules of EN 1990 [1] and relevant findings in other recent studies [5, 6, 7]. Similarly as in previous investigations [4, 5, 6, 7] the submitted study is based on probabilistic analysis of selected reinforced concrete members (slab, beam and column). The probabilistic approach guarantees a compliance of derived global factors with reliability requirements of the new European documents [1, 2, 3].

 The global resistance factors are derived for two fundamental cases, when the design resistance is derived from

- the characteristic value of resistance,

- the mean value of resistance.

The first approach may be useful when the serviceability limit states are verified simultaneously, the second approach when non-linear or dynamic analysis is required.

2   Design value of a resistance

The New European document EN 1990 [1] gives a recommendation for determining the design value R_d of a resistance R. Based on the FORM reliability procedure the following probabilistic relationship is provided:

$$\text{Prob}(R \le R_d) = \Phi\,(-\alpha_R \beta) \tag{1}$$

Here Φ denotes the distribution function of standardised normal distribution, α_R resistance sensitivity factor, for which [1] allows an approximation $\alpha_R = 0.8$ and β is the reliability index that is in common cases of structures with the design lifetime 50 years considered as $\beta = 3.8$ [1]. When $\alpha_R = 0.8$ and $\beta = 3.8$, the design resistance R_d is a fractile of R corresponding to the probability

$$\Phi\,(-\alpha_R \beta) \sim \Phi\,(-3.04) = 0.00118 \tag{2}$$

It is generally expected [3, 4, 5] that the resistance of reinforced concrete members may be described by two-parameter lognormal distribution with the lower bound at the origin. The design value R_d can be then approximated as

$$R_d = \mu_R \exp(-\alpha_R \beta\, V_R) \tag{3}$$

where μ_R denotes the mean and V_R the coefficient of variation σ_R/μ_R of R.

Note that the characteristic value R_k is the fractile of R corresponding to the probability 0.05, thus

$$R_k = \mu_R \exp(-1.65\, V_R) \tag{4}$$

Here the factor -1.65 is the fractile of standardised normal distribution corresponding to the same probability 0.05. Equations (3) and (4) provide a good approximation if the coefficient of variation V_R is small, say $V_R < 0.25$.

3   Global resistance factor

The design resistance R_d may be derived from the characteristic value R_k or from the mean μ_R of R using formulae

$$R_d = R_k / \gamma_R \tag{5}$$

$$R_d = \mu_R / \gamma^*_R \tag{6}$$

where the global resistance factors γ_R and γ^*_R follow from (3), (4), (5) and (6) as

$$\gamma_R = \exp(-1.645\ V_R)/\exp(-\alpha_R\beta V_R) = \exp((\alpha_R\beta - 1.65)\ V_R) \sim \exp(1.39\ V_R) \tag{7}$$

$$\gamma^*_R = 1/\exp(-\alpha_R\beta V_R) = \exp(\alpha_R\beta V_R) \sim \exp(3.04\ V_R) \tag{8}$$

The global factors are obviously dependent on the coefficient of variation V_R that should be somehow estimated. However, the coefficient V_R depends on the type of member and its reinforcement ratio. In common cases (slab, beam and column) may be expected within the interval from 0.1 to 0.2. In addition the characteristic and the mean value R_k and μ_R should be assessed. Approximately they may be estimated from the characteristic and mean values of the basic variables X describing the resistance $R = R(X)$, thus $R_k \approx R(X_k)$ and $\mu_R \approx R(\mu_X)$ (see an example in the following Section 4). Figure 1 shows variation of the global resistance factors γ_R a γ^*_R with the coefficient of variation V_R.
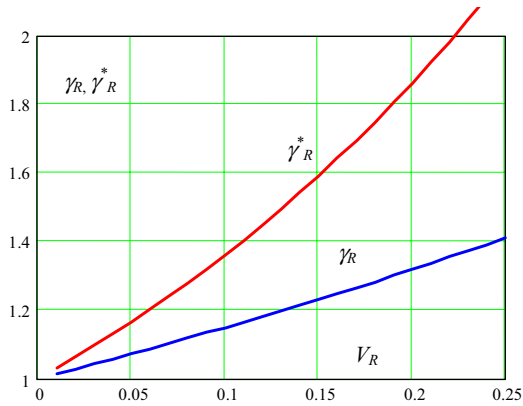

Fig. 1: Variation of the global resistance factors γ_R and γ^*_R with the coefficient V_R

It follows from Fig. 1 that for V_R within the interval from 0.1 to 0.2 the global factor γ_M varies from 1.17 to 1.26, the global factor γ^*_R from 1.27 to 1.85. As a first approximation the values $\gamma_R = 1.25$ and $\gamma^*_R = 1.60$ corresponding to the coefficient of variation $V_R = 0.15$ may be used.

Significance of the global resistance factors is evident from Fig. 2 assuming the lognormal distribution with the lower bound at the origin, the mean $\mu_R = 1$ and the coefficient of variation $V_R = 0.1$ and 0.2. Fig. 2 shows the corresponding characteristic and design values R_k and R_d of R. It should be however noted that the assumed lognormal distribution may be just an approximation of the actual distribution.
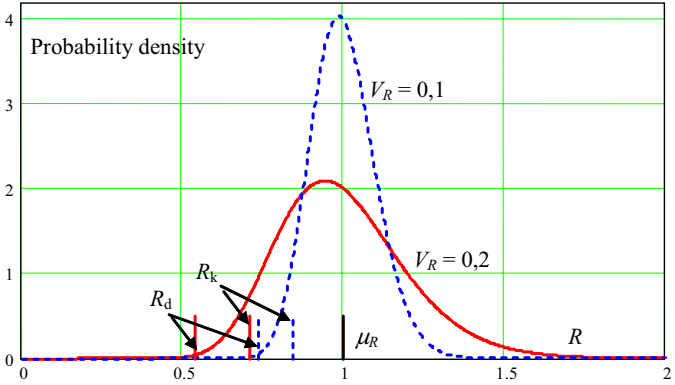

Fig. 2: The characteristic and design values R_k and R_d assuming a lognormal distribution of R and the coefficient of variation $V_R = 0.1$ and 0.2

Figures 1 and 2 clearly indicate that the coefficient of variation V_R may significantly affect estimation of the characteristic and design resistance. Indicative values of V_R for selected reinforced concrete members (slab, beam and column) are shown in Fig.3.
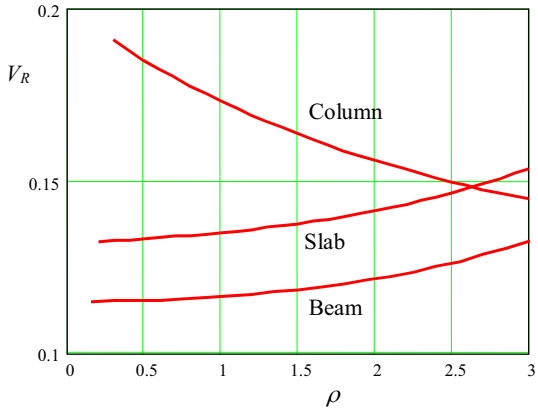

Fig. 3: Variation of the coefficient V_R with the reinforcement ratio ρ

Variation of the coefficient V_R with the reinforcement ratio ρ is derived using probabilistic methods for a slab of a thickness 0.25 m, a beam of cross-section dimensions 0.30×0.60 m, and a centrically loaded short column of cross-section dimensions 0.30×0.30 m, concrete C20/25 and steel S500. An effect of model uncertainties (the coefficient of variation 0.1) is included.

It follows from Fig. 3 that with the increasing reinforcement ratio ρ the coefficient of variation V_R decreases in the case of the centrically loaded short column (from 0.18 to 0.15) and increases in the case of the slab or beam (up to 0.15).

4   The global resistance factor for a slab

An example of the global resistance factor for the reinforced concrete slab assumes that the resistance may be expressed as

$$R = \mathrm{R}\,(\boldsymbol{X}) = K_R\,A_s f_y\,(h - a - 0.5\,A_s f_y/(b\alpha_c f_c)) \tag{9}$$

The vector of basic variables $\boldsymbol{X}$ includes the coefficient of model uncertainty K_R, reinforcement area A_s (the mean corresponds to the reinforcement ratio 0.01), steel strength f_y, slab depth $h=0.25$ m, the distance of the reinforcement centre form the surface $a=0.03$ m, slab width b (deterministic quantity 1 m), the coefficient of concrete strength α_c (deterministic value $\alpha_c = 0.85$) and concrete strength f_c. Basic variables and probabilistic models taken from the previous studies [4, 5, 6] and working materials of JCSS [7] are transparently listed in Tab. 1.

Tab. 1: Probabilistic models of basic variables

Variable	Symbol	Basic variables	Distrib.	Unit	Mean	St. dev.	Char. v.	Des. v.
Material	A_s	Reinforcement area	LN	m^2	0.0022	0.00011	0.0022	0.0022
properties	f_c	Concrete strength	LN	MPa	30	5	20	13.30
	f_y	Steel strength	LN	MPa	560	30	500	435
Geometric	h	Slab height	N	m	0.25	0.008	0.25	0.25
data	a	Distance	GAM	m	0.03	0.006	0.03	0.03
Model unc	K_R	Uncertainty	N	-	1.0	0.10	1.0	1.0

Partial factors for concrete and steel are considered by recommended values in [2] as $\gamma_c = 1.5$ and $\gamma_s = 1.15$. It follows from Fig. 2 that the coefficient of variation $V_R = 0.125$. The mean, characteristic value and the design value may be estimated from equation (9) and appropriate data in Table 1 as

$$\mu_R \approx 0.241 \text{ kNm},\ R_k \approx 0.206 \text{ kNm},\ R_d \approx 0.170 \text{ kNm} \tag{10}$$

The global resistance factors γ_R and γ^*_R follow from (7) a (8) or from Fig. 1 as

$$\gamma_R = \exp(1.39 \ V_R) \approx 1.19 \tag{11}$$

$$\gamma^*_R = \exp(3.04 \ V_R) \approx 1.46 \tag{12}$$

Using the global resistance factors it follows from (5) and (6) that

$$R_d = R_k/\gamma_R = 0.206/1.19 = 0.173 \text{ kNm} \tag{13}$$

$$R_d = \mu_R/\gamma^*_R = 0.241/1.46 = 0.165 \text{ kNm} \tag{14}$$

Note that R_d determined from R_k using the global factor γ_R is very close to the estimated value (0.170 kNm) given in (9), R_d determined from μ_R using the global factor γ^*_R is slightly more conservative than that given in (9); nevertheless, the differences are negligible.

The probability density function of resistance R and the estimated characteristic and design values R_k and R_d given in equation (9) (determined using equation (9) and appropriate data from Tab. 1) are indicated in Fig. 4.
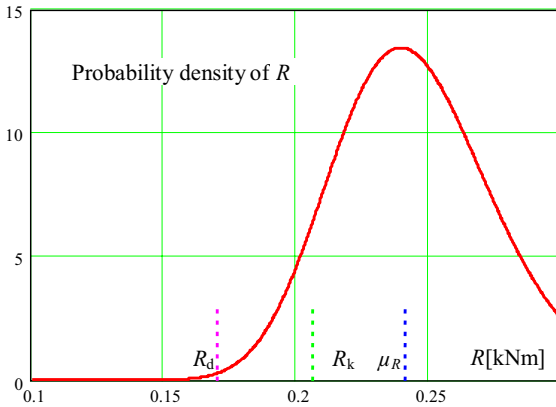

Fig.4: Probability density of R

It should be noted that the coefficient of model uncertainty K_R (see Table 1) is only estimated. Available information including working materials of JCSS [8] are, unfortunately, incomplete and inconclusive.

5   Resistance described by three-parameter lognormal distribution

The two-parameter lognormal distribution (having the lower bound at the origin) assumed above for the resistance of reinforced concrete members may not be always an appropriate approximation. In such a case a more general three-parameter lognormal distribution, when the asymmetry is considered as an independent parameter, may be a more suitable theoretical model.

As an example, Fig. 5 shows the global resistance factors γ_R and γ^*_R derived for the considered concrete members (slab, beam and column) assuming three-parameter lognormal distribution of the resistance R. The asymmetry of the distribution is obtained from the input data for the basic variables X (given in Tab. 1).
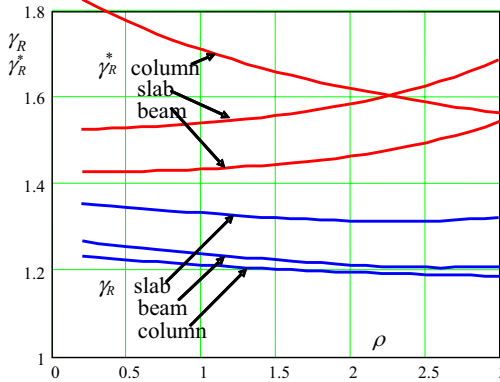

Fig. 5. Variation of the global resistance factors γ_R and γ^*_R with the reinforcement ratio ρ assuming three-parameter lognormal distribution

It appears that the global resistance factors γ_R and γ^*_R are slightly greater than those corresponding to the two-parameter lognormal distribution considered above. This increase is due to a lower asymmetry of the derived three-parameter distribution than the asymmetry corresponding to the two-parameter lognormal distribution. The differences are however insignificant.

Fig. 5 confirms the previous finding [4] that the global resistance factors γ_R and γ^*_R are dependent on both, the type of reinforced concrete member and the reinforcement ratio ρ. It appears that a simple approximation valid in general for all members and reinforcement ratios may be incorrect. The factors $\gamma_R \approx 1.3$ and $\gamma^*_R \approx 1.6$ should be considered as informative estimates only.

6 Global load factor and total factor of safety

An anticipated extension of the concept of global resistance factor is the idea of global load factor and the total factor of safety (reliability). Similarly to the case of resistance, the new European document EN 1990 [1] gives a recommendation for determining the design value E_d of a load effect E. The following probabilistic relationship is provided.

$$\text{Prob}(E > E_d) = \Phi\left(\alpha_E \beta\right) \tag{15}$$

Here Φ denotes a distribution function of the standardized normal distribution, α_R resistance sensitivity factor, for which [1] allows approximation $\alpha_E = -0.7$ and β is the reliabil-

ity index that is in common cases of structures with the design lifetime 50 years considered as $\beta = 3.8$ [1]. When $\alpha_R = -0.7$ and $\beta = 3.8$ the design resistance E_d is a fractile of E corresponding to the probability

$$\Phi(-\alpha_R\beta) \sim \Phi(-2.77) = 0.00309 \tag{16}$$

The permanent load is usually described by a normal distribution, variable action often by Gumbel distribution [3, 4, 5, 8]. The combination of actions (the total load effect) is considered here as a simple sum of one permanent load G and one variable load Q. It may be well approximated by three-parameter lognormal distribution. However, the resulting coefficient of variation and the skewness of the load effect E are strongly dependent on the load ratio χ of variable and the total actions defined for one permanent action G and one variable action Q as

$$\chi = Q_k /(Q_k + G_k) \tag{17}$$

where G_k and Q_k denote the characteristic values of G and Q. As an example consider a permanent action G described by a normal distribution having the mean $\mu_G = G_k$ and the coefficient of variation $V_G = 0.1$, and one variable action described by Gumbel distribution having the mean $\mu = 0.8\,G_k$ and the coefficient of variation $V_G = 0.3$. In addition, the coefficient of model uncertainty is considered by a normal distribution having the mean 1 and the coefficient of variation 0.05. These characteristics are listed in Tab. 2.

Tab. 2: Probabilistic models of actions

Variable	Symbol	Basic variables	Distrib.	Unit	Mean	St. dev.	Char. v.	Des. v.
Actions	G	Permanet load	N	kPa	G_k	$0.1\,G_k$	Q_k	$1.35\,G_k$
	Q	Variable load	GUM	kPa	$0.8\,Q_k$	$0.24\,Q_k$	Q_k	$1.5\,Q_k$
Model unc	K_R	Uncertainty	N	-	1.0	0.05	1.0	1.0

The global load factors γ_E and γ^*_E of the load effect E related to the characteristic value E_k and the mean μ_E are defined as

$$E_d = E_k /\gamma_E \tag{18}$$

$$E_d = \mu_E /\gamma^*_E \tag{19}$$

where the design value E_d of the load effect is defined by the probabilistic relationship given in equation (15).

Fig. 6 shows the variation of the global load effect factor $\gamma_E = E_d/E_k$, $\gamma^*_E = E_d/\mu_E$ and the variation of the coefficient of variation V_E with the load ratio χ (the skewness, not indicated in Fig. 6, varies within the range from 0 to 1.1). Obviously, both the global factors γ_E and γ^*_E are significantly dependent on the load ratio χ. Considering a practical range of the load ratio from 0 up to 0.8, the global factor γ_E varies within the interval from 1.2 to 1.4 (the value 1.3 might be considered as an informative approximation), the factor γ^*_E varies within the interval from 1.3 to 1.7 (an indicative value 1.4 may be considered for the load ratio χ around 0.4).

The fundamental reliability conditions $E_d < R_d$ may be expressed in terms of the characteristic values E_k and R_k using the factors γ_E, γ_R as

$$R_k > \gamma_E\, \gamma_R\, E_k \tag{20}$$

Similarly in terms of the mean values μ_R, μ_E using the factors γ^*_E, γ^*_R the fundamental inequality $E_d < R_d$ may be expressed as

$$\mu_R > \gamma^*_E\, \gamma^*_R\, \mu_E \tag{21}$$
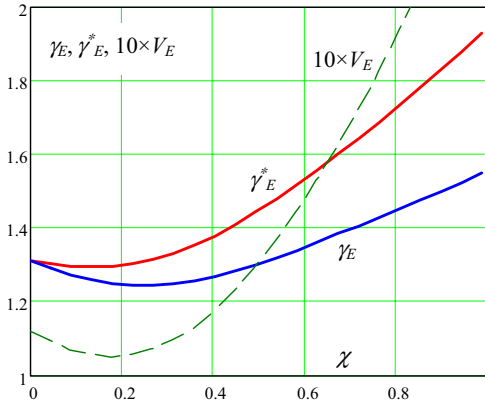
Fig. 6: Variation of the global factors γ_E and γ^*_E and the coefficient of variation V_E with the load ratio $\chi = G_k /(Q_k + G_k)$

Other possible combinations of the mean and characteristic values of the resistance R and load effect E are obvious. The products $\gamma_E\, \gamma_R$ and $\gamma^*_E\, \gamma^*_R < \gamma_E\, \gamma_R$, corresponding to the total factor of safety (reliability) used in one of the historical design method, may be assessed using both graphs in Fig. 5 and 6. However, it follows from Fig. 5 and Fig. 6 that the total factor of safety is dependent on the reinforcement ratio ρ and load ratio χ and a simple approximation is rather difficult.

7 Concluding remarks

The resistance of reinforced concrete members can be well approximated by two-parameter lognormal distribution having the lower bound at the origin. The coefficient of variation of the reinforced concrete members investigated here seems to be within an interval from 0.12 to 0.18. The coefficient of variation is however dependent on the reinforcement ratio; it increases in the case of a slab and beam (is less than 0.15), decreases in the case of a column (from 0.18 to 0.15).

Having the mean μ_R or the characteristic value R_k and the coefficient of variation V_R of the resistance R, the design value R_d may be well estimated using the global resistance factors. In general, the type of member and its reinforcement ratio should be taken into account. As a first (informative) approximation the following global resistance factors may be considered: $\gamma_R = 1.30$ for the global factors related to the characteristic value R_k, and $\gamma^*_R = 1.60$ for the global factors related to the mean μ_R.

The global factors γ_E and γ^*_E of the load effects are strongly dependent on the load ratio χ of variable and total actions. Considering a practical range of the load ratio up to 0.8, the global factor γ_E varies within the interval from 1.2 to 1.4 (the value 1.3 may be used as a first approximation), the factor γ^*_E varies within the interval from 1.3 to 1.6 (the value 1.4 may be used as a first approximation). The products $\gamma_E\,\gamma_R < \gamma^*_E\,\gamma^*_R$ correspond to the total factor of safety used in one of the historical design method.

Acknowledgement

8   References

[1] EN 1990: *Eurocode: Basis of structural design*. CEN 2002.

[2] EN 1992-1 *Design of concrete structures. General rules and rules for buildings*. CEN 2004.

[3] Gulvanessian, H. – Calgaro, J.-A. – Holický, M.: *Designer's Guide to EN 1990, Eurocode: Basis of Structural Design*; Thomas Telford, London, 2002,192 pp.

[4] Holický M. – Holická N.: Globální součinitele odolnosti železobetonových prvků. (Global resistance factors for concrete members, in Czech). 11. *Betonářské dny*, Hradec Králové 2004, pp. 287-292.

[5] Holický M. – Marková J.: Reliability of Concrete Elements Designed for Alternative Load Combinations Provided in Eurocodes. *Acta polytechnica*, 2003/1, pp.29-33.

[6] Holický M. – Retief J.V., Reliability assessment of alternative Eurocode and South African load combination schemes for structural design. *Journal of South African Institution of Civil Engineering*. Vol. 47, No 1, 2005, pp. 15-20.

[7] Gulvanessian, H. – Holický, M., Eurocodes: Using reliability analysis to combine action effects, *Proceedings of the Institution of Civil Engineers, Structures and Buildings*, Thomas Telford. August 2005, pp. 243-251.

[8] JCSS: *Probabilistic model code.* JCSS working materials, http://www.jcss.ethz.ch/

Keynote lecture: Economic Potentials of Probabilistic Optimization Methods

Carl-Alexander Graubner, Eric Brehm & Simon Glowienka
Institute for Concrete and Masonry Structures
University of Technology, Darmstadt

Abstract: A structure's efficiency is strongly influenced by the respective level of reliability. In Germany, this level is defined in DIN 1055-100 and is valid for all structure types in common construction. Considering that this level represents a compromise solution of economy and safety aspects, the question that arises is whether an overall requirement in reliability is adequate. In this paper, the optimization potential is exemplarily assessed for a concrete structure, due to different utilizations of the structure and thus different failure scenarios. The level of reliability is optimized and the saving potential is analyzed.

1   Introduction

The cost effectiveness of structures depends on many parameters. One of the strongest is the stipulated level of reliability. A too high level leads to oversized members that cause unnecessary cost for the owner. This level represents a compromise between efficiency and safety. Therefore, an average failure scenario has been considered in the determination process in many codes. To assess the optimum level considering different failure scenarios, a structure will be designed according to the latest German design codes and then a stochastic analysis is carried out to assess the member's reliability. Subsequently, the structure is optimized on the basis of the results of the stochastic analysis.

2   Examined Structure

2.1   Load-carrying behaviour

The observed structure is a concrete hall consisting of pre-cast elements. The building is 500 m long and 35 m wide. The main load carrying element is a concrete frame composed

of concrete columns, single foundations and a prestressed concrete girder. The single foundations of the columns act as fixed ends so that the structure is braced in this direction. The bracing in longitudinal direction of the structure is realized using walls. For the design according to DIN 1045-1 [2], a distance of the frames, further referred to as "*n*", of 5m is assumed, see Figure 1. Later, this will be the optimization parameter. Figure 1 gives an impression of the structure and of the cross section of the girder.

Cross-section of the girder at
the decisive location

Plan view of the structure

C35/45
St 1570/1770
Bst 500S

n

500m

35m

case I: $A_{p,\,I} = 22.32$ cm²; $d_I = 1.91$ m
case II: $A_{p,\,II} = 26.04$ cm²; $d_{II} = 2.14$m
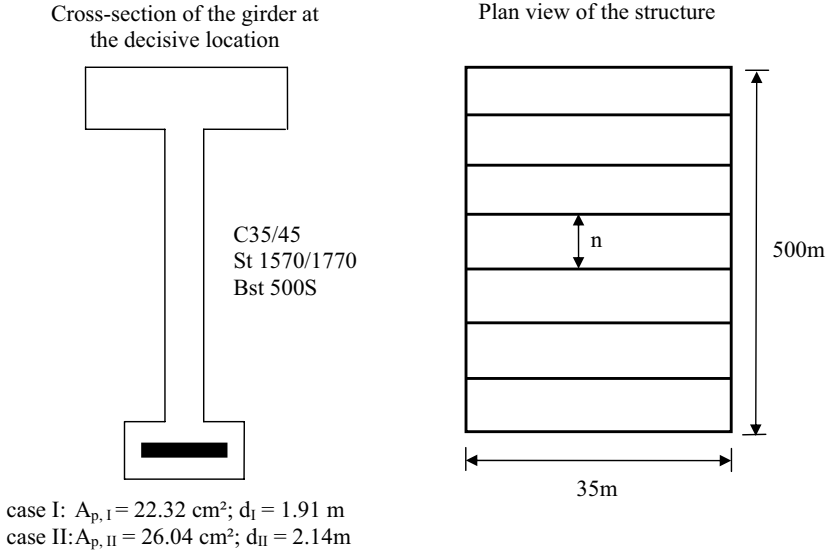
Figure 1: Cross section of the girder and impression of the concrete frames

The considered failure mode is flexural failure of the prestressed concrete girder. Shear failure is not considered due to the large shear capacity. Lateral buckling does also not become decisive.

2.2   Loads

The loads acting on the girder are summarized in Tab. 1. It has to be noticed that two different snow loads are considered due to different locations of the structure to assess the influence of the snow load. The self-weight of the girder is also a little different in both cases due to the different dimensions of the cross sections. In DIN 1055-4 [3], the snow load depends on the location of the structure in a certain snow load zone. The two loading cases represent snow load zone I and III.

Tab. 1: Loads acting on the girder

Kind of load	Referred to as	X_k	
		Case I	Case II
self-weight roof	g	1.41 kN/m²	
Snow	s	0.68 kN/m²	1.78 kN/m²
self-weight girder	G	13.48 kN/m	13.80 kN/m

3   Stochastic Analysis

3.1   Stochastic Modelling

The random variables of the resistance are model uncertainty, material parameters (strength of prestressing steel and reinforcing steel, concrete compressive strength), as well as the dimensions (depth, concrete cover, distance of the strands). They are modelled according to the recommendations of the JCSS [4] and SPAETHE [11]. The chosen type of distribution for the material parameters is lognormal due to the fact that negative values are not to be allowed. The chosen parameters can be taken from Tab. 2.

The modelling of the loads acting on the girder also mostly follows the recommendations of the JCSS [4]. Only the snow load is modelled using a different approach. The snow load is influenced by the altitude, by the depth of the snow layer, by wind action and melting behaviour. For further information see RACKWITZ [1]. As probabilistic model, an extreme value distribution (type Gumbel) was used for the snow load.

The dimensions only play a minor role in the stochastic analysis (see 3.2.2). They are also considered in the analysis but are not given in Tab. 2 since their influence on the failure probability is small in most cases.

Tab. 2: Stochastic model of the girder

Parameter	Mean	CoV	X_k	Distr. Type
Strength of prestressing steel f_p	1566 N/mm²	2.6	1500	LN
Strength of reinforcing steel f_y	560 N/mm²	5.4	500	LN
Concrete compressive strength f_c	48 N/mm²	6.3	40	LN
Model uncertainty resistance Θ_R	1.1	10	1	LN
Model uncertainty actions Θ_S	1.0	10	1	LN
Self-weight roof g	1.41 kN/m²	5	1.41	N
Self-weight girder G	13.48; 13.80 kN/m	5	13.48; 13.80	N
Snow load s	0.64; 1.59 kN/m²	25; 23	0.68; 1.78	Gumbel

Another important subject for the stochastic analysis is the limit state function. To obtain a practical model of the flexural failure of the girder, a stress block according to DIN 1045-1 [2] was used. The limit state function derives to

$$g_{(x)} = \Theta_R \cdot \left(A_p \cdot f_p + A_s \cdot f_y \right) \cdot z - \Theta_s \cdot M_s = 0 \tag{1}$$

Θ_R and Θ_s represent the model uncertainties. Considering a stress block, the inner lever z can be modelled only using the dimensions. This yield eq. (2).

$$g_{(x)} = \Theta_R \cdot \left(A_p \cdot f_p + A_s \cdot f_y \right) \cdot \left(d - \frac{A_p \cdot f_p + A_s \cdot f_y}{2 \cdot b \cdot 0.81 \cdot f_c} \right) - \Theta_E \cdot M_E \tag{2}$$

3.2   Results

3.2.1   Reliability Indices

First the reliability according to DIN 1055-100 [3] was analysed. The analysis was carried out for the design of the structure according to DIN 1045-1 [2], i.e. the distance of the frames is 5m. The results of the analysis for the different loading cases can be taken from Tab. 3.

Tab. 3:   Reliability Indices

Loading Case	Reliability Index β	
	1 a	50 a
I	4.85	4.22
II	4.36	3.68

The target values according to DIN 1055-100 in ultimate limit state [3] are 3.8 for an observation period of 50 years and 4.7 for 1 year. The reliability indices are within an acceptable range. In loading case I the indices are a little larger than the target values and loading case II they are a little smaller but still acceptable. So the girder fulfils the code requirements in ultimate limit state for the reference distance of the girders of 5 m.

3.2.2   Sensitivity Values and Partial Safety Factors

The sensitivity factors of the analysis showed that the strongest influences on the analysis are the model uncertainties and the snow load, see Tab. 4. The partial safety factors, calculated for the required target reliability index $\beta_T = 3.8$ according to DIN 1055-100 [3] are more or less similar to the ones given in the code. The factors on the steel are close to the ones based on DIN 1055 [3] but the factor on compressive strength of concrete is smaller. The biggest difference can be seen for the factor on the snow load which is the only considered live load. It is 12 % or 42 % larger than the stipulated value of the code, respectively. Considering the fact that the reliability indexes meet the code values, it can be estimated that the factor on compressive strength of concrete equalizes the large required partial safety factor on the live load.

Tab. 4   Sensitivity values

Quantity	sensitivity value α			
	case I		case II	
	1 year	50 years	1 year	50 year
Strength of prestressing steel f_p	0.15	0.15	0.11	0.13
Concrete compressive strength f_c	0.01	0.01	0.01	0.01
Self-weight roof g	-0.09	-0.09	-0.05	-0.06
Self-weight girder G	-0.18	-0.17	0.09	-0.11
Model uncertainty resistance M_R	0.63	0.65	0.46	0.55
Model uncertainty actions M_E	-0.63	-0.65	-0.46	-0.55
Strength of reinforcing steel f_y	0.02	0.02	0.01	0.02
Snow load s	-0.37	-0.29	-0.75	-0.60
Width of flange b	0.00	0.00	0.00	0.00
Depth of girder h	0.04	0.04	0.03	0.03
Distances of the strands Δ	-0.02	-0.02	-0.01	-0.01
Concrete cover c_{nom}	-0.02	-0.02	-0.01	-0.02

4   Probabilistic Optimization

4.1   Procedure and Objective Function

The optimization is linked to the failure scenarios. Therefore it is necessary to determine the scenario specific attributes. In this paper, an economic optimization is carried out, considering economic parameters as e.g. interest rate and costs due to reconstruction and fatalities. The target of the optimization is cost reduction in terms of saving of concrete frames.

Furthermore, the failure scenario has to be defined by a probability tree to assess the probability of the failure consequences. The probabilities in the probabilities trees have been estimated on basis of literature research.

The objective function is supposed to include all influencing parameters. The target is to find the optimum solution considering economic aspects. Therefore interest rates have to be considered. ROSENBLUETH and MENDOZA [9] formulated an equation that is used as basis for the optimization, see eq. (3).

$$Z(p) = B(p) - C(p) - D(p) \tag{3}$$

In this equation, $B(p)$ is the benefit derived from a structure, $C(p)$ is the structural cost and $D(p)$ is the risk. In this case, the risk is defined as the total cost, explained later in the paper, in case of failure multiplied by the probability of failure. p is the parameter of the optimization. Here, it is the distance of the concrete frames. This means that a change in this parameter will result in a larger or smaller number of concrete frames and so directly in increased or reduced structural cost.

It is essential to consider the fact that the optimization is done for a future event. So, the decision whether the structure will be built takes place at t = 0 considering a failure in the

future. The following approach using a continuous interest rate has proven to be sufficient in the past, eq. (4).

$$\delta(t) = \exp[-\gamma t_s]$$ (4)

If an annual interest rate γ' is defined, the interest rate has to be converted using eq. (5).

$$\gamma = \ln(1 + \gamma')$$ (5)

Further, the risk $D(p)$ has to be analyzed. In case of failure, a large number of different reasons for costs appear. Assuming a reconstruction of the structure after failure, they can be divided into the cost of the reconstruction $C^*(p)$ and the indirect cost H. The latter is difficult to define. It can be calculated by eq. (6).

$$H = \sum p_i \cdot K_i$$ (6)

Where p_i are the probabilities of the event on the observed level of the probability tree and K_i are the corresponding costs. Under the assumption of $C^*(p) \approx C(p)$, RACKWITZ [8] gives the following objective function for the case of reconstruction.

$$Z(p) = B^* - C(p) - (C(p) + H) \cdot \frac{P_f(p)}{1 - P_f(p)}$$ (7)

If a reconstruction is considered, the time span of the reconstruction has to be taken into account. Therefore, RACKWITZ [8] introduced the factor A_w.

$$A_w = \frac{E[T_S]}{E[T_S] + E[T_W]}$$ (8)

Where $E[T_S]$ is the service life of the structure and $E[T_W]$ is the reconstruction time. The factor has to be applied on the benefit and on the risk due to the fact that the structure can neither fail nor produce benefit during reconstruction time. Including eq. (4) and eq. (8) in eq. (7), modelling the failure rate by a Poisson Process with intensity λ and considering constant benefit leads to the final objective function, eq. (9).

$$Z(p) = \frac{b}{\gamma} \exp(-\gamma t_s) A_w - C(p) - (C(p) + H) \frac{\lambda(p)}{\gamma} \exp(-\gamma t_s) A_w$$ (9)

4.2   Approach to Assess Fatalities

The failure cost H in eq.(6) depends on the factor K_i. This factor represents the failure cost for a single failure scenario. To assess the optimal level of reliability, it has to include the cost due to fatalities. While an attempt at finding a model for the monetary assessment of fatalities may seem unwarranted, it is absolutely necessary to consider fatalities in an economic optimization. Fatalities do not only cause direct cost, such as insurance or funeral cost, but also the damage to the national economy is large due to the fact that the deceased will not pay taxes or be of use to the society. LIND [6] gives an approach to assess the con-

sequences to national economy due to a fatality. This approach was extended by NATHWANI, LIND und PANDEY [7]. The defined factor that regards social conditions is termed, the so called Life Quality Index. It includes three major factors: the gross national product per capita, the average expectation of life and the percentage of time that a person spends to earn a living. Based on this factor, SKJONG and RONOLD [10] developed a model that calculates the **Implied Costs of Averting a Fatality**, further referred to as *ICAF*. If it is assumed that the victims of structural failure averagely reached the half their life expectancy and produce the average gross national product per capita, *ICAF* can be calculated from eq. (10).

$$ICAF = \frac{g \cdot e}{q \cdot 4} \qquad (10)$$

Where g is the gross national product per capita, e is the expectation of life. The factor q is the percentage of time that people need to earn their living is estimated to be approx. 18% for western industrial nations according to RACKWITZ [1]. The failure costs due to fatalities can be calculated from eq. (11) where N_f is the number of persons in the building at the time of failure. However, because not every individual will be a fatality, the factor k represents the percentage of fatalities. Reference values for k can be taken from Tab. 5. Here, H_f was calculated to 1.2 Mio. € per fatality ($k = 0.5$).

$$H_f = k \cdot N_f \cdot ICAF \qquad (11)$$

Tab. 5   Reference values for the factor k according to Rackwitz [8]

Kind and reason of failure	k [-]
Earthquake	0.01-1.0
Avalanche, rockfall, blast, impact etc.	0.01-1.0
Floodings, storms	0.0001-0.01
Sudden structural failure in recreational areas	0.1-0.5
Fire in structures	0.0005-0.002
Fire in car tunnels	0.01-1.0

4.3   Optimization Results

4.3.1   General Assumptions

All analyses were done with an annual true interest rate of $\gamma' = 3\%$. The recommendations in the literature scatter from 2% to 5%. Furthermore, the structural cost $C(p)$ must be noted. This value is not constant because it depends on the number of concrete frames. The structural cost $C(p)$ can be calculated using eq. (12).

$$C(p) = \frac{l}{n} \cdot C_{frame} + C_{int} \qquad (12)$$

Where C_{frame} is the cost of one concrete frame (columns, foundations, girder, transport and installation), C_{int} is the cost of the interior fitting, l is the length of the structure and n is the distance of the frames. C_{frame} was calculated based on data of pre-cast concrete elements

manufacturers; it equates to 12,000 €. The following analyses were done for a service life (observation period) of t_s = 50 years and a reconstruction time of 1.5 years.

4.3.2 Classification of the Scenarios

To classify the risk of a failure scenario, JCSS [5] gives a criterion, defined as follows.

$$f(p) = \frac{C(p) + H}{C(p)} \tag{13}$$

Also, reference values are given. Structures with a value $f(p)$ smaller than 2 suggests that the risk is small. For *2 < f(p) < 5*, the risk is considered to be average. A high risk is given in cases of *5 < f(p) < 10*. For larger values of *f(p)*, an exact cost-benefit analysis should be carried out according to the JCSS [5]. In the following, the values of *f(p)* for the different scenarios corresponds to the reference distance of the concrete frames of 5m due to the fact that *f(p)* depends on the failure probability and the distance of the frames.

4.3.3 First Scenario: Print Shop

The first scenario corresponds to the use of the structure as a print shop. It is assumed that there is a maximum number of 4 persons working in the print shop at the same time. In case of failure, substitute machine rentals during the reconstruction time have to be considered. In this scenario, *f(p)* equals 1.0. So, the risk can be considered as small. Figure 2 gives the impression of the objective function *Z(p)*. As it can be seen from eq. (3), the rising parts are governed by the benefit while the falling parts are governed by the risk. The optimization result is the distance of the girders for the maximum value of the objective function.

Tab. 6   Parameters of the first scenario

| Parameter	Cost in Mio. €
Annual benefit	1.0
Retrieval of printing machines	20.0
Rent of printing machines during reconstruction time	7.5
Cost of interior work	2.5
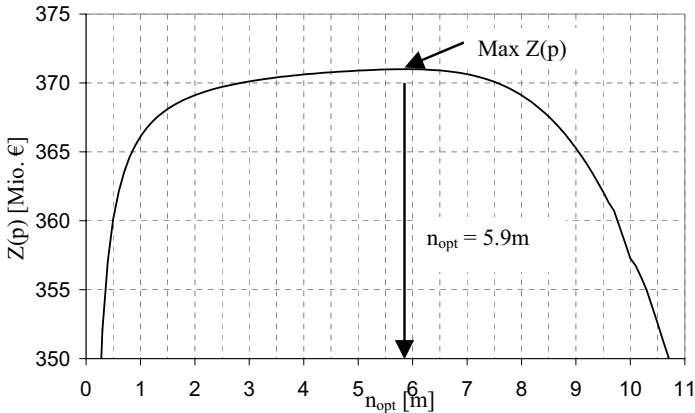
Figure 2:   Objective function for the first scenario with loading case II

The optimized distance of the girders is 6.9m in loading case I and 5.9m in loading case II. This corresponds to a number of 27 and 15 concrete frames saved. Considering the cost for a frame this leads to a saving of 324,000 € and 180,000 €, respectively. It has to be mentioned again that just the influence of the snow load yield a difference of 144.000 € in the optimization results. As another result, the risk H corresponding to the optimized distances of the beams can be compared. In loading case I, H equals 13.9 Mio.€ and $D(p)$ in eq. (3) becomes 9,780 €. In loading case II, H is 14.0 Mio. € and D(p) equals 12,600€. The optimum structural cost C(p) is 3.38 Mio.€ in loading case I and 3.52 Mio. € in loading case II. The optimum can be found where the minimum of the sum of $C(p)$ and $D(p)$ is reached, eq. (7).

$$C(p) + D(p) = \min \tag{14}$$

4.3.4   Second Scenario: Furniture Market

This scenario represents the worst failure consequences. The parameters used were converted from data of a big furniture company. The maximum number of people in the building at the time of failure is 615. Opening times and holidays have been regarded, as well as the goods in stock and in the exhibition. Here, $f(p)$ equals 17.2, so this is a structure with very high risk. This scenario considers the largest risk. Therefore, the optimization potential is smaller than in the other cases. In loading case II, the optimized distance of the girders equals $n_{ref} = 5.0$m. In loading case I, the optimization result is 5.7m. This leads to a saving of 144,000 € in the case of minor influence of the snow load. The corresponding risk H for the optimized distances of the beams is 132.2 Mio. € in loading case I. Multiplying with the failure probability, this yield $D(p) = 8,860$ €. For loading case II, H equals 132.2 Mio. € and $D(p)$ becomes 15,200 €. The risk H is similar because the risk is governed by the costs due to fatalities. Therefore, the change in structural cost does not affect the risk H significantly.

Tab. 7   Parameters of the second scenario

Parameter	Cost in Mio. €
Annual benefit	3.3
Value of goods in the building at the time of failure	30.0
Cost of interior work	6.5

4.3.5   Third Scenario: Ice Rink

The last scenario represents medium failure consequences. The maximum number of people in the building at the failure is 250. In this case, *f(p)* = 4.4. The risk can be classified as average according to JCSS [5]. Opening times were considered in the probability tree. It has to be mentioned that the structure's commercial area is very large and so the maximum number of persons in the structure, calculated using the number of persons per m² of a typical ice rink, is also large.

Tab. 8   Parameters of the third scenario

Parameter	Cost in Mio. €
Annual benefit	1.0
Cost of interior work	5.0

Due to the fact that this scenario ranges between the print shop and the furniture market concerning the risk, the optimization result is expected to be in between the results of the previous scenarios. In the first loading case, the result is 6.5 m; in loading case II it is 5.5 m. This corresponds to a saving potential of 23 and 9 concrete frames, respectively. To express it in a monetary way, 276,000 € in loading case I and 108,000 € can be saved to obtain the most economic result. The corresponding risk *H* for the optimized distances of the beams is 27.3 Mio. € in loading case I. This yield *D(p)* = 9,380 €. For loading case II, *H* equals 27.5 Mio. € and *D(p)* becomes 10,600 €.

4.4   General Results

4.4.1   Sensitivity of the Model

A parameters study showed that only a small number of parameters significantly influenced the optimization results. A short summary is given by Tab. 9. The parameters were varied up to 10 %. If a parameter's sensitivity is classified as minor, the optimization result changed less than 3 %. It is found that the only major influences are the annual interest rate and the failure probability i.e. the stochastic model of the girder.

Tab. 9   Qualitative statements concerning the model's sensitivity

| Parameter	Sensitivity
Changes in the probability tree	minor
Annual interest rate γ'	major
Percentage of fatalities k	negligible
Failure probability Pf	major
Cost of a frame C_{frame}	minor
ICAF	negligible

4.4.2   Optimized Reliability Index

The optimized reliability indices for different annual interest rates in loading case II (large snow load) can be taken from Figure 3. It can be detected that the larger the interest rate is, the larger the optimized reliability index becomes. This is logical since in case of small interest rates, the benefit due to the interest is small and so the risk is dominating the objective function. This also explains the strong exponential behaviour for small interest rates because the exponential interest rate governs the optimization. It also can be seen that the optimized reliability indices are smaller than the stipulated ones according to DIN 1055 even for small interest rates. In loading case I, the optimized reliability indices are in every case smaller than in loading case II.

4.4.3   Saving Potential

Due to the fact that the distance of the concrete frames is optimized and so the number of frames changes, the saving potential is the difference between the structural cost for a reference distance of the frames of 5 m and the structural cost for the optimized distance. As mentioned in the previous paragraph, the major influence is the annual interest rate. Therefore, this is taken as the main parameter for the following analyses.

Figure 4 shows the relation between the saving potential and the interest rate for loading case II (large snow load). It can be seen that the interest rate alone can change the result from saving to more expensive solutions. As it can also be seen from Figure 4, the saving potential already starts to leave the negative for interest rates larger than 1 % in cases of minor risk (print shop) and 3 % in case of major risk (furniture market).
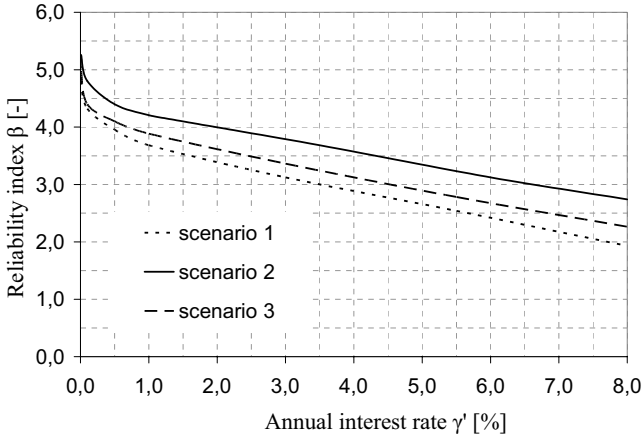
Figure 3   Optimized reliability indices depending on the interest rate
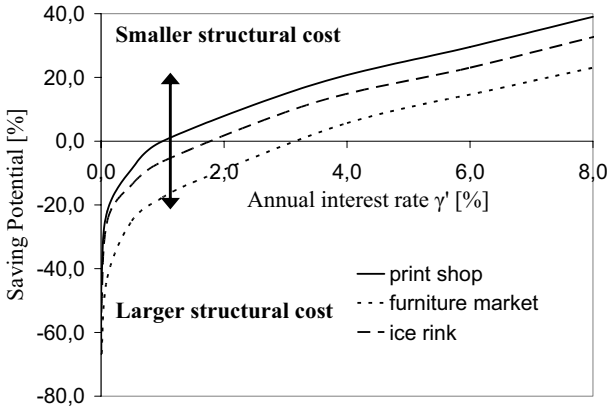
Figure 4   Saving potential depending on the annual interest rate for loading case II

5   Summary

In this paper, a probabilistic optimization of a concrete structure is carried out to show potentials of probabilistic optimization methods. The considered limit state is flexural failure of the main load-carrying member, a concrete frame with a prestressed concrete girder, columns and single foundations. In the first step, the girder is designed according to the latest German standard. Then a stochastic analysis is conducted. It is shown that the target reliability indices according to DIN 1055-100 are reached. The optimization is done focussing on economic parameters, such as interest rates, benefit, structural cost and costs due to fatalities, for three different failure scenarios. Subject of the optimization is the distance of the fames. It is shown that the optimum distance of the girders is larger than according to

DIN 1045-1 and so the optimized reliability is smaller than the target values. Thus, significant saving potential is found. The strong influence of the snow load is also shown. Even in case of large risk, saving potential up to 23 % of the structural cost compared to the code design is found. Because of these results, probabilistic optimizations methods are recommended for special structures with large structural cost. Dividing the required level of reliability depending on the kind and use of a structure seems to be reasonable as long as risks are small.

6   References

[1]   Bachmann, H.; Rackwitz, R.; Schuëller, G.: *Tragwerkszuverlässigkeit/Einwirkungen*, in *Der Ingenieurbau* edited by Mehlhorn, G.; Berlin: Ernst und Sohn, 1996

[2]   Deutsches Institut für Normung: *DIN 1045-1: Tragwerke aus Beton, Stahlbeton und Spannbeton*. Berlin: Beuth Verlag, 2001

[3]   Deutsches Institut für Normung: *DIN 1055: Einwirkungen auf Tragwerke.* Berlin: Beuth Verlag, 2005

[4]   Joint Committee on Structural Safety (JCSS): *Probabilistic Model Code*, www.jcss.ethz.ch

[5]   Joint Committee on Structural Safety: *Probabilistic Assessment of Existing Structures*. RILEM Publications S.A.R.L.

[6]   Lind, N.C.: *Target Reliabilities from Social Indicators*. Balkema: Proceedings, ICOSSAR93, 1994

[7]   Nathwani, J.S.; Lind, N.C.; Pandey, M.D.: *Affordable Safety by Choice: The Life Quality Method*. Waterloo, Canada: Institute of Risk Research, 1997

[8]   Rackwitz, R.; Lentz, A.; Faber, M.: *Socio-economically sustainable civil engineering infrastructures by optimization*. Structural Safety, Vol. 27, 2005

[9]   Rosenblueth, E.; Mendoza, E.: *Reliability Optimization in Isostatic Structures*. Journal of the Engineering Mechanics Division, Proceedings of the American Society of Civil Engineers, 1971

[10]   Skjong, R. und Ronold, K.O.: *Societal Indicators and Risk Acceptance*. Proceedings 17th Int. Conference Offshore Mech. and Arctic Eng. (OMAE98), Paper No. 1488, 1998

[11]   Spaethe, G.; *Die Sicherheit tragender Baukonstruktionen*. Wien: Springer Verlag, 1992

Estimation of concrete strength from small samples

Milan Holický, Karel Jung & Miroslav Sýkora
Czech Technical University in Prague, Klokner Institute

Abstract: Statistical procedures for estimating concrete strength from small samples provided in the new European document EN 13791 (2007) are different from those accepted in material independent Eurocode EN 1990 (2002). Differences between these two approaches are not negligible and appear to be important particularly for assessment of existing structures. The characteristic values (5% fractiles) of concrete strength determined in accordance with EN 13791 are systematically greater than values obtained using EN 1990 procedure. The differences increase up to 8 MPa with decreasing number of tests. Moreover, according to EN 13791, the variation of the characteristic strength with number of tests results is discontinuous. Thus, it is desirable to harmonise the procedures given in EN 13791 for determining compressive concrete strength with those provided for any material in EN 1990.

1   Introduction

A traditional task of estimating concrete strength using small samples has recently been discussed in connection with the new European document EN 13791 [2] published in January 2007. The document is intended for new as well as existing concrete structures. However, statistical procedures provided in the document seem to be rather different from those given in material independent Eurocode EN 1990 [3], which is consistent with ISO 12491 [6], ISO 13822 [7] and ISO 2394 [8].

Differences between EN 13791 [2] and EN 1990 [3] are not negligible and appear to be important particularly in case of assessment of existing structures, for which estimation of material properties from limited data is an important and sensitive task. Moreover, repair and upgrading of existing structures is becoming more and more frequent construction activity of increasing economic significance. Therefore, assessment of existing structures is treated in the recent document ISO 13822 [2], which refers to ISO 2394 [8] and ISO 12491 [6]. Statistical procedures given in these ISO documents are consistent with the rules provided by EN 1990 [3]. Taking this into account, the inconsistency of EN 13791 [2] and EN 1990 [3] is obviously an urgent topic.

The question arising out of this situation is clear: which of these two different procedures should be accepted and used in practise?

Procedures in both the documents EN 13791 [2] and EN 1990 [3] are analysed using the sampling theory described in ANG and TANG [1] and ISO 12491 [6] in conjunction with a simulation technique. Normal distribution of the population of concrete strength is considered only. However, similar results may be obtained for a two-parameter lognormal distribution. To illustrate differences between the procedures, a representative population of test results having the mean 30 MPa and the standard deviation 5 MPa (common characteristics of concrete in accordance with JCSS [10]) is considered in numerical simulations. It is emphasized that test results are considered to be statistically independent which may be a realistic assumption in assessment of existing structures. In case of compliance control of concrete, autocorrelation between consecutive test results may occur and should be then taken into account as indicated by TAERWE [11,12].

2   Estimation of the characteristic strength in EN 1990

In accordance with the Annex D of EN 1990 [3] (see also GULVANESSIAN and HOLICKÝ [5], ISO 12491 [6] and ISO 2394 [8]), the characteristic in-situ compressive strength $f_{ck,is}$ may be determined from n tests results using the prediction method, ISO 12491 [6] (in EN 1990 [3] the prediction method is referred to as "Bayesian procedures with vague prior distributions").

$$f_{ck,is} = f_{m(n),is} (1 - k_n \times V) \qquad (1)$$

with k_n Coefficient obtained from Tab. 1
       V Coefficient of variation
       $f_{m(n),is}$ The mean of test results

Tab. 1:   Values k_n for the 5% characteristic value

N	1	2	3	4	5	6	8	10	20	30	∞
V known	2.31	2.01	1.89	1.83	1.80	1.77	1.74	1.72	1.68	1.67	1.64
V unknown	–	–	3.37	2.63	2.33	2.18	2.00	1.92	1.76	1.73	1.64

The terminology and symbols defined in EN 13791 [2] are accepted here. Note that the characteristic value $f_{ck,is}$ given by equation (1) may be affected by various conversion factors η_d not included in this study to simplify the analysis.

The coefficient k_n in Tab. 1 for the known coefficient of variation V is given as

$$k_n = u_{0.05} (1 + 1/n)^{0.5} \qquad (2)$$

with $u_{0.05}$ Fractile of the standardized normal distribution for
             the probability 0.05

When the coefficient of variation V is unknown, the sample standard deviation s (or sample coefficient of variation v) shall be used. The coefficient k_n then becomes in accordance with ISO 12491 [6]

$$k_n = t_{0.05} (1 + 1/n)^{0.5} \tag{3}$$

with $t_{0.05}$ Fractile of the t-distribution for the probability 0.05

Similar expressions are valid for fractiles corresponding to any probability, for example to the probability 0.001 when a design value of a material property is estimated. As indicated by GULVANESSIAN and HOLICKÝ [5], the prediction method accepted for fractile estimation in EN 1990 [3] corresponds approximately to the classical coverage method with the confidence level 0.75 (as described in ISO 12491 [6]).

3 Estimation of the characteristic strength in EN 13791

3.1 Approach A

EN 13791 [2] distinguishes statistical procedures for 15 and more test results (Approach A) and for 3 to 14 test results (Approach B). When the characteristic in-situ compressive strength $f_{ck,is}$ is estimated from $n = 15$ or more test results (Approach A), $f_{ck,is}$ is equal to the lower of two values obtained from the following expressions

$$f_{ck,is} = f_{m(n),is} - k_2 \times s$$
$$f_{ck,is} = f_{is,lowest} + 4 \tag{4}$$

with k_2 Coefficient provided by national provisions, if no
value is given, then $k_2 = 1.48$
s Standard deviation of test results
$f_{m(n),is}$ The mean of test results
$f_{is,\,lowest}$ The lowest test result

The coefficient k_2 is further considered as $k_2 = 1.48$. The sample standard deviation should be considered not lower than 2 MPa.

3.2 Approach B

When 3 to 14 test results are available (Approach B), the characteristic strength $f_{ck,is}$ is estimated as the lowest value obtained from

$$f_{ck,is} = f_{m(n),is} - k$$
$$f_{ck,is} = f_{is,lowest} + 4 \tag{5}$$

with k Margin associated with small numbers n of tests

The additive margin k in the first equation (5) is given in Tab. 2 for selected intervals of n.

Obviously, the approaches A and B given in EN 13791 [2] for concrete compressive strength (similar to those accepted in EN 206-1 [4] for conformity criteria) differ from a general procedure provided in EN 1990 [3] valid for any material including the compres-

sive concrete strength. The following analysis is focused on a quantitative comparison of both the methods and on prediction of possible differences that might occur in practice.

Tab. 2: The margin k associated with small number of test results n

n	k
10 to 14	5
7 to 9	6
3 to 6	7

The stepwise margins k cause a discontinuity in variation of the strength estimates with the number of test results n.

4 Comparison of EN 13791 and EN 1990

4.1 Approach A

A simple comparison between EN 13791 [2] and EN 1990 [3] follows from equation (1) and the first equation (4) provided that the first equation (4) is decisive. The expected difference $E(\Delta f_{ck,is})$ between the characteristic values given by equation (4) and (1) is simply

$$E(\Delta f_{ck,is}) = (-1.48 + k_n) \times E(s) = (-1.48 + k_n) \times c \times \sigma \qquad (6)$$

Here $E(s)$ denotes the expected sample standard deviation, σ is the standard deviation of population and constant c (denoted in the quality control literature by c_4) is given by WADSWORTH [13] as

$$c = \sqrt{\frac{2}{n-1}} \frac{\Gamma\left(\dfrac{n}{2}\right)}{\Gamma\left(\dfrac{n-1}{2}\right)} \qquad (7)$$

Consider the lowest sample size $n = 15$ of the Approach A in EN 13791 [2]. It follows from Tab. 1 or equation (3) that $k_n = 1.82$ is applied in equation (1). If the standard deviation of a population is $\sigma = 5$ MPa, then the expected difference (6) becomes $E(\Delta f_{ck,is}) = 1.67$ MPa. However, in few cases the second equation (4) is decisive and, consequently, the expected difference slightly decreases, $E(\Delta f_{ck,is}) \approx 1.6$ MPa. This may be easily verified by simulations of test results indicated in Fig. 1.

Fig. 1 shows results of 100 simulations of samples of test results of the size $n = 15$ from a population having the mean 30 MPa and standard deviation 5 MPa (somewhat high coefficient of variation 0,17). It follows that the expected difference $E(\Delta f_{ck,is})$ of the indicated simulation is 1.57 MPa. Note that in two cases (samples number 67 and 73) the character-

istic value predicted using EN 13791 [2] is lower than the corresponding value determined using EN 1990 [2]. In these cases, the second equation (4) leads to the lower value than the first equation (4). It should be mentioned that for the number of tests greater than 15, the difference between the characteristic values $\Delta f_{ck,is}$ slightly decreases.
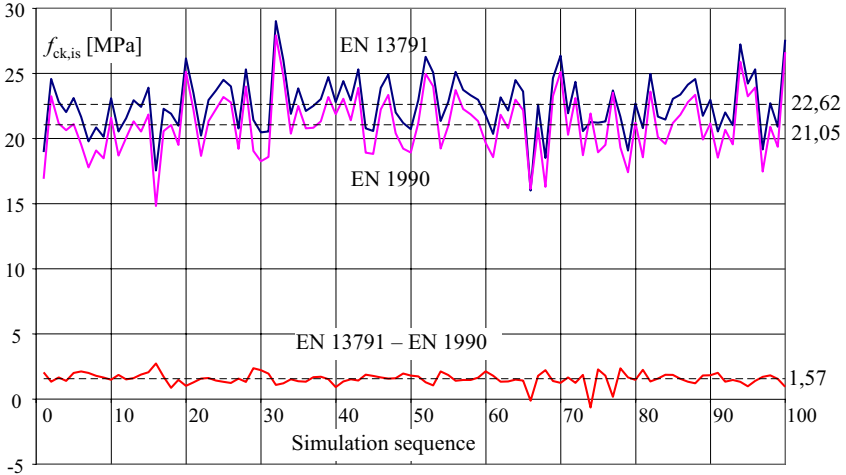

Fig. 1: The characteristic strength $f_{ck,is}$ derived from simulated samples of the size $n = 15$ taken from the population having the mean 30 MPa and standard deviation 5 MPa

4.2   Approach B

Comparison of the approach B of EN 13791 [2] and EN 1990 [3] is based on a simulation technique only. Fig. 2 shows results of 100 simulations of samples of the size $n = 7$ taken from the population of test results having the mean 30 MPa and standard deviation 5 MPa. The expected difference $E(\Delta f_{ck,is})$ is 4.02 MPa as indicated in Fig. 2, thus more than two times greater than for $n = 15$. Note that in several cases (for example sample 6) the characteristic value predicted using EN 13791 [2] is lower than the corresponding value determined using EN 1990 [3].

4.3   Variation of the expected characteristic strength with the number of tests

Variation of the expected characteristic values determined using EN 13791 [2] and EN 1990 [3] with the number of tests (sample size) n is shown in Fig. 3. Simulation of samples having different sizes n (number of simulations from 1 000 up to 10 000 for each n) based on equations (4) and (5) is used in case of EN 13791 [2]. Both simulation technique and analytical approach using directly expressions (1) and (3) are applied in case of EN 1990

[3]. A population of concrete strength having the mean 30 MPa and standard deviation 5 MPa is considered again to illustrate different procedures.
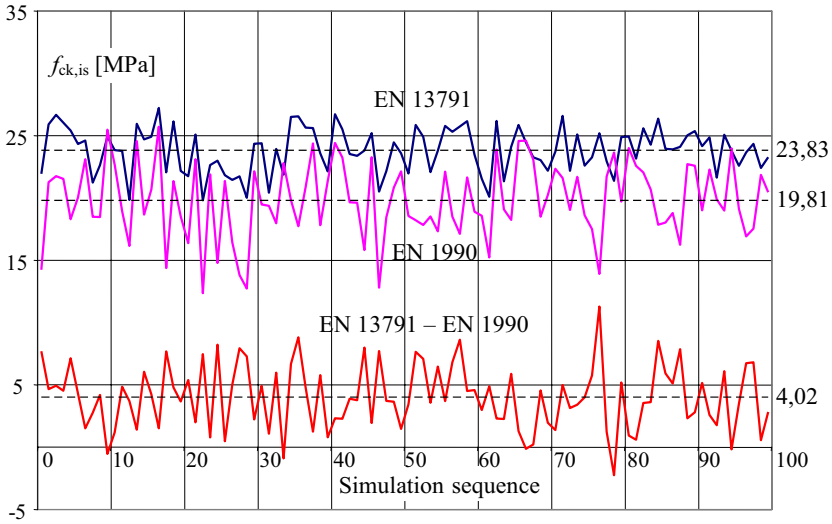

Fig. 2: The characteristic strength $f_{ck,is}$ derived from simulated samples of the size $n = 7$ taken from the population having the mean 30 MPa and standard deviation 5 MPa

It follows from Fig. 3 that the characteristic in-situ strength $f_{ck,is}$ determined using the procedure given in EN 13791 [2] is systematically greater than the corresponding values derived in accordance with EN 1990 [3]. Moreover, $f_{ck,is}$ determined using the procedure given in EN 13791 [2] is even greater than the theoretical 5% fractile of the population shown in Fig. 3 by the dashed line (21.78 MPa is the limit value for an increasing number of test results n).

Fig. 3 also shows the discontinuity of the expected characteristic strength derived in accordance with EN 13791 [2] for $n < 15$. For $n = 14$ the expected difference $E(\Delta f_{ck,is})$ suddenly increases by about 1.5 MPa. This alarming and illogical increase of the characteristic strength is due to the discontinuity of Approach B provided in EN 13791 [2] (as described above by equation (5) in conjunction with the stepwise margins k given in Tab. 2). Note that for very small numbers of test results $n = 3, 4$ and 5, the expected difference $E(\Delta f_{ck,is})$ increases up to almost 8 MPa.

It is interesting to note that Fig. 3 also indicates estimates of the characteristic value (sample 5% fractiles) obtained by the classical coverage method (described e.g. in ISO 12491 [6] and ISO 3207 [9]) assuming the confidence levels 0.75 and 0.90. These estimates are obviously conservative as compared with those obtained by the prediction method accepted in EN 1990 [3]. It also follows from Fig. 3 that the confidence level of the prediction method is about 0.75, however for $n > 5$ decreases below 0.75.
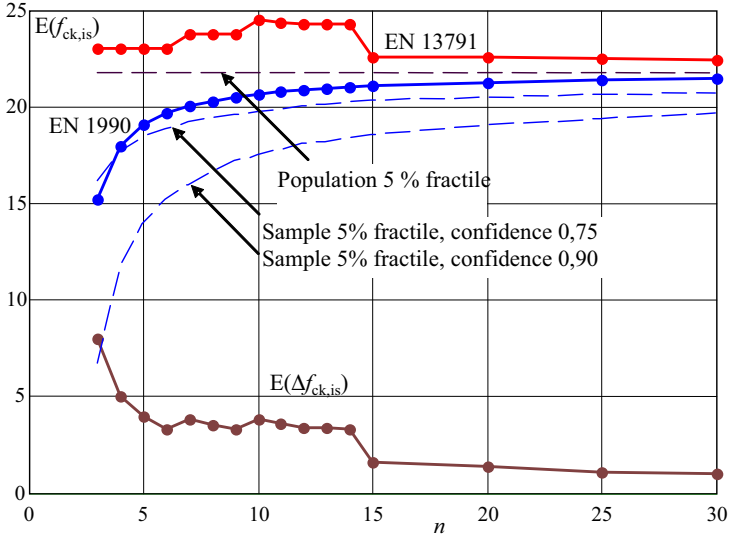
Fig. 3: Variation of the expected characteristic value with number of tests n derived from samples taken from the population having the mean 30 MPa and standard deviation 5 MPa

5 Conclusions

The new European document EN 13791 [2] provides operational rules for estimation of the characteristic compressive strength of concrete that are different from those provided by material independent Eurocode EN 1990 [3]. The following conclusions are drawn from the analysis of the population with the mean 30 MPa and standard deviation 5 MPa.

- The characteristic values determined in accordance with EN 13791 [2] are systematically greater than values based on the procedure given in EN 1990 (for number of tests from 6 up to 14 commonly by 3 MPa).

- The differences between the approaches increase up to 8 MPa with a decreasing number of test results.

- According to EN 13791 [2] the variation of the characteristic values with the number of tests is discontinuous.

- In case of assessment of existing structures, it is recommended to use the procedure given in EN 1990 [3].

- Harmonisation of the procedure given in EN 13791 [2] for determining concrete strength with the statistical technique provided in material independent EN 1990 [3] is desirable.

Literature

[1]   Ang, A.H.S.; Tang, W.H.: *Probabilistic concepts in engineering planning and design*. New York: John Wiley and Sons, 1975.

[2]   EN 13791 Assessment of in-situ compressive strength in structures and precast concrete components. CEN, 2007.

[3]   EN 1990 Eurocode: Basis of structural design. CEN, 2002.

[4]   EN 206-1 Concrete – Part 1: Specification, performance, production and conformity. CEN, 2000.

[5]   Gulvanessian, H.; Holický, M.: *Designers' Handbook to Eurocode 1*. London: Thomas Telford, 1996.

[6]   ISO 12491 Statistical methods for durability control of building materials and components. ISO, 1997.

[7]   ISO 13822 Bases for design of structures – Assessment of existing structures. ISO, 2003.

[8]   ISO 2394 General principles on reliability for structures. ISO, 1998.

[9]   ISO 3207 Statistical interpretation of data – Determination of a statistical tolerance interval. ISO, 1975.

[10]   Probabilistic Model Code, JCSS, 2001.

[11]   Taerwe, L.: The Influence of Autocorrelation on OC-lines of Compliance Criteria for Concrete Strength. *Materials and Structures* 20, 1987, p. 418-427.

[12]   Taerwe, L.: Serial Correlation in Concrete Strength Records, Special Publication ACI SP-104, *Lewis H. Tuthill International Symposium on Concrete and Concrete Construction*, Detroit, 1987, pp. 223-240.

[13]   Wadsworth, H.M. (jr.): *Handbook of statistical methods for engineers and scientists* (2nd ed.), New York: McGraw-Hill, 1998.

Conformity control of concrete
based on the "concrete family" concept

Robby Caspeele & Luc Taerwe

Magnel Laboratory for Concrete Research,
Faculty of Engineering, Department of Structural Engineering,
Ghent University, Belgium

Abstract: This paper describes how the concept of concrete families can be used for the conformity control of concrete strength. The principles of the concept are explained and an original probabilistic evaluation is introduced. A parameter evaluation approach is explained and the guidelines and conformity criteria for concrete families in EN 206-1 are discussed.

1   Introduction

Concrete factories are asked to supply a very wide range of concrete mixes, with different strengths, consistencies, admixtures, aggregate sizes, etc. As a result of this largely differentiated request, a plant does often not produce enough of certain concrete mixes in order to apply the conformity criteria applicable to an individual concrete according to EN 206-1. The family concept allows to obtain a sufficiently high number of strength results and allows a more continuous control of the production process and consequently a more rapid detection of significant changes in quality level.

2   The "concrete family" concept

2.1   Principles

Concretes that can be reliably related to each other can be grouped into families and the combined data from the family can be used for conformity control. As a suitable starting point for a basic family description, the following guidelines are available [6]:

- Cement of one type, strength class and source

- Similar aggregates

- Concretes with or without a water reducing/plasticizing admixture

- Full range of slump classes

- Concretes of a few strength classes

Furthermore, concretes containing a Type II addition (i.e. a pozzolanic or latent hydraulic addition) or a high range of water reducing/superplasticizing, retarding or air entraining admixtures should be put into a separate family or treated as an individual concrete [6].

In order to check whether the concrete production complies with the specified properties, conformity criteria are used. For the application of the family concept, the strength results of the family members are transposed into an equivalent value of a reference concrete, which is most often the member with the highest number of test results or the concrete type closest to the average strength of the family [1]. This larger group of transposed data is then used to check the conformity criteria for the compressive strength.

Theoretically, this procedure leads to a smaller consumer's and producer's risk in comparison to the conformity control of individual family members with less data [8,9,13], because a higher number of test results can be used to perform the conformity control. However, an additional uncertainty is introduced, which is related to the transformation relation between the strength results of family members and the reference concrete.

2.2   Transformation methods

In order to transform the test results of the family members to test results of the reference concrete different transformation methods can be used. In [3] the following methods are mentioned:

- Strength method based on a straight-line relation between strength and W/C ratio

- Strength method based on a proportional effect

- W/C ratio method for transposing data

The last two methods are not frequently used [7]. In the first method the difference in strength between the specified characteristic strength of the family member and each individual strength result is determined and this difference is then applied to the characteristic strength of the reference concrete to obtain the equivalent strength [3]. This yields equation (1), which can be translated into the transformation rule formulated in equation (2).

$$x_i - f_{ck,member} = x_i^* - f_{ck,reference} \qquad (1)$$

$$x_i^* = x_i + \left(f_{ck,reference} - f_{ck,member} \right) \tag{2}$$

with x_i^* the transposed (or equivalent) test result

x_i the original test result of the family member

Some examples of the application of the concrete family concept in practice can be found in [1, 5, 7].

2.3   Advantages and disadvantages of the family concept

By using the family concept, concrete producers are able to check conformity on a higher number of concrete mixtures, which is both in the benefit of the producer and the consumer. The producer can improve the quality of his product and is able to detect changes in his production more rapidly. The consumer, for his part, gets a higher assurance of the quality of the obtained product.

There exists however also a disadvantage in using the family concept. Since the test results of the different family members are combined and tested together, "bad" test results can be masked by "good" test results. This concern is one of the main objections for using the family concept in practice, because it could be used to disguise "bad" production. Currently, the conformity criteria for concrete families in EN 206-1 do not exclude this problem, as will be shown further in this paper.

3   The probability of acceptance and the AOQL concept

3.1   The m-dimensional P_a-function

The specified characteristic strength f_{ck}, used in design and production, corresponds to the 5%-fractile of the theoretical strength distribution of the considered concrete class. In practice, however, the fraction below f_{ck} will be lower or higher than 5%. This fraction is called the fraction defectives $\theta = P[X \leq f_{ck}]$, with X the compressive strength, considered as a random variable. The probability that a concrete lot – characterized by a fraction defectives θ – is accepted with a certain conformity criterion, is called the probability of acceptance P_a. The function $P_a(\theta)$ is called the operating characteristic (OC-curve) of the criterion and allows to visualize the discriminating capacity of the criterion in order to distinguish "good" from "bad" production. In the case of a concrete family consisting of m family members – each characterised by a number of test results n_j, a known specified characteristic strength $f_{ck,j}$ and an unknown fraction defectives θ_j – the probability of acceptance of the complete family becomes a m-dimensional surface $P_a(\theta_1, \theta_2, ..., \theta_m)$.

Let us for example first consider the individual criterion (3).

$$\overline{x_n} \geq f_{ck,ref} + \lambda_0 \sigma \tag{3}$$

With $\quad \overline{x_n} \quad$ the sample mean of the transposed test results

$\lambda_0 \quad$ a parameter

$\sigma \quad$ the standard deviation (supposed to be known)

When the transformation of the test results is performed according to (2) and all family members are supposed to have the same standard deviation $\sigma_1 = \sigma_2 = ... = \sigma_m = \sigma$, it can be shown that the exact probability of acceptance is given by equation (4), assuming a normal strength distribution. This $\tilde{P}_a$ is the probability of acceptance of all (transposed) test values, resulting from the accepted family members and as such, it is a function of the m parameters $\theta_1,...,\theta_m$.

$$\tilde{P}_a(\theta_1, \theta_2,...,\theta_m) = \Phi\left[-\sqrt{n}(\tilde{u}_\theta + \lambda_0)\right] \tag{4}$$

With $\quad n = \sum_{i=1}^{m} n_i$, $u_{\theta,i} = \Phi^{-1}(\theta_i)$ and $\tilde{u}_\theta = \dfrac{\sum_{i=1}^{m} n_i u_{\theta,i}}{n}$

As an example this surface is illustrated in Fig. 1 for a concrete family with 2 members (the reference concrete and 1 other member), a parameter $\lambda = 1.48$ and a test sample consisting of 10 samples for the reference concrete and 5 samples for the transformed family member.
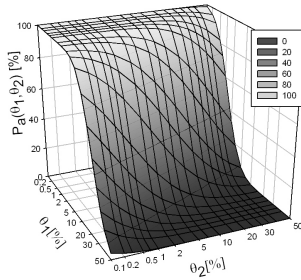

Fig. 1: Example of the probability of acceptance $\tilde{P}_a(\theta_1, \theta_2)$ for a concrete family of 2 members with parameters $n_1 = 10$, $n_2 = 5$ and $\lambda = 1.48$

Let us now consider the case where besides (3) also a criterion of type (5) is used to check each concrete family member individually.

$$\overline{x_{n,i}} \geq f_{ck,i} + \lambda_i \sigma \tag{5}$$

with $\overline{x_{n,i}}$ the sample mean of the original test results of the family member

           λ_i a parameter

           σ the standard deviation (supposed to be known)

The calculation of the global probability of acceptance P_a becomes more complex since criterion (3) is not independent from the criteria of type (5). The exact calculation of P_a is complicated and uses Monte-Carlo simulation techniques. However, when the dependency of the criteria is neglected, a lower bound for P_a can be derived under the same assumptions as mentioned before, which leads to (6).

$$P_a(\theta_1, \theta_2, ..., \theta_m) = \Phi\left[-\sqrt{n}(\tilde{u}_\theta + \lambda_0)\right] \cdot \prod_{i=1}^{m} \Phi\left[-\sqrt{n_i}(u_{\theta,i} + \lambda_i)\right] \tag{6}$$

with $n = \sum_{i=1}^{m} n_i$ and $\tilde{u}_\theta = \dfrac{\sum_{i=1}^{m} n_i u_{\theta,i}}{n}$

This global probability of acceptance is related to the total population, consisting of all potential family members, including those which do not satisfy (5).

3.2   Parameter evaluation based on the AOQL concept

In order to make a parameter selection or evaluation without arbitrary assumptions, the AOQL concept (Average Outgoing Quality Limit) can be used [4,9,10,13]. The limit of the average outgoing quality AOQ of a certain family member is set to 5%, corresponding to the definition of the characteristic strength. If θ_j is the incoming quality of the j-th family member, equation (7) has to be checked for each family member.

$$\forall j \in \{1, ..., m\}: P_a\left(\theta_j | \theta_1, ..., \theta_{j-1}, \theta_{j+1}, .., \theta_m\right) \cdot \theta_j \leq 0.05 \tag{7}$$

Equation (7) formulates that on average, no more than 5% of the population of each family member, that passes the conformity criteria, is lower than the specified characteristic strength of that member.

Based on (7), for each member it thus has to be checked if the conditional probabilities of acceptance $P_a\left(\theta_j | \theta_1, ..., \theta_{j-1}, \theta_{j+1}, .., \theta_m\right)$ remain lower than a boundary curve defined by the AOQL $P_a(\theta_j) \cdot \theta_j = 0.05$, as can be seen in Fig. 3 for $m = 2$. The values of P_a have been obtained by Monte-Carlo simulation as mentioned in section 3.1.

4   Discussion of the EN 206-1 criteria for concrete families

4.1   EN 206-1 criteria

In the current standard EN 206-1, 3 conformity criteria for compressive strength are mentioned for the continuous production control of concrete families. Criterion 1 and 2 are indicated in Tab. 1. Criterion 1 checks the conformity of the group mean (based on the transposed test results), while criterion 2 is a minimum value criterion that needs to be applied on each individual (non-transformed) test result. To confirm that each individual member belongs to the family, the mean of all non-transposed test results for a single family member must be assessed against criterion 3 [2], described in Tab. 2. The derivation of the parameters for criterion 3 can be found in [3], and is based on a 99% confidence interval and an assumed standard deviation $\sigma = 5 MPa$ for the family members.

Tab. 1:   Criterion 1 and 2 for continuous production according to EN 206-1 [2]

Number "n" of test results for compressive strength in the group	Criterion 1 Mean of "n" results (f_{cm}) for the group [N/mm²]	Criterion 2 Any individual test result (f_{ci}) for a single family member [N/mm²]
15	$\geq f_{ck} + 1.48\sigma$	$\geq f_{ck} - 4$

Tab. 2:   Criterion 3 according to EN 206-1 [2]

Number "n" of test results for compressive strength for a single concrete	Criterion 3 Mean of "n" results (f_{cm}) for a single family member [N/mm²]
2	$\geq f_{ck} - 1.0$
3	$\geq f_{ck} + 1.0$
4	$\geq f_{ck} + 2.0$
5	$\geq f_{ck} + 2.5$
6	$\geq f_{ck} + 3.0$

For the application of criterion 1 σ has to be estimated on the basis of at least 35 consecutive transposed strength values taken over a period exceeding three months and which is immediately prior to the production period during which conformity is to be checked [2]. This σ value may be introduced in criterion 1 on condition that the sample standard deviation of the latest 15 transposed results (s_{15}) does not deviate significantly from σ. This is considered to be the case if (8) holds, which is the 95% acceptance interval. If (8) is not satisfied, a new estimate of σ has to be calculated from the last available 35 test results.

$$0.63\,\sigma \leq s_{15} \leq 1.37\,\sigma \tag{8}$$

4.2   Analysis of a concrete family with 2 members

In the case of a concrete family with 2 members – a reference concrete (indicated with '1') and a second member (indicated with '2') – the criteria mentioned in 4.1 can be written in the form of the compound criterion (9).

$$\begin{cases} \overline{x_{15}} \geq f_{ck,ref} + 1,48\sigma \\ \overline{x_{n1}} \geq f_{ck,ref} + k_{2,1} \\ \overline{x_{n2}} \geq f_{ck,2} + k_{2,2} \\ x_{1,min} \geq f_{ck,ref} - 4 \\ x_{2,min} \geq f_{ck,2} - 4 \end{cases} \tag{9}$$

with $k_{2,i}$ according to Tab. 2 with $n = n_i$

σ satisfying equation (8)

Let us first consider a family composed of 10 test results of a reference concrete (with unknown fraction defectives θ_1) and 5 results of the other member (with unknown fraction defectives θ_2). The standard deviation is supposed to be known and $\sigma_1 = \sigma_2 = \sigma = 5MPa$. The OC-surface $P_a(\theta_1,\theta_2)$ is calculated by Monte Carlo simulation and is illustrated in Fig. 2 (a). The conditional probabilities of acceptance $P_a(\theta_1|\theta_2)$ and $P_a(\theta_2|\theta_1)$ are illustrated in Figs. 3 (a) and (b). In these last 2 figures the AOQL is illustrated as 'Boundary 1'. The second boundary is an economic boundary, based on [9,10].

Fig. 3 (a) indicates that the specified quality (based on the AOQL concept) is obtained for the reference concrete. In the case where a member with a high fraction defectives is added to the family, the criteria become uneconomical. For the other family member however, Fig. 3 (b) proves that the specified quality is in some cases not obtained, namely when the quality of the reference concrete is good (with a percentage defectives 5% or lower). This indicates that with the current conformity criteria bad test results can be masked by good test results.

Figs. 2 (b)-(e) visualize the relative probabilities of rejection of the different criteria in (9) for the specified example. This relative probability is the probability that a certain criterion rejects the lot divided by the probability of rejection of the lot, hence

$$\frac{P[\text{criterion rejects the lot}]}{P_r} = \frac{P[\text{criterion rejects the lot}]}{1 - P_a} \tag{10}$$

Criterion 1 rejects the lot in a large range of the domain (θ_1,θ_2). The criteria 3 reject the lot if the assessed family member has a high fraction defectives. Finally, the added value of the criteria 2 to the corresponding criteria 3 is only located in the region of lower fraction defectives of the assessed family member, where it isn't necessary to reject the lot as mentioned in [9, 10, 13] for the conformity control of individual concretes.
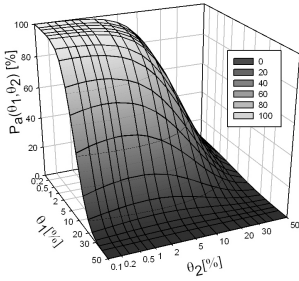
(a) $P_a(\theta_1,\theta_2)$
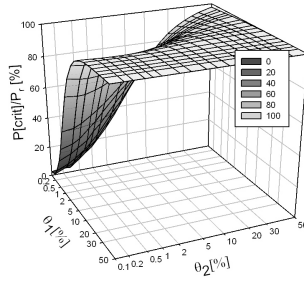
(b) Relative probability of rejection of criterion 1
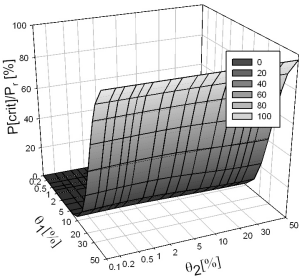
(c) Relative probability of rejection for criterion 3 for the reference concrete
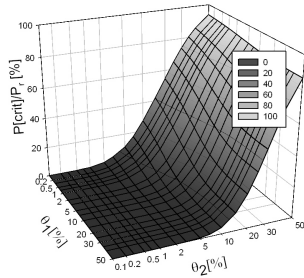
(d) Relative probability of rejection for criterion 3 for the family member
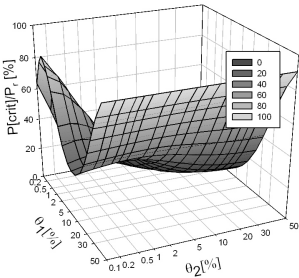
(e) Relative probability of rejection for criterion 2 for the reference concrete.
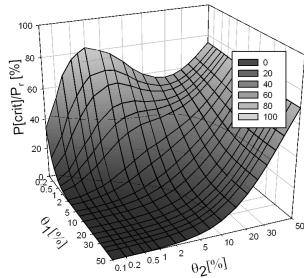
(f) Relative probability of rejection for criterion 2 for the family member

Fig. 2: OC-curve and relative probabilities of rejection according to EN 206-1 for a concrete family with 2 members ($n_1 = 10$, $n_2 = 5$) and $\sigma_1 = \sigma_2 = \sigma = 5 MPa$
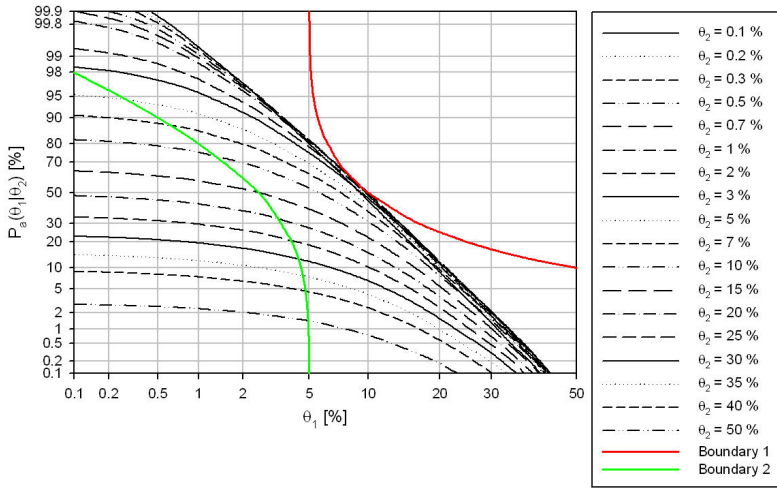
(a) Conditional OC-curves $P_a\left(\theta_1|\theta_2\right)$
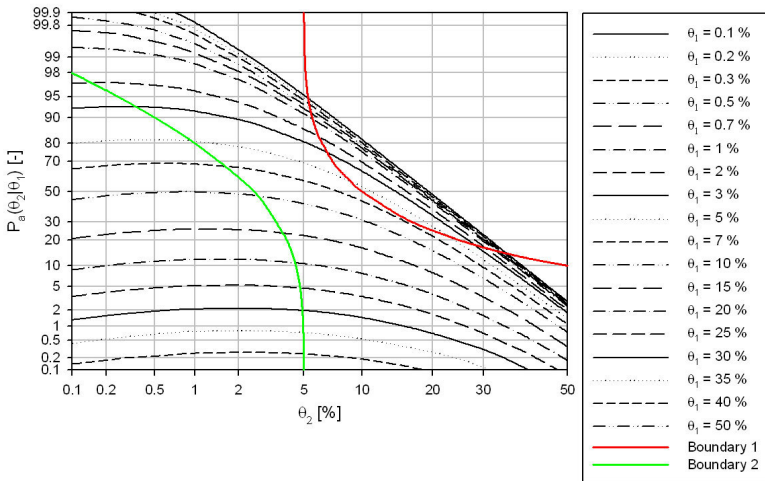
(b) Conditional OC-curves $P_a\left(\theta_2|\theta_1\right)$

Fig. 3: Conditional OC-curves of $P_a\left(\theta_1, \theta_2\right)$, extracted from Fig. 2 (a)

In order to quantify the influence of different family compositions and different assumed standard deviations $\sigma_1 = \sigma_2 = \sigma$, the most negative conditional probability $P_a\left(\theta_2\middle|\theta_1 = 0.1\right)$ is compared for different simulations. Fig. 4 (a) illustrates that for all relevant compositions of a concrete family with 2 members and $n = 15$ the same conclusions apply as drawn from Fig. 3. From Fig. 4 (b) it can be seen that (for the example with $n_1 = 10$ and $n_2 = 5$) the choice of σ has only small influence on the conditional probabilities of Figs. 3 and 4 (a) and the same remarks are valid.

5   Conclusions

The principles, advantages and disadvantages of the use of a "concrete family" concept for the conformity control of concrete strength are explained.

The probabilistic evaluation of the conformity criteria for concrete families, using the AOQL concept, is explained and some theoretical formulae for OC-surfaces are mentioned for some special cases.

The conformity criteria for concrete families in EN 206-1 are explained and analyzed with some Monte Carlo simulations for the special case of a concrete family with 2 members. All these simulations show that the current criteria for concrete families in EN 206-1 do not exclude that "bad" test results mask "good" test results. In order to avoid this hiatus more appropriate parameters must be derived or additional criteria must be presented.

6   Further research and a note on autocorrelation

In the continuation of this research project more appropriate parameters and possibly additional criteria will be proposed. Also the influence of the used transformation method will be investigated and possibly propositions will be made for other transformation methods.

Realistic concrete strength records present an undeniable autocorrelation between consecutive values [11,12]. This can be modelled in Monte Carlo simulations by using an AR(2)-model as selected in [9,11]. For concrete families however, this model does not necessarily hold, because the test results are not always obtained from a continuous production.

7   Acknowledgements
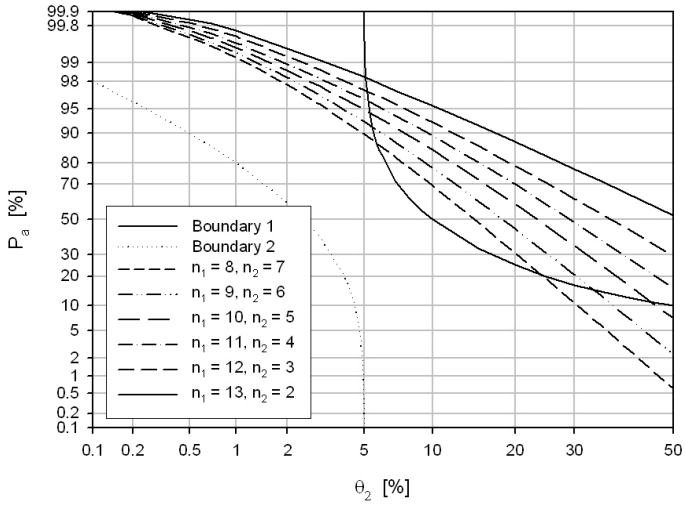
(a) $P_a\left(\theta_2 \middle| \theta_1 = 0.1\right)$ for different compositions of a concrete family with 2 members
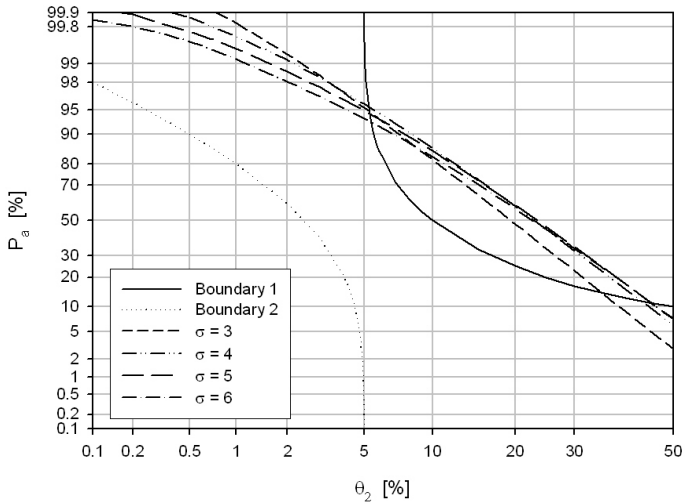
(b) $P_a\left(\theta_2 \middle| \theta_1 = 0.1\right)$ for different σ values

Fig. 4: Conditional OC-curves $P_a\left(\theta_2 \middle| \theta_1 = 0.1\right)$ for different simulations

8 References

[1] Böing, R.; Konformitätskontrolle der Druckfestigkeit nach DIN EN 206-1/DIN 1045-2. *Beton*, 2002, Vol. 6, pp. 306-311.

[2] CEN; Concrete – Part 1 : Specification, performance, production and conformity. *EN-206-1*, 2000.

[3] CEN; The use of the concept of concrete families for the production and conformity control of concrete. *CEN Technical Report*, 2000.

[4] Govindaraju, K.; Single sampling plans for variables indexed by AQL and AOQL. *Journal of Quality Technology*, Vol. 22, No. 4, pp. 310-313.

[5] Grübl, P.; Rühl, M.; Berger, A.; Ratgeber für den Konformitätsnachweis für die Druckfestigkeit von Beton nach DIN EN 206-1 und DIN 1045-2 (Teil 3). *Beton*, 2005, Vol. 3, pp. 100-105.

[6] Harrison, T. A.; The use of concrete families in the control of concrete. *Proceedings International Congress 'Creating with Concrete', 'Utilising Ready-mixed Concrete and Mortar'*, 1999, pp 269-276.

[7] Helm, M.; Zeh, D.; Konformitätskontrolle unter Nutzung des Betonfamilienkonzepts – ein Beispiel für die praktische Umsetzung. *Beton*, 2007, Vol. 5, pp. 210-219.

[8] Taerwe, L.; A general basis for the selection of compliance criteria. *IABSE Proceedings P-102/86*, 1986, pp. 113-127.

[9] Taerwe, L.; Aspects of the stochastic nature of concrete strength including compliance control (in Dutch). *Doctoral thesis*, Ghent University, Ghent, Belgium, 1985.

[10] Taerwe, L.; Evaluation of compound compliance criteria for concrete strength. *Materials and Structures*, 1988, pp. 13-20.

[11] Taerwe, L.; Influence of autocorrelation on OC-lines of compliance criteria for concrete strength. *Materials and Structures*, 1987, Vol. 20, pp. 418-427.

[12] Taerwe, L.; Serial correlation in concrete strength records. *Special Publication ACI SP-104 "Lewis H. Tuthill International Symposium on Concrete and Concrete Construction"*, Detroit, 1987, pp. 223-240.

[13] Taerwe, L.; Caspeele, R.: Conformity control of concrete: some basic aspects. *Proceedings 4th International Probabilistic Symposium*, Berlin, 2006, pp. 57-70.

Construction producer's and user's risks
from a testing uncertainty point of view

Wilfried Hinrichs

Materialprüfanstalt für das Bauwesen Braunschweig (Germany)

Abstract: The uncertainty of test results influences the risks of producers and consumers due to fail and pass errors. In construction the uncertainty of test methods is often considerable. In this contribution the producer's and user's (consumer's) risks have either been estimated on a half-quantitative basis (pressure differential system kits in multi-story buildings according to EN 12101-6) or quantitatively calculated (flatness of floors according to DIN 18202). An important feature of the simulation model used was the implementation of guard bands which generally offer the possibility to influence risks. As a result the application of the two test methods leads to considerable risks both for producers and users as well as for product certification bodies. Consequently, a mere agreement on a test method may not be sufficient in some cases. Statements on conformity with an appropriate product standards is rather uncertain and guard-banding seems not to be a helpful tool for the parties involved in all cases.

1   Introduction

The focus of the author's presentation on the 4TH INTERNATIONAL PROBABILISTIC WORKSHOP [1] was on the estimation of measurement uncertainty and the subsequent use of risk analysis techniques for categorisation and classification purposes. The result was a quantitative approach to probability estimates of 'correct' results predominantly for construction products. Based on these methods described the research has been broadened in two directions:

- A construction product is usually not a final product as such but an element of a final product building. Suppliers of construction products need test results for documentation but users, owners, designers, insuring companies etc. are more interested in the 'product' building. Therefore further effort has been put in arriving at data that are directly applicable for stakeholders. In other words, certification of construction

products is a 'third party' business whereas the quantitative estimation of producer's and user's (owner's etc.) risks address 'first' and 'second' parties.

- It is interesting to note that the EU Commission has identified an acceptance problem with the CONSTRUCTION PRODUCT DIRECTIVE [2]. Some private users, in particular insurance companies, are reluctant with the implemented system which indicates a basic problem of reliability with the regulations. The unknown risks about the validity of statements on certificates may contribute to this phenomenon.

- Statements containing quantitative data on risks are often not fully understood. The significance of such figures may be increased when they are clearer and can be reasonably influenced by the parties involved.

2   First approach to producer's and user's risks

2.1   General remarks

Both the producer and the user (users are often referred to as 'consumers') have to accept risks due to pass and fail errors which are mainly caused by the variability of the product (u_P) and the testing (measurement) uncertainty (u_m). As regards the parameter u_P it can be estimated on the basis of data from former testing of the same product. In some cases u_m-related data are published in test standards.

Quantitative details on the risk of making wrong decisions in compliance assessment which encompass measurement uncertainty are mostly lacking. In the areas investigated neither the test nor the product standards provide any help. This situation is by no means exceptional. In principle, assessment bodies are aware of the problem but it is often hardly possible to address it using reliable figures. An important reason for that is that both clients and other parties involved do not want to be confronted with (avoidable) problems and a certification body would usually not have all necessary information to professionally include the results of a risk analysis in its decision when the clients do not wish to address this subject.

Strictly speaking, in compliance assessment a test result as such does not contain a crucial information for external parties. Relevant for them are statements whether or not a product meets specified requirements. But as all decisions are wrong to a certain degree users of certificates should get an idea on the reliability of a decision. That could be done by a quantitative statement on the probability to what extent a decision may be right or wrong.

The determination of producer's and user's risks is usually done in some consecutive steps. In a first approach one tries to identify the main influences on the parameters. At this stage the components are introduced qualitatively or half-quantitatively. The discussion below on risks in testing pressure differential system kits in multi-story buildings is such a first approach whereas the second example on the flatness of floors is fully quantitative.

2.2   Pressure differential system kits in multi-story buildings

2.2.1   Function

Smoke and heat-exhaust ventilation systems are used to create a smoke-free layer above a floor by removing fire effluents and thus improve the conditions for safe escape and/or rescue of people and animals. They further help to permit a fire to be fought while it is still in its early stages.

Pressure differential system kits are mainly used to protect staircases and floors to be used as escape routes. In fire safety concepts their function is to inhibit the entrance of smoke into such areas by the creation of a slight overpressure in the rooms to be protected.

Provided that both the system works and its design is appropriate the user's risk is that smoke flows into the escape routes due to the uncertainty of statements that are based on tests of the kit (which would be a so-called 'pass error' as referred to in chap. 3.1). The producer's risk is that only due to measurement uncertainty a test may indicate that the system does not meet the requirements after the installation ('fail error').

2.2.2   Test procedures and uncertainty

General sources of uncertainty are the procedures for the inspection of installed kits. According to EN 12101-6 [3] the inspection encompasses five tests:

- **Test 1**: Estimation of the influence of wind outside the building and realisation of a natural chimney effect with the pressure differential system switched off

- **Test 2**: Determination of the effective pressure difference

- **Test 3**: Measurement of the velocity of air flowing through an open door connecting protected and unprotected rooms

- **Test 4**: Measurement of the manual force required to open a door connecting protected and unprotected rooms

- **Test 5**: Testing of the reaction to smoke of the smoke detector

The test procedures are not described in much detail in the standard which obliges the inspection body to work on additional specifications. Table 1 contains some qualitative data on uncertainty components which should have an impact on the results without any statement whether this impact may be significant or not. Sufficient data for a calculation of risks have not been available.

Table 1: Possible influence of testing uncertainty on compliance statements

Test No.	Uncertainty component	Estimation: Significant influence of measurement uncertainty on compliance statement?
1	Period of time after switch-off of the differential pressure system	No. The pressure equalization in buildings is usually very fast.
	Air temperature	No.
	Performance of the test	No.
	Correctness of the pressure gauge	No.
2	Working stability of the pressure system	May be. The impact depends on the pressure variability of the working control system installed.
	Measurement of difference pressures	No.
	Correctness of the pressure gauge	No.
3	Working stability of the pressure system	May be (see 2).
	Measurement of the velocity of air	Yes. The determination of air velocity in openings is a difficult task from a measurement point of view.
	Correctness of the anemometer	May be. The uncertainty of calibration is considerable.
4	Working stability of the pressure system	May be (see 2).
	Performance of the test	No.
	Correctness of the spring balance	No.
5	Density and application of the test smoke	No. The reliability of new smoke detectors is known to be high.

2.2.3 Uncertainty components

Statements on the compliance of an installed pressure differential system kit with EN 12101-6 are assumed to be (possibly) significantly influenced by three parameters:

- the measurement of the velocity of air flowing through a door frame,

- the correctness of the anemometer and

- the working stability of the pressure system.

The standard requires a minimum air velocity of 0.75 m/s … 2.0 m/s depending on the specific situation. The air velocity shall be measured as an average of at least 8 results which have to be taken homogeneously distributed across the open door area. This requirement implies an (almost) evenly distributed air velocity. It is doubtful that this assumption is correct. The air velocity in a door frame due to a small difference in pressure between large rooms is far from being such easily to determine. The velocity – which is usually in the range of about 2 m/s – depends upon the effective pressure difference as well as on the size and the shape of the door. The spread of results measured across the whole area should also be considerable. As the air is pressed from the protected area into a possi-

ble fire zone through a relatively small opening the air flow in the door frame should not or not fully be undisturbed, in spite of the very low velocity. Therefore the often used so-called 'log-Tchebychev' method for ventilation lines or testing channels should not be fully applicable. Even if it were applicable the test prescription does not provide information on the position where to make the measurements in the door frame. In addition the measuring personnel has an influence on the result if the anemometer is manually applied, i.e. with looping or screening across the door frame to get a mean value of the air velocity.

In order to avoid such difficulties in practice, the air velocity in the door frame is often not measured as required but calculated on the basis of the measured pressure difference. However, for this alterative method one has to take into account general estimations on the leakage of the doors with connection to the protected areas, the loss of pressure in the staircase, the reaction time of the ventilator creating the pressure etc. The uncertainty of a calculation thus depends upon the 'quality' of these additional data. In both cases the quantitative outcome of test 3 should not be a sound basis for conformity statements.

Suitable instruments for measurements of low air velocities (2 … 3 m/s) are thermic probes or impellers with large diameters. The precision of thermic probes at low air velocities should be about 0.2 m/s whereas that of an adequate impeller is about 0.3 m/s. In both cases the uncertainty is in the range of 10% of the result.

A further uncertainty component that can be found at different stages of the inspection is the pressure variability of the working system. The standard only specifies that the test has to be performed within 15 minutes after reaching the required testing conditions. The systems mainly influence the difference pressure and the air velocity which means that in a calculation the interdependence of the parameters would have to be considered. Variations in pressure of about 5 Pa at a difference pressure of 50 Pa seem to be an adequate approach.

2.3   Result

To sum up the 'over-all measurement uncertainty of tests' on the basis of EN 12101-6 is estimated to be considerable. The result should strongly depend on the experience of the inspecting personnel. On this basis it can be assumed that there is a relatively large gap between repeated and reproduced test results.

3   Quantitative approach

3.1   General remarks

In general, the calculation of consumer's and producer's risk is in no way news. The basic principles are a well-known method in statistics and explained in detail in many standards. However, the application of these methods for such purposes as the specification of construction products and the use of test data uncertainty for the calculation of risks has rarely

been a scientific topic. General principles are object of recent discussion. A major example is a draft paper of JCGM/WG1/SC3 [4].

Conformance (and conformity) testing do not have only the two outcomes 'yes' (specification has been met) and 'no' (specification has not been met). In decision-making it has to be taken into account that there are four possible results of product tests.

- A product passes because a test result correctly indicates that it conforms with the specification ('yes').

- A product is rejected because a test result correctly indicates that it does not conform with the specification ('no').

- A product is rejected because a test result incorrectly indicates – due to the measurement uncertainty – that it does not conform with the specification ('no, but …'). This 'fail error' is the producer's risk (R_P).

- A product passes because a test result incorrectly indicates – due to the measurement uncertainty – that it conforms with the specification ('yes, but …'). This 'pass error' is the user's risk (R_U).

3.2 Mathematical model

In many cases tolerances are two-sided and a normal distribution of the test results is deemed to be appropriate. However, parameters like flatness have one-sided tolerances and the choice of a normal distribution would cause a situation in which (impossible) test results $x < 0$ mm could significantly contribute to the final result. Therefore the calculations are based on a gamma distribution

$$g(x;a,b) = \left(\frac{b^a}{\Gamma(a)} \cdot x^{a-1} \cdot e^{-bx} \right) \qquad (1)$$

$$\Gamma(a) = \int_0^\infty x^{a-1} \cdot e^{-x} \cdot dx \qquad (2)$$

with
a parameter of the distribution
b parameter of the distribution
x test result

The quantification of the parameters a and b of the distribution requires a detailed knowledge on both appropriate expectation values and their variances. This is a major task in the preparation of an applicable model. Provided a gamma distribution the formulae for the producer's and the user's risks run as follows:

$$R_P = g(x;a,b) \cdot \int_0^T \left[1 - \Phi\left(\frac{G-x}{u_m} \right) \right] \cdot dx \tag{3}$$

$$R_U = g(x;a,b) \cdot \int_T^\infty \left[\Phi\left(\frac{G-x}{u_m} \right) \right] \cdot dx \tag{4}$$

with

R_P	producer's risk
R_U	user's risk
T	tolerance limit
u_m	associated measurement uncertainty
G	guard band
x	measurement value

The formulae 3 and 4 differ from those proposed in [4, formula B.65]. From the author's point of view the preconditions for two-sided tolerances cannot not be transferred unchanged to one-sided applications. Both a *lower* tolerance limit and, consequently, a *lower* guard band limit are not merely zero, they do not exist and must therefore be deleted. It can easily be shown that an application of the formula given in the JCGM/WG1/SC3-document, would lead to implausible results: The producer's and the user's risks would increase with expectation values smaller half of the tolerance limit, which would imply higher risks with increasingly good products. As shown below the deletion of the term for the lower tolerance limit does not produce such strange results. However, this modification has a significant influence on the results. As a consequence the validity of the numerical example for the one-sided tolerance in [4] becomes questionable (R_P = 0.089 or 0.076, respectively), if the author's assumption is correct.

Remark: The approach of the draft guide to use a gamma function to estimate the distribution of measurement results is reasonable because the introduction of impossible negative measurement values is being avoided. But, strictly speaking, the use of a normal distribution for the calculation of the risks is not fully plausible on this background. It is therefore important to take the remark into consideration that the approach becomes less reliable when the expectation value is close to zero. A deeper look into possible solutions in such a situation is not done in this contribution. Here a binomial distribution could be appropriate.

4   Flatness of floors

4.1   Test procedures

The flatness or evenness of floors is a basic requirement which necessary 'degree' strongly depends upon the intended use. It is obvious that requirements for unfinished upper surfaces and concrete bases are less stringent than those for finished floors. An example for a normative document with tolerances for the flatness of floors in buildings is DIN 18202 [5]. As this standard does not specify a test method, the parties involved have to agree on the test procedure. Prevalent methods are described by HINRICHS [6]:

- Straight-edge and V head (here referred to as 'test A')

- Grid levelling / area levelling ('test B')

- Continuous profile analysis ('test C')

4.2 Testing uncertainty

The application of different testing principles usually causes problems with the reproduci-bility of test results. Small numbers of test results is another important matter as the stan-dard deviations are far from being statistically reliable. Beforehand it is therefore very likely that the uncertainty of test results is not negligible when reference is made to DIN 18202. This is a reason for additional explanations in branch-specific test procedures and for detailed comments [7].

An investigation has shown that the main influences on the uncertainty are the floor itself as the object of measurement, the number of measured distances per square unit, the test method applied, the measuring conditions and the skill of the personnel. The quantified estimates in table 2 are valid for favourable measurement conditions. 'Favourable' means good practice, not best measurement capability.

According to DIN 18202 the flatness in a single test is determined as the maximum devia-tion from a horizontal line of a defined length (test A and C) or as the distance of a position from a reference plane in a virtual grid (test B). The tolerances depend on the length L of the 'horizontal line' or the mesh of the grid respectively ($L \geq 0.1$ m). The German term 'Grenzwert' (limiting value) indicates that no single result is allowed to be larger than an upper tolerance for a specific purpose (finished or unfinished floor, regular or restricted requirements).

In order to arrive at some exemplary data the lengths L_1 (1 m), L_2 (4 m) and L_3 (10 m) have been chosen for which the tolerances $T_1 = 4$ mm, $T_2 = 10$ mm and $T_3 = 12$ mm are given for floors ready for use.

Table 2: Uncertainty data of test results with different lengths L of the 'horizontal lines'

Test procedure	u_m in mm		
Straight-edge and V head (test A)	$L_1 = 1$ m	$L_2 = 4$ m	$L_3 = 10$ m
	0.9	1.1	2.0
Optical levelling (test B)	1.0		
Continuous profile analysis (test C)	0.5		

4.3   Specification of the mathematic model

A general problem with DIN 18202 is the requirement that no single result is allowed to be larger than the tolerance. As it is impossible to test 100% of the floor's surface such a requirement is difficult to deal with from a statistical point of view. The 'detection' of a single or very few non-conforming spots out of an unlimited number of spots is a question of probability. In this contribution it is therefore assumed that the probability of conformity must be high or very high ($p_C \geq 0.950$).

The quantification of the parameters a and b of the gamma distribution requires a statement on the variability (u_P) of the flatness of floors[1]. It is important to highlight that the term u_P depends upon several factors such as the material (concrete, polymer modified cementitious levelling screeds, laminate etc.), the working conditions, the workers experience and skill and so on. Test results always contain the uncertainty of both test procedure and surface variations. In order to arrive at reliable results it is important not to 'double-count' uncertainty components. Taking these considerations into account an estimate for $u_P = 1.0$ mm seems to be reasonable for sophisticated applications, and $u_P = 2.0$ mm for all other finished surfaces.

With the assumption of a given probability of conformity p_C the calculation of risks becomes a second step. As p_C is a function of the variability of the floor ($p_C = f(u_P)$) but not a function of the measurement uncertainty ($p_C \neq f(u_m)$) a preparatory step for the risk calculations aims at identifying possible combinations of T and u_P. The results are listed in table 3 for five tolerances T according to DIN 18202, the two chosen variability factors u_P and three probability levels of conformity $p_C \geq 0.95$. The figures for the expectation values are the mean values of the distributions in mm. Combinations of T, u_P and p_C with no result are not possible.

Table 3: Calculation of the expectations for the identification of possible combinations of T, u_P and p_C (in brackets: percentages of the expectations of the tolerances T)

		$p_C = 0.9990$	$p_C = 0.990$	$p_C = 0.950$
$T = 2$ mm	$u_P = 1.0$ mm	-	-	-
	$u_P = 2.0$ mm	-	-	-
$T = 4$ mm	$u_P = 1.0$ mm	-	-	2.13 (53 %)
	$u_P = 2.0$ mm	-	-	-
$T = 10$ mm	$u_P = 1.0$ mm	6.45 (64.5 %)	7.48 (74.8 %)	8.29 (82.9 %)
	$u_P = 2.0$ mm	-	4.00 (40.0 %)	6.40 (64.0 %)
$T = 12$ mm	$u_P = 1.0$ mm	8.57 (71.4 %)	9.52 (79.3 %)	10.30 (85.8 %)
	$u_P = 2.0$ mm	-	6.47 (53.9 %)	8.46 (70.5 %)
$T = 15$ mm	$u_P = 1.0$ mm	11.67 (77.8 %)	12.56 (83.7 %)	13.32 (88.8 %)
	$u_P = 2.0$ mm	7.20 (48.0 %)	9.75 (65.0 %)	11.53 (76.9 %)

It becomes clear that the statistical basis of the requirements according to DIN 18202 for finished floors seems not to be fully adequate. Unspecified test procedures can only be

---

[1] u_P is the variance $Var(x)$ of the expectation $E(x)$ of the gamma distribution.

applied for tolerances $T \geq 4$ mm. For floors with an increased u_P the procedure is only useful for tolerances $T \geq 8$ mm.

Calculations of the producer's (R_P) and the user's risk (R_U) have been carried out for some of the possible combinations according to table 3 with $G = 0$. The chosen measurement results are all well below the tolerances in consideration. It is therefore not surprising that the producer's risks are all higher than those of the users.

4.4   Results

Results are presented in the following figures. In the Figures 1 and 2 the producer's and the user's risks are plotted against the variability of the floor flatness as the variable at different testing uncertainties for a situation where the probability of conformity is large. It is not surprising that the risk increases with increasing both flatness variability and testing uncertainty. The variability of the floor flatness is less important for the producer's risk than the testing uncertainty. In contrast to that the user's risk sharply increase with larger variability of the floor. As in the scenario chosen the producer's risks are mostly significantly larger than the user's one. However, producers should generally be interested in using precise procedures, especially in cases where the expectation value is estimated to be more than half the tolerance. With no knowledge about the variability of a floor the user's primary risk is when a reference value is agreed. For example, with $E(x) = 7,48$ mm, $T = 10$ mm and $u_m = 2,0$ mm the factor R_U sharply increases from 0.4 % to 3.3 % for $u_P = 1.0$ or $u_P = 2.0$ respectively.

The influence of the testing uncertainty is more prominent for the producer's risk but at low levels of u_m the differences become smaller. With lower probability of conformity p_C the absolute values of the particular risk increase significantly but the general statements above remain valid.

For contingency reasons the four fractions of a particular conformity statement sum up to 100 % (see chap. 3.1). Of course, the particular percentages of the fractions vary with increasing variability of the floor flatness as shown in Figure 3. The plot makes clear that the testing uncertainty plays an important role as at a low degree of variability it creates a considerable fail error.
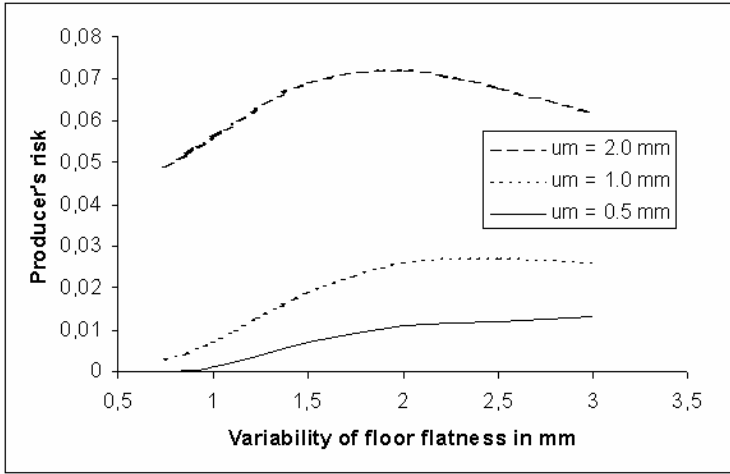
Figure 1: Producer's risk as a function of the variability u_P of flatness and of the testing uncertainty u_m [$x = 6{,}45$ mm ($p_C = 0.999$ at $u_P = 1$ mm) and $T = 10$ mm]
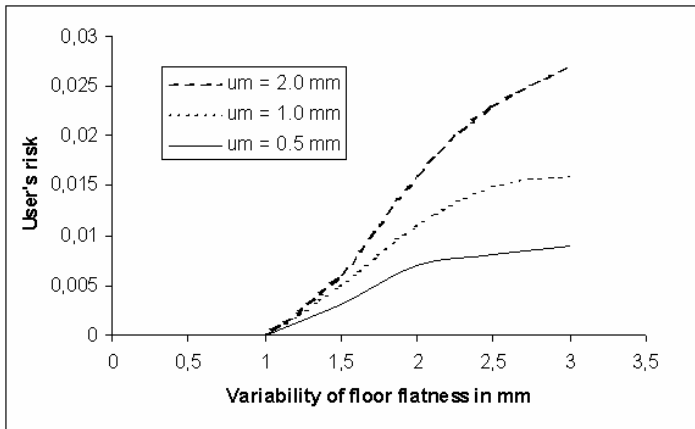

Figure 2: User's risk as a function of the variability u_P of flatness and testing uncertainty u_m [$x = 6{,}45$ mm ($p_C = 0.999$ at $u_P = 1$ mm) and $T = 10$ mm]
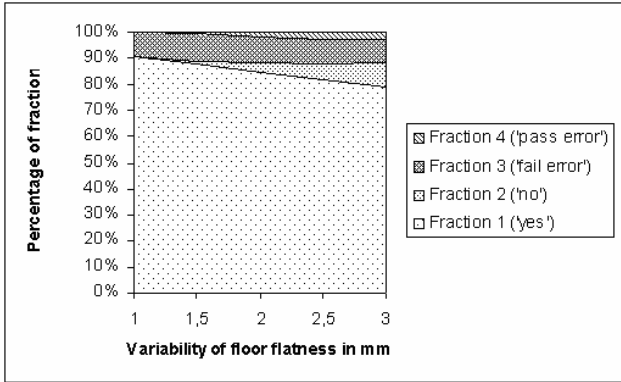
Figure 3: The contingency for the four possible outcomes as a function of the variability u_P of the flatness with $u_m = 1.0$ mm [$x = 6,45$ mm and $T = 10$ mm]

The particular risks can be influenced by the setting guard-bands according to the formulae 3 and 4. A positive factor G reduces the user's, a negative one the producer's risk. With $p_C \neq f(u_m)$ the setting of a guard band only influences the parameter R_P and R_U, i.e. the fractions 3 and 4 (see Figure 3). With

$$G = T - 2 \cdot h \cdot u_m \qquad (5)$$

with
T tolerance
h guard band multiplier
u_m measurement uncertainty

the influence of guard band setting can be studied. An example with a fix $R_U = 1$ % is shown in Figure 4. The R_P-curve shows clearly that a producer can influence his risks considerably.

5   Discussion

The investigation has produced results at two levels: 1. data usable for producers, users and conformity assessment bodies (level testing) and 2. information on the reliability of test procedures as prescribed in two test standards (level standards).

1. If reference has to be made to EN 12101-6 or DIN 18202 respectively, on the one hand the user of the standard should try to gather additional information both on the object of testing and on the test procedure. On the other hand the applicant of the standard should try to define the testing situation as clear as possible in order to reduce risks or to increase the reliability of statements on conformity.
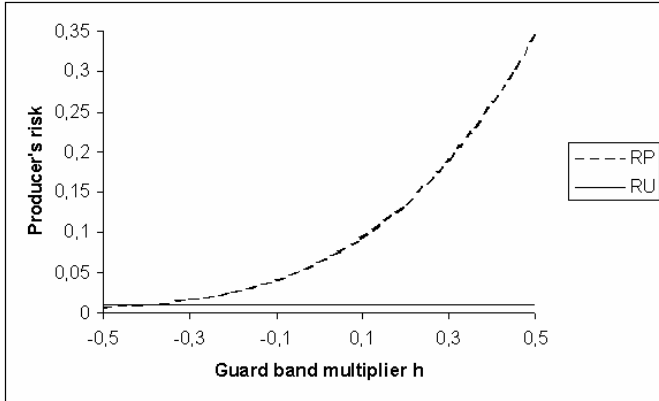
Figure 4: Producer's risk as a function of the guard band multiplier h with $u_m = 1.0$ mm, $u_P = 1.0$ mm, $T = 10$ mm and $R_U = 1$ %

2a. It seems to be doubtful that test procedures as given in EN 12101-6 are a reliable basis for subsequent conformity statements.

2b. The applicability of DIN 18202 procedure for the flatness of floors is limited. It has become apparent that, strictly speaking, the standard is no good basis for testing from different points of view:

- the required statement on the uncertainty of the test is too difficult a task for most testing personnel without detailed further instructions

- tolerances $T \leq 4$ mm (or even $T \leq 8$ mm) are not suitable for the given test procedure

- the conformity procedure is statistically not appropriate

When imprecise test procedures are used for the specification of products the application of safe-guard limits in production cannot be a satisfying tool to influence the particular risks. Primarily the test precision should be increased, if possible.

6   Acknowledgement

7   Literature

[1] HINRICHS, W.; *Measurement uncertainty and risk analysis – examples from civil engineering products*; PROSKE, D.; MEHDIANPOUR, M.; GUCMA, L. [Eds.]; 4th International Probabilistic Workshop, 12-13 October 2006, Berlin, 265-278

[2] *Construction Product Directive* (89/106/EEC); OJ No. L40, 11.02.1989, 12

[3] EN 12101-6:2005; *Specification for pressure differential systems, Kits*

[4] JCGM/WG1/SC3: *Measurement Uncertainty and Conformance Testing: Risk Analysis*; Draft 2; October 2003

[5] DIN 18202:2005: *Tolerances in building construction – Buildings*

[6] HINRICHS, W.; *Flatness – a Risk Analysis of Test Methods*; Proceedings 6th International Colloquium Industrial Floors '07, 16-18 January 2007, Esslingen, 723-729

[7] ERTL, R.; *Toleranzen im Hochbau. Kommentar zur DIN 18202*; Cologne 2006

On the Integration of Equality Considerations into the Life Quality Index Concept for Managing Disaster Risk

Timm Pliefke & Udo Peil

Institute of Steel Structures, Technical University of Braunschweig, Braunschweig, Germany

Abstract: Decisions about investments into public disaster risk mitigation projects are to be made in presence of many other investments a society could possibly perform. In order to derive a statement about the advantageousness of a particular disaster risk reduction initiative in comparison to other potential investments, the cost of the intervention has to be put in relation to the expected benefits that go in line with it. The question if the benefits outweigh the cost entails a transformation of the primary non monetary benefits due to disaster risk reduction into monetary units, where especially the valuation of reduced mortality risk can be conveniently assessed by applying the net benefit criterion derived from the life quality index (*LQI*). But as public risk reduction interventions usually involve a great variety of affected people, cost effectiveness is only one determinant in declaring a project as being socially beneficial. Only if the concept is widened to also account for the distributional consequences, i.e. the identification of winners and losers from the intervention, it can be guaranteed that a great number of individuals profit from the enhanced safety standards. This paper addresses this issue by extending the conventional net benefit criterion to also incorporating distributional effects in the decision process and demanding an equally distributed share of cost and benefits throughout society. Thus, in a welfare economic sense more comprehensive risk reduction acceptance criteria are derived.

1   Introduction

The term risk describes a potential adverse event that might endanger an existing valuable element over a certain time horizon and can be calculated by taking the product of probability of occurrence over a predefined time period and the expected consequences that go in line with it. In this context, risk mitigation defines one strategy of risk management that subsumes all activities to reduce the severity of consequences in case the adverse event

occurs. In this very general formulated pattern, the management of natural disaster risk has to be clearly separated from risk management throughout other application areas. This distinction has to be made due to two main motives:

1. Firstly, the occurrence of a natural disaster leads to a great variety of consequences that might occur over a comparatively long period of time. A major natural disaster can result in serious damage to buildings and infrastructure, in injuries and loss of life, in pollution and devastation of the environment, the loss of cultural, social and historical values and in various other harms to the affected region. In this respect, it differs from many other risks like for instance risks existing in financial markets as a large part of the consequences can not directly be measured in monetary terms, i.e. are characterized by the loss of intangible values.

2. Secondly, the happening of a natural disaster has an impact on a large number of people that are dissimilarly exposed and thus, have to bear the consequences to different extends. In the case of financial risks on the contrary, one single investor or institution has to face the adverse effects of the unexpected volatility of performance himself or by equal shares respectively.

Consequently, when it comes to appraise disaster risk reduction interventions in societal interest, one immediate challenge is induced by the monetary evaluation of intangible values. Only if this can be done comprehensively, the risk reduction investment can be related to other investments a society can possibly perform. By comparing the mone-tarized benefits of the intervention with the entailed cost, statements about the efficient allocation of money can be derived and it can be reassured that the invested money could not have been spent more efficiently elsewhere. On basis of social indicators that are designed to reflect the most important societal concerns as well as their relative contribution to social well-being, a social willingness to pay for certain intangible values can be estimated and included in the cost benefit analysis. In this respect the *LQI* has recently received growing attention as a social indicator to evaluate reductions in mortality risk.

The second concern that has to be addressed in the societal risk mitigation process is the fact that public risk reduction efforts usually alleviate the consequences of natural disasters quite unevenly. Whereas some subgroups of the total endangered population might derive large advantages in terms of increased safety from the intervention, other fractions of the population might only be forced to bear the burden of the cost without profiting to large extends. For this reason a reflective analysis about the distributional effects of risk reduction interventions must be included in a profound decision making process.

2   The LQI in public risk management

How should a nation, a region or a community, exposed to the impact of a natural catastrophe and facing uncertainty over future conditions, decide whether to invest in a risk reduction program? From an economic point of view most people would agree to judge on the effectiveness of such an intervention by applying one simple rule. Firstly, the expected stream of expenditures over time that is necessary to implement the project is calculated

and discounted back to the present time by including proper time preferences of money. Secondly, the expected stream of benefits the project might generate over time is estimated and transferred back to the decision point. Finally, if the difference between discounted benefits and cost, the net present value, is positive, the project is declared as being beneficial and advice is given to perform the intervention. While the cost that go in line with a disaster mitigation project, such as reinforcing building codes or the construction of a dike, can usually be estimated with some accuracy, the benefits are highly uncertain and entail a great variety of incommensurable gains. The latter are compounded of benefits that can directly be expressed in monetary units, such as reduced damage to buildings and infrastructure elements, and intangible benefits such as loss of life, environmental devastation and the destruction of cultural social and historical values such as hospitals, schools and churches. Only if these values can be assessed and reasonably be transformed into monetary units a meaningful analysis of cost effectiveness can be performed. Especially with focus on the evaluation of mortality risks, in recent years several compound social indicators have been developed to indicate the ability of nations to provide the resources for mastering extreme events according to their social development status. Relying on these indicators, the arbitrary determination of safety standards can be overcome by setting a clear rationale what is necessary and affordable by a society to spend into risk mitigation.

2.1 Life Quality Index

One of these social indicators that is especially designed to support managing risks to life is the LQI introduced by NATHWANI et al. [9]. Based on the assumption that a long and healthy life with high income and a great fraction of leisure time to enjoy life are among the most important human concerns, the *LQI* has been presented as a function of the GDP per capita g adjusted for purchasing power parity, the life expectancy at birth e, and the fraction of lifetime devoted to work w. Based on a life time model of consumption as well as a chain of mathematical derivations, relying on some reasonable assumptions that can best be reviewed in PANDEY at al. [12], the *LQI* has been extracted to have the following functional form:

(1) $\quad LQI = g^{\frac{w}{1-w}}e \quad$ or more conveniently $\quad LQI = g^q e, \quad q = \dfrac{w}{1-w}$

The LQI is to be interpreted as an anonymous individual's utility function deriving its life quality to unequal parts from longevity and consumption. Furthermore, the *LQI* constitutes an ordinal utility function, indicating that the actual value of life quality has no significance, different bundles of consumption and longevity are merely put into a preference ordering. Without going deeper into the mathematical derivations, it has to be emphasised at this point that the labour leisure trade-off principle, i.e. the assumption that people on average maximize their life quality with respect to working time, is implicit in the *LQI* equation. Thus, w is a stationary variable for the considered social economy and can not be varied. Consequently, in order to judge on the effectiveness of risk reduction efforts, it has to be analyzed, how changes in life expectancy e due to the increased safety level and changes in the GDP per capita g due to the implementation cost of the intervention influence the *LQI*, as is demonstrated in section 2.3. Finally, a conclusion must be drawn

whether this change is desirable and in compliance with welfare economic theory, that is discussed briefly in the following.

2.2   Welfare Economics

Welfare economics is a subfield of modern economic theory that is concerned with capturing and maximizing the overall social welfare of a society by examining the economic activities of the individuals that comprise society. It assumes that the individual is the basic unit of measurement and provides the best judges of its own welfare. The welfare or the level of satisfaction each individual derives from a certain bundle of goods is specified in terms of utility functions that need to be aggregated on societal level to define the overall welfare or utilitarian state of a society. In this sense welfare economics is devoted to fulfil two major objectives:

1. Economic Efficiency:

The first aim is to allocate societies scarce resources most efficiently in order to supply the maximum achievable wealth and prosperity for a society as a whole. To determine whether an activity is driving society towards efficiency is usually assessed by the PARETO criterion PARETO [14] or more practicable by the KALDOR-HICKS compensation tests KALDOR [6] HICKS [5] or potential Pareto improvements which are essentially identical to cost benefit analysis. Questions of economic efficiency are nowadays almost exclusively assessed on basis of ordinal utility theory and can be looked upon as a largely positive science, i.e. efficiency judgements can be made objectively, without relying on subjective personal allocation attitudes.

2. Income Distribution:

The second goal in contrast, is assigned to the task to select this solution among all Pareto efficient allocations which is most desirable for society from a distributional point of view. Income distributional considerations usually entail normative value judgements which have to be included in the construction of a social welfare function. The primary purpose of the latter is to integrate PARETO optimal allocations on basis of individual utilities into a full societal preference order and so to determine the most desirable solution.

According to the second fundamental theorem of welfare economics DEBREU [2], the two sub disciplines can be separated and need not involve a trade-off. Consequently, any statement about the advantageousness of an investment into risk reduction has to be tested for compliance with the demands of each of the two welfare economic sub disciplines.

2.3   Risk management in public interest

When judging on risk reduction interventions that have an impact on human safety on basis of the *LQI*, it is obvious that the two scarce resources that have to be allocated efficiently and distributed equally among the members of society are given through the money available for consumption represented through GDP per capita and life expectancy at birth,

standing for longevity in good health. As already mentioned above, the life working fraction w instead, is assumed to be held fixed according to the assumption that people on average maximize their life quality with respect to working time. So, to formalize the effect of risk reduction a three step distinction is introduced:
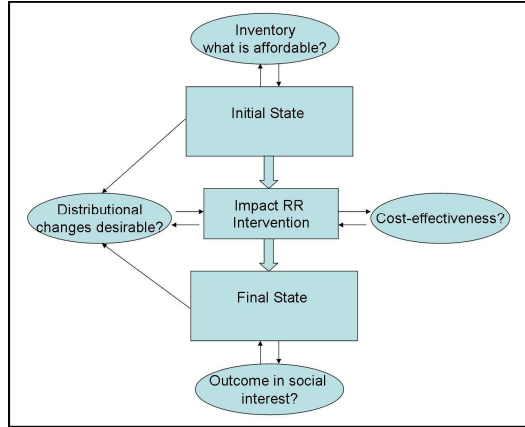

Fig. 1: 3 step division for risk reduction in public interest

1. Initial State:

represents the initial absolute level of money available for consumption and longevity in society as well as its distribution among the members of society before performing a risk reduction intervention. $LQI_{initial}$ represents the initial level of life quality accordingly. The determination of these initial values is to be seen as an assessment of inventory values in order to determine a societies capacity to allocate resources into risk reduction. .

2. Impact of risk reduction initiative:

Any risk reduction project that is performed on behalf of society has an impact on the absolute level and the distribution of the two scarce resources. Firstly, an expenditure is necessary in order to implement the intervention, which is to be expressed in terms of reduced money available for consumption $-dg$ and secondly, the enhanced safety level that goes in line leads to an increase in life expectancy $+de$. Moreover, as the gainers and the losers of the intervention are usually not identical, changes in the distribution are imposed as well.

3. Final State

defines the resulting level of money available for consumption and life expectancy on absolute levels as well as an alternation in distribution of the two goods after having performed the risk reduction intervention. LQI_{final} represents the final level of life quality respectively. Finally, by comparing the final to the initial distribution of goods, the distributional consequences of the intervention can be assessed.

Figure 1 provides a schematic overview of the public risk management process, following this three step division. To conclude, the approval of a risk reduction intervention in societal sense entails the investigation under which conditions the final state is more desirable than the initial state from a welfare economic point of view.

Conventionally, this investigation is carried out by taking the so called net benefit criterion into account. This criterion takes notice of the fact that the *LQI* is an ordinal utility function and requires that LQI_{final} is greater than or at least equal to $LQI_{initial}$ for a risk reduction intervention to be performed. In this sense it is analyzed by the criterion, how marginal changes in consumption together with marginal changes in life expectancy influence the *LQI* by taking the total differential into consideration:

$$(2) \qquad \frac{dLQI}{LQI} = \frac{\partial LQI}{\partial g} dg + \frac{\partial LQI}{\partial e} de = \frac{dg}{g} + \frac{1}{q}\frac{de}{e} \geq 0 \longleftrightarrow LQI_{final} \geq LQI_{initial}$$

According to this equation, any change from the initial to the final state is socially beneficial, that involves a cost satisfying the following requirement:

$$(3) \qquad -dg \leq \frac{1}{q} g \frac{de}{e}$$

As the LQI is designed for the evaluation of reductions in mortality risk only, it should be emphasised at this point that the cost that is used in this formula, is the net expenditure into human safety, i.e. the expected benefits that result from reduced damage to buildings and infrastructure, environment and cultural, social and historical values are already subtracted from the total project cost to calculate *dg*. Substituting the inequality sign in equation (3) through an equality sign, the change in the cost represents exactly the change that is necessary to remain on the same indifference curve given a predefined change in life expectancy and is called the social willingness to pay. With this willingness to pay it is possible to transfer the benefits of a risk reduction intervention in terms of prolonged life expectancy into monetary units and relate these monetarized benefits to the entailed cost. If the benefits are higher than the involved cost, the price for safety is judged to be below the societal threshold level and contributes to a more efficient allocation of resources. Thus, the criterion given in (3) is essentially analogous to conventional cost benefit analysis and therefore in accordance with the potential Pareto improvement criterion as well as the requirements of the first sub-discipline of welfare economics.

2.4 Shortcomings of the concept

The ease with which the net benefit criterion (3) can be used comes at the price of one major shortcoming when it is applied without caution to judge on the effectiveness of public disaster risk reduction expenditures. The net benefit criterion does not allow for the incorporation of distributional effects of the risk reduction investments. In particular this is due to two main motives:

1. The first reason for this is that the LQI is based on average values only, which signifies that it can only be seen if the population as a whole derives a gain from the intervention on

average, without identifying the actual winners and losers from the project. Thus, if a small group of individuals derives a large gain in terms of prolonged life expectancy for a relatively moderate decrease in income and on the other hand the great majority of the population only pays for the intervention without profiting from the benefits to large extents, the net benefit criterion will give advice to perform the action as long as the average benefits outweigh the average costs. But this certainly would be not be contributing to social welfare. By applying the net benefit criterion, the problem of public decision making is reduced to a decision problem of only one affected person, the average individual of society. Since societal risk reduction expenditures or investment decisions entail a broad variety of effected people, the efficiency requirement will clearly not be sufficient to derive a statement if the invested money is spent in public interest.

2. The second reason why it is difficult to incorporate distributional effects in the decision process is that the *LQI* constitutes an ordinal utility function. This signifies that even if it were possible to identify all winners and losers from a risk reduction intervention, the gains and losses could not be meaningfully quantified in terms of life quality and in addition they could not be compared interpersonally. Thus, it could only be said that a particular group of individuals derives a higher or a lower life quality utility from the new distribution of resources in terms of a preference ranking. According to ARROWS impossibility theorem ARROW [1], a social welfare function that is able to integrate different Pareto optimal solutions in a social preference ordering and at the same time fulfils several reasonable requirements cannot be constructed without relying on interpersonal comparable and fully measurable individual utility functions.

3   Measuring multidimensional inequality

In order extend the LQI concept by incorporating inequality considerations, it is necessary to first answer two major questions that were posed by SEN [15] addressing this problematic:

1. Inequality of what?

2. What is inequality?

Traditional welfare economic concepts that are concerned with distributional consequences of societal decisions are mainly restricted to the analysis of the distribution of income or the distribution of individual utilities directly derived from income. In the area of income distribution measurement a great number of analytical tools, measures as well as methods have been designed to compare distributions, some of which are widely accepted in scientific community SEN [15], LOVE et al. [7], NYGARD et al. [10]. But with the management of risk based on the *LQI*, the traditional definitions of well-being have been extended to have two dimensions, i.e. income and longevity, and therefore require also an extension of the existing techniques to measure inequality or, if necessary, the design of new ones. Consequently, the answers to the above stated questions is that the two attributes income and longevity are taken into account for the inequality consideration and a statement about the

degree of inequality is determined by the specialisation of an multidimensional inequality measure.

3.1   Mathematical framework

In the following a population or society consisting of n individuals or groups of individuals that are endowed with k attributes is considered. The set $N=\{1,...,n\}$ defines the set of individuals or groups of individuals and, to maintain generality, $K=\{1,...,k\}$ defines the set of attributes, which is given by the GDP per capita and life expectancy at birth in the particular case. Moreover, $M(n,k)$ is written for the set of all possible multidimensional distribution $n \times k$-matrices $X=(x_{i,j})$ of attributes j to individuals i. Furthermore, $x_{i,j}$ represents the individual i's share of attribute j, and x_i denotes the row vector of attributes for the i-th individual. The k-th column vector defines the distribution of attribute k among the individuals. Then, a multidimensional measure of inequality is given through

(4) $I(X):M(N,K)\rightarrow\Re$,

i.e. a continuous realvalued function summarising the information about a given distribution. Like in the univariate case, inevitably each mutivariate inequality measure I is required to satisfy a series of properties together with some majorization criteria, that can be reviewed in Lugo [8] and Diez [3].

In general, there are two different ways of aggregating the information of the distribution in a real valued number:

1. Two-stage inequality indices

In the first stage of this approach, a single composite measure $U_i(x_i):\Re^k\rightarrow\Re$ for each individual or group of individuals i is developed that indicates the utility the individual derives from the attributes it possesses. In the second stage, a simple conventional univariate inequality measure $I_{\dim1}(U):\Re^n\rightarrow\Re$ is applied to analyze the distribution of the individual utilities.

2. One-step inequality indices

The one-step approaches in contrast have the valuation function of all the attributes implicit in the definition of the inequality measure.

To conclude, in each of the two strategies the weighting structure $(w_1,...w_k)$, i.e. the extend to which dimension each attribute is contributing to an individuals wellbeing, the degree of substitution β_{km} , $k, m=1,...k$, between each pair of attributes and the degree of inequality aversion α have to be determined to finally construct the multidimensional inequality measure.

3.2   Quality Adjusted Income

At this point it is discussed how the quality adjusted income approach introduced by PANDEY et al. [13] fits in the above introduced terminology of multidimensional inequality measures and how it can be used to incorporate inequality considerations in the decision process. The quality adjusted income is a cardinal construct that integrates income inequality and inequality in life expectancy into one scale by using the *LQI* and therefore accounts for a wider range of socio economic inequality across various population segments. Its application to inequality measurement is analogous to the above introduced two-stage inequality measures methodology.

To calculate the quality adjusted income, first of all the whole population is subdivided into *n* population classes which contain exactly the same number of individuals each. Subsequently, the individuals are classified into the population classes depending on their personal income. Consequently, if $g_1,...,g_n$ and $e_1,...,e_n$ represent the average incomes and the average life expectancies in each population class *k=1,...,n* respectively, the above introduced *nx2* distribution matrix of attributes to individuals is fully characterized. Furthermore, $g_1 \le g_2 \le ... \le g_n$ is valid and the life quality indexes for each class can be calculated to be

(5) $LQI_k = g_k^q e_k, \ \ k = 1,...,n$

The average LQI across all population segments is identical to the conventional LQI of the entire society and is given through

(6) $L = g^q e$, with $g = \frac{1}{n}\sum_{k=1}^{n} g_k$ and $e = \frac{1}{n}\sum_{k=1}^{n} e_k$

If it is assumed that perfect socio economic equality implies a constant value of LQI across all the population classes, i.e. $LQI_k = LQI, k=1,...,n$, then it will be possible to quantify the income equivalent δ_k of the differences in life quality LQI_k-LQI an individual of population class *k* experiences on average resulting from differences in life expectancy. For population class *k* this can be obtained by solving the following chain of equations for δ_k :

(7) $(g + \delta_k)^q e_k = g^q e = LQI$

$\Leftrightarrow \delta_k = g(\frac{e}{e_k})^{\frac{1}{q}} - g$

It is straightforward that this term δ_k is positive for all population classes that have a life expectancy e_k that is below the average life expectancy *e* throughout the society. To finally calculate the quality adjusted income, the actual income of each population segment is adjusted by the monetarized inequalities that result from differences in segment life expectancy to societal life expectancy as follows

(8) $g_{QAI\ k} = g_k - \delta_k$ for all population classes $k=1,...,n.$

Obviously, the calculation of the quality adjusted income for each group of individuals is analogous to defining the individual utility functions U_i that indicated the individual level of satisfaction with the assignment of attributes that has been introduced in the description of the two-stage inequality measure calculation. Consequently, the quality adjusted income combines differences in income and in life expectancy into one number, that is cardinally measurable and fully interpersonal comparable. Accordingly, a proper univariate inequality measure can be applied to measure the quality adjusted income inequalities throughout the predefined groups of individuals. This inequality measure is eventually taken into account to measure the quality adjusted income inequality before and after the risk reduction project in order to net out the distributional effects of the intervention and to evaluate whether it contributes to more equality in distribution of the two attributes throughout society.

Without further specifying the problematic of choosing the right inequality measure that is most suitable to be integrated into the concept, three distinctive approaches to include inequality considerations in the *LQI* concept have been developed and are introduced in the following. To facilitate the presentation, all the approaches are illustrated on basis of the Gini coefficient inequality measure applied to the quality adjusted income, which can be shown to fulfil the stated requirements for multidimensional inequality measures. Nevertheless, any other suitable multidimensional inequality measure could have been used instead.

4   Incorporation of inequality considerations in the decision process

As already stated above, the inclusion of inequality in longevity and consumption into the decision process of risk reduction on basis of the *LQI* constitutes a fairly normative issue, as some people will argue that inequality is highly important while others will be convinced of the opposite. For this reason, it is important in the development of extended risk reduction acceptance criteria to be explicit and open about the relative weights assigned to the two considered components of well-being rather then leaving them implicit and hidden OSBERG et al. [11]. Furthermore, leaving sufficient space for problem specific modifications as well as for the decision-makers personal attitudes towards inequality should be inherent in the problem formulation. In economic literature it is generally distinguished between two characteristics of inequality. On the one hand, there is inequality in opportunity that reflects factors that lie beyond a persons control and characterize the circumstances under which people are living, i.e. access to educational system, heath care etc. On the other hand, there is inequality of outcomes that result from factors that individuals can be judged upon to be responsible for, i.e. personal diligence, working moral etc. As most people would agree, the first source of inequality is not morally acceptable, whereas inequality resulting from differences in efforts need not to be corrected. In the authors' opinion, inequalities resulting from public risk reduction interventions can clearly be classified into the first category of economic inequalities considering that an exposure to natural dis-

aster risk is without doubt an involuntary issue that determines the circumstances people are living in. From this point of view, a maximum amount of equality in providing safety to population, with a great number of people sharing those standards should be aspired. In the following, three conceptually different approaches of integrating inequality considerations into the *LQI* concept are presented and pros and cons in application are discussed.

4.1   Derivation of a new index of life quality

The first way to include inequality considerations into the LQI concept is based on the idea, that not only a long healthy life with high income on average define life quality in a society but also the distribution of those two goods, with a great number of individuals sharing those standards is significant. This assumption goes in line with the fundamentals of happiness economics, a recently emerging field that is concerned with the determination of attributes from which people derive their well-being. One of the major findings within this research area is the so called EASTERLIN paradox (EASTERLIN [4]), which states that peoples happiness rises with income to a certain threshold level but not significantly beyond it. If the basic needs are met, relative rather than absolute levels of income matter to well-being as people tend to "look over their shoulders", which can be captured by the analysis of the distribution functions. Thus, a modified newly developed social indicator, the so called equality adjusted life quality index (*EALQI*), is supposed to best go in line with this way of thinking and has the following form:

(9) $EALQI = LQI \times \alpha(1\text{-}Gini(QAI))$

In this equation α represents a parameter to adjust the relative importance of distributional equality throughout the society. When applying the net benefit criterion derived from *EALQI* to judge on risk reduction interventions and requiring that

(10) $EALQI_{final} \geq EALQI_{initial}$

the efficiency and the distributional part are judged upon simultaneously. Furthermore, this approach is not compulsory in the sense that it also lets interventions pass that do not necessarily lead to an increased equality in distribution as long as the benefits strongly outweigh the cost. And also the reverse situation is possible. If the risk reduction initiative has strongly equality supportive consequences, even slightly ineffective risk reduction interventions will pass the test. In this context, the parameter α must be calibrated very carefully as it strongly influences the trade-off between efficiency and equality.

When distributional aspects are incorporated in this way, the trade-off between consumption and longevity is not influenced because only a multiplicative factor is added to the original *LQI* formula. Nevertheless, when relying on *EALQI* only, the contributions of efficiency and equality to the new level of equality adjusted life quality are blurred as it is not directly possible to retrace whether the more efficient allocation or distribution of the goods is responsible for the increase. Furthermore, as the inclusion of distributional aspects clearly represents a normative concern, i.e. it is strongly dependent on the political attitude of the decision-maker, the pure adjustment of the parameter α might not leave sufficient

flexibility to address this issue. Finally, the question remains to which extend efficiency and equality should be traded off against each other, if this is reasonably possible at all.

4.2   Addition of an extra constraint beside the net benefit criterion

The second possible way to include distributional considerations in the risk management process on basis of the LQI is to attach an additional equality constraint to the net benefit criterion. This further constraint could be:

$$(11) \qquad Gini_{initial}(QAI) - Gini_{final}(QAI) \geq a$$

Extending the concept in this way, the efficiency and the distributional sub disciplines of welfare economics are judged upon separately. As the criterion only lets interventions pass which are at the same time efficient and contribute to more equality in distribution at a minimum threshold level ($a \geq 0$) or alternatively do not increase inequality over a certain amount ($a < 0$), it is being referred to as the compulsory equality approach. It can easily been seen that the parameter a is somehow an inequality aversion parameter, i.e. the higher its value is set, the more strict are the requirements with respect to distribution. Efficiency and distribution are considered to be non substitutive and to a certain extend both mandatory for approving a safety regulation in societal sense. Moreover, the effects of the risk reduction intervention with respect to efficiency and distribution of the goods are not accumulated in one number, but can clearly be seen and treated separately. Consequently, it is not necessary to define a trade-off between equity and efficiency. Furthermore, incorporating an additional constraint leaves more space to include individual attitudes towards equality.

As first two introduced approaches have in common to simply evaluate if the risk reduction intervention is efficient and contributes to equality to a certain extend, the approach to be discussed next makes explicitly use of the second welfare economic theorem and considers efficiency and equality as two different fields to interact.

4.3   The two step procedure

In this approach the two welfare economic sub-disciplines are explicitly treated separately and in addition the term compensation payment is introduced. Figure 2 provides an schematic overview of the method's workflow:
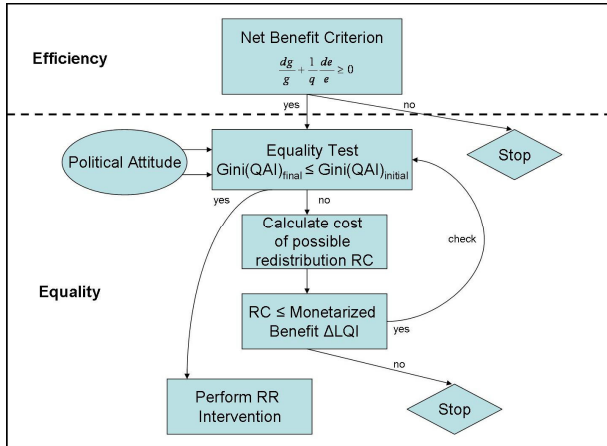
Fig. 2: The two step procedure

The two step procedure starts with checking if the risk reduction intervention is efficient in terms of positive net benefit by taking the conventional net benefit criterion into account. If it is not, no further evaluation is necessary because the evaluated risk reduction intervention is life consuming and the invested money could be spend more efficiently into safety elsewhere. If the net benefit criterion is met, the approach proceeds with an equality test, where the distributional consequences are analyzed. This equality test is to be specified with respect to the political attitudes of the decision maker towards distribution and could be for instance the comparison of the Gini coefficients of the quality adjusted income before and after the intervention. Should the intervention pass also this second test, it is approved in social sense and should be performed. Otherwise, it is analyzed in the next step how the two attributes could be redistributed to compensate the losers for their losses while the winners still should have some benefit left over. This certainly comes at a certain additional cost. If the redistribution cost is lower than the monetarized average benefits of the risk reduction intervention, the equality test is being performed once again to check for the distributional admissibility of the project after the compensation. If the test is passed this time, the project is to be implemented, if not a distinct way of compensation that meets the cost restriction of the redistribution has to be found. These steps are executed until either an admissible redistribution has been found and the project is declared as efficient as well as distributionally desirable or rejected, if the cost of all possible compensations efforts will exceed the montarized benefits of the project.

Judging on a risk reduction project on basis of the illustrated two step procedure has several advantages. The first one might be seen in the fact that the consequences of the risk reduction project can clearly be split with respect to efficiency and equality. Furthermore, the decision maker leaves his passive role behind and is required not only to check if the efficient investment meets the stated equality requirement but is challenged to widen his horizon for possibilities of compensation. Finally, the procedure leaves sufficient space for the specialisation of political attitudes with respect to distribution.

5   Conclusion

In this article the problematic of public disaster mitigation investments is illustrated. By characterizing a public investment to be in social interest when the expenditure is both cost efficient and guarantees a homogeneous distribution of cost an benefits to a certain extend, it is demonstrated, that the sole application of the net benefit criterion, derived from the *LQI*, is insufficient to approve a public risk reduction project as being beneficial for society. This is due to the fact that the *LQI* is based on average values only and moreover doesn't allow for interpersonal utility comparisons. After it has been clearly outlined that inequality considerations based on the *LQI* ought to have two dimensions, the basic framework of multidimensional inequality measurement is provided and it is demonstrated how the quality adjusted income can be used to construct a two stage inequality measure. Leaving adequate space for problem specific modifications, three different approaches to integrate inequality aspects in the *LQI* framework are eventually presented and their pros and cons are discussed. The rather general formulation of the three approaches is to be specified especially with respect to the relative importance to assign to inequality relative to effectiveness. Furthermore, it has to be investigated if other existing multidimensional inequality measures will be better suited to be incorporated in the analysis. In order to finally be able to draw a conclusion about the advantageousness of one approach in comparison to another, the performances of the approaches have to be tested on basis of microsimulation techniques and real world data.

6   Literature

[1]   Arrow, K.J.; *Social Choice and Individual Values*, Wiley, New York, 1951

[2]   Debreu, G.: *Valuation Equilibrium and Pareto Optimum*. Porceedings of National Academics of Science 40, 1954

[3]   Diez, H.: Unit-Consistent Aggregative Multidimensional Inequality Measures: A Characterization. Society for the Study of Economic Inequality, Working Paper 66, 2007

[4]   Easterlin, R.: Does Economic Growth Improve the Human Lot. Nations and Households in Economic Growth: Essays in Honor of Moses Abramovitz, New York Academic Press, Inc., N.Y., USA 1974

[5]   Hicks, J.: *Value and Capital*, Clarendon Oxford, 1939

[6]   Kaldor, N.: Welfare Propositions of Economics and Interpersonal Comparisons of Utility. Economic Journal 49, 549-552, 1939

[7]   Love, R.; Wolfson, M.C.: *Income Inequality: Statistical methodology and Canadian illustrations*, Statistics Canada Cataloguo No.13-559, 1986

[8] Lugo, M.A.: *Comparing Multidimensional Indices of Inequality: Methods and Application*. Society for the Study of Economic Inequality, Working Paper 14, 2005

[9] Nathwani, J. S.; Lind, N.C.; Pandey, M.D.: *Affordable Safety by Choice: The Life Quality Method*. Institute of Risk Research, University of Waterloo, Ontario, Canada, 1997

[10] Nygard, F.; Sandstrom, A.: *Measuring Income Inequality*, Almqvist & Wiksell International, Sweden, 1981

[11] Osberg, L.; Sharpe, A.: *Human and Economic Well Being: What Values are Implicit in Current Indices?* Conference Proceedings WIDER Conference on Inequality, Poverty and Human Well-being, Helsinki 2003

[12] Pandey, M.D.; Nathwani, J.S.: *Life quality index for the estimation of societal willingness to pay for safety*. Structural Safety, 26, 181-199, Elsevier Science, 2004

[13] Pandey, M.D.; Nathwani, J.S.: *Measurement of Socio-Economic Inequality Using the Life Quality Index*. Social Indicators Research 39: 187-202, Kluwer Academic Publishers, 1997

[14] Pareto, V.: *Manuel d'economic politique*, Girard, Paris, 1904

[15] Sen, A.: *On Economic Inequality*. Oxford University Press, Oxford 1973

A Standardized Methodology for Managing Disaster Risk – An Attempt to Remove Ambiguity

T. Pliefke [1], S.T. Sperbeck[2], M. Urban[3], U. Peil[4] & H. Budelmann[5]

[1] International Graduate College 802 "Risk Management on the Built Environment",
Institute of Steel Structures, TU Braunschweig, Braunschweig, Germany

[2] International Graduate College 802 "Risk Management on the Built Environment",
Institute of Building Materials, Concrete Structures and Fire Protection, TU Braunschweig,
Braunschweig, Germany

[3] German Research Foundation, Bonn, Germany

[4] Institute of Steel Structures, TU Braunschweig, Braunschweig, Germany

[5] Institute of Building Materials, Concrete Structures and Fire Protection,
TU Braunschweig, Braunschweig, Germany

Abstract: A major natural disaster can result in serious damage to buildings and infrastructure, in loss of life and in various other harms to the affected region. Earthquakes, floods, storms as well as their immediate aftermaths such as fires are among the most disruptive natural disasters that occurred worldwide in the last century. Even though the miscellaneous catastrophes are very different in nature and imply various impacts on the affected surrounding area, the general approach to assess, compare and treat disaster risk is quite similar. It is best done on basis of a probabilistic risk management framework that is developed and discussed in detail in this article. With respect to the many different definitions of disaster risk and an inhomogeneous understanding of the risk defining terms in literature, this paper is a contribution to create a unified language as a basis for communication among stakeholders.

1 Introduction

The application of risk management throughout several disciplines and for various perils has led to the development of a great diversity of risk management definitions and methods within the scientific community. Areas of application include finance, medical science, insurance industry, mechanical engineering as well as disaster management. Even within the latter so far no consistency in the risk management terminology has been achieved as the miscellaneous catastrophes, such as earthquakes, storms or floods are very different in nature and cause various harms to the affected region. The many existing definitions for similar principles within the risk management processes often result in confusion. Espe-

cially when it comes to interdisciplinary co-operations, an inhomogeneous understanding of basal terms might impose problems in communication. Moreover, different definitions as well as ways to estimate and evaluate risk frequently lead to results, which are not comparable as the underlying range of consequences that is included in the calculation is quite uneven. Therefore, costly risk studies often do not provide sufficient assistance to decision makers and accordingly, huge mistakes can be made. As a result, a unified methodology to define and to calculate risk throughout various disciplines is indispensable for a rational quantification, comparison, and treating of risks. Only in this way an effective expenditure of societies resources into risk reduction can be guaranteed and thus, an adequate safety level obtained.

This article is a contribution to approach these tasks. It provides reasonable definitions and a standardized language for communicating and managing risk among stakeholders. To do this in a justifiable manner, firstly risk definitions and concepts existing in literature are reviewed and out of these, classes of risk calculation schemes are extracted. Subsequently, an exhaustive risk management concept is presented that covers the whole risk management chain, starting from risk identification over risk assessment up to risk treatment. The discussion of the risk management workflow is accompanied by delineating the repeatedly occurring basal risk terms and illustrating their interrelations graphically. Eventually, the risk calculation schemes are integrated in the concept and their advantageousness with respect to different application fields are discussed.

2 Definitions of disaster risk – A literature review

The analysis and management of natural disaster risk is a highly multidisciplinary field of research. It involves the work of natural scientists to determine the hazard characteristic parameters such as probability of occurrence and intensity of an event for a special location, followed by a profound engineering analysis about the building structure and infrastructural responses due to natural disaster loads. Moreover, investigations of economists are need to estimate the monetary consequences of the damages and harms to the affected region, resulting in a political discussion about how to handle the peril in order to guarantee an adequate safety level for society. This necessity to consider disaster management from the perspective of a great variety of sciences has led to the development of various quantitative as well as qualitative approaches towards disaster management. Each field is trying to cultivate their own understanding of disaster related terms. As a result, communication within the disaster management community is often accompanied by misunderstandings and confusion due to colliding definitions and concepts. Therefore, an homogeneous understanding of disaster management is crucial for an efficient coordination of the important sub-steps and collaboration throughout the various disciplines. Due to this problematic an extensive literature review has been performed. In the following, exemplary definitions of risk are provided to demonstrate the wide range of definitions existing in literature.

- "The risk is associated with flood disaster for any region is a *product of both the region's exposure to the hazard (natural event) and the vulnerability* of objects (so-

ciety) to the hazard. It suggests that three main factors contribute to a region's flood disaster risk: *hazard, exposure and vulnerability*." HORI et al. [9]

- "Risk is the *product of hazard* (H) *and vulnerability* (V) as they affect a *series of elements* (E) comprising the population, properties, economic activities, public services, and so on, *under the threat* of disaster in a given area" ALEXANDER [1]

- "The *probability of harmful consequences*, or *expected loss* of lives, people injured, property, livelihoods, economic activity disrupted (or environment damaged) resulting from interactions between natural and human induced hazards and vulnerable conditions. Risk is conventionally expressed by the equation: *Risk = Hazard x Vulnerability*." UNDP [13]

- "Risk is the *probability of an event multiplied by the consequences* if the event occurs." EINSTEIN [4]

- "A combination of the *probability or frequency of occurrence of a defined hazard and the magnitude of the consequences* of the occurrence. More specific, a risk is defined as the probability of harmful consequences, or expected loss (of lives, people, injured, property, livelihoods, economic activity disrupted or environment damaged) resulting from interactions between natural or human induced hazards." Europ. Spatial Planning Observ. Netw. [5]

- "Risk is an expression or *possible loss* over a specific period of time or number of operational cycles. It may be indicated by the *probability of an accident times the damage* in dollars, lives, or operating units." HAMMER [8]

Out of these citations basically five widespread classes of definitions of disaster risks can be extracted and are categorized subsequently:

1. risk = hazard × vulnerability × exposure

2. risk = hazard × vulnerability

3. risk = probability × consequences

4. risk = probability × loss

5. risk = probability × damage

These risk formulae as well as the exemplary verbal definitions make clear that the different understanding of the term risk is mainly due to the diverse meanings of the terms hazard, vulnerability, exposure, damage and loss. Obviously, the definition boundaries are blurred and intersecting between the understandings of the authors. Therefore, there is the need to clearly clarify what is understood by each term. Furthermore, it is evident throughout the definitions that no clear formula is used to define the risk. Whereas some authors define risk as a product of several terms, others even avoid any mathematical deepness by simply arguing that risk is a function of several terms. This observation has also been made THYWISSEN [12] that even goes a step further in arguing "Risk is seen as a function of haz-

ard, vulnerability, exposure and resilience, while the mathematical relationship between the variables is unknown". In this sense also the above collected risk formulae (1)-(5) are not to be understood too mathematically, but more illustrative to show the composition of disaster risk. The only clear mathematical formula to quantify risk that is known by the authors is the PEER equation for earthquake risk that is provided in BAKER et al [3]. In the next section a fully developed disaster management methodology is presented that clearly outlines the important sub-steps of risk management and supplies unambiguous definitions of the risk defining terms. After this has been illustrated, the theoretical background is sufficient to demonstrate, how the above listed definitions interrelate and can be included in the framework.

3   Proposed risk management framework

The proposed risk management framework that is presented in this section has been developed in close correlation to Pliefke [10] and is structured in compliance with AS/NZS 4360 [2] that define a risk management process as the:

"Systematic application of policies, procedures and practices to the task of identifying, analysing, evaluating, treating and monitoring risk."
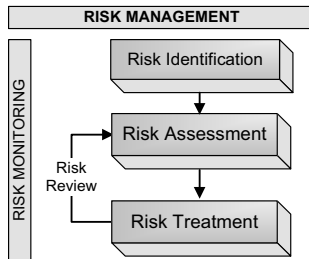
Fig. 1: The concept of risk management in first order subdivision

As illustrated in Fig. 1 the three main components are risk identification, risk assessment and risk treatment and are performed sequentially throughout the risk management process, accompanied by a risk review step and continuous risk monitoring. The risk review process is assigned to the task to constantly include all new information, knowledge and experience about the risk and to indicate it's evolution within the process over time. Thus, the risk is updated on a regular basis. It should be emphasised that the risk review process is only performed for risks that have already run through the whole process at least once. Consequently, in each risk review iteration the effectiveness of possibly implemented risk reduction interventions is indicated. The risk monitoring procedure in contrast, captures the exchange of information of all persons actively or passively involved or participating in the risk management process. This exchange of information is necessary to guarantee a good collaboration between interdisciplinary researchers and to discover new hazards due to the ever changing environment.

3.1   Risk identification

The prerequisite for performing the risk identification phase and therefore to initiate the operation of the risk management chain is the condition of being aware of a dangerous situation. If this is met, first of all the boundaries of the model domain have to be circumscribed by defining the system under analysis. The system can be composed of a single building or infrastructure element, a city, a region or even a whole country. Next, all sources of events that are able to endanger the functionality of the system have to be identified and are characterized by the term hazard. Thus, the risk identification step leads to an answer to the question "what can happen and where?" As soon as this analysis is completed for a particular location, it is proceeded with the risk assessment phase.

3.2   Risk Assessment

After having outlined the model domain and identified all possible hazards to the system, the risk assessment phase starts to operate, representing the first crucial step of the risk management framework. The risk assessment itself consists of two sub-procedures, the risk analysis and the risk evaluation module, whose tasks are to be seen in quantifying the risk and comparing it to other competing risks, respectively.

3.2.1   Risk analysis

The risk analysis procedure (depicted in Fig. 2) represents the most sophisticated part of the risk assessment phase, whose major objective lies in the quantification of the risk defining parameters and finally the risk itself, most desirably in monetary units per time unit (i.e. \$/year). In order to reach this ambition, first of all a hazard analysis is being performed where the intensity and frequency parameters of each identified hazard type with respect to the predefined system are estimated. Once the hazard data are quantified, it has to be analysed, which components of the system are exposed, i.e. potentially endangered by the
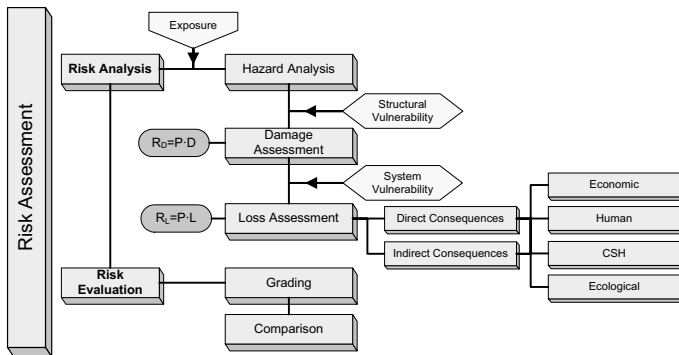
Fig. 2: The risk assessment phase

impact of the hazard. In this way, a subdivision of the system into elements at risk (EaR) and elements at non risk (EaNR) is performed, depending on the hazard under consideration. As the EaNR by definition are not exposed, they are not threatened by the hazard and can therefore be excluded from the further analysis. An EaR on the contrary, represents a building or an other arbitrary infrastructure element that is characterized by several parameters that have to be determined. Among these are precise location parameters within the system, information about the functional use (residential, commercial, industrial), occupancy (inventory of contents, number of people living or working inside) and construction type (building material, number of stories, construction year). A detailed discussion about the EaR parameters is provided in GROSSI et al. [7]. Furthermore, to facilitate the analysis, EaR with similar characteristics can be grouped together into EaR classes, depending on the hazard under consideration. Then, the further analysis can concentrate on one typical representant out of each EaR class, assuming that all other EaR of the same category will show similar behaviour. After all the EaR (classes) have been identified and clearly delineated, the structural behaviour of each EaR (class) has to be predicted depending on the hazard load. The damage module of an EaR is strongly dependent on the structural response of the EaR and captures the physical harm only. It is expressed by a large variety of measures, e.g. water height, crack width, story drift, which are used to derive damage states. It has to be clearly emphasised that damage is not measured in monetary values. The relation between the hazard intensity and the resulting damage is called structural vulnerability. Thus, the structural vulnerability is an EaR (class) specific characteristic that indicates the degree of physical susceptibility towards the impact of the hazard. After the structural behaviour of all EaR (classes) has been predicted, the consequences for the system that might go in line with a given level of damage of the exposed elements have to be analysed. For this investigation the characteristic parameters of each EaR (class) have to be taken into account. It is distinguished between direct consequences, that occur simultaneously to the time the disaster takes place and indirect consequences, that occur with a time shift as a result of the direct consequences. Whereas direct consequences are in a straight line linked to the coping capacity of the system, i.e. the ability to withstand the natural forces and to provide immediate help, indirect consequences are linked to the resilience, i.e. the capacity to remain functional and recover from the disaster. In addition, each consequence class is further subdivided into tangible or economic consequences, that are directly measurable in monetary terms and intangible consequences, that are not directly appraisable, e.g. injuries and fatalities, pollution of the environment, loss of cultural social and historical values etc. Fig. 2 provides an overview of the consequence division. After all possible consequences for each EaR (class) and thus for the system have been determined, loss appraises and eventually accumulates all direct and indirect consequences at the time the disaster takes place. In this respect, the indirect consequences that occur later in time have to be discounted on basis of a properly defined discount rate that is specific for each consequence class. In this context, system vulnerability is an EaR (class) specific characteristic, that links the hazard parameters directly to the loss and indicates the total potential the hazard has on the EaR (class). Thus, it indicates the physical susceptibility of the EaR (class) itself, it's contents as well as the resulting degree of disruption of it's functionality within the system. Consequently, the structural vulnerability is included in the broader concept of system vulnerability. The risk analysis phase terminates with the quantification of risk where all the previously collected information is comprised. It is distinguished be-

tween two different types of risks. Firstly, risk can be calculated by taking the product of the annual probability of occurrence of the hazard multiplied by the expected damage that goes in line with it.

Structural Risk = Probability × Damage   [Damage measure / year]

Evidently, the structural risk is of primary importance for engineers in order to predict the behaviour and the response of a structure or structural element under potential hazard load. The second way to express the risk is to take the product of the annual probability of occurrence of the hazard and the expected loss.

Total Risk = Probability × Loss   [Loss unit / year]

It is being referred to as total risk. The total risk can comprise all consequences, both tangible and intangible, if a reasonable way has been found to convert the primarily non appraisable harms into monetary units. Alternatively, this transformation of intangible outcomes need not be done and the total risk can be split according to the respective consequence classes, to indicate their relative contribution to risk. In any case the total risk is more exhaustive than the structural risk as the full hazard potential to the system is taken in account.

3.2.2   Risk evaluation

Subsequent to the termination of the risk analysis procedure, the risk evaluation phase is initiated. The purpose of risk evaluation is to make the considered risk comparable to other competing risks to the system, by the use of adequate risk measures. In this context, so called exceedance probability curves have found wide acceptance as a common tool to illustrate risk graphically. In an exceedance probability curve the probability that a certain level of loss is surpassed in a specific time period is plotted against different loss levels. Hereby, the loss to the system can be specified in terms of monetary loss, of fatalities or of other suitable impact measures. An insightful overview of common risk measures and tools to compare risks is provided in PROSKE [11]. Finally, after having analysed the risk on basis of adequate risk measures, it may be graded into a certain risk class, depending on individual risk perceptions.

3.3   Risk treatment

After the risk to the predefined system has been analysed and graded into a risk class, the last procedure of the risk management framework, the risk treatment phase begins to operate. This procedure is assigned to the task to create a rational basis for deciding about how to handle the risk in the presence of other competing risks. Based on several analytical tools from decision mathematics, economics and public choice theory, a decision whether to accept, to transfer, to reject or to reduce a given risk can be derived. In the latter case, risk mitigation initiatives are implemented. Fig. 3 visualizes the process of risk treatment schematically.
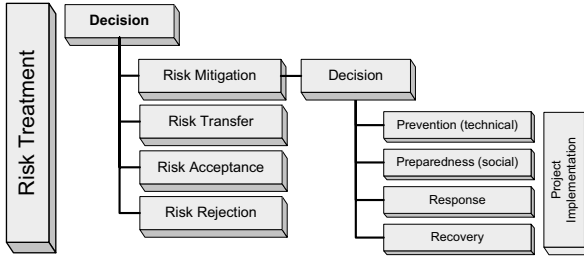
Fig. 3: The risk treatment phase

If the risk is to be mitigated, decision makers have several opportunities to implement a risk reduction project. All the possible risk reduction strategies have in common that they reduce the vulnerability of the system. Depending on the specific strategy that is chosen, they can either reduce structural vulnerability by increasing the resistance of structures or system vulnerability by strengthening the system to recover from the disaster as quickly as possible. The strategies are subdivided with respect to the time the risk reduction project is implemented. Firstly, so called pre-disaster interventions, such as prevention and preparedness, are available. Prevention includes technical measures like structural strengthening that are to be performed with an accurate time horizon before the disaster takes place. Typical examples are dykes against floods or dampers against dynamic actions. Preparedness contains all social activities, e.g. evacuation plans and emergency training, that are necessary to limit harm shortly before the disaster takes place. Secondly, post-disaster strategies can be pursued to reduce the risk. Among these, response covers all activities that are performed immediately after the occurrence of the disaster, such as the organization of help and shelter for the injured and harmed as well as the coordination of emergency forces. Recovery on the contrary, subsumes all activities that need to be taken until the pre-disaster status of the system is restored again. Obviously, also a combination of the mentioned possibilities can be applied to mitigate the risk. Eventually, for clarity reasons, Figure 4 reviews the entire risk management framework schematically.

4   Evaluation and integration of most common definitions

After the general risk management framework has been introduced in the last section, at this point it is discussed, how the risk definitions of section 2 are to be seen in relation to each other. Even if the referenced authors might have had different understandings in their risk characterization, it is shown now, how the diverse formulae can be retraced in the above described methodology. This ambition is approached, by taking the previously established basal terms and definitions as a baseline for argumentation. In the following, the review of the risk Def. (1)-(5) is separated in two passages with respect to the affinity of formulation.
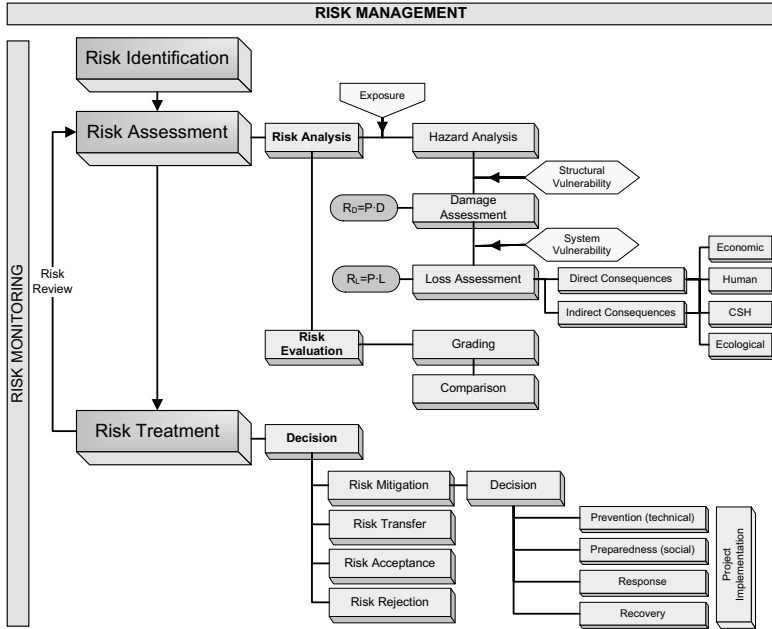
Fig. 4: Overview of the whole risk management process

The first two formulae (1) and (2) have the hazard and the vulnerability module in common, while Def. (1) contains an additional exposure multiplier. Therefore, Def. (1) is better suited for the analysis of entire systems, that are composed both of endangered objects (EaR) and non endangered objects (NEaR) that are distributed unevenly within the system. Consequently, the exposure term has to be included in the definition in order to first identify the exposed elements for which the further analysis is being performed. Def. (2) on the contrary is superior in application for risk analysis of one single structural element, where the exposure to the impact of the hazard is a prerequisite for initiating the investigation. In this case, risk is sufficiently described by the product of hazard times vulnerability. In both definitions of risk it is to be specified case specifically whether structural vulnerability or system vulnerability is employed to calculate the risk. If structural vulnerability is taken into consideration, the formulae (1) and (2) are principally identical to Def. (5), as structural vulnerability links the hazard to the damage state of each exposed element of system or the single EaR respectively. If system vulnerability is used instead, Def. (1) and (2) are analog to risk formula (4) as system vulnerability connects the hazard module directly to the loss of the system or the single EaR, by incorporating all direct and indirect consequences that might go in line with the disaster and transforming them to the time the disaster takes place.

Secondly, risk Def. (3)-(5) are considered together as they differ in their understanding of hazard outcome, while they have the hazard impact implicit in their probability multiplier.

There are basically two ways to interpret the probability multiplier. On the one hand it can refer to the probability that a hazard occurs, while on the other hand the probability of an adverse outcome, specified in terms of consequences, loss or damage could be meant. The variation in the outcome term in contrast, is directly related to the depth of investigation as well as the width of demonstration.

In this respect, the use of the term consequence, in Def (3) is most general and makes a detailed listing of the diverse harms to the system necessary. The depth of analysis cannot be judged upon on basis of the formula. It can either finish with the determination of the physical harm to the considered system or include the total spectrum of adverse outcomes over time. Therefore, formula (3) is most suitable to be applied in political decision processes as in this area, it is essentially to know which parts of the system are especially endangered by the hazard and to which extend. With this information specifically tailored risk reduction interventions can be implemented to guarantee an adequate safety level throughout the population.

The use of loss (Def. (4)) and damage (Def. (5)) as an outcome measure however, usually entail an evaluation of the consequences on basis of a suitable impact measure, and differ in the depth of analysis. If loss is taken into account, it is implicit in the definition that all possible consequences, both direct and indirect, need to be considered and evaluated, dependent on their occurrence in time. Hereby, the loss can be either subdivided by consequence classes, so that it is distinguished between economic loss, loss of life etc., or accumulated in one single number, which entails finding a common scale of evaluation for both tangible and intangible consequences. The use of loss as an outcome indicator is predominantly advantageous in economic considerations, where it is important for instance to express disaster risk as a percentage of national income. Furthermore, on a loss basis it can be judged on the effectiveness of risk reduction interventions, as the benefits in terms of reduced loss can directly be incorporated in cost-benefit analysis. Also in insurance industry it is essential to rely on loss in the calculation of premiums for disaster insurance.

Finally, if damage is taken to convey the outcome, the consideration will be restricted to the physical harm of the elements of the system. Only the immediate reactions of the structures are included in the analysis without questioning the aftermaths. Consequently, the expression of risk in terms of damage is of primary importance in civil engineering, to indicate the structural behaviour under hazard load. Based on this consideration, the engineer can decide for instance whether a strengthening measure of a building is necessary to reduce the structural risk.

5   Conclusion

This article demonstrates how widely the definitions and understandings of the term risk can range. Applied across various disciplines and often used in multidisciplinary collaborations, so far no consistency in delineating the borders of disaster risk could be reached. By providing some exemplary risk definitions from literature and extracting classes of risk calculation formulae, it is shown that the heterogeneity of risk definitions is mainly due to

different understandings of the basal terms hazard, vulnerability, exposure, consequences, damage and loss. These terms that occur repeatedly throughout the diverse risk definitions, are often used interchangeably and so far no clear concept to circumscribe the terms from each other has been developed. This lack of a harmonized concept is addressed by introducing a clear and flexible risk management framework that provides assistance in analysing, comparing and treating disaster risk. Each step in this chain is precisely defined and graphically illustrated, leaving some range for problem specific modifications. Finally, the initially listed risk definitions are integrated in the concept and their interrelations are shown. It is illustrated how the definitions vary with respect to the object or system under consideration and differ in the depth of analysis as well as the level of detail. To conclude, the question which formula to use depends strongly on the field of application, which makes it necessary to emphasise certain aspects of the risk composition. Therefore, none of the risk formulae can be shown to be superior to another and even less to be universal. However a "communication in the same language" is indispensable for an efficient multidisciplinary collaboration in implementing all the sub-steps of the risk management chain.

6　　Literature

[1]　Alexander, D.: Theoretical Aspects of Risk Estimation, Analysis and Management. No Date.

[2]　Australian and New Zealand Standard AS/NZS 4360–1999, Risk Management.

[3]　Baker, J.W., Cornell, C.A.: *Uncertainty Specification and Propagation for Loss Estimation Using FOSM Methods*. PEER Report 2003/07, Pacific Earthquake Engineering Research Center, College of Engineering, University of California, Berkeley, 2003

[4]　Einstein, H.H.: *Landslide Risk Assessment Procedure.* Proceedings Fifth International Symposium On Landslides, Lausanne, Switzerland 1988

[5]　European Spatial Planning Observation Network: *Glossary of Terms*, 2003

[6]　Faizian, M., Schalcher, H.R., Faber, M.H.: *Consequence Assessment in Earthquake Risk Management Using Damage Indicators*. Discussion Paper, ETH-Hönggerberg

[7]　Grossi, P., Kunreuther, H.: *Catastrophe Modeling: A New Approach to Managing Risk*, Springer Science Business and Media Inc, 2005

[8]　Hammer, W.: *Handbook of System and Product Safety.* Englewood Cliffs, NJ: Prentice-Hall, Inc. 1972

[9]　Hori, T., Zhang, J., Tatano, H., Okada ;N., Likebuchi, S.: *Micro-zonation-based Flood Risk Assessment in Urbanized Floodplain.* Second Annual IIASA-DPRI Meeting Integrated Disaster Risk Management Megacity Vulnerability and Resilience, Laxenburg, Austria, 2002

[10] Pliefke, T.; Sperbeck, S.T.; Urban, M.: The Probabilistic Risk Management Chain - General Concept and Definitions. Internal Discussion Paper, International Graduate College 802, 2006

[11] Proske, D. (2004): *Katalog der Risiken – Risiken und ihre Darstellung*, Eigenverlag Dresden, ISBN 3-00-014396-3

[12] Thywissen, K.: *Components of Risk - A Comparative Glossary*. Publication Series of United Nations University-EHS, No.2, 2006

[13] UNDP (United Nations Development Programme) Bureau for Crisis Prevention and Recovery: *Reduced Disaster Risk: A Challenge for Development*. A Global Report, 2004

A genetic algorithm for the discretization of homogeneous random fields

Diego Lorenzo Allaix, Vincenzo Ilario Carbone & Giuseppe Mancini
Department of Structural and Geotechnical Engineering, Politecnico di Torino, Torino

Abstract: The description of the spatial variability of model parameters is an important task in the reliability analysis of concrete structures. In this paper, the theory of the random fields is used for this purpose and a generalized Fourier-type series expansion of a continuous random field is considered. In order to use this representation in any reliability analysis, the problem of the optimal discretization with respect to an error estimator arises. It is possible to obtain a relationship between the discretization error and the truncation order of the series expansion. The discretization procedure can be intended as an optimization problem, where the optimization variable is the truncation order and the objective function depends on a target value of the error. In this paper, a genetic algorithm is used to solve the optimization problem. The procedure is applied to a 2D random field defined on a square plate, whose analytical solution is available, and to the description of the concrete compressive strength of a bridge deck.

1   Introduction

The probabilistic mechanical analysis of structural systems should take in account the variability of the model parameters both in time and space, when their influence on the structural behaviour is significant. The representation of those parameters as random fields leads to a more accurate description of the input of the structural system, but also increases the complexity of the computational problem. In practical application, in particular when the stochastic finite element method is used, the discretization of continuous random fields is necessary. The aim of the discretization is to approximate the random field by a finite set of random variables. In this paper, the Karhunen-Loeve expansion is employed to represent analytically the random field by a generalized Fourier-type series expansion. A numerical technique based on finite elements with Lagrange interpolation functions allows to achieve an optimal discretization, referring to a global error estimator over the structural domain and a prescribed accuracy. The procedure is considered as an optimization problem, where

the truncation order is the optimization variable and the objective function depends on the discretization error and the prescribed accuracy. While in the 1D domains the discretization can be achieved in a non trivial manner, refined strategies are desirable in the case of 2D and 3D domains. A genetic algorithm has been implemented for this purpose. The solution obtained by this algorithm consists in the number of elements of the finite element mesh representing the random field. From the solution, the number of terms of the aforementioned generalized Fourier-type series expansion can be obtained.

2   Karhunen-Loeve expansion

Consider an homogeneous random field $w(\mathbf{x}, \theta)$ with mean $\overline{w}(\mathbf{x})$ and finite, constant variance σ^2, defined on a probability space (Ω, A, P) and indexed on a bounded domain D. The Karhunen-Loeve expansion of the random field is:

$$w(\mathbf{x}, \theta) = \overline{w}(\mathbf{x}) + \sum_{i=1}^{\infty} \sqrt{\lambda_i} f_i(\mathbf{x}) \xi_i(\theta) \tag{1}$$

where $\{\lambda_i\}$ and $\{f_i(\mathbf{x})\}$ are, respectively, its eigenvalues and eigenfunctions of the covariance function $C_{ww}(\mathbf{x}_1, \mathbf{x}_2)$ and $\{\xi_i(\theta)\}$ are uncorrelated zero mean random variables [1]. By definition, this function is bounded, symmetric and positive definite. Therefore it has the following spectral decomposition:

$$C_{ww}(\mathbf{x}_1, \mathbf{x}_2) = \sum_{i=1}^{\infty} \lambda_i f_i(\mathbf{x}_1) f_i(\mathbf{x}_2) \tag{2}$$

The eigenvalues $\{\lambda_i\}$ and eigenfunctions $\{f_i(\mathbf{x})\}$ are the solution of the Fredholm integral equation of the second kind:

$$\int_D C_{ww}(\mathbf{x}_1, \mathbf{x}_2) f_i(\mathbf{x}_2) dx_2 = \lambda_i f_i(\mathbf{x}_1) \tag{3}$$

Due to the aforementioned properties of the covariance function, the eigenfunctions $\{f_i(x)\}$ form a complete base of orthogonal functions. The truncation of the series at the M-th term gives:

$$\hat{w}(\mathbf{x}, \theta) = \overline{w}(\mathbf{x}) + \sum_{i=1}^{M} \sqrt{\lambda_i} f_i(\mathbf{x}) \xi_i(\theta) \tag{4}$$

The variance function corresponding to the truncation series of equation (4) is:

$$\hat{C}_{ww}(\mathbf{x}_1) = \sum_{i=1}^{M} \lambda_i f_i^2(\mathbf{x}_1) \tag{5}$$

It can be shown that the truncated Karhunen-Loeve expansion underestimates the variance of the random field. Indeed, the variance of the error associated to the approximation of the random field can be written as:

$$Var[w(\mathbf{x},\theta) - \hat{w}(\mathbf{x},\theta)] = Var[w(\mathbf{x},\theta)] - \hat{C}_{ww}(\mathbf{x}_1) \tag{6}$$

The left hand side is positive by definition, therefore the variance of the random field is larger than the variance of its truncation at the M-th order.

2.1 Numerical solution of the Fredholm integral equation

An analytical solution of the eigenproblem of equation (3) is available only for a set of covariance functions. Otherwise a numerical solution has to be used. The Galerkin procedure has been used in literature for this purpose, adopting as basis functions piecewise polynomials [1], Legendre orthogonal polynomials [2] and Haar wavelets [3]. In this paper, the shape functions of quadratic quadrilateral elements are used. The peculiarity of this class of finite elements is that the shape functions are Lagrange interpolation polynomials. This choice allows to write the eigenfunctions of the covariance function as linear combination of the interpolation functions $\{N_k(\mathbf{x})\}$:

$$f_i(\mathbf{x}) = \sum_{k=1}^{n} f_{ki} N_k(\mathbf{x}) \tag{7}$$

where the coefficients $\{f_{ki}\}$ are the nodal values of the eigenfunctions. Substituting equation (7) in equation (3) and applying a Galerkin procedure to the corresponding residual, the following generalized algebraic eigenvalue problem is obtained:

$$\mathbf{Cf} = \mathbf{\Lambda Bf} \tag{8}$$

where:

$$\mathbf{C}_{ij} = \int_D \int_D C_{ww}(\mathbf{x}_1, \mathbf{x}_2) N_i(\mathbf{x}_1) N_j(\mathbf{x}_2) d\mathbf{x}_1 \, d\mathbf{x}_2 \tag{9}$$

$$\mathbf{B}_{ij} = \int_D N_i(\mathbf{x}_1) N_j(\mathbf{x}_1) d\mathbf{x}_1 \tag{10}$$

$$\mathbf{f}_{ij} = f_{ij} \tag{11}$$

$$\mathbf{\Lambda}_{ij} = \delta_{ij} \lambda_i \tag{12}$$

The eigenvalues $\{\lambda_i\}$ are located on the diagonal of the matrix $\mathbf{\Lambda}$ and the eigenfunctions $\{f_i(\mathbf{x})\}$ are obtained by substitution of the coefficients $\{f_{ki}\}$ in equation (7). The computation of the matrix $\mathbf{C}$ and $\mathbf{B}$ is the time consuming part of the numerical procedure. The matrix $\mathbf{C}$ is obtained from the contribution $\mathbf{C^{mn}}$ of the finite elements m and n:

$$\mathbf{C}^{mn} = \int_{D^m} \int_{D^n} C_{ww}(\mathbf{x}_1, \mathbf{x}_2) \mathbf{N}^m(\mathbf{x}_1) \mathbf{N}^{nT}(\mathbf{x}_2) d\mathbf{x}_1 \, d\mathbf{x}_2 \qquad (13)$$

The dimension of these matrices is equal to the number of nodes per element. The elements $\mathbf{C}_{ij}^{mn}$ are assembled into the matrix $\mathbf{C}$ combining the values corresponding to the same node. The matrix $\mathbf{B}$ is obtained by assembling, as in the case of the matrix $\mathbf{C}$, the elements of the matrix $\mathbf{B}^{mm}$:

$$\mathbf{B}^{mm} = \int_{D^m} \mathbf{N}^m(\mathbf{x}_1) \mathbf{N}^{mT}(\mathbf{x}_1) d\mathbf{x}_1 \qquad (14)$$

It should be noted that the due to the symmetry of the covariance function, the matrix $\mathbf{C}^{mm}$ and $\mathbf{C}$ are symmetric. The same property holds also for the matrices $\mathbf{B}^{mm}$ and $\mathbf{B}$, due to their definition. The integrals defining the elements of the matrix $\mathbf{C}$ and $\mathbf{B}$ are calculated according to Gauss-Legendre quadrature rule. The number of integration points (named also Gauss points) per element necessary for the computation of the elements of the matrix $\mathbf{B}$ depends on the shape functions and can be determined easily in order to reach the order of exactness of the Gauss-Legendre rule. In the case of the quadratic quadrilateral elements nine Gauss points per element are considered. The integration of the elements of the matrix $\mathbf{C}$ is more complex and, in general, requires a larger number of Gauss points depending on the covariance function. The influence of the number of integration points, necessary for the integration of the elements of the matrix $\mathbf{C}$, on the discretization accuracy in terms of eigenvalues and eigenfunctions is discussed. The relative difference between the exact and numerical value of each eigenvalue is considered as error estimator for the eigenvalues:

$$\varepsilon_\lambda = \left| \frac{\lambda_{exact} - \lambda_{numerical}}{\lambda_{exact}} \right| \qquad (15)$$

A global error estimator is considered for the eigenfunctions:

$$\varepsilon_f = \left[\int_D (f_{exact} - f_{numerical})^2 \, dD \right]^{1/2} \qquad (16)$$

As stated before, the truncated Karhunen-Loeve expansion underestimates the variance of the random field. Therefore only the modes that allow to satisfy this property point wise in a suitable grid of points have to be considered in the series expansion. Two examples are considered to discuss the sensitivity of the quality of the discretization to the number of integration points per element. In the first example, a Gaussian random field is defined on a 10 m long square plate. A unit mean a variance are considered. The following correlation function is assumed:

$$\rho_{ww}(\mathbf{x}_1, \mathbf{x}_2) = \exp\left(-\frac{|\mathbf{x}_1 - \mathbf{x}_2|_x}{l_{cx}} \right) \exp\left(-\frac{|\mathbf{x}_1 - \mathbf{x}_2|_y}{l_{cy}} \right) \qquad (17)$$

where the correlation lengths l_{cx} and l_{cy} are assumed, respectively, equal to 10.0 and 5.0 m. The analytical solution is known in this case [1]. The numerical solution is based on a mesh of sixteen finite elements of equal size. The first eight modes, representing approximately 80% of the variance σ^2 of the random field are considered (figure 1). In the following the term "exact" refers to the analytical solution. The exact eigenvalues and their numerical approximations, depending on the number of Gauss points (NGP) per element, are listed in table 1 and the error ε_λ is plotted in figure 2. It can be observed that in the case of four Gauss points per element only six modes can be considered in the series expansion. Moreover, the accuracy of each eigenvalue increases with the number of integration points. The percentage increment of the accuracy is significant when nine Gauss points are used instead of four. However, the advantage of using a more refined integration decreases when twenty-five or thirty-six Gauss points are considered, as shown for the first eigenvalue in figure 3.
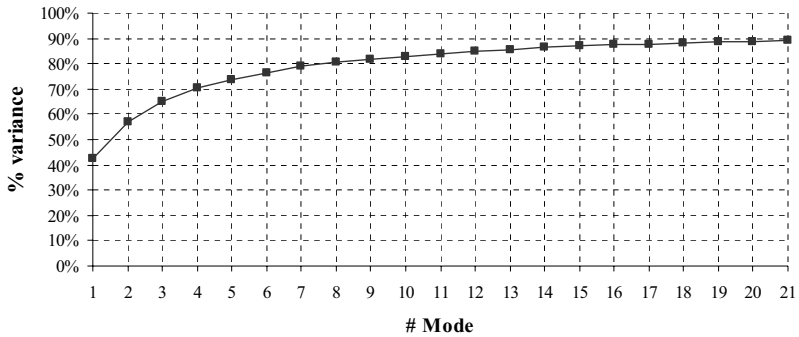
Fig. 1: Influence of the Karhunen-Loeve modes in the representation of the variance

Tab. 1. Exact and numerical eigenvalues

# mode	λ_{exact}	λ (NGP=4)	λ (NGP=9)	λ (NGP=16)	λ (NGP=25)	λ (NGP=36)
1	42.45	43.03	42.75	42.63	42.57	42.54
2	14.42	14.91	14.68	14.59	14.54	14.51
3	7.93	8.17	8.05	8.00	7.98	7.97
4	5.80	6.24	6.03	5.94	5.89	5.86
5	2.94	3.37	3.17	3.07	3.02	3.00
6	2.70	2.83	2.77	2.74	2.73	2.72
7	2.59		2.69	2.65	2.63	2.6
8	1.74		1.86	1.80	1.77	1.75
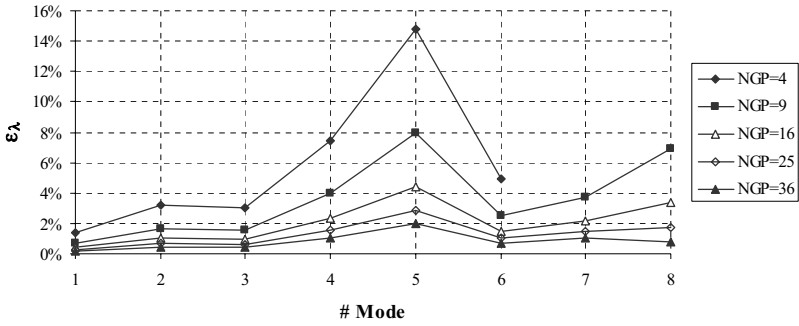
Fig. 2: Error in the estimation of the eigenvalues
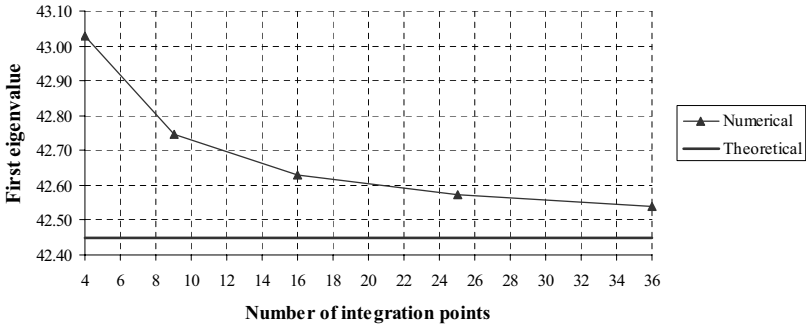
Fig. 3: Accuracy of the first eigenmode

Similar considerations about the influence of the number of integration points on the accuracy can be drawn for the error estimator ε_f for the eigenfunctions. The error in the eigenfunctions induced by the numerical procedure is listed in table 2.

Tab. 2. Error related to the eigenfunctions

# mode	ε_f (NGP=4) [%]	ε_f (NGP=9) [%]	ε_f (NGP=16) [%]	ε_f (NGP=25) [%]	ε_f (NGP=36) [%]
1	0.80	0.26	0.15	0.10	0.07
2	3.77	0.87	0.60	0.51	0.48
3	3.12	0.68	0.47	0.41	0.39
4	10.47	2.84	2.24	2.11	2.07
5	26.05	7.39	5.63	5.30	5.15
6	4.83	1.07	0.76	0.67	0.63
7		2.55	2.07	1.97	1.93
8		13.89	13.77	13.76	13.76

Even with nine Gauss points the error in the first seven eigenfunctions is less than 8%. The error in the last mode does not decrease when more than sixteen Gauss points are used and it could be influenced by the chosen mesh for the random field. Considering also the accuracy for the eigenvalues, the solution with sixteen Gauss points per element is suggested as first trial. In the second example, a 40m long (direction x) and 13 m wide (direction y) bridge concrete deck slab is considered. The concrete compressive strength f_c is described by a 2D lognormal random field. The mean value and the standard deviation are, respectively, $\overline{w} = 40.5$ MPa and $\sigma_w = 5.3$ MPa. The correlation function of the underlying Gaussian field is [6]:

$$\rho_{ww}(\mathbf{x}_1, \mathbf{x}_2) = 0.5 + 0.5 \cdot \exp\left(-\frac{\|\mathbf{x}_1 - \mathbf{x}_2\|^2}{l_c^2}\right) \tag{18}$$

A correlation length l_c of 5 m is adopted [6]. A mesh of five elements in the x direction and two elements in the y direction is considered. In this case an analytical solution is not available. Therefore, the solution obtained with sixty-four Gauss points per element is referred as the "exact" solution. The exact and the approximated eigenvalues (table 3), the error estimators ε_λ (figure 4) and ε_f (table 4) are shown for the first eight modes.

Tab. 3. Exact and numerical eigenvalues

# mode	λ_{exact}	λ (NGP=4)	λ (NGP=9)	λ (NGP=16)	λ (NGP=25)	λ (NGP=36)
1	288.72	288.69	288.72	288.72	288.72	288.72
2	28.06	28.23	28.06	28.06	28.06	28.06
3	24.57	24.75	24.59	24.57	24.57	24.57
4	19.20	19.39	19.24	19.20	19.20	19.20
5	16.65	15.98	16.70	16.65	16.65	16.65
6	15.15		15.19	15.14	15.14	15.14
7	14.87		14.96	14.84	14.85	14.85
8	12.92		12.96	12.92	12.92	12.92

The solution with four Gauss points per element is not able to represent correctly the modes higher than the fifth order. It can be observed that an integration scheme with nine or sixteen integration points per element leads to a solution extremely accurate in terms of the eigenvalues. Therefore, the computational effort required by a more refined scheme is not worthwhile in terms of accuracy for the considered modes.
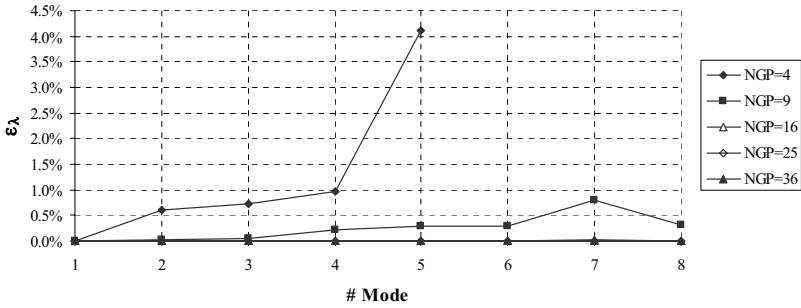
Fig. 4: Error in the estimation of the eigenvalues

Tab 4. Error related to the eigenfunctions

# mode	ε_f (NGP=4) [%]	ε_f (NGP=9) [%]	ε_f (NGP=16) [%]	ε_f (NGP=25) [%]	ε_f (NGP=36) [%]
1	0.47	0.02	0.00	0.00	0.00
2	6.96	0.28	0.01	0.00	0.00
3	12.10	0.52	0.02	0.00	0.00
4	25.15	1.17	0.03	0.00	0.00
5	14.78	0.71	0.02	0.00	0.00
6		0.74	0.02	0.00	0.00
7		2.15	0.05	0.00	0.00
8		0.86	0.02	0.00	0.00

In conclusion, sixteen integration points per element are suggested for both examples. Due to the increasing accuracy in the integrations, the number of modes that can be used correctly in the series expansion increases with the number of integration points. Furthermore, an increment of the accuracy of the integration requires a huge increment of the computational effort. Therefore, the number of integration points, depending on the geometrical domain and correlation properties of the random field, should be chosen carefully as a balance between the accuracy and the CPU time. In conclusion, it should be noted that the finite elements involved in the structural analysis can be of different type respect to the quadratic quadrilateral elements used in this paper. It means that the choice of the class of finite elements used in the discretization of the random field and in the solution of the structural problem (is dependent on the structural model adopted) are completely uncorrelated.

2.2 Discretization error estimator

A discretization error estimator has to be formulated, in order to give a measure of the goodness of the aforementioned procedure. The error in representing the exact variance function is the difference between the exact variance and equation (5):

$$\varepsilon_M(\mathbf{x}_1) = C_{ww}(\mathbf{x}_1) - \hat{C}_{ww}(\mathbf{x}_1) = Var[w(\mathbf{x},\theta)] - \sum_{i=1}^{M} \lambda_i \, f_i^2(\mathbf{x}_1) \tag{19}$$

The mean value of the estimator of the accuracy of the discretization is considered:

$$\overline{\varepsilon}_M = \frac{1}{|D|} \int_D \frac{\varepsilon_M(\mathbf{x},\mathbf{x})}{Var[w(\mathbf{x},\theta)]} d\mathbf{x} \tag{20}$$

where $|D|$ is the area of the domain D, in the case of 2D random fields.

2.3   The structure of the genetic algorithm

A genetic algorithm attempts to solve any optimization problem by search through a space (population) of solutions, that evolve due to the actions of genetic operators [4, 5]. Therefore, a genetic algorithm performs a multi-directional search within the population of solutions. In this paper, a genetic algorithm is proposed to solve efficiently the discretization of a 2D random field. Let denote with $\overline{\varepsilon}_M$ and $\overline{\varepsilon}_{t\arg et}$, respectively, the discretization error (equation 20) and a prescribed accuracy. The optimization problem can be written as:

$$\begin{aligned} &\text{maximize } f_{obj} = f_{obj}\left(\overline{\varepsilon}_M, \varepsilon_{t\arg et}\right) \\ &\text{s.t. } M \in E. \end{aligned} \tag{21}$$

where E is a set of integers. This set has a unit lower bound and the upper bound depends on the specific random field under investigation. The objective function is written as as a linear combination of the absolute value of the difference between the discretization error and the prescribed accuracy and a penalty function that improves the overall efficiency:

$$f_{obj} = -\left|\overline{\varepsilon}_M - \varepsilon_{t\arg et}\right| + f_p\left(\overline{\varepsilon}_M, \varepsilon_{t\arg et}\right) \tag{22}$$

where the penalty function $f_p\left(\overline{\varepsilon}_M, \varepsilon_{t\arg et}\right)$ is defined as:

$$f_p\left(\overline{\varepsilon}_M, \varepsilon_{t\arg et}\right) = \begin{cases} -1 & \text{if } \overline{\varepsilon}_M > \varepsilon_{t\arg et} \\ 0 & \text{otherwise} \end{cases} \tag{23}$$

This penalty function is used to ensure that the potential solution, characterized by an error higher than the required value, have a low chance to survive. It can be observed that the penalty function is applied to those potential solution characterized by an error higher than the required value. In figure 5 the discretization error and the objective function are plotted, for a simple 1D example. It can be observed that the slope of the objective function is small after the solution M=7. Therefore, an adequate number of individuals has to be used to reach the global optimum.
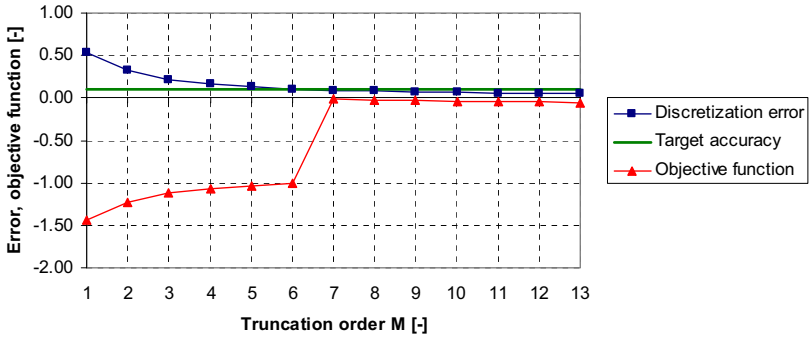
Fig. 5: The objective function

The optimization problem of equation (21) is solved as follows. Each solution is a vector of two components denoting the number of subdivisions of the finite element mesh in the x and y directions. The truncation order corresponding to each mesh is then calculated. The initialization involves the definition of the parameters of the genetic algorithm (population size, probabilities of crossover and mutation, representation of the population). The following values have been chosen as initial guess:

- population size = 50 individuals;

- probability of crossover = 0.80;

- probability of mutation = 0.001.

Each individual has a Gray-coded representation. The advantage is that neighbouring integers are represented by binary strings that differ in only one bit. After the definition of the inputs of the algorithm, the population is ready to start the iterative loop. During each iteration, it will undergo to four genetic operators: selection of the parent individuals, crossover, mutation and selection of the survivor individuals. The convergence criterion of the genetic algorithm is not based on information from the search process, since the population converges to the solution in few iterations. Therefore the iterative scheme is performed for a prescribed number of iterations. The flowchart of the genetic algorithm is shown in figure 6.
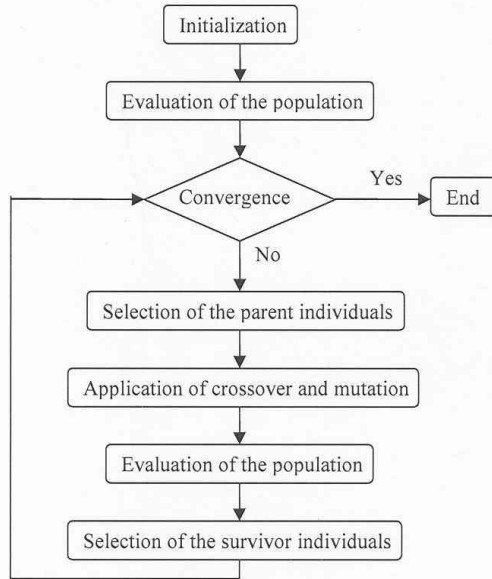
Fig. 6: Flow chart of the genetic algorithm

3   Application examples

The solution strategy is applied to the test cases used in the section 2.1. The target discretization error is 0.10. The domain of the solution is considered between one and ten elements in each direction. The ratio between the CPU time required by the proposed algorithm and a simple solver, consisting in adding iteratively elements in both directions, is considered as a measure of efficiency. In the first example, an optimal mesh of ten elements in the x direction and five elements in the second direction is obtained. The corresponding discretization error is equal to 0.0998 and twenty modes are used in the Karhunen-Loeve expansion. The genetic algorithm is able to find the solution at the third iteration, requiring only fifty objective function evaluations. In terms of efficiency, the genetic algorithm is 1.5 times faster than the aforementioned iterative algorithm. In the second example, the proposed algorithm finds the optimal solution of eight elements in the direction x and two elements in the direction y. This solution leads to a discretization error of 0.0996 and fourteen modes can be used in the series expansion of the random field. The genetic algorithm is able to find the solution in three iterations and forty-eight objective function evaluations are required. The speed-up with respect to the simple iterative solver is about 1.7.

4   Conclusions

A genetic algorithm has been developed to obtain an optimal discretization of stationary random fields, with respect to a global error estimator. The objective function is formulated by considering a linear combination of the absolute value of the difference between the discretization error and the prescribed accuracy and a penalty function. This latter function is used to ensure that the potential solution, characterized by an error higher than the required value, have a low chance to survive. The proposed procedure is applied to an example of a 2D random field defined on a square plate, whose analytical solution is available, and to 2D random field describing the concrete compressive strength of a bridge deck. The genetic algorithm is able to find in few iterations the solution. Therefore, the approximation of the random field can be used to deal with the spatial variability of model parameters within a reliability analysis.

5   References

[1] Ghanem, R.G.; Spanos, P.D., *Stochastic finite elements: a spectral approach*. New York: Springer-Verlag, 1991.

[2] Zhang, J.; Ellingwood, B. Orthogonal series expansion of random fields in reliability analysis. *Journal of Engineering Mechanics*, 120 (1994), pp.2660-2677.

[3] Phoon, K.K.; Huang, H.W.; Quek, S.T. Comparison between Karhunen-Loeve and wavelet expansion for simulation of Gaussian processes. *Computers & Structures*, 82 (2004), pp.985-991.

[4] Michalewicz, Z., *Genetic Algorithms + Data Structures = Evolution Programs*. Berlin: Springer-Verlag, 1996.

[5] Srinivas, M.; Patnaik, L.M. Genetic Algorithms: A Survey. *Computer*, 27 (1994), pp.17-26.

[6] Joint Committee on Structural Safety. *Probabilistic Model Code*, Internet publication, 2001, www.jcss.ethz.ch

On the Moments of Functions of Random Variables Using Multivariate Taylor Expansion, Part I

Noel van Erp & Pieter van Gelder

Structural Hydraulic Engineering and Probabilistic Design, TU Delft

Delft, The Netherlands

1. Introduction

In this article we give a general procedure to find the mean, variance and higher order centralized moments for arbitrary functions of random variables, provided these functions have partial derivatives of order $(n+1)$ equal to zero. We will demonstrate this procedure by finding the general equations for the mean, variance and skewness for sample means; of which the general equations for the mean and variance respectively, equations (13) and (16) given below, are well-known from the various statistical textbooks. Van Erp and Van Gelder (2007) present an algorithm for the developed models in this paper.

2. Multivariate Taylor Expansion

The following Taylor's Theorem in m variables is a generalization of Taylor's Theorem in 2 variables as given in the standard calculus text by Thomas and Finney (1996). We simply state the result here, and for a proof we refer to (Thomas and Finney, 1996).

Taylor's Theorem

Suppose that $g(x_1,\ldots,x_m)$ and all its partial derivatives of order less than or equal to $(n+1)$ are continuous on $D = \{(x_1,\ldots,x_m) \mid a_1 \leq x_1 \leq b_1,\ldots,a_m \leq x_m \leq b_m\}$, and let $(c_1,\ldots,c_m) \in D$. For every $(x_1,\ldots,x_m) \in D$ of $(x_1,\ldots,x_m)$, there exists a point $(\xi_1,\ldots,\xi_m) \in D$ lying in between $(x_1,\ldots,x_m)$ and $(c_1,\ldots,c_m)$ with

$$g(x_1,\ldots,x_m) = P_n(x_1,\ldots,x_m) + R_n(x_1,\ldots,x_m) \tag{1}$$

where

$$P_n(x_1,\ldots,x_m) = g(c_1,\ldots,c_m) + \sum_{j=1}^{m}\left[\frac{\partial g}{\partial x_j}(c_1,\ldots,c_m)\right](x_j - c_j)$$

$$+ \frac{1}{2}\sum_{j_1=1}^{m}\sum_{j_2=1}^{m}\left[\frac{\partial^2 g}{\partial x_{j_1}\partial x_{j_2}}(c_1,\ldots,c_m)\right](x_{j_1} - c_{j_1})(x_{j_2} - c_{j_2})$$

$$+ \cdots$$

$$+ \frac{1}{n!}\sum_{j_1=1}^{m}\cdots\sum_{j_n=1}^{m}\left[\frac{\partial^n g}{\partial x_{j_1}\cdots\partial x_{j_n}}(c_1,\ldots,c_m)\right](x_{j_1} - c_{j_1})\cdots(x_{j_n} - c_{j_n})$$

$$(2)$$

and

$$R_n(x_1,\ldots,x_m) = \frac{1}{(n+1)!}\sum_{j_1=1}^{m}\cdots\sum_{j_{n+1}=1}^{m}\left[\frac{\partial^{n+1} g}{\partial x_{j_1}\cdots\partial x_{j_{n+1}}}(\xi_1,\ldots,\xi_m)\right](x_{j_1} - c_{j_1})\cdots(x_{j_{n+1}} - c_{j_{n+1}})$$

$$(3)$$

The function P_n is called the nth order Taylor polynomial in m variables for the function g about $(c_1,\ldots,c_m)$, and R_n is the remainder term associated with P_n.

Corollary

If all the partial derivatives of order $(n+1)$ of $g(x_1,\ldots,x_m)$ equal zero then, we have that

$$g(x_1,\ldots,x_m) = P_n(x_1,\ldots,x_m) \tag{4}$$

The proof for this Corollary follows trivially from the fact that the remainder term R_n must equal zero if all the partial derivatives of order $(n+1)$ also equal zero, as can be seen in (3).

[1] Functions of Random variables

We now want to determine for an arbitrary function

$$Z = g(X_1,\ldots,X_m) \tag{5}$$

of m known random variables, $(X_1\cdots X_m) \sim p(x_1\cdots x_m\,|\,\{\theta\})$, what the centralized moments are of the probability density function of $Z \sim p(z\,|\,\{\theta\})$.

If all the partial derivatives of order $(n+1)$ of $g(x_1,\ldots,x_m)$ equal zero, then we have with our Corollary that equality (5) may be written as $Z = P_n(X_1,\ldots,X_m)$, which in turn implies the following equality

$$E(Z^k) = E\left\{[P_n(X_1,\ldots,X_m)]^k\right\}, \qquad k = 1,2,\ldots \qquad (6)$$

Now if we let P_n be about the point $(\mu_1,\ldots,\mu_m)$, where the μ_j's, $j = 1,\ldots,m$, are the expectation values of the known random variables $(X_1 \cdots X_m) \sim p(x_1 \cdots x_m \mid \{\theta\})$, then we may rewrite (3) as a function of centralized random variables

$$P_n(X_1,\ldots,X_m) = g(\mu_1,\ldots,\mu_m) + \sum_{j=1}^{m}\left[\frac{\partial g}{\partial X_j}(\mu_1,\ldots,\mu_m)\right](X_j - \mu_j)$$

$$+ \frac{1}{2}\sum_{j_1=1}^{m}\sum_{j_2=1}^{m}\left[\frac{\partial^2 g}{\partial X_{j_1}\partial X_{j_2}}(\mu_1,\ldots,\mu_m)\right](X_{j_1} - \mu_{j_1})(X_{j_2} - \mu_{j_2})$$

$$+ \cdots$$

$$+ \frac{1}{n!}\sum_{j_1=1}^{m}\cdots\sum_{j_n=1}^{m}\left[\frac{\partial^n g}{\partial X_{j_1}\cdots\partial X_{j_n}}(\mu_1,\ldots,\mu_m)\right](X_{j_1} - \mu_{j_1})\cdots(X_{j_n} - \mu_{j_n})$$

$$(7)$$

What we have accomplished in (5) – (7) is the following. The Corollary tells us that if all the partial derivatives of order $(n+1)$ of $g(x_1,\ldots,x_m)$ equal zero we may, without any loss off generality, make the transformation from our original function g to its nth order Taylor expansion P_n. This Taylor expansion P_n, if developed about the point $(\mu_1,\ldots,\mu_m)$, is a function of centralized random variables. So by taking expectation values of P_n, or powers of P_n, we find that the expectation value of g, or powers of g, can be written as a function of (known) centralized moments of the (known) random variables $(X_1 \cdots X_m) \sim p(x_1 \cdots x_m \mid \{\theta\})$.

Procedure (5) – (7) can be computationally very tedious, even in the most simplest of cases, as shall be demonstrated below when we find the mean, variance and skewness for the a sample mean of m known random variables. For more complicated functions of random variables one would probably like to use symbolic computing packages like Maple or Mathematica. In VAN ERP & VAN GELDER (2007), we will give such a routine for Mathematica.

Example: Finding the Mean, Variance and Skewness of the Sample Mean

One of the most well known functions of random variables is the sample mean:

$$Z = g(X_1,\ldots,X_m) = \frac{1}{m}\sum_{j=1}^{m} X_j \tag{8}$$

Since all the second order partial derivatives of (8) equal zero we have, by our corollary, that

$$Z = g(\mu_1,\ldots,\mu_m) + \sum_{j=1}^{m}\left[\frac{\partial g}{\partial X_j}(\mu_1,\ldots,\mu_m)\right](X_j - \mu_j)$$

$$\tag{9}$$

$$= \frac{1}{m}\sum_{j=1}^{m}\mu_j + \sum_{j=1}^{m}\frac{1}{m}(X_j - \mu_j)$$

And it follows that

$$Z^2 = \left\{\frac{1}{m}\sum_{j=1}^{m}\mu_j + \sum_{j=1}^{m}\frac{1}{m}(X_j - \mu_j)\right\}^2$$

$$= \left(\frac{1}{m}\sum_{j=1}^{m}\mu_j\right)^2 + 2\left(\frac{1}{m}\sum_{j=1}^{m}\mu_j\right)\sum_{j=1}^{m}\frac{1}{m}(X_j - \mu_j) + \sum_{j_1=1}^{m}\sum_{j_2=1}^{m}\frac{1}{m^2}(X_{j_1} - \mu_{j_1})(X_{j_2} - \mu_{j_2})$$

$$\tag{10}$$

As well as

$$Z^3 = \left\{\frac{1}{m}\sum_{j=1}^{m}\mu_j + \sum_{j=1}^{m}\frac{1}{m}(X_j - \mu_j)\right\}^3$$

$$= \left(\frac{1}{m}\sum_{j=1}^{m}\mu_j\right)^3 + 3\left(\frac{1}{m}\sum_{j=1}^{m}\mu_j\right)^2\sum_{j=1}^{m}\frac{1}{m}(X_j - \mu_j)$$

$$\tag{11}$$

$$+ 3\left(\frac{1}{m}\sum_{j=1}^{m}\mu_j\right)\sum_{j_1=1}^{m}\sum_{j_2=1}^{m}\frac{1}{m^2}(X_{j_1} - \mu_{j_1})(X_{j_2} - \mu_{j_2})$$

$$+ \sum_{j_1=1}^{m}\sum_{j_2=1}^{m}\sum_{j_3=1}^{m}\frac{1}{m^3}(X_{j_1} - \mu_{j_1})(X_{j_2} - \mu_{j_2})(X_{j_3} - \mu_{j_3})$$

In what follows we will need the following properties of expectation values

$$E(c) = c, \tag{12a}$$

$$E(X_j - \mu_j) = 0, \tag{12b}$$

$$E\left[(X_{j_1} - \mu_{j_1})(X_{j_2} - \mu_{j_2})\right] = \text{cov}(X_{j_1}, X_{j_2}), \tag{12c}$$

$$E\left[(X_{j_1} - \mu_{j_1})(X_{j_2} - \mu_{j_2})(X_{j_3} - \mu_{j_3})\right] = \text{M}_3(X_{j_1}, X_{j_2}, X_{j_3}). \tag{12d}$$

where we let the symbol M_3 in (12d) stand for the third order mixed centralized moments. Using the results (12a) and (12b), we find the expectation value of (9) to be

$$
\begin{aligned}
E(Z) &= E\left[\frac{1}{m}\sum_{j=1}^{m}\mu_j + \sum_{j=1}^{m}\frac{1}{m}(X_j - \mu_j)\right] \\[2mm]
&= E\left(\frac{1}{m}\sum_{j=1}^{m}\mu_j\right) + E\left[\sum_{j=1}^{m}\frac{1}{m}(X_j - \mu_j)\right] \\[2mm]
&= \frac{1}{m}\sum_{j=1}^{m}\mu_j + \sum_{j=1}^{m}\frac{1}{m}E(X_j - \mu_j) \\[2mm]
&= \frac{1}{m}\sum_{j=1}^{m}\mu_j
\end{aligned}
\tag{13}
$$

Using the results (12a), (12b) and (12c), we find the expectation value of (10) to be

$$
\begin{aligned}
Z^2 &= \left(\frac{1}{m}\sum_{j=1}^{m}\mu_j\right)^2 + 2\left(\frac{1}{m}\sum_{j=1}^{m}\mu_j\right)\sum_{j=1}^{m}\frac{1}{m}E(X_j - \mu_j) + \sum_{j_1=1}^{m}\sum_{j_2=1}^{m}\frac{1}{m^2}E\left[(X_{j_1} - \mu_{j_1})(X_{j_2} - \mu_{j_2})\right] \\[2mm]
&= \left(\frac{1}{m}\sum_{j=1}^{m}\mu_j\right)^2 + \sum_{j_1=1}^{m}\sum_{j_2=1}^{m}\frac{1}{m^2}\text{cov}(X_{j_1}, X_{j_2})
\end{aligned}
\tag{14}
$$

Using the results (12a), (12b), (12c) and (12d), we find the expectation value of (11) to be

$$E\left(Z^{3}\right)=\left(\frac{1}{m}\sum_{j=1}^{m}\mu_{j}\right)^{3}+3\left(\frac{1}{m}\sum_{j=1}^{m}\mu_{j}\right)^{2}\sum_{j=1}^{m}\frac{1}{m}E\left(X_{j}-\mu_{j}\right)$$

$$+3\left(\frac{1}{m}\sum_{j=1}^{m}\mu_{j}\right)\sum_{j_{1}=1}^{m}\sum_{j_{2}=1}^{m}\frac{1}{m^{2}}E\left[\left(X_{j_{1}}-\mu_{j_{1}}\right)\left(X_{j_{2}}-\mu_{j_{2}}\right)\right]$$

$$+\sum_{j_{1}=1}^{m}\sum_{j_{2}=1}^{m}\sum_{j_{3}=1}^{m}\frac{1}{m^{3}}E\left[\left(X_{j_{1}}-\mu_{j_{1}}\right)\left(X_{j_{2}}-\mu_{j_{2}}\right)\left(X_{j_{3}}-\mu_{j_{3}}\right)\right]$$

$$=\left(\frac{1}{m}\sum_{j=1}^{m}\mu_{j}\right)^{3}+3\left(\frac{1}{m}\sum_{j=1}^{m}\mu_{j}\right)\sum_{j_{1}=1}^{m}\sum_{j_{2}=1}^{m}\frac{1}{m^{2}}\mathrm{cov}\left(X_{j_{1}},X_{j_{2}}\right)+\sum_{j_{1}=1}^{m}\sum_{j_{2}=1}^{m}\sum_{j_{3}=1}^{m}\frac{1}{m^{3}}\mathrm{M}_{3}\left(X_{j_{1}},X_{j_{2}},X_{j_{3}}\right)$$

$$(15)$$

If we substitute (13) and (14) in the equation for the variance of Z, then we find

$$\mathrm{var}(Z)=E\left(Z^{2}\right)-\left[E(Z)\right]^{2}$$

$$=\left(\frac{1}{m}\sum_{j=1}^{m}\mu_{j}\right)^{2}+\sum_{j_{1}=1}^{m}\sum_{j_{2}=1}^{m}\frac{1}{m^{2}}\mathrm{cov}\left(X_{j_{1}},X_{j_{2}}\right)-\left(\frac{1}{m}\sum_{j=1}^{m}\mu_{j}\right)^{2} \qquad (16)$$

$$=\frac{1}{m^{2}}\sum_{j_{1}=1}^{m}\sum_{j_{2}=1}^{m}\mathrm{cov}\left(X_{j_{1}},X_{j_{2}}\right)$$

Likewise if we substitute (13), (14) and (15) in the equation for the third centralized moment of Z, then it can be verified that we find

$$\mathrm{M}_{3}(Z)=E\left(Z^{3}\right)-3E\left(Z^{2}\right)E(Z)+2\left[E(Z)\right]^{3}$$

$$(17)$$

$$=\sum_{j_{1}=1}^{m}\sum_{j_{2}=1}^{m}\sum_{j_{3}=1}^{m}\frac{1}{m^{3}}\mathrm{M}_{3}\left(X_{j_{1}},X_{j_{2}},X_{j_{3}}\right)$$

We now define the skewness of Z to be its standardized third moment

$$\mathrm{skew}(Z)=\frac{\mathrm{M}_{3}(Z)}{\mathrm{var}(Z)^{3/2}} \qquad (18)$$

If the X_{i}, $i=1,\ldots,m$, are independent and identically distributed with common distribution $X_{i}\sim N\left(\mu,\sigma^{2}\right)$, $i=1,\ldots,m$, or equivalently, if

$$E\left(X_{i}\right)=\mu, \quad \mathrm{cov}\left(X_{i},X_{i}\right)=\sigma^{2}, \quad M_{3}\left(X_{i},X_{i},X_{i}\right)=0 \qquad (19)$$

for $i = 1,\ldots,m$, then we find, using (9) – (18), the mean, variance and skewness of Z to be, respectively

$$E(Z) = \mu, \qquad \text{var}(Z) = \frac{\sigma^2}{m}, \qquad \text{skew}(Z) = 0 \qquad (20)$$

But if the X_i, $i = 1,\ldots,m$, are independent and identically distributed with common distribution $X_i \sim Exp(\mu)$, $i = 1,\ldots,m$, or equivalently, if

$$E(X_i) = \mu, \qquad \text{cov}(X_i, X_i) = \mu^2, \qquad M_3(X_i, X_i, X_i) = 2\mu^3 \qquad (21)$$

for $i = 1,\ldots,m$, then we find, using (9) – (18), the mean, variance and skewness of Z to be, respectively

$$E(Z) = \mu, \qquad \text{var}(Z) = \frac{\mu^2}{m}, \qquad \text{skew}(Z) = \frac{2}{\sqrt{m}} \qquad (22)$$

3.   Summary

In this article, a general procedure to find the mean, variance and higher order centralized moments for arbitrary functions of random variables has been presented. A case study and algorithm of the general procedure will be described in part II of this paper (VAN ERP & VAN GELDER, 2007).

4.   References

[1]   George B. Thomas, Ross L. Finney, Calculus, 1264 pages, Publisher: Addison Wesley; 9th edition (1 Jan 1996) ISBN-10: 0201531747.

[2]   Van Erp, N., and Van Gelder, P.H.A.J.M., 2007. A Mathematica Algorithm for Finding Moments of Functions of Random variables Using Multivariate Taylor Expansion, Part II, 5th International Probabilistic Workshop - Taerwe & Proske (eds), Ghent, 2007.

On the Moments of Functions of Random variables Using Multivariate Taylor Expansion, Part II: A Mathematica Algorithm

Noel van Erp & Pieter van Gelder

Structural Hydraulic Engineering and Probabilistic Design, TU Delft,
Delft, The Netherlands

1   Introduction

Part I has presented a general procedure to find the mean, variance and higher order centralized moments for arbitrary functions of random variables (Van Erp and Van Gelder, 2007). In this paper, Part II, an algorithm will be presented with an application to a simplified case study.

2   Case study and algorithm

We give here an algorithm using to find the first two moments of

$$g(x, y) = \frac{\pi x^2 y}{4} - 1000 .$$

We first declare the function g, the lists u and A, and the multivariate Taylor polynomial Q_3, which represents g without any loss off generality. The list u controls the partial derivatives in Q_3 and the a, b in A will later on be replaced by $(X - \mu), (Y - \nu)$ as we go from $(Q_3)^k \rightarrow P^k$.

$$\text{In[1]:= } g[x\_, y\_] := \frac{\pi x^2 y}{4} - 1000$$

$$\text{In[2]:= } u = \{x, y\};$$
$$A = \{a, b\};$$

$$\text{In[4]:= } Q_3 =$$

$$\left(g[x, y] + \sum_{i=1}^{2} \left(\partial_{u[\![i]\!]} g[x, y] \right) A_{[\![i]\!]} + \frac{1}{2!} \sum_{i=1}^{2} \sum_{j=1}^{2} \left(\partial_{u[\![i]\!], u[\![j]\!]} g[x, y] \right) A_{[\![i]\!]} A_{[\![j]\!]} + \right.$$

$$\left. \frac{1}{3!} \sum_{i=1}^{2} \sum_{j=1}^{2} \sum_{k=1}^{2} \left(\partial_{u[\![i]\!], u[\![j]\!], u[\![k]\!]} g[x, y] \right) A_{[\![i]\!]} A_{[\![j]\!]} A_{[\![k]\!]} \right) /. \{x \to \mu, y \to \nu\}$$

$$\text{Out[4]= } -1000 + \frac{1}{4} a^2 b \pi + \frac{1}{4} b \pi \mu^2 + \frac{1}{2} a \pi \mu \nu + \frac{1}{4} \pi \mu^2 \nu + \frac{1}{2} \left(a b \pi \mu + \frac{1}{2} a^2 \pi \nu \right)$$

One might wonder why we do not immediately state

$$A = \{(X - \mu), (Y - \nu)\} ,$$

The reason for not doing this is that second and higher order moments of Z powers of Taylor polynomials will need to be expanded by Mathematica. But if Q_3 is a function of $(X - \mu), (Y - \nu)$ Mathematica will also expand these terms. This is undesirable because the terms $(X - \mu), (Y - \nu)$ correspond to centralized random variables which later on have to be replaced, in their totality, by their corresponding centralized moments. So, we define Q_3 as a function of the symbols a, b, and replace these symbols, respectively, with $(X - \mu), (Y - \nu)$, after we have expanded Q_3.

$$\text{In[5]:=}$$
$$P = Q_3 \ /. \ \{a \to (X - \mu), b \to (Y - \nu)\}$$

$$\text{Out[5]= } -1000 + \frac{1}{4} \pi (X - \mu)^2 (Y - \nu) + \frac{1}{4} \pi \mu^2 (Y - \nu) +$$

$$\frac{1}{2} \pi (X - \mu) \mu \nu + \frac{1}{4} \pi \mu^2 \nu + \frac{1}{2} \left(\pi (X - \mu) \mu (Y - \nu) + \frac{1}{2} \pi (X - \mu)^2 \nu \right)$$

We assume that X and Y are bivariate normal, or, $(X, Y) \sim N(\boldsymbol{\mu}, \boldsymbol{\Sigma})$, with mean vector and covariance matrix

$$\boldsymbol{\mu} = \begin{pmatrix} \mu \\ \nu \end{pmatrix}, \qquad \Sigma = \begin{pmatrix} \sigma^2 & \rho\sigma\zeta \\ \rho\sigma\zeta & \zeta^2 \end{pmatrix}$$

where ρ is the correlation between X and Y.

We now replace the centralized random variables in P by their corresponding centralized moments; i.e., we go from

$$(X - \mu)^k (Y - \nu)^l \rightarrow E\left[(X - \mu)^k (Y - \nu)^l\right]$$

We do this by way of the Mathematica replace command '/.'. Now care must be taken with this replace command. One must start with the highest sum of powers of $(X - \mu)$ and $(Y - \nu)$, since Mathematica replaces the first statements it encounters in the list the first; so if we write

$$/. \{(X - \mu) \rightarrow 0, (Y - \nu) \rightarrow 0, (X - \mu)(Y - \nu) \rightarrow \rho\sigma\xi, \ldots\}$$

then every $(X - \mu)$ and $(Y - \nu)$ in P will be replaced by zeros, and there will be no more $(X - \mu) \cdot (Y - \nu)$ terms left in P (only $0 \cdot 0 = 0$ terms). where ρ is the correlation between X and Y.

```
In[6]:=  EZ = P /. { (X - μ)² (Y - ν) → 0, (X - μ) (Y - ν) → ρσξ,
          (X - μ)² → σ², (X - μ) → 0, (Y - ν) → 0}

Out[6]= -1000 + 1/4 π μ² ν + 1/2 (π ξ μ ρ σ + 1/2 π ν σ²)
```

Now we go on to the second moment of $Z = g(x, y)$. We start by taking the second power of Q_3, and then proceeding in likewise fashion

In[7]:= **P2 = Expand$\left[(Q_3)^2\right]$ /. {a → (X − μ), b → (Y − ν)}**

Out[7]= $1000000 - 500\pi (X-\mu)^2 (Y-\nu) - 1000\pi (X-\mu) \mu (Y-\nu) -$

$500\pi\mu^2 (Y-\nu) + \frac{1}{16}\pi^2 (X-\mu)^4 (Y-\nu)^2 + \frac{1}{4}\pi^2 (X-\mu)^3 \mu (Y-\nu)^2 +$

$\frac{3}{8}\pi^2 (X-\mu)^2 \mu^2 (Y-\nu)^2 + \frac{1}{4}\pi^2 (X-\mu) \mu^3 (Y-\nu)^2 + \frac{1}{16}\pi^2\mu^4 (Y-\nu)^2 -$

$500\pi (X-\mu)^2 \nu - 1000\pi (X-\mu) \mu \nu - 500\pi\mu^2 \nu + \frac{1}{8}\pi^2 (X-\mu)^4 (Y-\nu) \nu +$

$\frac{1}{2}\pi^2 (X-\mu)^3 \mu (Y-\nu) \nu + \frac{3}{4}\pi^2 (X-\mu)^2 \mu^2 (Y-\nu) \nu +$

$\frac{1}{2}\pi^2 (X-\mu) \mu^3 (Y-\nu) \nu + \frac{1}{8}\pi^2\mu^4 (Y-\nu) \nu + \frac{1}{16}\pi^2 (X-\mu)^4 \nu^2 +$

$\frac{1}{4}\pi^2 (X-\mu)^3 \mu \nu^2 + \frac{3}{8}\pi^2 (X-\mu)^2 \mu^2 \nu^2 + \frac{1}{4}\pi^2 (X-\mu) \mu^3 \nu^2 + \frac{1}{16}\pi^2\mu^4 \nu^2$

Again we take care to start with the highest sum of powers of $(X-\mu)$ and $(Y-\nu)$ in the replace command '/.'.

In[8]:= **EZ2 = P2 /. $\left\{ (X-\mu)^4 (Y-\nu)^2 \to 3 \left(1+4\rho^2\right) \sigma^4 \xi^2 , \right.$**

$(X-\mu)^4 (Y-\nu) \to 0,$

$(X-\mu)^3 (Y-\nu)^2 \to 0,$

$(X-\mu)^2 (Y-\nu)^2 \to \left(1+2\rho^2\right) \sigma^2 \xi^2 ,$

$(X-\mu)^3 (Y-\nu) \to 3\rho\sigma^3 \xi ,$

$(X-\mu)^4 \to 3\sigma^4 ,$

$(X-\mu)^2 (Y-\nu) \to 0,$

$(X-\mu) (Y-\nu)^2 \to 0,$

$(X-\mu)^3 \to 0,$

$(X-\mu) (Y-\nu) \to \rho\sigma\xi ,$

$(Y-\nu)^2 \to \xi^2 ,$

$(X-\mu)^2 \to \sigma^2 ,$

$(Y-\nu) \to 0,$

$(X-\mu) \to 0\}$

Out[8]= $1000000 + \frac{1}{16}\pi^2 \xi^2\mu^4 - 500\pi\mu^2\nu + \frac{1}{16}\pi^2\mu^4 \nu^2 - 1000\pi\xi\mu\rho\sigma +$

$\frac{1}{2}\pi^2\xi\mu^3 \nu\rho\sigma - 500\pi\nu\sigma^2 + \frac{3}{8}\pi^2\mu^2 \nu^2\sigma^2 + \frac{3}{8}\pi^2\xi^2\mu^2 \left(1+2\rho^2\right)\sigma^2 +$

$\frac{3}{2}\pi^2\xi\mu\nu\rho\sigma^3 + \frac{3}{16}\pi^2\nu^2\sigma^4 + \frac{3}{16}\pi^2\xi^2 \left(1+4\rho^2\right)\sigma^4$

So we find the mean of Z to be

In[9]:= **MeanZ = EZ**

Out[9]= $-1000 + \dfrac{1}{4}\,\pi\,\mu^2\,\nu + \dfrac{1}{2}\left(\pi\,\zeta\,\mu\,\rho\,\sigma + \dfrac{1}{2}\,\pi\,\nu\,\sigma^2\right)$

and the variance of Z

In[10]:= **VarZ = Expand[EZ2 - (EZ)^2]**

Out[10]= $\dfrac{1}{16}\,\pi^2\,\zeta^2\,\mu^4 + \dfrac{1}{4}\,\pi^2\,\zeta\,\mu^3\,\nu\,\rho\,\sigma + \dfrac{3}{8}\,\pi^2\,\zeta^2\,\mu^2\,\sigma^2 + \dfrac{1}{4}\,\pi^2\,\mu^2\,\nu^2\,\sigma^2 +$

$\dfrac{1}{2}\,\pi^2\,\zeta^2\,\mu^2\,\rho^2\,\sigma^2 + \dfrac{5}{4}\,\pi^2\,\zeta\,\mu\,\nu\,\rho\,\sigma^3 + \dfrac{3}{16}\,\pi^2\,\zeta^2\,\sigma^4 + \dfrac{1}{8}\,\pi^2\,\nu^2\,\sigma^4 + \dfrac{3}{4}\,\pi^2\,\zeta^2\,\rho^2\,\sigma^4$

Say that we have means $\mu = 10$, $\nu = 20$, variances $\sigma^2 = 1$, $\zeta^2 = 1$ and correlation $\rho = 0.2$, then we find the find the following numerical values of the mean and variance of Z

In[11]:= **MeanZ /. {$\rho \to$ 0.2, $\mu \to$ 10, $\sigma \to$ 1, $\nu \to$ 20, $\zeta \to$ 1}**

Out[11]= 589.646

and

In[12]:= **VarZ = Expand[EZ2 - (EZ)^2] /. {$\rho \to$ 0.2, $\mu \to$ 10, $\sigma \to$ 1, $\nu \to$ 20, $\zeta \to$ 1}**

Out[12]= 116113.

These values have found to be correct using a numerical transformation of variables.

The third order moments of Z can be found by taking the third power of Q_3, expanding it , and replacing the a, b by $(X - \mu)$, $(Y - \nu)$, respectively. The resulting centralized random variables can then be replaced, using the Mathematica replace command '/.', by their corresponding centralized moments, and we have $E(Z^3)$. We already had $E(Z)$, $E(Z^2)$, and σ_Z^2, we can now find the skewness Z using the following identity

$$\gamma_Z = \frac{E(Z^3) - 3E(Z^2)E(Z) + 2[E(Z)]^3}{\sigma_Z^3}$$

3 Summary

This paper has described an algorithm (based on Mathematica) for finding moments of functions of random variables using multivariate Taylor expansions.

4. References

[1]   Van Erp, N., and Van Gelder, P.H.A.J.M., 2007. On the Moments of Functions of Random Variables Using Multivariate Taylor Expansion, Part I, 5th International Probabilistic Workshop - Taerwe & Proske (eds), Ghent, 2007.

Perceived safety with regards to the optimal safety of structures

Dirk Proske [1], Pieter van Gelder [2] & Han Vrijling [2]

[1] Institute of Mountain Risk Engineering, University of Natural Resources and Applied Life Sciences, Vienna, Austria

[2] Structural Hydraulic Engineering and Probabilistic Design, TU Delft, Delft, Netherlands

Abstract: This paper gives a critical view about the development and application of optimisation procedures for the safety of structures. Optimisation techniques for the safety of structures have experienced major progress over the last decade based on, for example, the introduction of quality of life parameters in engineering. Nevertheless such models still incorporate many major assumptions about the behaviour of humans and societies. Some of these assumptions and limitations are mentioned briefly in this paper. These assumptions heavily influence the outcome of such optimisation investigations and can not be neglected in realistic scenarios. Therefore, the authors advise against the application of such optimisation techniques under real world conditions. An alternative for such optimisation procedures can be seen in the concept of integral risk management. Finally examples are given to illustrate effects of individual and social behaviour under stressed situations, which are not considered in the optimisation techniques mentioned. These effects are potentially considered within the concepts of integral risk management.

1 Problem

Over the last few years the question about the optimal safety of structures has been discussed intensively in the field of structural engineering. This question is of particular interest for the development of general safety requirements in codes of practices for structures. Within the last decades, the general safety concept has been updated from the global safety factor concept to the semi-probabilistic safety concept initiating debates regarding the optimal safety of structures.

The question of optimal safety has mainly been answered based on the idea of the optimal economical spending of resources. This includes the important and true consideration that resources for humans and societies are limited.

In structural engineering usually the sum of the production cost and the cost of failure are compared with the possible gains of creating such a structure. The combination of these two cost components mentioned gives an overall cost function with an minimum value according to some adaptable structural design parameters included, for example the chosen concrete strength (Fig. 1). This overall cost function is based on economic considerations. Sometimes additional measures such as those found within the quality of life parameters are incorporated. For example the Life Quality Index *LQI* by NATHWANI, LIND & PANDEY [21] has become widely used in several engineering fields. The development of quality of life parameters can not only be seen in the field of structural engineering, but also in other fields like social sciences or medicine (PROSKE [23]).
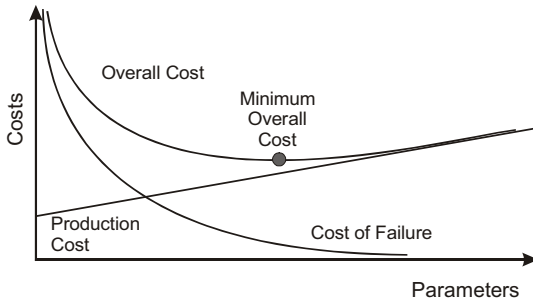
Fig. 1. Widely used function of overall structural cost depending on several parameters

2   Drawbacks of optimisation procedures for safety

2.1   Some limitations of LQI definitions

Although the search for performance measures as a basis of optimisation procedures has yielded in many fields to the application of quality of life parameters, it does not necessarily mean that this strategy has been successful. It shows only that entirely pecuniary based performance measures might be insufficient. If one considers for example the history of quality of life measures in medicine since 1948, now a huge variety of such parameters (more than 1000) has been developed for very special applications. Such a specialisation requires major assumptions inside the parameters. Considering for example the *LQI* it assumes a trade-off between working time and leisure time for individuals. Although this might be true for some people, most people enjoy working (VON CUBE [34]) if the working conditions and the working content is fitting to personal preferences. The choice of using the average lifetime as a major indicator for damage has also been criticized (PROSKE [25]). The question, whether a quality of life parameter can be constructed on only a very

limited number of parameters remains. Fig 2. gives an impression about the dimensions of quality of life (KÜCHLER & SCHREIBER [17]). The comparison between the different dimensions and the simplified definition of the *LQI* makes limitations visible. For example, many psychological effects are not considered, which most of us can agree through personal experience will have an effect.
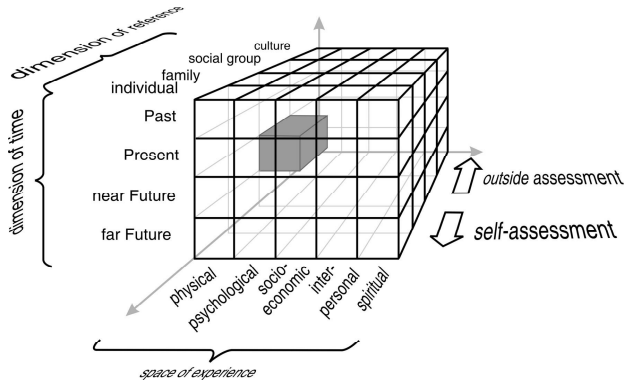

Fig. 2. Dimension of quality of life according to KÜCHLER & SCHREIBER [17]

2.2   Some subjective judgement effects

Since people are so strongly affected by their personal experiences, this chapter discusses some issues of subjective and psychological judgement of safety which influences not only quality of life, but also the investigation of optimal safety. Many works have been done in the field of subjective risk judgement such as, FISCHHOFF et al. [9], SLOVIC [27], COVELLO [6], ZWICK & RENN [36] or WIEDEMANN. For a general summary see PROSKE [24]. The authors here define "safety" as a feeling under which no further resources have to be spent to decrease a hazard or a danger (Fig. 3 bottom diagram – the change of slope in the function). By definition, this is a subjective evaluation of a situation and therefore the term "perceived safety" is actually a pleonasm. Often the term "subjective risk judgement" or "subjective safety assessment" are used as well. Nevertheless the term "perceived safety" has become very popular in scientific literature and shall be used here. Since the term safety considers subjective effects, the property of trust should be mentioned. COVELLO et al. [7] have stated that trust might shift the individual acceptable risk by a factor of 2 000. That means, if one convinces people through dialogue that a house is safe, a much higher risk (no resources are spent) will be accepted, whereas with only a few negative words trust can be destroyed and further resources for protection are spent.

Incidentally the introduced definition of safety also gives the opportunity to define a relationship between the terms disaster, danger and safety and the freedom of resources (Fig. 3 bottom). The discussion on safety has already introduced danger as a situation, where the majority of resources are spent to re-establish the condition of safety, e.g. not spending resources. Under an extreme situation of danger, no freedom of resources exists anymore; since all resources are spent to re-establish safety. Actually the term disaster then describes

a circumstance, where the resources are overloaded (negative). Here external resources are required to re-establish safety. This indeed fits very well to common definitions of disaster stating, that external help is required. Additionally the introduced definitions can be transferred to the time scale of planning and spending resources, as shown in Fig. 3 top diagram.

The time horizon of planning alters dramatically in correlation with the states of danger and safety. Under the state of safety and peace of mind the time horizon shows a great diversity of planning times ranging from almost zero time to decades or even longer. In emergency states, the time horizon only considers very short time durations, such as seconds or minutes.
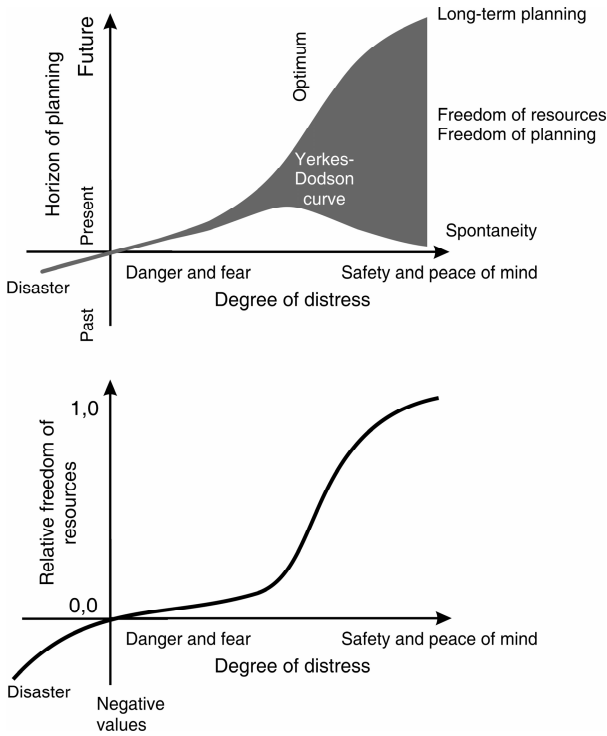
Fig. 3: Relationship between horizon of planning and degree of distress (top) and freedom of resources and degree of distress (bottom)

The choice of the time horizon is very important for optimizations: It determines the results. Short term optimization procedures are often criticized as yielding unethical results. If economic based optimizations are implemented with sufficiently long time horizons then more ethical solutions arise (MÜNCH [20]). For example, IMHOF [13] has chosen a time

horizon of 50 years for the maintenance planning of Swiss railway bridges based on a cost-benefit-analysis optimization. In general such long time horizons are required not only for structures, but for many human activities (economical aid, school systems etc.). But using such long time horizons introduces major indeterminations through assumptions about the future behavior of the social system. An example of this is the uncertainty in predicting the traffic volumes in 50 years

But on which time horizon are usually decisions taken? Here the techniques of the human brain for identifying major hazards and therefore ruling resources should be of interest.

The awareness of danger depends very strongly on the presence of thoughts. But the presence of many different thoughts at the same time is limited. In general, the human short term memory can only consider up to ten items, but usually only three to seven items are used. This obviously limits the comparison of different risks and the consequent spending of resources to the most important ones. Secondly the repetition, for example in media, is important for human memory. Fig. 4 shows several thoughts about risk considering the intensity and EBBINGHAUS'es memory curvature. It should be mentioned here, that after several years the amount of information about a certain event is less then $1/10^{12}$ of the original information. Therefore many scientists speak about the invention of reality. This is of utmost importance as it shows the high degree of individual risk judgement.

Fig. 4. fails to consider inconsistency of thoughts, which has been shown by many psychological investigations. Instead of a continuous flow of topics in thoughts, permanent interruptions of the topics can be experienced. Such intrusive thoughts might be considered as positive or negative depending on the situation. So far, there are no techniques for the evaluation of such switching of or missing thoughts in advance. But such intrusive thoughts can heavily influence the perceived safety (FEHM [10]).

Even the intrusive thoughts might cause problems with safety assessments as it seems that they are rather important for humans. BIRKHOFF [1] has introduced a general numerical measure for the aesthetical assessment of objects based on a simple formula. Additionally many scientists have discussed the issue, whether high aesthetical evaluation is strongly correlated with high utility for humans. One additional issue of aesthetics is a positive disturbance of thoughts (PIECHA [22], RICHTER [27]). Positive disturbing elements, such as a flower decoration on a table, might increase efficiency over the long term: a sparkling idea might be caused by the disturbance.

The briefly mentioned psychological effects are to the knowledge of the authors not included in the optimisation techniques for the safety of structures; however, these effects influence heavily the way in which decisions under real world conditions are made.
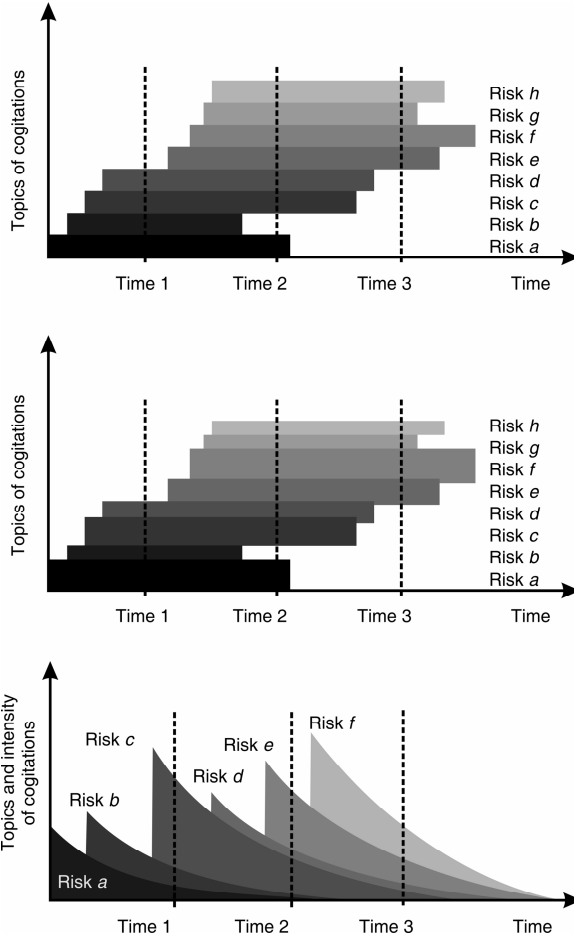
Fig. 4: Risks as topics of cogitations, first only considering the length of the thoughts (top), then considering the intensity (middle) and considering the memory function (bottom)

2.3 Limitations of the economic models used

Most quality of life parameters consider the economy as a system, which functions under all circumstances. For example, assuming a major disaster killing one billion people, the *LQI* assumes that the economy still functions as before. Such assumptions only become visible under extreme situations, such as some of the major economical crises which have occurred in the last century or the current decline of states such as Zimbabwe or Iraq. Changes in economical behaviour under such conditions can occur and will be shown in one example.

Many people live in countries where the social conditions motivate people to produce further wealth. This seems to be valid for all developed countries in the world, especially for countries, where scientists investigate the optimal safety of structures. This is not, however, a concrete behaviour of humans, since one can also detect countries where the social conditions motivate people to take wealth from other people instead producing the wealth (KNACK & ZACK [15], KNACK & KEEFER [14], WELTER [35]). Those countries can be easily described as having a lack of trust in the social system. After major disasters in developed countries such behaviour can also be observed. Here people have the impression that the state as a representative of the society is unable to fulfil the duty of safety, the major task of states (HUBER [12]). As already mentioned, people lose trust in the functioning of the social system. But how is the property of trust influenced by the actions of a state and can this trust be destroyed? To answer this question a short look into the properties of trust is worthwhile.

Trust is a main indicator of social capital and the basis for developing cooperation with other humans and/or organisations. Since the success of the economy is mainly based on specialization, which requires cooperation then the success of the economy in terms of developing wealth is connected to trust. It is not the main goal of this paper to define trust, just one adapted definition should be mentioned (CONCHIE & DONALD [5]):

"*Interpersonal trust is a psychological state that involves the reliance on other people in* certain *situations based upon a positive expectation of their intentions or behaviour*."

Coming back to the simple example mentioned above, where potential economic actors cannot trust each other, the private returns of predation increase while the returns of production decrease. Unfortunately over the long term, this strategy yields to the complete failure of the society and the individuals. So if actions destroy trust, they also destroy the social system including the economy.

As an example the information inserts in pharmaceutical products are mentioned. These inserts are not only considered as information material, but also as a protection measure because they inform about the risks. Recent investigations, however, have shown that the inserts actually increase risk, since people in real need of the medication refuse to accept it due to the fear caused by the inserts. They simply do not trust the medicaments.

In contrast the safety regulations in air planes, such as lifejackets on board, increase the trust and the perceived safety of the passengers. In reality, however, the number of people actually saved by the lifejacket is negligible. Therefore this equipment could be saved and the resources spent on other activities based on optimisation investigations. Nevertheless not only the authorities, but also the airlines themselves refuse to implement this, since the major goal of the lifejacket is to create an atmosphere of carrying and trust, not to function under real life conditions. Only if such subjective effects are considered during the optimisation procedure can realistic results be yielded.

The question then arises, whether optimisation procedures can increase or decrease trust. This has not yet been proven, but simple considerations show, that trust is decreased by optimisation procedures in safety. See also the examples at the end.

2.4   System Requirements

Whereas the one chapter discussed mainly some effects of individual information processing, this chapter focuses more on the behavior of social systems and system theory. The membership of elements, such as humans, belonging to a system might influence required safety levels. First of all, the objectivity of risk assessment depends very strongly on the distance of the endangered elements to the damaged system. A scientist usually works in safe environment thinking about the optimization of the safety of structures. What would happen, however, if the concrete slab inside the office crunches and shows cracks? Would the scientist continue to work or would he spend resources checking the safety of the office? Here system theory might help: If elements of a system are endangered, the system will spend resources in a short term non-optimal way, just defending the integrity of the system. Only if the system exceeds a certain degree of seriousness, then the behavior of the system might shift back to taking economical considerations into account. This has been heavily investigated by looking at parent animals protecting their children. Under normal conditions the parents attack even stronger animals therefore endangering their own life; however, under extreme situations (hunger or drought) they leave their children without care. Also rules for military rescue actions quite often endanger more people to rescue a small number of military staff. Based on a theoretical optimisation analysis these actions should never be carried out, but under real world conditions it is of overwhelming importance that the people keep their trust in the system.

This behaviour can also be seen in constitutions: Here governments promise some properties without any considerations of limited resources. Such statements might be complete nonsense but their goal is to give the elements of the system the impression and the trust, that the system itself will do everything required to save the element.

In general, treating elements of a system with a short term optimal solution can yield to long term failure of the system, since the elements will not function anymore. The problem of long term efficiency, however, can not yet be solved, since that would require the prediction of the behaviour of humans and social systems. Further research especially in the social systems field needs to be carried out. Where we have NEWTON's law in physics, we do not yet have something comparable for societies and predictions are difficult (Fig. 5). In other terms, the behaviour of humans and social systems is highly indeterminate (PROSKE [26]).

This yields to another problem in the field of optimal safety of structures. It is known, that most structural failures are caused by human failure (MATOUSSEK & SCHNEIDER [19]). But the overwhelming number of probabilistic calculations used as input data for optimisation procedures does not consider human failure (avoiding the prediction of human and social behaviour). Therefore the optimisation procedures are only partly connected to realistic problems.
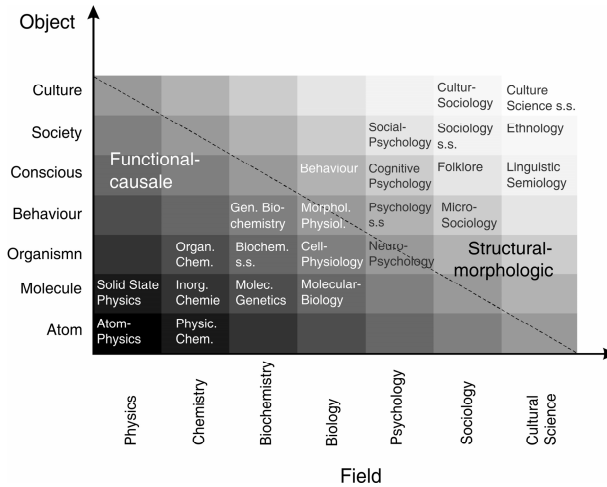
Fig. 5: Causality and field of science: High causality exists at the bottom left (in many cases), whereas low causality exists in the top right area (RIEDL [28])

3   Examples

The following few examples should illustrate the considerations.

Fig. 6. Ford Pinto Case in the US

① The famous Fort Pinto Case (Fig. 6) in the US in the 70s is the first example. Here the company Ford made an optimisation analysis about whether to make changes in the construction of the car concerning safety against fire and explosion. The analysis recommended no changes but financial compensation should be provided. During the court case (Ford vs. Romeo Weinberger) the analysis become public and Ford was heavily punished in terms of compensation (128 Million US $). During the public discussion the question whether the number of fatalities exceeded a permitted level was not so much of concern, but the idea, that any fatalities were accepted was the major critic. General Motor also used

such a procedure and experienced the same effects in public in the 90s [32]. In both cases the loss of trust and other individual and social effects of the optimisation strategy were not considered, but heavily affected the outcome. The actual optimisation procedure did more harm than good.

Fig. 7. Collapsed sport hall in Bad Reichenhall, Germany

② On January 2nd 2006 at 3:54 pm the sport hall in Bad Reichenhall (Fig. 7) collapsed. 15 people, many of them children, died in the collapse and 30 people were hurt. The failure of the structure led to an intensive debate about the safety of public buildings in Germany. First, it was assumed that snow overload caused the failure, since during the same winter a hall collapsed in Poland for this reason. This discussion reminds one very much of a discussion in the beginning of the seventies, when many light weight constructions in East and West Germany failed under the snow load. Here first sabotage was assumed to be the cause of failure in East Germany. Later, however, very optimistic assumptions about snow load and a change of construction material from wood to steel were identified as the causes. The discussion about the cause of failure in Bad Reichenhall turned more into a discussion on maintenance and the required level of safety over time.

"*The question of safety is now answered by business people and legalese, not by engineers.*" said the president of the German Association of inspection engineers on German television (ZDF) in 2006. He actually complains about an inherently economic based optimisation procedure. Independent from such optimisation considerations the ministers for building structures decided in December 2006 to change the law considering the safety requirements of public buildings in terms of additional inspections based only on the singular event in January 2006. This is very common in politics. Still, even with that event, structures in Germany remain an extremely safe technical product (17 293 678 residential buildings in Germany 2004, 5 247 000 non-residential buildings in Germany, 120 000 bridges in Germany, 20 hours exposed per day [16], [8], [31], less then 10 fatalities per year on average) either in terms of mortality, fatal accident rates, *F-N*-Diagrams or optimisation procedures using quality of life parameters. As clearly seen from the words by the

president of the Germany Association of inspection engineers, the optimisation procedures (using risk parameters) are criticised and not helpful in the case of a collapse. One can not simply state after a disaster, that the disaster was an acceptable one and business as usually should continue. For an example the goal of predictions is referred to (TORGERSON [33]).

Here trust in the safety of buildings can be identified as a major requirement which has to be included in optimisation investigations. It should be mentioned, that the efficiency of trust destroying actions is three times higher than trust building. If optimisation procedures for safety are really considered as trust decreasing actions, the procedure itself has to be balanced by much higher investigations.

Fig. 8. Newspaper report in Germany, 2003

③ The Saxon Newspaper (Sächsische Zeitung) from November 8th 2003 reported that the permission to work as a physician has been withdrawn for a doctor due to the uneconomic treatment of patients (Fig. 8). Currently in Germany physicians have a budget which they can spend to treat people. If the budget is completely spent, either the doctor works for free or they may receive a penalty if they stop working. Nevertheless it is prohibited to inform patients about the current status of the budget or give any information about the budget to the patients in the waiting room. Most patients are not aware about such budgets and officials and politicians blame doctors if they refuse to treat people due to an exhausted budget. Here an optimisation procedure is carried out but is kept confidential. Obviously there must be a reason to keep it confidential, and the reason might be feared loss of trust.

So if people are aware of optimisation procedures for safety, they feel a strong damage of trust and develop social prevention actions, which yield to political decisions in terms of laws.

If one assumes, that the definition for safety given in this paper is valid, then it can be proved, that optimisation procedures for safety are actually decreasing safety. Consider the definition of safety as the freedom of resources which have not to be spent immediately for safety measures against a danger. If optimisation procedures, however, imply that re-

sources should be spent in one way or another, people lose the freedom of resources. Actually the goal of optimisation procedures to improve safety, fails since the definition of safety is not fulfilled, e.g. freedom of resources. One could argue that optimisation procedures extend the life time of a person but this does not necessarily mean freedom of resources.

4   Possible solution and conclusion

In the last few years the topic of the optimisation of the safety of structures has been of major importance in engineering, especially since the wide spread application of quality of life parameters. Nevertheless in medicine the application of quality of life parameters has been discussed for over 50 years now. As shown in this paper, social, psychological and other effects have to be considered in the optimisations of safety. Additionally here ARROWS [1] the impossibility theorem should only be mentioned to give an impression about the magnitude of problems.

Nevertheless somehow some decisions have to be made. The only ones able to carry out decisions are empirics. They never declare their solutions as optimal, are aware of the limitations of their models and check carefully the validity. Consider for example the idea of integral risk management, which follows the concept of empirics not assuming an optimal solution, but inherently including an indefinite improvement. From the authors' point of view this seems to be the most promising way. It responds better to social and psychological needs, such as disaster management and increased resources in disaster situations independent of some synthetic optimisation criteria. Therefore integral risk management builds, as just mentioned, a never-ending circle (Fig. 9). Sometimes also the term risk informed decision making is used and helpful (ARROW et al. [2]).

Considering the mentioned drawbacks for optimisation, it is not surprising, that in different fields of science, many authors actually have turned away from optimisation, looking for substitution parameters, such as robustness (HARTE et al.[11], BUCHER [4], MARCZYK [18]). Without going into detail, one of the definitions of robustness of structures consists of satisfying behaviour under non-considered conditions. Again here by definition the limitation of the current knowledge is accepted.

This critique about the possible application of optimisation procedures for the safety of structures will be finished by some remarks taken from a mathematical research project called "Robust mathematical modelling" [30].
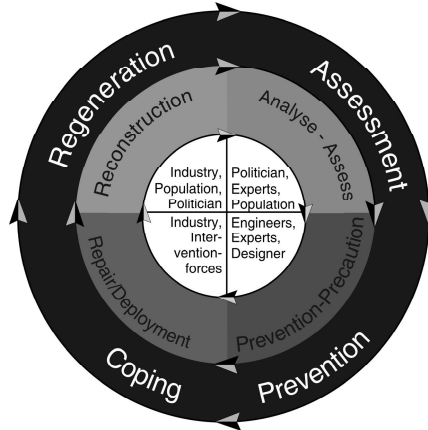
Fig. 9. Integral Risk Management Concept

1. There is no such thing, in real life, as a precise problem. As we already saw, the objectives are usually uncertain, the laws are vague and data is missing. If you take a general problem and make it precise, you always make it precise in the wrong way. Or, if your description is correct now, it will not be tomorrow, because some things will have changed.

2. If you bring a precise answer, it seems to indicate that the problem was exactly this one, which is not the case. The precision of the answer is a wrong indication of the precision of the question. There is now a dishonest dissimulation of the true nature of the problem.

5 Acknowledgement

6 References

[1] Arrow, K.J.; *Social Choice and Individual Values*, Wiley, New York, 1951

[2] Arrow, K.J.; Cropper, M.L., Eads, G.C.; Hahn, R.W., Lave, L.B., Noll, R.G., Portney, P.R., Russell, M.; Schmalensee, R.; Smith, V.K. and Stavins, R.N.: Is there a role for benefit-cost analysis in environmental, health and safety regulations. Science, 272, 1996, pp. 221-222

[3] Birkhoff, G. D.: *Aesthetic Measure*. Cambridge, MA: Harvard University Press, 1933

[4] Bucher, C.: Robustness analysis in structural optimization. *3rd Probabilistic Workshop – Technical Systems – Natural Hazards*. Schriftenreihe des Departments für Bautechnik und Naturgefahren, Universität für Bodenkultur Wien, Nr. 7 – November 2005, Hrsg. Bergmeister, Rickenmann & Strauss, Seite 31-40

[5] Conchie, S.M. & Donald, I.J.: The relative importance of cognition-based and effect-based trust in safety. In: *Safety and Reliability for Managing Risks* – Guedes Soares & Zio (Eds.) Taylor and Francis Group, London 2006, pp. 301-308

[6] Covello, V.T. 1991 Risk comparisons and risk communications: Issues and problems in comparing health and environmental risks. Kasperson, R.E. (Edr): Communicating Risk to the Public. Kluwer Academic Publishers, pp.79-124

[7] Covello, V.T.; Peters, R.G.; Wojtecki, J.G.; Hyde, R.C.: Risk Communication, the West Nile Virus Epidemic, and Bioterrorism: Responding to the Communication Challenges Posed by the Intentional or Unintentional Release of a Pathogen in an Urban Setting. *Journal of Urban Health*: Bulletin of the New York Academy of Medicine, Volume 78, No. 2, Juni 2001, pp. 382-391

[8] *Der Prüfingenieur*, April 2004, Nachrichten, p. 7

[9] Fischhoff, B., Lichtenstein, S.; Slovic, P.; Derby, S.L. & Keeney, R.L. 1981, Acceptable Risk, Cambridge: Cambridge University Press

[10] Fehm, L.B.: *Unerwünschte Gedanken bei Angststörungen: Diagnostik und experimentelle Befunde.* Promotion, Technische Universität Dresden, 2001

[11] Harte, R.; Krätzig, W.B.; Petyna, Y.S.: Robustheit von Tragwerken – das vergessene Entwurfsziel? *Bautechnik* 84 (2007), Heft 4, Seite 225-234

[12] Huber, P.M.: Die Verantwortung für den Schutz vor terroristischen Angriffen. 12. *Deutsches Atomrechtssymposium*. Forum Energierecht 8, Nomos Verlagsgesellschaft, 2004, pp 195-215

[13] Imhof, D.; Hitz, P.; Jordi, R.: Optimal asset management strategy for the bridge of the Swiss deeral railways. *32nd ESReDA meeting*, 8.-9. May 2007, Sardinian, pp. 25-36

[14] Knack, S.; Keefer, P.: Does Social Capital Have an Economic Payoff? A Cross-Country Investigation. *Quarterly Journal of Economics*, 112 (4), 1997, pp. 1251-88.

[15] Knack, S.; Zack, P.: Trust and Growth. *Economic Journal*, April 2001.

[16] Knobloch, B.: *EURO FINANCE WEEK* – Initiative Finanzstandort Deutschland am 25.10.2005, Frankfurt am Main, EuroHypo AG.

[17] Küchler T., Schreiber H.W.: Lebensqualität in der Allgemeinchirurgie - Konzepte und praktische Möglichkeiten der Messung, Hamburger Ärzteblatt, 1989, 43, pp. 246-250

[18] Marczyk, J.: Does optimal mean best? In: NAFEMS-Seminar: *Einsatz der Stochastik in FEM-Berechnungen*, 7.-8. Mai 2003, Wiesbaden

[19] Matoussek, M., Schneider, J.: *Untersuchungen zur Struktur des Sicherheitsproblems*, IBK-Bericht 59, ETH Zürich, 1976

[20] Münch, E.: Medizinische Ethik und Ökonomie – Widerspruch oder Bedingung. Vortrag am 8. Dezember 2005 zum Symposium: *Das Gute – das Mögliche – das Machbare*, Symposium am Klinikum der Universität Regensburg

[21] Nathwani, J. S.; Lind, N.C.; Pandey, M.D.: *Affordable Safety by Choice: The Life Quality Method*. Institute of Risk Research, University of Waterloo, Ontario, Canada, 1997

[22] Piecha, A.: *Die Begründbarkeit ästhetischer Werturteile*. Fachbereich: Kultur- u. Geowissenschaften, Universität Osnabrück, Dissertation 1999

[23] Proske, D.: *Katalog der Risiken*. Eigenverlag Dresden 2004

[24] Proske, D.: Catalogue of risks. Springer: Heidelberg, Berlin, New York 2008

[25] Proske, D.: Limitation of interdisciplinary Quality of Life parameters. Research proposal, Dresden 2003

[26] Proske, D.: Unbestimmte Welt. Dirk Proske Verlag, Dresden Wien 2006

[27] Richter, U.R.: Redundanz bleibt überflüssig? *LACER (Leipzig Annual Civil Engineering Report)* 8, 2003, Universität Leipzig, pp. 609-617

[28] Riedl, R.: *Strukturen der Komplexität – Eine Morphologie des Erkennens und Erklärens*. Springer Verlag, Heidelberg, 2000

[29] Slovic, P. 1999. Trust, Emotion, Sex, Politics, and Science: Surveying the Risk-Assessment Battlefield, *Risk Analysis*, Vol. 19, No. 4, pp. 689-701

[30] Société de Calcul Mathématique, SA : Robust mathematical modeling, 2007 http://perso.orange.fr/scmsa/robust.htm

[31] Statistisches Bundesamt, ifo Institut für Wirtschaftsforschung e. V.: *Die volkswirtschaftliche Bedeutung der Immobilienwirtschaft*, Sonderausgabe 2005, p. 47

[32] Stern: Eiskalte Rechnung. 22.7.1999

[33] Torgersen, H.: Wozu Prognose. Beitrag zu den Salzburger Pfingstgesprächen 2000: Ist das Ende absehbar? - Zwischen Prognosen und Prophetie. 6.8.2000

[34] von Cube, F.: Lust an Leistung. Piper 1997

[35] Welter, F.: Vertrauen und Unternehmertum im Ost-West-Vergleich. In: *Vertrauen und Marktwirtschaft – Die Bedeutung von Vertrauen beim Aufbau marktwirtschaftli-*

cher Strukturen in Osteuropa. Jörg Maier (Hrsg.) Forschungsverband Ost- und Süd-osteuropa (forost) Arbeitspapier Nr. 22, Mai 2004, München, pp. 7-18

[36] Zwick, M. M.; Renn, O. 2002. Wahrnehmung und Bewertung von Risiken: Ergeb-nisse des Risikosurvey Baden-Württemberg 2001. Nr. 202, Mai 2002, Arbeitsbericht der Akademie für Technikfolgenabschätzung und der Universität Stuttgart, Lehrstuhl für Technik- und Umweltsoziologie

Probabilistic method and decision support system for ships underkeel clearance evaluation in port entrances

Lucjan Gucma & Marta Schoeneich

Institute of Marine Traffic Engineering, Institiute of Marine Navigation,
Maritime University of Szczecin, Szczecin

Abstract: The paper presents probabilistic method of underkeel clearance evaluation dedicated for ships approaching to ports. The method is based on Monte Carlo model. The method enables to determine the distribution of underkeel clearance in several ships passages and in further step to assess the probability of ships grounding accident during the port approach. To support the decision of Port Captain the probabilistic decision support model is applied. The system was implemented in Polish ports and is used in risk based decision support practice of large ships entrance.

1   Introduction

Underkeel clearance of ships is the most important factor which determines the possibility of ships grounding. Maintaining safe clearance is the basic navigator's responsibility among his other usual duties. Until now method of constant clearances has been used to determine the minimal safe underkeel clearance. This method calculates safe underkeel clearance as a sum of several components. Many factors are taken into account within this method which has constant values for a particular area. In many cases this solution might be too general.

The paper presents a practical implementation of ships underkeel clearance determination based on probabilistic method and decision support system for port captains. The most important groups of uncertainties taken into account within the model are depth, draught and water level. The paper presents practical use of the model. Model presents predicted underkeel clearance distribution. The method allows to determine the probability of ships hull hitting the bottom, which is helpful to assess whether large vessel are allowed or not to enter to the port.

2 Probabilistic method of ships underkeel clearance determination

The stochastic model of under keel clearance evaluation was presented in [3, 5] (Fig.1). It is based on Monte Carlo methodology where overall ships underkeel clearance is described by following formula:

$$UKC = (H_0 + \sum \delta_{Hoi}) - (T + \sum \delta_{Ti}) + (\Delta_{Swa} + \sum \delta_{Swi}) + \delta_N$$

where:

δ_{Hoi} – the uncertainties concerned with depth and its determination,

δ_{Ti} – the uncertainties concerned with draught and its determination,

δ_{Swi} – the uncertainties concerned with water level and its determination.

δ_N – navigational and manoeuvring clearance.
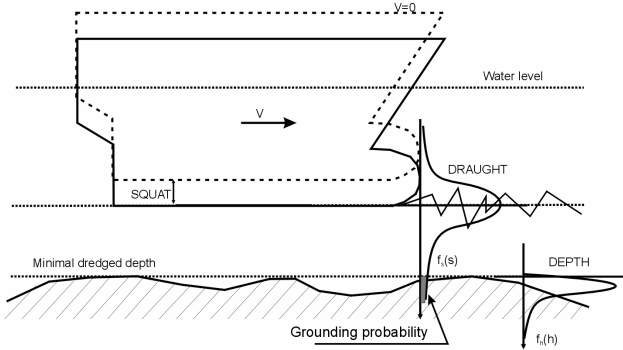
Fig. 1: Concept of probabilistic underkeel clearance of ships determination

The final model takes into account depth measurement uncertainty, uncertainty of draught determination in port, error of squat determination, bottom irregularity, tides and waves influence are deciding factors for underkeel clearance of ships. Program is modelling above mentioned uncertainties using distributions and their parameters. The following parameters are randomly selected from their distributions:

- depth - h_i ,
- sounding error- δ_{BS_i} ,
- mudding component clearance - δ_{Z_i} ,
- draught determination error - δ_{T_i} ,
- ship's heel error - δ_{P_i} .

Length between perpendiculars- L, ship service speed- V_{serv}, ship's block coefficient - C_b are determined on the basis of vessel type and length overall.

Random draught module

User-entered draught is corrected for draught determination error value and ship's heel error.Iterated draught (T_i) is calculated as follows:

$$T_i = T + \delta_{T_i} + \delta_{P_i} \tag{1}$$

where: T- Ships draught [m],

δ_{T_i} - draught determination error,

δ_{P_i} - ships heel error.

Water level module

Water level PW_i is automatically fed from Maritime Office in Szczecin.

Depth module

Random depth h_i and current water level in port are used to calculate up-to-date depth.

Squat module

Squat (ship sinkage due to decrease of water pressure during movement) is calculated in three stages. First module calculates squat with analytical methods used to obtain moving vessel squat (Huusk, Milword 2, Turner, Hooft, Barrass 1, Barrass 2) [7; 8]. Next standard errors of each method are applied. Squat model selection and their standard errors were verified by GPS-RTK experimental research [1;5]. As a result of the experiment uncertainty of each model was assessed and each squat method assigned weight factor. Method's weights and Bootsrap method are then used to calculate final ship's squat.

Underkeel clearance module

Underkeel clearance Z_i is determined by using draught, depth, water level and squat results which were calculated before. Underkeel clearance is defined as:

$$Z_i = (h_i + \delta_{Z_i} + \delta_{BS_i}) - (T_i + O_i + \delta_N + \delta_{WP_i} + \delta_F) \tag{2}$$

where: h_i – up-to-date depth in each iteration,

δ_{Z_i} – mudding component clearance,

δ_{BS_i} – sounding error,

T_i – ships draught with its uncertainty,

O_i – iterated squat,

δ_N – navigational clearance,

δ_{WP_i} – high of tide error,

δ_F – wave clearance.

The result of method of constant clearances is presented to compare it with the proposed probabilistic method. This method calculates safe underkeel clearance as a sum of several components. Any probabilistic characteristics of underkeel clearance can be taken account. The value of this clearance is calculated in accord with "The guidelines for Designing of Maritime Engineering Structures".

3 Decision support application

Simplified decision model is presented as decision tree in Fig.2 [4]. The actions are denoted as *A*, possible state of nature as *P* and outcomes as *U*. The *P* can be understood as state of nature (multidimensional random variable) that could lead in result to ship accident. The main objective of decision can be considered as minimisation of accident costs and ship delays for entrance to the harbour due to unfavourable conditions. The limitation of this function can be minimal acceptable (tolerable) risk level. The expected costs of certain actions (or more accurate distribution of costs) can be calculated with knowledge of possible consequences of accident and costs of ship delays. The consequences of given decision actions expressed in monetary value can be considered as highly non-deterministic variables which complicates the decision model. For example the cost of single ship accident consists of:

- salvage action,
- ship repair,
- ship cargo damages,
- ship delay,
- closing port due to accident (lose the potential gains),etc.

The decision tree can be used also for determination of acceptable level of accident probability if there are no regulations or recommendations relating to it. If we assume that accident cost is deterministic and simplified decision model is applied (Fig.1) then with assumption that the maximum expected value criterion is used in decision process, the probability $p_a{}^*$ can be set as a limit value of probability where there is no difference for the decision maker between given action a_1 and a_2. This value can be expressed as follows:

$$p_a^* = \frac{1}{\dfrac{u_1 - u_3}{u_4 - u_2} + 1} \qquad (3)$$

where: u_1, u_2, u_3, u_4-consequences of different decisions expressed in monetary values.
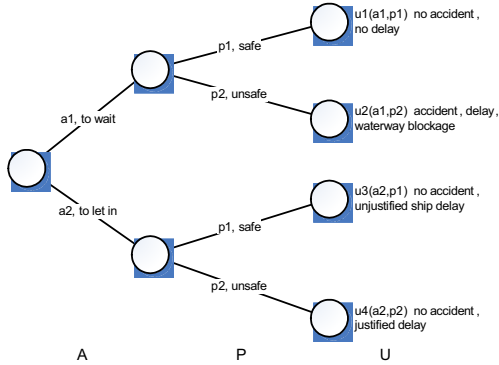
Fig. 2: Simplified decision tree of ship entrance to the port.

3.1   Costs of ships accident and delay

Usually during the investigation of ship grounding accident are restricted waters it is not necessary to take into consideration the possibility of human fatalities nor injures. The cost of accident Ca could be divided into following costs:

$$Ca = Cr + Cra + Cos + Cpc \qquad (4)$$

where: Cr – cost of ships repair,
   Cra – cost of rescue action,
   Cos – cost of potential oil spill,
   Cpc – cost of port closure.

The mean cost of grounding accident in these researches was calculated for typical ship (bulk carrier of 260m). The mean estimated cost of serious ship accident is assumed as C_l=2,500,000 zl (around 700,000 Euro) [6]. The oil spill cost is not considered. Following assumption has been taken in calculations:

- number of tugs taking part in rescue action: 3 tugs,

- mean time of rescue action.: 1 day,

- trip to nearest shipyard: 0.5 day,

- discharging of ship: 4 days,

- repair on the dry dock: 2 days,

- total of oil spilled: 0 tons.

Mean cost of loses due to unjustified ships delay according to standard charter rate can be estimated as 90,000 zl/day. It is assumed that after one day the conditions will change scientifically and the decision process will start from the beginning.

3.2   The decision making process

The maximization of mean expected value criterion is used to support the decision of port captain. Decision tree leads to only 4 solutions. Each decision could be described in monetary values. The expected results (losses) of given decisions are as follows:

- $u1$= 0 zl;

- $u2$= - 2,500,000 zl;

- $u3$= - 90,000 zl;

- $u4$= 0 zl.

Taking into consideration the results of grounding probability calculations of example ship entering to Świnoujscie Port (Fig.4) the probability of ship under keel clearance is less then zero equals $p2$=0 which is assumed as accident probability. No accident probability in this case is estimated as $p1$=1-$p2$=1. We can evaluate the mean expected values of given decisions $a1$ and $a2$ as:

- $a1$=0zl+(-0,0×2,500,000zl)= 0zl;

- $a2$=-(-1×90,000zl)+0zl= - 90,000zl;

With use of mean expected value it is obvious to prefer action $a1$ (to let the ship to enter the port) because total mean expected loses are smaller in compare to unjustified delay due to decision $a2$.

4   Computer implementation of the model

The model was implemented using Python compiler and it is available "on-line" on Maritime Traffic Engineering Institute web site. Figure 3 presents form for entering parameters. It is possible to enter the basic ship and water region data. The remaining necessary data are taken from XML file located from the server.

Model underkeel clearance is evaluated after running the application. The results are presented as a histogram (Fig. 4).

Fig. 3. User defined data form for probabilistic model of underkeel clearance (UKC)

5   Example results

Example entering to the harbours of Świnoujście, Szczecin, Police and Gdańsk were simulated with reference water level at 5,0 m. Maximum draught for these harbours decided of vessels' parameters selection [2]. In the Table 1 harbour and input data are presented. Simulation results are presented in Figures 4, 5.

Tab. 1: Ship parameters used in simulation

Harbour Ships parameters	Świnoujście	Szczecin	Police	Gdańsk
Vessel type	ULCC	Bulk Carrier	Chemical Tanker	Panamax
L[m]	240	160	170	280
T[m]	12.8	9.15	9.15	15
B[m]	36.5	24.2	23.7	43.3
V[kt]	6	8	8	7

The most important result is the probability that clearance is less than zero. This is the probability of accident due to insufficient water depth. Table 2 present's result of simulations as probability, values of mean squat, conventional calculated underkeel clearance, 5% and 95% percentiles of under keel clearance (UKC).

Tab. 2: Simulation results

Harbour Simulation results	Świnoujście	Szczecin	Police	Gdańsk
P(UKC<0)	0.0	0.0	0.0	0.0
Mean squat	0.23 m	0.35 m	0.32 m	0.22 m
Constant UKC component method	3.11 m	2.59 m	2.57 m	3.02 m
5% UKC percentile	0.73 m	0.58 m	0.64 m	1.09 m
95% UKC percentile	2.07 m	3.53 m	3.31 m	1.81 m

Results show zero values of probability that clearance is less than zero. It is obvious that all the cases when UKC<0 show safety entrance to the port.
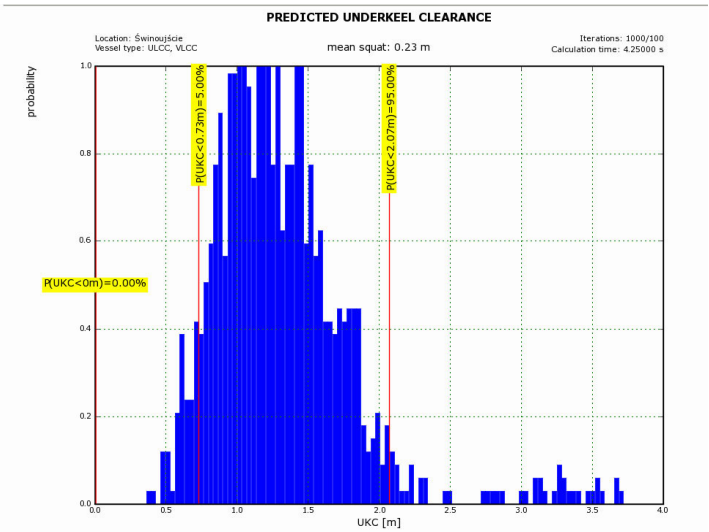
Fig. 4. Underkeel clearance distribution in simulations of the maximum vessel's draught in Świnoujście Port (Górników Wharf)

The distribution has positive asymmetry. Mean underkeel clearance of maximal ships is equal to UKC_M = 1,2 m. 95% values are less than 2.07 m when value conventional calculated underkeel clearance is equal to 3.11m.
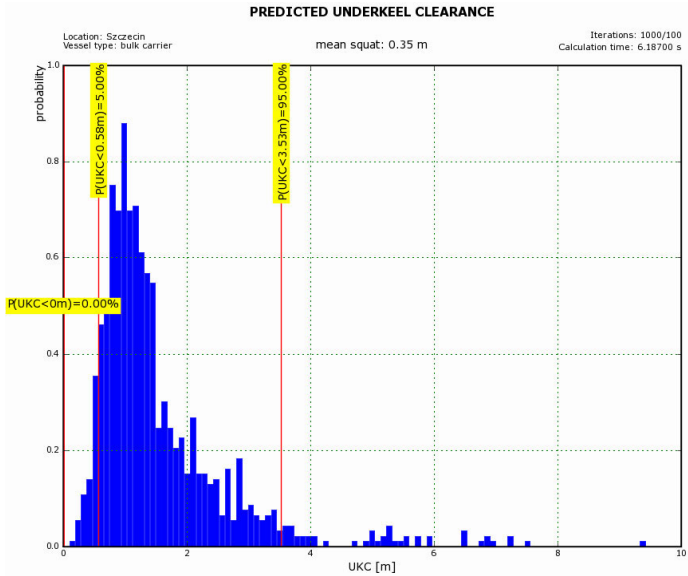
Fig. 5. Underkeel clearance simulation results at the maximum vessel's draught in Szczecin Port.

In this case (Figure 5) the disribution have positive asymmetry too. Mean underkeel clearance of maximal ships is equal 1.0m. 95% values are less than 3.53 m.

In Figure 6 presents decision support aplication result. In this case simulated ship's draught in Świnoujście Port was increase to 13.3 m.
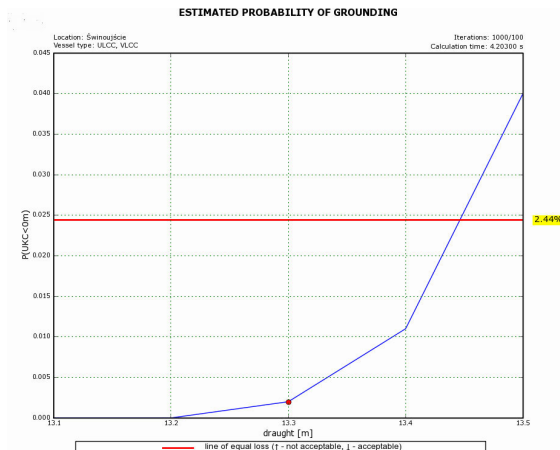
Fig. 6. Example of decision support aplication result (line of equal loss is 2.44%, ship can enter to the port)

6   Conclusion

The paper presents probabilistic method of ships dynamic underkeel evaluation. Previously developed Monte Carlo model was implemented as online program. The program allows assessing the probability of grounding accident with consideration of several uncertainties.

Simplified decision model based on mean expected value was presented and applied in case study of ships entering Świnoujscie Port. Results were discussed.

The model after validation is intended to be used in every day decision making practice of port captains and VTS operators.

References

[1]   Określenie dopuszczalnego zanurzenia statków mogących bezpiecznie wchodzić do portu handlowego w Świnoujściu w różnych warunkach hydrometeorologicznych. Praca naukowo-badawcza. Akademia Morska, Szczecin 2004.

[2]   Określenie minimalnej rezerwy wody pod stępką przy nabrzeżach portu handlowego Świnoujście. Praca naukowo-badawcza, Akademia Morska, Szczecin, 2004.

[3]   Gucma, L.: Probabilistic Monte Carlo method of determination safe underkeel clearance, Proc. of the XIV International Conference: The Role of Navigation in Support of Human Activity on the Sea, Gdynia 2004.

[4]   Gucma L..: Risk Based Decision Model for Maximal Ship Entry to the Ports. PSAM7-ESREL04, C. Spitzer et. al (eds.), Springer-Verlag, Berlin, 2004.

[5]   Gucma, L.: Risk Modelling of Ship Collisions Factors with Fixed Port and Offshore Structures (in polish). Maritime University of Szczecin 2005.

[6]   Gucma, L.; Schoeneich, M.: Określanie niepewności metod osiadania na podstawie badań rzeczywistych przeprowadzonych na promie m/f Jan Śniadecki w porcie Świnoujście. Proceedings of the XV-th International Scientific and Technical Conference The Role of Navigation in Support of Human Activity on the Sea, Gdynia, 2006.

[7]   Gucma, L.; Schoeneich, M.: Probabilistic model of underkeel clearance in decision-making process of port captain. Transport XXI Conference Warsaw 2007.

[8]   MUS 2000: Efficiency evaluation of Swinouscie – Zalew Szczeciniski (0,0 – 18,8 km) waterway modernization. Unpublished results of researches, Maritime University of Szczecin 2000.

[9]   PIANC 1997: Approach Channels. A Guide for Design. Final Report of the Joint PIANC-IAPH Working group II-30 in cooperation with IMPA and IALA. June 1997.

[10] PIANC 2002: Dynamic Squat and Under-Keel Clearance of Ships in confined Channels, 30th International Navigation Congress, Sydney, September 2002, S10B P152.

Probabilistic method of ships navigational safety assessment on large sea areas with consideration of oil spills possibility

Lucjan Gucma & Marcin Przywarty
Maritime University of Szczecin, Poland

Abstract: The paper presents the implementation of probabilistic method of ships collision and grounding model to evaluate the risk of oil spills. The model is capable to assess the risk of large complex systems with consideration of human (navigator) behaviour models, ship dynamics model, real traffic streams parameters and external conditions like wind current visibility etc. The model works in fast time and could simulate large number of scenarios. The output of the model as the collision place, ships involved and navigational conditions could be useful for risk assessment of large sea areas.

1   Introduction

The presented methodology is used for assessment of oil spill possibility due to navigational accidents of ships in the Baltic Sea area. The collisions and groundings in different conditions were modelled with use of complex stochastic safety model and real statistical data. The model could assess the navigational risk in large complex system with consideration of navigators behaviour models, ship dynamics model, real traffic streams parameters and external conditions like wind current visibility etc. The model works in fast time and could simulate large number of scenarios. The most important output of the model is time, place and size of oil spills in the Southern Baltic Sea area. The collision and grounding probability together with potential oil spill size in different conditions (environmental, traffic etc) evaluated in this researches will be used in the further step for risk assessment in the Baltic Sea area.

The collision between ships, grounding and fire on board are most contributing factor in ship accident. The consequences of considered accidents especially in coastal waters due to possibility of oil spill could be catastrophic. The paper presents methodology of ships accident probability evaluation in different conditions with use of complex stochastic safety model and real statistical data.

To achieve the aims of the paper stochastic model of ships traffic was developed and applied on the Southern Baltic Sea area. The model is capable to assess the risk of large complex system with consideration of human (navigator) behaviour models, ship dynamics model, real traffic streams parameters and external conditions like wind current visibility etc (Fig. 1). The model works in fast time and could simulate large number of scenarios.

In the second step the statistical data of real collision accidents was collected. With the number of collision situations, assessed, in previous step, the collision probability in different scenarios was evaluated. This probability of collision in different encounter situations was estimated.

In the third stage of researches calibrated model was run with the traffic data estimated at level 2010 and routing schemes introduced in 2006. The output from model as collision and grounding places, ships involved, and navigational conditions could be useful for further risk assessment.

2   Stochastic model of ships accidents

One of the most appropriate approaches to assess the safety of complex marine traffic engineering systems is use of stochastic simulation models [GUCMA 2005, GUCMA 2003]. The model presented in Figure 1 could be used for almost all navigational accidents assessment like collisions, groundings, collision with fixed object [GUCMA 2003], indirect accidents such as anchor accidents or accidents caused by ship generated waves [GUCMA & ZALEWSKI 2003]. The model could comprise several modules responsible for different navigational accidents.

This methodology was used already by several authors before with different effect [Friis-HANSEN & SIMONSEN 2000, MERRICK et al. 2001, OTAY & TAN 1998]. In presented studies the model was used to assess the probability of oil spills in the Southern Baltic Sea area.
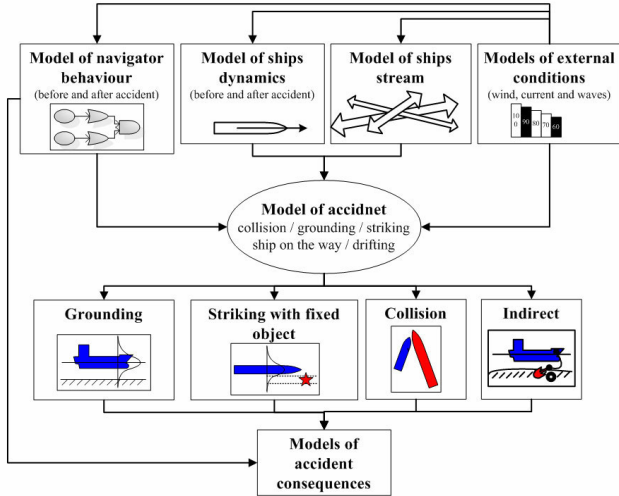
Fig. 1. Diagram of fully developed stochastic model of navigation safety assessment

2.1 Traffic data

There are several sources of data necessary for the running of simulation model. The data of traffic was obtained by analysis of AIS records [Assessment 2005] Polish national AIS network studies, and statistics of ships calls to given ports. The weather data was obtained from Polish meteorological stations and extrapolated in order achieves open sea conditions [Risk 2002]. The navigation data was obtained from navigational charts, guides and own seamanship experience. The simulated ships routes are presented in Figure 3.
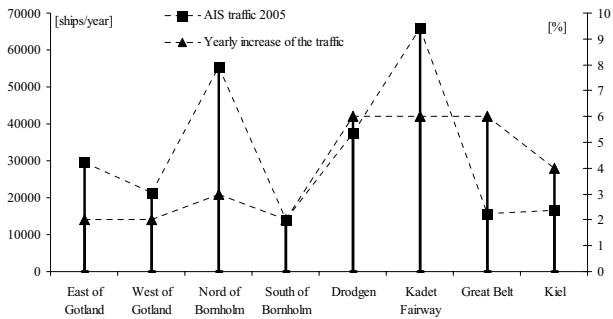
Fig. 2. Traffic of ships and its increase on analyzed part of the Baltic Sea
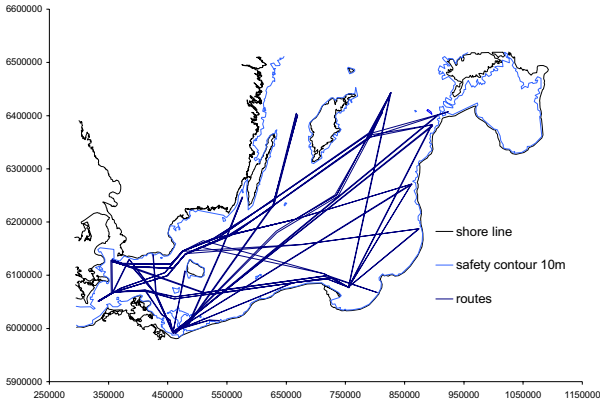
Figure. 3. Simulated ships routes in examined area

2.2 Collision accident models

To model the collisions simplified statistical model is used. The model neglects several dependencies but because it is based on real statistical data the achieved results are very close to reality. The most unknown parameter necessary for collision probability assessment on large sea areas is number of ships encounter situations. In complex systems with several traffic routes this number could be evaluated only by traffic streams simulation models such as the one presented in this study.

The traffic of ships is modelled by nonhomogenous Poison process where actual intensity of traffic is evaluated on the basis of real AIS (Automatic Identification System) data from the Helcom network which is operated since mid 2005. The collected AIS data is used also for determination of ships routes, types, length and draught distribution. The variability of mean ships routes is modelled by two-dimensional normal distribution which parameters were estimated by AIS data and expert-navigators opinion. New ships routings were considered. Routes are presented on Figure 8. Ships traffic and its annual increase in different Baltic Sea regions is presented on Figure 2.

After collecting necessary input data the simulation experiment was carried out and the expected number of encounter situation was calculated. The critical distance where navigators perform anti-collision manoeuvre was assumed on the base of expert opinion separate for head on (heading difference ±170°), crossing and overtaking situations (heading difference ±10°). These distances called minimal distances of navigator's reaction were estimated by expert opinion and real time non-autonomous simulation experiment performed on ARPA simulator. The mean distances of reaction were estimated to 0.35; 1.0; 0.45 Nm for head on collision avoidance, crossing and overtaking [KOBAYASHI 2006].

The overall number of encounter situation estimated by simulation model is around 140000 per year where 30% of them are head on situations, 40% of crossing and 30% of overtaking (Figure 4).
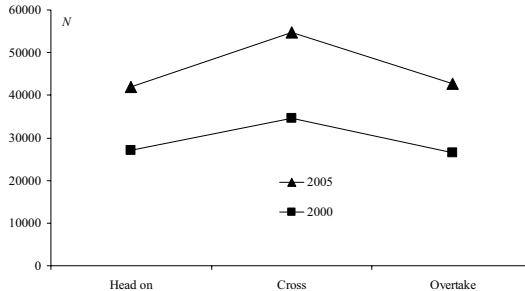

Fig. 4. Simulated number of encounter situations N (the influence of traffic increase)

Statistical data from southern part of the Baltic Sea accidents were used for evaluation of mean intensity of ship collision accidents in the Southern Baltic. The number of accidents significantly increases mostly due to traffic increase. Only the accidents on the open sea area were considered. Figure 5 presents number of accidents per year on the investigated area. The mean intensity of collision accidents equals 2.2 per year and grounding 0.4 accidents per year. Observation of tendency of accidents shows high correlation of collision accidents of traffic intensity. The grounding accidents are not dependant of traffic intensity in such extend.
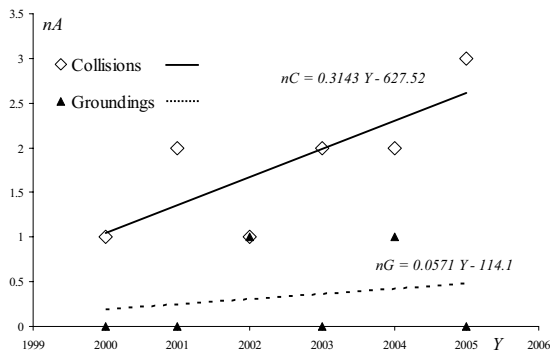
Fig. 5. Number of collision (nC) and grounding (nG) accidents per year located at the open sea of the Southern Baltic

Data presented on Figure 5 and the simulation results of ships encounter situation (Figure 3) have been used for estimating the number of collisions. To simplify the calculations it was assumed that probability of collision is equal in all considered situations. The existing databases of real accidents scenarios justify this assumption.

The calculated probability of collision in single encounter situation (Figure 6) is higher than 1×10^{-5} which is the typical mean value of probability used in safety of collision assessment. The difference between probability in 2000 and 2005 can be justified only by the error of estimation and simplicity of applied model. Normally minor decrease of collision probability could be expected due to better navigational and positioning systems, traffic regulations, better training of navigator.
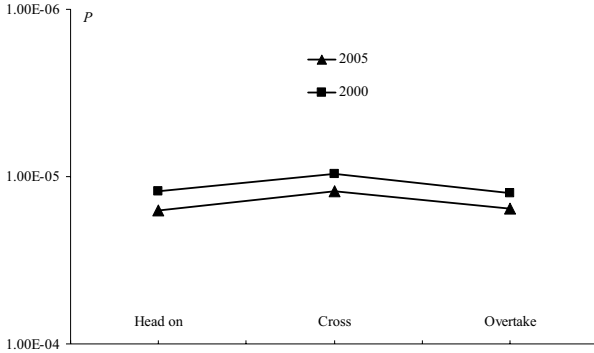

Fig. 6. Probability of collision accident (P) in different encounter situations
in 2000 and 2005

2.3   Grounding accident model

The model of grounding was developed with assumption that probability of accident is dependant of distance to the given safety contour (or shore). The following formula is used:

$$P_{Gr} = P_G P_H \tag{1}$$

where: P_G=geometrical probability;
P_H=probability of human error.

Geometrical probability is calculated on the basis of observation of real traffic. To describe traffic near by navigational obstacles the special mixed distribution could be used (Fig. 7). This distribution is the mixture of two normal distributions with mean equals zero:

$$f(x) = \frac{1}{\sigma\sqrt{2\pi}} \exp\frac{1}{2}(\frac{x}{\sigma})^2 \quad \text{where:} \quad \sigma = \begin{cases} \sigma_r & if \quad x > 0 \\ \sigma_l & if \quad x < 0 \end{cases} \tag{2}$$

where: σ_r= standard deviation of the right side of distribution σ_l =standard deviation of the left side of the distribution.
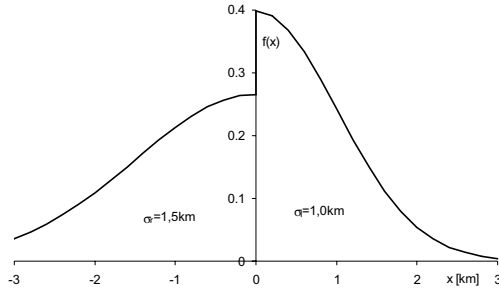
Fig. 7. Density function of ships positions (mixture of two normal distributions) for geometrical probability evaluation

The studies on ships traffic carried out on the Baltic Sea (real traffic) and on the restricted area (simulation studies) lead to assumption that standard deviation of ships traffic is mostly dependent from distance to the danger and size of ships. Following relation could be used to define the standard deviation of ships routes (Fig. 9):

$$\sigma = aD + b \qquad (3)$$

where: a, b=coefficients of regression,
D=distance to navigational danger (safety contour, isolated depth).

The factors a is dependant of ships size and type In the researches these factors were represented by ships length (L). The factor a is around 0,1 and its dependence of ships length L could be expressed as:

$$a = -0.0002L + 0.12$$

The factor b varies from 450 to 550 and was estimated as mean value as 500.

The typical behaviour of ships traffic near the Bornholm is presented in Fig. 8. The behaviour of traffic is very similar to proposed approach with using two different normal distributions.
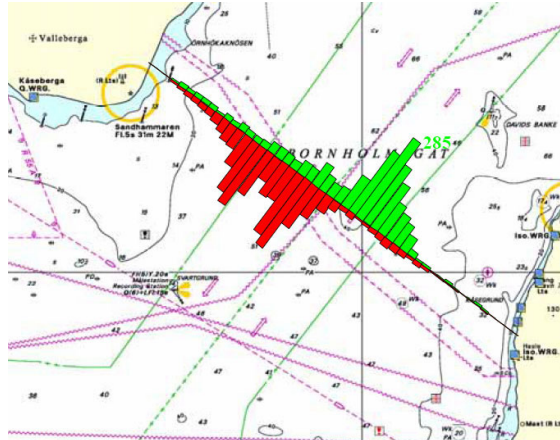
Fig. 8. Typical ships traffic behaviour real data from AIS 2004

Probability of human error is estimated on the level P_H=1 × 10^{-4} which is the standard value assumed in human reliability assessment confirmed in several maritime studies [GUCMA 2005] for grounding assessment.
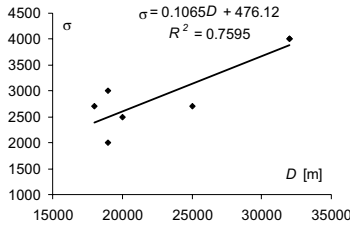
Fig. 9. One of the several studies of route standard deviation in relation to distance to the danger D (here based on the AIS data from Southern Baltic Sea)

Finally the probability of grounding accident P_{Gr} is evaluated by the following formula:

$$P_{Gr} = P_{GrL} + P_{GrR} \tag{4}$$

where: P_{GrL}=probability of grounding on the left side of the waterway;
P_{GrR}=probability of grounding on the right side of the waterway

2.4   Fire on board accident model

The analysis of several databases and study results [MEHRA 1999, ITOPF 1998, MAIB 2005, LMIS 2004, HECSALV 1996, IMO 2001] leads to assumption that probability of fire on board of merchant ship is dependant of kilometres travelled. During the sea travel of typical merchant ship this probability equals 5.18×10^{-5} 1/km. Distribution of mean time to

fire extinguishing of is presented in Figure 10. It was assumed that the fire could be extinguished by the crew only when time is less than 0.5 h.
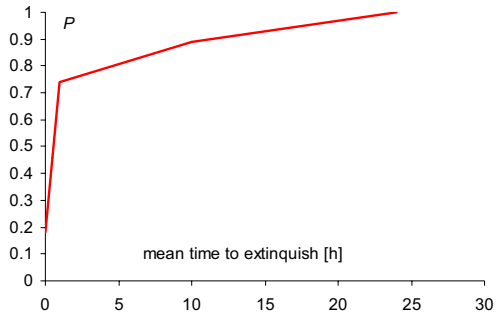
Fig. 10. Probability of time to extinguish the fire

3   Oil spill model

The collision, grounding and fire on ship accident could be followed by the oil spills. The conditional probability is used and finally the probability of oil spill accident (P_S) is calculated as follows:

$$P_S = P_A P_{A/OS} \tag{5}$$

where: P_A=probability of accident;
$P_{A/OS}$=conditional probability of oil spill if accident occur.

Several databases [MEHRA 1999, ITOPF 1998, MAIB 2005, LMIS 2004, HECSALV 1996, IMO 2001] was used to find the conditional probability of oil spills if given accident occurs. Fig. 11 shows conditional probability of oil spills in different accidents.

Oil spills due to collision is estimated with the double bottom tankers with relation to ships size expressed in DWT. Identical procedure was followed to find probability of oil spill after grounding and fire. Fire on ships is highly unlike to be the result of oil spill. Only about 10% of fire accident is ended with oil spill.
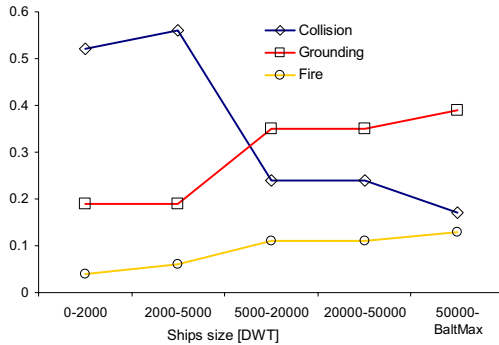
Fig. 11. Conditional probability of oil spill if given kind of accident occurs

3.1 Estimation of oil spill size after collisions

To evaluate the probability oil spill size after ships collision several databases and another study results was used [MEHRA 1999, ITOPF 1998, MAIB 2005, LMIS 2004, HECSALV 1996, IMO 2001]. The simplified statistical model is used. The model assumes that the size of oil spill is dependant only of ships size expressed in DWT in tons. The results are presented on Fig. 12.
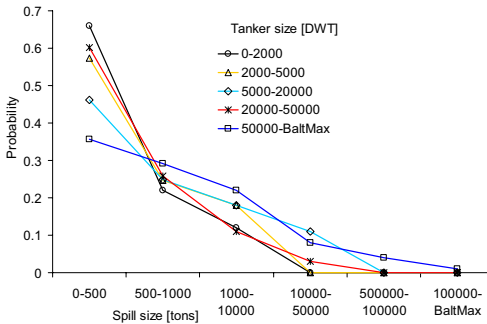

Fig. 12. The probability of given oil spill size for different size of tankers in collision accident

3.2 Estimation of oil spill size after grounding

To evaluate the probability oil spill size after ships grounding several databases and another study results was used [MEHRA 1999, ITOPF 1998, MAIB 2005, LMIS 2004, HECSALV 1996, IMO 2001]. The simplified statistical model is used. The model assumes

that the size of oil spill is dependant only of ships size expressed in DWT in tons. The results are presented in Fig. 13.
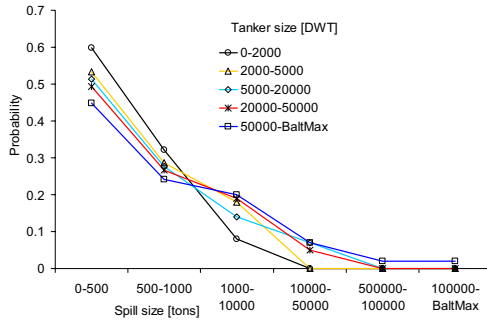

Fig. 13. The probability of given oil spill size for different size of tankers in grounding accident

3.3   Estimation of oil spill size after fire on board

To evaluate the probability oil spill size after fire on board several databases and another study results was used [MEHRA 1999, ITOPF 1998, MAIB 2005, LMIS 2004, HECSALV 1996, IMO 2001]. The simplified statistical model is used. The model assumes that the size of oil spill is dependant only of ships size expressed in DWT in tons. The results are presented in Fig. 14.
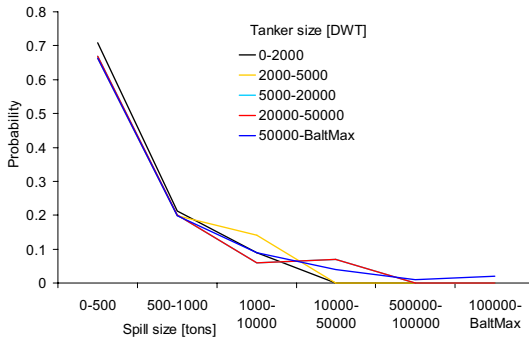
Fig.14. Statistical oil spill model (based on more than 1000 accidents from 3 independent sources)

3.4   Bunker spills after collisions and groundings

Bunker spills was estimated with use of accident databases [MEHRA 1999, ITOPF 1998, MAIB 2005, LMIS 2004, HECSALV 1996, IMO 2001]. The following formula is used for finding the bunker spill accident probability:

$$P_{BS} = P_A P_{A/BS} \tag{6}$$

where: P_A=probability of accident;
          $P_{A/BS}$=conditional probability of bunker spill if accident occur.

It was found that the conditional probability of bunker spill is dependant only of kind of accident and for collision equals $P_{BS/C}$=0.125 for grounding $P_{BS/G}$=0.12 and is smallest for fire accidents $P_{BS/F}$=0.017.

To find the size of bunker spill the mean capacity of bunker tanks in different ships was used. It was assumed that only 50% to 30% of bunker could be spilled after accident. This value is dependant of ships size. The results as mean bunker spill can were fitted to exponential function (Fig. 15).
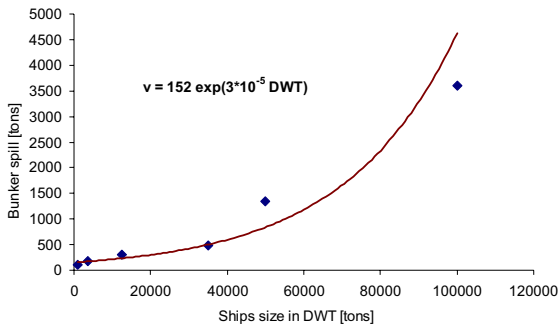

Fig. 15. The model of bunker spill size

4   Results

New routing measures have been adopted in July 2006. Traffic separation scheme established north of Bornholm significantly changed the traffic layout in the Southern Baltic Sea. This phenomenon could be observed during AIS data analysis. The most reliable accident database is carried out by Maris database of Helcom. The accident statistics between 2000 and 2005 are presented in Figure 16.

In the further step the presented simulation model was applied for the Southern Baltic Sea region to assess the expected number of accidents. The following assumptions have been made:

- traffic of ships with new routing measures applied;

- traffic on estimated level in 2010 year applied according to data of Figure 2;

- time of simulation: >300 years until stabilisation of parameters is achieved;

- the mean encounter reaction distances same as for probability of collision evaluation;

- no influence of weather for simplification reasons;

The results of simulation are presented in Figure 17, 18 and 19. The quantitative results of simulation are presented in Table 2.

Fig. 16. Statistical data of collision accidents in the Southern Baltic Sea (2000-2005) [Helcom 2006]
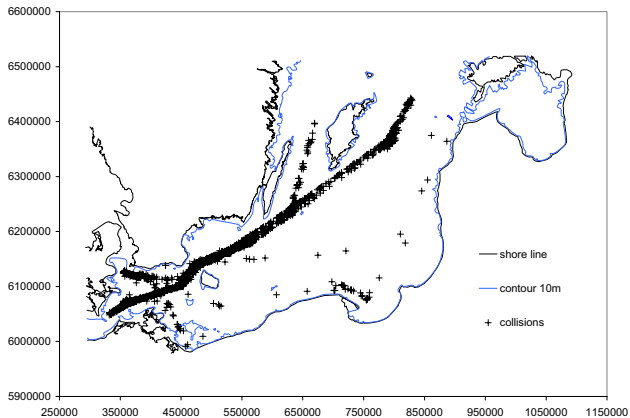
Fig. 17. Simulation data of collision accidents on the Southern Baltic Sea
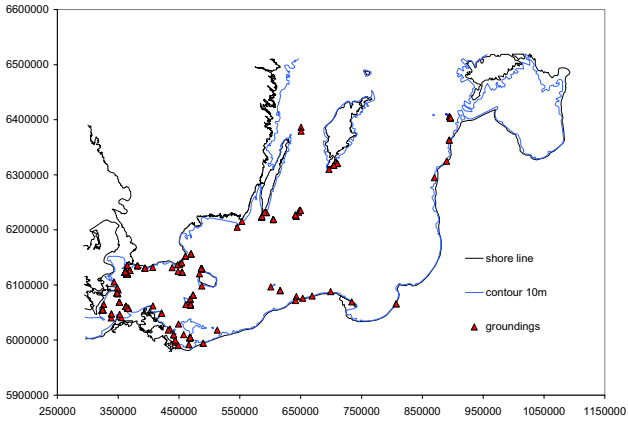
Fig. 18. Places of simulated ships groundings (700 calculation years)
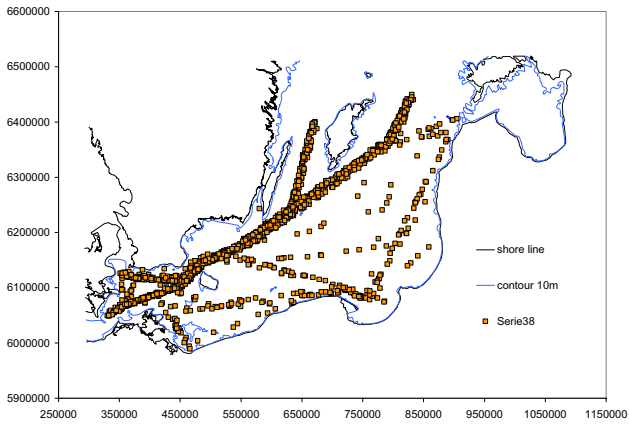
Fig. 19. Places of simulated ships fire accidents (700 calculation years)

The real oil spill accidents in analysed area are presented in Table 1. Mean intensity of oil spill accidents in Southern Baltic Sea equals 0.20 oil spill per year which gives mean time between accidents on the level of 5.0 years.

Tab. 1: The major oil spill accidents on whole Baltic Sea (Helcom 2007)

Year	Name of ship	Oil spill [t]	Location
2003	Fu Shan Hai	1,200	Bornholm, Denmark/Sweden
2001	Baltic Carrier	2,700	Kadetrenden, Denmark
1998	Nunki	100	Kalundborg Fjord, Denmark
1995	Hual Trooper	180	The Sound, Sweden
1990	Volgoneft	1,000	Karlskrona, Sweden

Tab. 2: Statistical data (700 calculation years to stabilise of statistical parameters)

Accident class	All	No spill	With spill	Time between accidents [ys]	Time between spills [ys]
Collision	1904	1584	320	0.37	2.19
Grounding	488	399	89	1.43	7.87
Fire	1382	1344	38	0.51	18.42
Total	3774	3327	447	0.19	1.57

The simulated oil spill places due to collisions, groundings and fire are presented in Figure 20, 21 and 22. The data shows high dependency of oil spills after collisions of traffic in examined area.
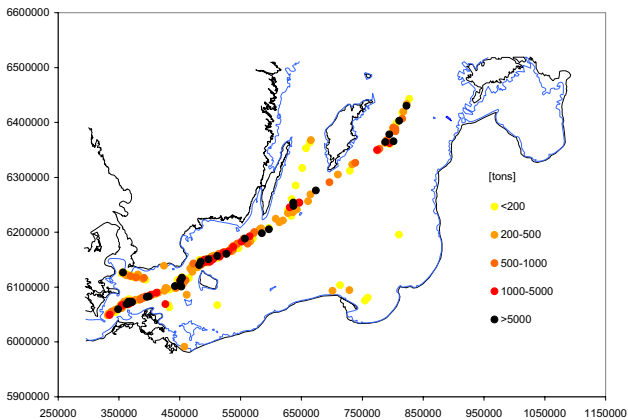

Fig. 20. Simulated oil spills accidents due to collisions with constant traffic estimated at 2010 year level (700 calculation years)
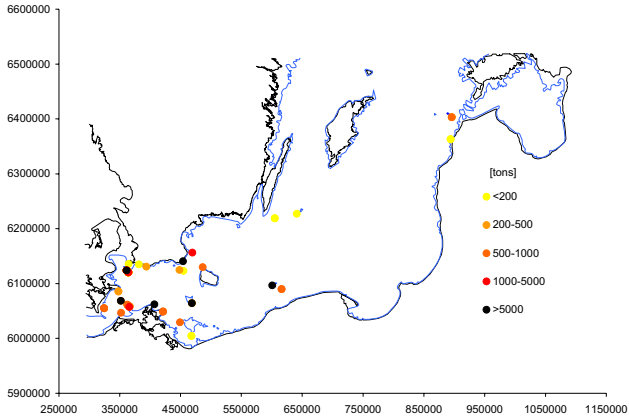
Fig. 21. Simulated oil spills accidents due to groundings with constant traffic estimated at 2010 year level (700 calculation years)
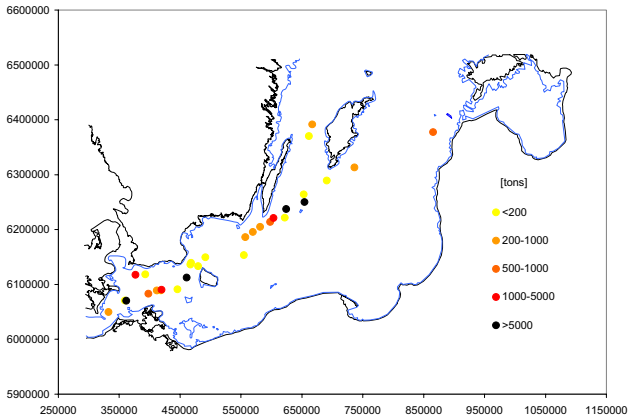

Fig. 22. Places and size of oil spills after fire accidents (700 calculation years)

5   Conclusions

Stochastic model of navigational safety was applied to assess the safety of Southern Baltic in respect of oil spills. The traffic on expected at 2010 level and new routing schemes on the Baltic Sea was applied. As it was expected the number of accidents will increase significantly.

The accident probability in different conditions (meteorological, traffic, navigational) evaluated in this researches will be used in the further step as the input value in navigational risk assessment models on large costal areas. The evaluation of ships traffic influence on environment due to possible oil spills after collision is also presented.

The comparison of simulation results with real data of oils spills shows significant discrepancy. As it was presented the simulated time between oil spills accidents is twice as high as the one from statistical data. It could mean that navigational conditions in the Baltic Sea are scientifically different from all over the world. From the other side it should be remembered that the oil spill accidents are very rare events and high uncertainty should be considered.

References

[1] Assessment of the traffic in the Baltic Sea. Study submitted on 51 session of Sub-Committee on Safety of Navigation by Denmark and Sweden, 2005.

[2] Friis-Hansen, P.; Simonsen, B.C.: GRACAT: Software for Grounding and Collision Risk Analysis. Collision and Grounding of Ships; *Proc. Intern. Conf.* Copenhagen, 2000.

[3] Gucma, L.; & Zalewski, P.: Damage probability of offshore pipelines due to anchoring ships. *Polish Maritime Research*. 2003.

[4] Gucma, L.: Models of ship's traffic flow for the safety of marine engineering structures evaluation. *Proc. of ESREL Conf.* Rotterdam: Balkema, 2003.

[5] Gucma, L.: Risk Modelling of Ship Collisions Factors with Fixed Port and Offshore Structures (in polish). Szczecin: Akademia Morska, 2005.

[6] Helcom. Report on shipping accidents in the Baltic Sea area for the year 2005. Helsinki Commission Baltic Marine Environment Protection Commission (HELCOM). Draft. 2006.

[7] Kobayashi, H.: Standard Mariners Behavior in Avoiding Collision Maneuver. *Proc. of Marsim Conf.* Terschelling. 2006.

[8] Merrick, J.R.W. et al.: Modelling Risk in Dynamic Environment of Maritime Transportation. *Proc. of Intern. Conf. of Winter Simulation.* Washington. 2001.

[9] Otay, E.; Tan, B.: Stochastic Modelling of Tanker Traffic Through Narrow Waterways *Proc. of Intern. Conf. on Oil Spills in the Mediterranean and Black Sea Regions.* 1998.

[10] Risk assessment of undersea gas pipeline Baltic-Pipe in Polish EEZ with consideration of shipping and fishery activities. 2002. Maritime University of Szczecin (draft).

[11] Severity, probability and risk of accidents during maritime transport of radioactive material Final report of a co-ordinated research project 1995-1999 Int. Atomic Agency 2001 Viena

[12] MEHRA 1999, Factors Influencing Vessel Risks in UK Waters, Appendix 6 1999.

[13] ITOPF 1998 (The International Tanker Owners Pollution Federation Limited), Database of Oil Spills from Tankers, Combined Carriers and Barges, 1974-1998.

[14] LMIS 2004. Lloyds Maritime Information Services The database of maritime incidents and accidents reported to Lloyd

[15] MAIB 2005. Maritime Accident Investigation Branch. UK registered ships accident database.

[16] HECSALV1996. Herbert Engineering Corporation. Salvage Engineering Software 5.08 Huston.

[17] IMO 2001 International Maritime Organisation, Fire Casualty Database.

Multi-factor MANOVA method for determination of pilot system interface

Maciej Gucma
Marine Traffic Engineering Institute, Maritime University, Szczecin, Poland

Abstract: The paper proposes a statistical approach to the solution of practically very important problem, of risk based criteria's, in field of testing and development of a sea pilot electronic chart. Multi Factor Analysis of Variance Method (MANOVA) was applied to assess different visualizations types in Pilot Navigation System. Results concerning optimal solution are presented. Construction of quantity criteria for assessment and development of navigational chart and interface is also shown.

1   Introduction

1.1   The Problem

Safe passage of vessel at confined area depends on several phenomena's that occurs during dynamic movement. These phenomena's are described by marine traffic engineering (MTE) and particularly these are: safe maneuvering of vessel by means of its destination with acceptable movement risk level.

Practically MTE leads to choose of most efficient maneuver for given vessel type at given area and in given conditions. Researches over navigator-vessel-environment system are indispensable for decision making support systems construction. These systems contribute to increase of safety level at area. Information provided by such system must have following attributes [2]:

- be sufficient for safe performance of given maneuver;

- displayed in optimal way that may be used directly by operator.

These assumptions could be fulfilled by:

- minimization of information required for safe performance of planned maneuver;

- such visualization of these information which allows operator to transform it to rudder and propeller settings without diversion of operator.

Although optimal visualization is very complex some elements are crucial for its safe improvement usability. These are chart and user interface.

Navigation in restricted waters is often referred to as pilotage or pilot navigation. In the process of navigating in restricted waters, because of the fast changes in the vessel's position in relation to objects ashore, the observed and the reckoned positions are not marked on the chart, as in navigation in unrestricted and coastal areas. The vessel's position is determined in the mind of the pilot or the master conducting the ship. In the process of conducting pilot navigation the pilot can be supported by the PNS (Pilot Navigation System).

1.2   The Solution

Currently, there are a few solutions of pilot navigational systems produced in the world. These systems are constructed on ECS basis (systems of electronic charts) or ECDIS (systems of imaging electronic charts and navigational information), the latter being a detailed development of the former. Their common characteristic is the vessel imaged on the electronic chart in the shape of an outline called "conventional waterline". The accuracy of the PNS depends on the positioning system applied and ranges from 1m to 20m.

The basic faults of the PNSs currently produced are [2]:

- the information presented is not the optimal information which causes it not to be taken advantage of in the utmost degree and there are difficulties with its being absorbed by the pilot;

- lack of special images useful in pilotage navigation, like: in relation to the shore, in relation to the fairway axis;

- lack of optimal user interface;

- lack of a maneuver prediction system.

These faults result from the systems being only modernizations of the systems functioning in unrestricted water areas (ECS or ECDIS) for the needs of pilotage, and were not worked out by scientific methods.

A team of scientists from the Navigational Department of the Maritime University of Szczecin, within the framework of a project co-financed by the Ministry of Education and Science, undertook to work out the optimal solution for a pilotage navigational system, making use of scientific methods of constructing navigational systems. As a result of research carried out, two PNS prototypes emerged:

- a stationary one, designed for sea ferries,

- a portable one, designed for pilotage.

At present these prototypes are undergoing experimental research and are being prepared for starting production. The following elements make up these systems:

- subsystem of electronic charts,

- positioning subsystem,

- information processing and imaging subsystem.

2   Research description and field

Optimization of presented visualization is one of problems in modern support system for aircrafts [3] as well as vessels. For the latter, very special demands are risen by sea pilots and this matter is presented in paper.

Complex system like Pilot Navigation System (PNS) consist of both hardware and software subsystems. Software is based at electronic chart, transformed for this special purpose. This transformation is subject to optimization. Thus development of PNS requires complete simulation solution. Such tool has been created in Marine Traffic Engineering Institute and consists of following elements:

- part time vessel simulator (pc based) presented at fig.1;

- fully functional PNS model presented at fig. 2;

- interfaces for visualization and control for simulator.
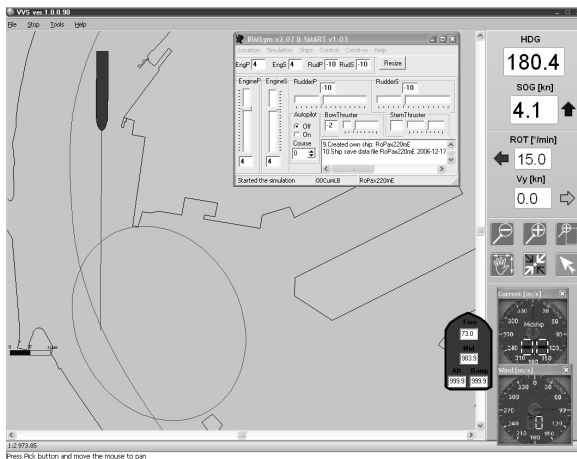

Fig. 1 Visualization in part time simulator
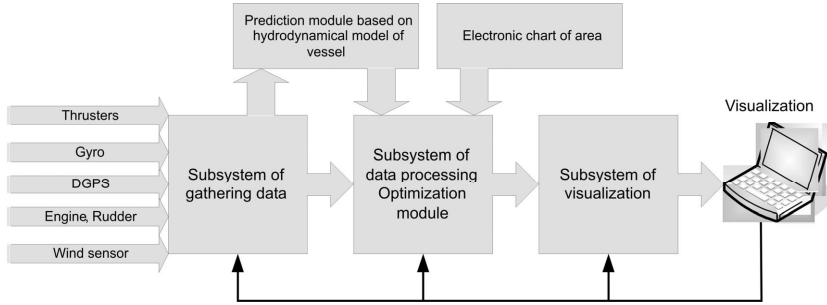
Fig.2. Model of Pilot Navigation System

For analysis set of simulations from 19 experts was taken. Simulations were performed at artificially created area where navigator was maneuvering at restricted (confined) waters. Vessel model was based on real vessel factors. Plan of passage for single experiment is presented at fig 3. Whole route consists of 2 arcs, entrance, exit and straight section. Each expert has performed 3 passages with different presentation orientations – here treated as classification factor for variance analysis. This factors are: N – representing North up chart orientation, R10 – representing Route Up with 10 deg change of course axis update, and R20 - representing Route Up with 20 deg change of course axis update. Orientations are presented at equation nr 4 and fig 4..
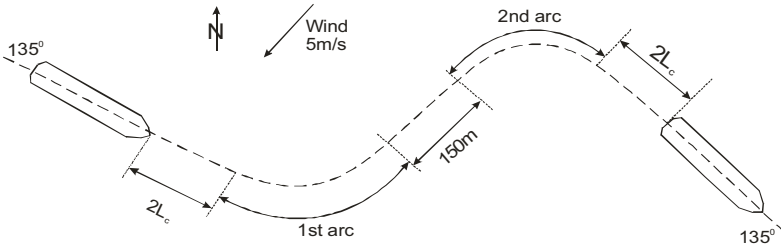

Fig.3. Simulation experiment overview

$$\left. \begin{array}{l} |\alpha_i - \alpha_{i+1}| \ge \alpha_z \Rightarrow Z = K_{i+1} \\ |\alpha_i - \alpha_{i+1}| < \alpha_z \Rightarrow Z = K_i \end{array} \right\} \qquad (1)$$

with:

K_i − waterway axis with width d_i and course α_i,

α_z − value of waterway axis change in system <10, 20> [°],

Z − orientation used for given waterway axis.
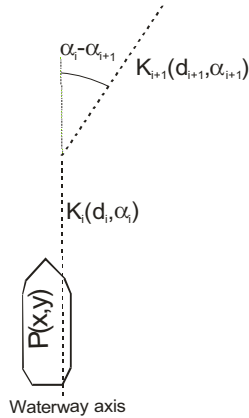
Fig. 4. Change of waterway axis in Route up (R) orientation

Analysis of traffic lanes at restricted area provides variety of information. These data are the consequence of steering of model with use of PNS, and especially:

- comparison of waterway width between different simulation runs within same classification factor group;

- conclusions over structure of width of traffic lanes population (maximums, mean values etc.)

- interference between type of area and width of traffic lane.

After initial analysis of total observed variances, some groups for MANOVA analysis can be obtained. There are 4 sections of data taken into consideration. Fig. 5 presents 95% traffic lanes for each section of data, as well as their total variances. For comparison waterway axis is presented.
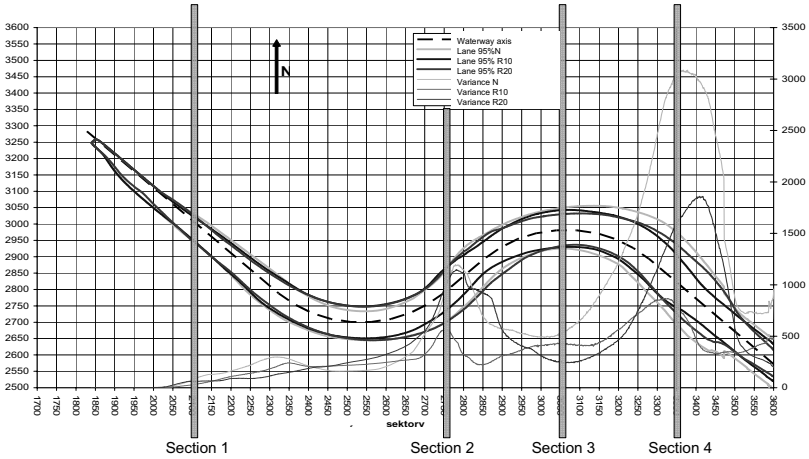
Fig. 5. Sections in experiment and total observed variances

3 Method of optimization

Optimization was performed in two steps: one factor variance analysis ANOVA, and multi dimensional MANOVA. ANOVA gave simple answer to existence of correlation between factors whilst MANOVA let to observe interactions between these factors. In presented article only MANOVA will be concerned. Interaction is here assumed as change of main factor during change of other factor. MANOVA sum of squares (*SS*) then will be:

$$\sum_{i=1}^{a}\sum_{j=1}^{b}\sum_{k=1}^{n}(x_{ijk}-\overline{x})^2 = \sum_{i=1}^{a}\sum_{j=1}^{b}\sum_{k=1}^{n}(x_i-\overline{x})^2 + \sum_{i=1}^{a}\sum_{j=1}^{b}\sum_{k=1}^{n}(x_j-\overline{x})^2 +$$
$$+\sum_{i=1}^{a}\sum_{j=1}^{b}\sum_{k=1}^{n}(x_{ij}-x_i-x_j+\overline{x})^2 + \sum_{i=1}^{a}\sum_{j=1}^{b}\sum_{k=1}^{n}(x_{ijk}-\overline{x}_{ij})^2 \qquad (2)$$

with:

x_{ijk} − k-th result of observation at i-th level of factor *A*, and j-th level of factor *B*.

$\overline{x}$ - general mean value

$\overline{x}_i$ - mean of all observations at i-th level of factor *A*

$\overline{x}_j$ - mean of all observations at j-th level of factor B

$\overline{x}_{ij}$ - mean value of all observations at i-th level of factor *A* and j-th level of factor *B*.

Simplifying this equation it can be stated:

$$SS_{total} + SS_A + SS_B + SS_{(AB)} + SS_{error}$$

(3)

with:

SS_A – sum of squares deviations related to influence of A factor

SS_B – sum of squares deviations related to influence of B factor

$SS_{(AB)}$ – sum of squares deviations related to influence of A and B factors (interactions)

Identically we can build equations defining degrees of freedom (*df*), mean squares (*MS*) and F-test. Tested hypothesis will be related with given factor A or B and interactions between them (*AB*). For generalization we it can be used two way classification model (cross classification model) and it is:

$$x_{ijk} = \mu + \alpha_1 + \beta_j + (\alpha\beta)_{ij} + \varepsilon_{ijk}$$

(4)

with

x_{ijk} – value from experiment. *K*-th value for *i*-th level of factor *A* an *j*-th level of factor *B*.

μ – mean value

α_i – main effect *i*-th level of factor *A*.

β_j – main effect of *j*-th level of factor *B*.

$(\alpha\beta)_{ij}$ – effect of interaction *i*-th level of factor *A* and *j*-th level of factor *B*

ε_{ijk} – random error from experiment with normal distribution (mean equals zero and variance equals σ^2)

Assuming:

$$\sum_i \alpha_i = \sum_j \beta_j = \sum_{ij} (\alpha\beta)_{ij} = 0$$

Hypotheses can be formulated as follows:

- H_{0A} : $\alpha_1 = \alpha_2 = ... = \alpha_a = 0$ H_{1A} : $\alpha_i \neq 0$ for certain *i*
- H_{0B} : $\beta_1 = \beta_2 = ... = \beta_b = 0$ H_{1B} : $\beta_j \neq 0$ for certain *j*
- H_{0AB} : $(\alpha\beta)_{11}$ $1 = (\alpha\beta)_{11} = ... = (\alpha\beta)_{ab} = 0$ H_{1A} : $(\alpha\beta)_{ij}$ $\neq 0$ fort certians *i, j*,

In presented example of optimization, linguistically formulated parameters influence can be described:

- orientation of chart (variants: N, R10, R20)

- waterway part (sections from 1 to 4 i.e: straight, exit from turn, double turn, exit from double turn)

Perimeter that will be evaluated is number of overriding 95 % traffic lane for right and left sides of waterway. Matrix of factors with dimension 3 x 20 can be defined. This matrix is presented in table 1.

Tab.1. Matrix of factors of MANOVA in investigated orientations [1].

Variant	Orientation of chart	Section - name	number of overrides
1	N	1 - straight	0
2	R10	1 - straight	0
3	R20	1 - straight	0
4	N	1 - straight	1
5	R10	1 - straight	0
6	R20	1 - straight	0
7	N	2 - exit from turn	1
8	R10	2 - exit from turn	1
9	R20	2 - exit from turn	1
10	N	2 - exit from turn	3
11	R10	2 - exit from turn	2
12	R20	2 - exit from turn	1
13	N	3 - double turn	3
14	R10	3 - double turn	2
15	R20	3 - double turn	1
16	N	3 - double turn	4
17	R10	3 - double turn	3
18	R20	3 - double turn	2
19	N	4 – exit from double turn	4
20	R10	4 – exit from double turn	2
21	R20	4 – exit from double turn	2
22	N	4 – exit from double turn	5
23	R10	4 – exit from double turn	4
24	R20	4 – exit from double turn	3

4 Research results

Results for significance test of MANOVA for overriding factor are presented in table 2. Whilst results of overriding for all sections depend from orientation at figure 4.

Tab. 2: Significance of dependant variables for overriding waterway factor

|	SS	df	MS	F	p
Orientation	7.75000	2	3.87500	6.2000	0.014150
Section	33.45833	3	11.15278	17.8444	0.000101
Orientation·Section	1.91667	6	0.31944	0.5111	0.789072
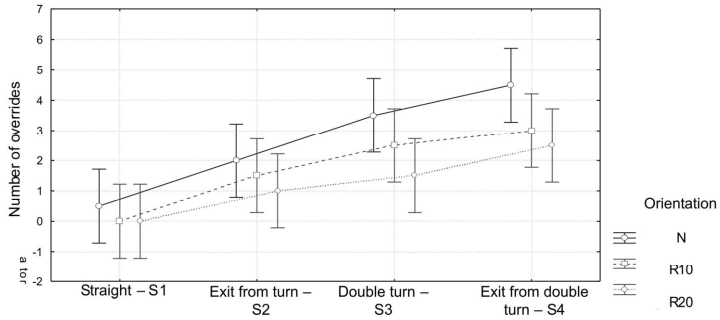
Fig. 6 Waterway overrides in function of section for all orientations.

Fig 7 presents mean square roots deviations for all orientations as function of waterway overrides. Whiskers represent 95% confidence values.
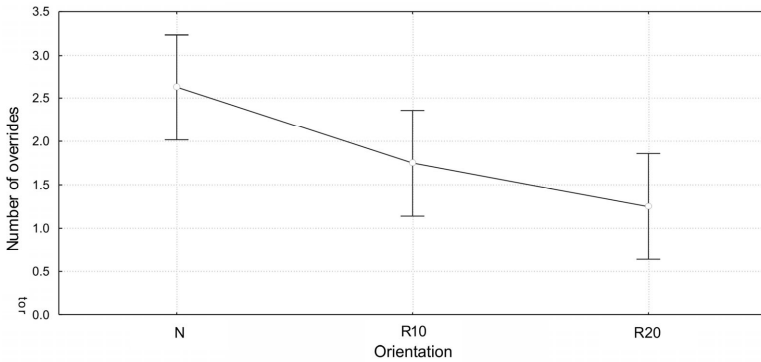
N R10 R20

Fig. 7. Orientation in function of waterway overrides.

5 Conclusions

In article model of information optimization in PNS is presented. In details MANOVA analysis of variance for traffic lanes shows following:

- values of waterway width are higher for third and fourth analyzed section,

- highest values of waterway width are at area of exit from double curve (section 4),

- depending on orientation big differentiation is observed,

- analyzing number of overrides of waterway, most sufficient orientation is in relation to waterway axis (R) with change of waterway every 20 deg (R20). Very low difference between variants R10 and R20 may suggest that additional researches between more variants shall be considered.

Literature

[1] Gucma, M., Optimization of navigational information in pilot decision support systems. unpublished PhD dissertation, Military University of Technology, Warsaw 2007.

[2] Gucma S.: Pilot Navigation, Fundacja Promocji Przemysłu Okrętowego i Gospodarki Morskiej, Gdańsk, 2004 (in Polish).

[3] Leiden, K., Keller, J., French, J., Information to Support the Human Performance Modeling of a B757 Flight Crew during Approach and Landing. Report NASA, California, 2001.

List of Probabilistic Symposiums in this Series

1st Dresden Probabilistic Symposium –
Safety and Risk in Civil Engineering (in German)
14th November 2003, Dresden
Dresden University of Technology
2nd Edition, 2006
ISBN-10: 3-00-019234-4 & ISBN-13: 978-3-00-019234-0
Price: 30 €
Order: Dirk Proske, Goetheallee 35, 01309 Dresden, Germany
E-mail: dirk.proske@boku.ac.at

2nd Dresden Probabilistic Symposium –
Safety and Risk in Civil Engineering (in German)
12th November 2004, Dresden
Dresden University of Technology
2nd Edition, 2006
ISBN-10: 3-00-019235-2 & ISBN-13: 978-3-00-019235-7
Price: 30 €
Order: Dirk Proske, Goetheallee 35, 01309 Dresden, Germany
E-mail: dirk.proske@boku.ac.at
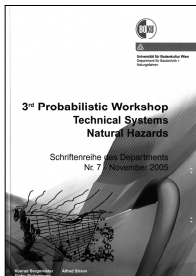
3rd Probabilistic Workshop –
Technical Systems & Natural Hazards,
12th-13th October 2005, Vienna
University of Natural Resources and Applied Life Sciences,
Vienna, Austria
Order: Department of Civil Engineering and Natural Hazards,
Peter Jordan Strasse 82, 1190 Vienna, Austria

4th International Probabilistic Symposium
12th-13th October 2006, Berlin
BAM - Federal Institute for Materials Research and Testing
ISBN-10: 3-00-019232-8 & ISBN-13: 978-3-00-019232-6
Order: Dirk Proske, Goetheallee 35, 01309 Dresden, Germany
E-mail: dirk.proske@boku.ac.at
or: Milad Mehdianpour, BAM-Fachgruppe VII.2 Ingenieurbau
Bundesanstalt für Materialforschung und –prüfung,
Unter den Eichen 87, 12205 Berlin

Magnel Laboratory for Concrete Research
Ghent University, Ghent, Belgium
University of Natural Resources and Applied Life Sciences, Vienna
Department of Civil Engineering and Natural Hazards, Austria
Supported by the European Safety and Reliability Association